APPLICATION OF AN EVOLUTIONARY DATA MINING TECHNIQUE FOR CONSTITUTIVE MODELLING OF GEOMATERIALS

Alireza Ahangarasr

PhD in Geotechnical Engineering

University of Exeter
December 2012

College of Engineering, Mathematics and Physical Sciences

APPLICATION OF AN EVOLUTIONARY DATA MINING TECHNIQUE FOR CONSTITUTIVE MODELLING OF GEOMATERIALS

Submitted by

ALIREZA AHANGARASR

to the University of Exeter as a thesis for the degree of

Doctor of Philosophy in Geotechnical Engineering

December 2012

I certify that all material in this thesis which is not my own work has been identified and that no material has previously been submitted and approved for the award of a degree by this or any other University.

……..

To My Family

ACKNOWLEDGEMENTS

Undertaking this PhD has been a life-changing experience for me and it would not have been possible to do without the support and guidance that I received from many people.

I would like to first say a very big thank you to my supervisor Professor Akbar Javadi for his help, support and encouragement all the time during my PhD studies. This PhD would not have been achievable without his very kind and ceaseless support.

Many thanks also to my second supervisor Professor Slobodan Djordjevic, very supportive mentor Dr Arnaud Marmier, and my very good friend and colleague Dr Asaad Faramarzi who helped and supported me all the way along with my PhD.

I would also like to say a heartfelt “thank you” to my parents, my wife, my brother, my grandma, and my aunt for always believing in me and encouraging me to follow my dreams and for all the priceless support that I have received from them during my PhD studies.

ABSTRACT

Modelling behaviour of materials involves approximating the actual behaviour with that of an idealised material that deforms in accordance with some constitutive relationships. Several constitutive models have been developed for various materials many of which involve determination of material parameters with no physical meaning. ANN is a computer-based modelling technique for computation and knowledge representation inspired by the neural architecture and operation of the human brain. It has been shown by various researchers that ANNs offer outstanding advantages in constitutive modelling of material; however, these networks have some shortcoming. In this thesis, the Evolutionary Polynomial Regression (EPR) was introduced as an alternative approach to constitutive modelling of the complex behaviour of saturated and unsaturated soils and also modelling of a number of other civil and geotechnical engineering materials and systems. EPR overcomes the shortcomings of ANN by providing a structured and transparent model representing the behaviour of the system. In this research EPR is applied to modelling of stress-strain and volume change behaviour of unsaturated soils, modelling of SWCC in unsaturated soils, hydro-thermo-mechanical modelling of unsaturated soils, identification of coupling parameters between shear strength behaviour and chemical's effects in compacted soils, modelling of permeability and compaction characteristics of soils, prediction of the stability status of soil and rock slopes and modelling the mechanical behaviour of rubber concrete. Comparisons between EPR-based material model predictions, the experimental data and the predictions from other data mining and regression modelling techniques and also the results of the parametric studies revealed the exceptional capabilities of the proposed methodology in modelling the very complicated behaviour of geotechnical and civil engineering materials.

UNIVERSITY OF EXETER

CONGRATULATIONS

Alireza Ahangarasr

on obtaining the

Exeter Research Scholarship

Dr Jonathan Barry
Dean of the Faculty of Taught Programmes
November 2008

UNIVERSITY OF EXETER

Advanced Technologies Research Institute

Prize for the Best PhD Student at Stage 1 2008/2009

Alireza Ahangarasr

In recognition of the best overall PhD student at stage 1 awarded by the Advanced Technologies Research Institute

Professor K E Evans CEng CPhys
Head of School

School of Engineering, Mathematics and Physical Sciences

LIST OF PUBLICATIONS

Journals papers

- Ahangar-Asr, A., Johari, A. and Javadi, A. A. (2012). "An Evolutionary Approach to Modelling the Soil-Water Characteristic Curve in Unsaturated Soils", *Computers and Geosciences*, 43, 25-33.

- Ahangar-Asr, A., Faramarzi, A., Mottaghifard, N. and Javadi, A. A. (2011). "Modelling of Permeability and Compaction Characteristics of Soils using Evolutionary Polynomial Regression", *Computers & Geosciences*, 37(11), 1860-1869.

- Ahangar-Asr, A., Faramarzi,A. and Javadi, A. A. (2011). "Modelling Mechanical Behaviour of Rubber Concrete Using Evolutionary Polynomial Regression" *Engineering Computations: International Journal for Computer-Aided Engineering*, 28(4), 492-507.

- Ahangar-Asr, A., Faramarzi, A. and Javadi, A. A. (2010). "A New Approach for Prediction of the Stability of Soil and Rock Slopes", *Engineering Computations: International Journal for Computer-Aided Engineering*, 27(7), 878-893.

- Javadi A.A., Ahangar-Asr A., Johari A., Faramarzi A., and Toll D.G. (2012). "Modelling Stress-Strain and Volume Change Behaviour of Unsaturated Soils using an Evolutionary Based Data Mining Technique, an Incremental Approach", *Engineering Applications of Artificial Intelligence Journal*, 25(5), 926-933.

- Cuisinier, O., Javadi, A., Ahangar-Asr, A. and Masrouri, F. (2013) "Identification of a Coupling Parameter between Hydro-mechanical Behaviour and Chemical's Effects in Compacted Soils with an Evolutionary Based Data Mining Technique", *Computers and Geotechnics Journal*, 48, 107-116.

Conference papers

- Ahangar-Asr A., and Javadi A. A. (2013): Modelling deviator stress-axial strain behaviour of unsaturated soils considering temperature effect, *Proceedings of the International Conference on Computational Mechanics (CM13)*, 25-27 March, Durham University, Durham, UK.

- Ahangar-Asr A., Javadi A. A., Faramarzi, A. (2012): Thermo-mechanical modelling of unsaturated soils using EPR, *Proceedings of the International Workshop: Intelligent Computing in Engineering (eg-ice)*, 4-6 July, in Herrsching (Munich), Germany.

- Ahangar-Asr, A., Javadi A. A., Faramarzi, A., Mottaghifard N. (2012): Rock Slope Stability Analysis; an Evolutionary Approach, *9th International Congress on Civil Engineering*, 8-10 May, Isfahan University of Technology (IUT), Isfahan, Iran.

- Ahangar-Asr, A., Johari, A., Javadi, A.A. (2011): Modelling Soil-water Characteristic Curve Using EPR, *Proceedings of the 5th Asia-Pacific Conference on Unsaturated Soils (AP-UNSAT)*, 29 February & 1-2 March 2012, Pattaya, Thailand.

- Ahangar-Asr, A., Faramarzi, A., Javadi, A. A., Mottaghifard, N. (2011): An Evolutionary Approach to Modelling Compaction Characteristics of Soils, *Proceedings of the 19th Annual Conference of the Association of Computational Mechanics in Engineering (ACME)*, 5-6 April, Heriot-Watt University, Edinburgh, UK, pp: 45-48.

- Ahangar-Asr, A. (2011): A New Approach to Modelling the Stability Behaviour of Soil and Rock Slopes in Civil and Structural Engineering, *Proceedings of the Young Researchers' Conference (YRC)*, 17 March, The Institute of Structural Engineers, London, UK.
- Ahangar-Asr, A., Mottaghifard, N., Faramarzi, A., Javadi, A.A. (2011): A Prediction Model for the Stability Factor of Safety in Soil Slopes, *Proceedings of the 2nd Post Graduate Conference on Computing: Application and Theory (PCCAT)*, 8th June, University of Exeter, UK, pp: 37-40.
- Ahangar-Asr, A., Javadi, A.A., Faramarzi, A., Mottaghifard, N. (2011): An evolutionary approach to modelling behaviour of geo-materials, *Proceedings of the 7th International PhD-DLA Symposium*, 24-25 October, Pollack Mihaly Faculty of Engineering, University of Pecs, Pecs, Hungary.
- Javadi, A.A., Johari, A., Ahangar-Asr, A., Faramarzi, A., and Toll D.G. (2010): Prediction of the Behaviour of Unsaturated Soils Using Evolutionary Polynomial Regression; an Incremental Approach, *Proceedings of the 5th International Conference on Unsaturated Soils, 6-8 September*, Barcelona, Spain, pp: 837-842.
- Ahangar-Asr, A., Faramarzi, A. and Javadi, A.A. (2010): An evolutionary numerical approach to modelling the mechanical properties of rubber concrete, *Proceedings of the International Conference on Computing in Civil and Building Engineering*, 30 June-2 July, Nottingham University, Nottingham, UK, pp 411, paper 206.
- Javadi, A. A., Johari, A., Ahangar-Asr, A., Faramarzi, A. and Toll, D. G. (2009): A New Approach to Constitutive Modelling of Unsaturated Soils Using Evolutionary Polynomial Regression, *Proceedings of the 4th Asia-Pacific Conference on Unsaturated Soils*, 23-25 November, Newcastle, Australia.
- Javadi, A. A., Johari, A., Ahangar-Asr, A., Faramarzi, A. and Toll, D. G. (2009): Using Evolutionary Polynomial Regression in Modelling of Unsaturated Soils, *Proceedings of the 19th Annual Conference of the Association of Computational Mechanics in Engineering (ACME)*, 6-8 April, Nottingham, UK, pp: 353-356.

Book chapter

- Javadi, A.A., Ahangar-Asr, A., Faramarzi, A., Mottaghifard, N. (2012) "An EPR Approach to Modelling of Civil and Geotechnical Engineering Systems", Chapter in *Metaheuristic Algorithms in Water, Geotechnical and Transport Engineering*, Yang X.S., Talatahari S., Gandomi A.H (eds), and Alavi A.H., First Edition, Elsevier, ISBN: 978-0-12-398296-4.

LIST OF ABBREVIATIONS

ASTM	American Society for Testing Materials
ABAQUS	A commercial finite element analysis software
ANN	Artificial Neural Network
BPNN	Back-propagation Neural Network
$Ca(OH)_2$	Calcium Hydroxide
CAH	Calcium Aluminate Hydrates
CaO	Calcium oxide
CoD	Coefficient of Determination
CSH	Calcium Silicate Hydrates
D	Stiffness (Jacobian) matrix
DEM	Discrete Element Method
DNA	Deoxyribonucleic Acid
DV	Design Variables
EAs	Evolutionary Algorithms
EEP	Extended-End-Plate
eM	Macropore void ratio
EPR	Evolutionary Polynomial Regression
FEA	Finite Element Analysis
FEM	Finite Element Method
Fm	Fineness Modulus
FRP	Fibre Reinforced Polymeric
FS	Factor of Safety
GA	Genetic Algorithm
GP	Genetic Programming
GUI	Graphical User Interface
GWC	Gravimetric Water Content
HMIM	Hybrid Modelling framework utilizing mathematics and Information-based Methodologies
K	Permeability
LR	Linear Regression
LS	Least Square
MA	Manois Argillite
MARC	Name for a commercial finite element software

MDD	Maximum Dry Density
MGU	Unsaturated Mataara-Granite
MHM	Meuse-Haute Marne
MIT-E3	An elasto-plastic constitutive model for Overconsolidated Clays
MOGA	Multi-objective Genetic Algorithm
MOGA-EPR	Multi-objective Genetic Algorithm-based Evolutionary Polynomial Regression
NANN	Nested Adaptive Neural Network
NaOH	Sodium Hydroxide
NeuroFEM	Neural Network-based Finite Element Method
NN	Neural Network
NNCM	Neural Network-based Constitutive Model
OCR	Overconsolidation Ratio
OMC	Optimum Moisture Content
PCS	Penalisation of Complex Structures
PDE	Partial Differential Equations
PLAXIS	A commercial geotechnical engineering software
PSSP	Plane-Strain Strain Probe
RTSM	Real Time Simulation Method
Self-Sim	Self-learning Simulation
SOGA	Single-objective Genetic Algorithm
SOGA-EPR	Single-objective Genetic Algorithm-based Evolutionary Polynomial Regression
SPSW	Steel Plate Shear Wall
SSE	Sum of Squared Errors
SWCC	Soil Water Characteristic Curve
THM	Thermo-Hydro-Mechanical
TSADWA	Top-and-Seat-Angle with Double Web-Angle
TTSP	True Triaxial Strain Probe
UMAT / VUMAT	User-defined Material subroutines in ABAQUS
Wsat	Saturated Water Content
XRD	X-Ray Diffraction Analysis - Investigates crystalline material structure, including atomic arrangement, crystallite size, and imperfections
pH	A measure of the activity of the (solvated) hydrogen ion. Solutions with a pH less than 7 are said to be acidic and solutions with a pH greater than 7 are basic or alkaline.
3D	Three-dimensional

TABLE OF CONTENTS

Chapter 1

INTRODUCTION

1.1 General background

Constitutive modelling involves approximating the actual behaviour of materials with that of an idealised material that deforms in accordance with some constitutive relationships. In the past decades several constitutive models have been developed for various materials. Most of these models involve determination of material parameters, many of which have no physical meaning. In spite of considerable complexities of constitutive theories, due to the erratic and complex nature of some materials such as soil, rock, etc, none of the existing constitutive models can completely describe the real behaviour of these materials under various stress paths and loading conditions.
Because of significant advances in computational power and the development of more efficient solvers, the models are getting more and more sophisticated and realistic. Available packages provide new and improved interfaces, better visualization of the developed results, more options for automatic searching for design solutions, etc; but, the constitutive laws used in the analyses remain mostly unchanged from the ones used years ago (Faramarzi, 2011). Traditional material models are not capable of addressing the complexities inherent in natural geomaterials, like soils and rocks, in a unified way and normally are developed for specific applications and target specific problems. One of the main roles of constitutive modelling is their application in describing the material behaviour in numerical analyses.

The finite element method is a very popular numerical modelling technique to find approximate solutions of partial differential equations (PDE). Most of the problems in engineering analysis and design can be represented as a single or a series of differential equations. These equations are used to explain the system response once it is subjected to external influences (loads, displacements, etc). Most differential equations do not have analytical solution and numerical techniques need to be used to find approximate solutions for this type of equations. Among numerical techniques available, the finite element method is one of the most powerful techniques for solving most engineering problems. In the finite element method the structure being analysed is divided into a large number of smaller parts called elements (Stasa, 1986).

The accuracy of the finite element analyses results greatly depends on the constitutive model chosen to represent the material behaviour. Therefore, one of the most important steps in finite element analysis is selecting the most appropriate constitutive model. Although there are a large number of constitutive models with high degrees of complexity, but none of these models are able to completely describe the real behaviour of some materials such as soils, rocks, composites, etc. under different loading conditions. Therefore alternative methods for describing the material behaviour would be very advantageous.

In recent years, the use of artificial intelligence and data mining techniques has been introduced, as an alternative approach, for constitutive modelling of complex materials (Javadi and Rezania, 2009a). The use of artificial neural network (ANN) for modelling the behaviour of concrete was first introduced by Ghaboussi et al (1991). After that, other researchers continued to apply ANN to model the behaviour of other materials. Some of these works incorporated neural network-based material models (NNCMs) in finite element method to analyse engineering problems. Ghaboussi et al. (1998), Shin & Pande (2000) and Hashash et al. (2006) proposed the autoprogressive or self-learning approach to train neural network-based material models. These models included sequences of training a neural network (NN) embedded in the finite element method using measured values of displacements and forces of a structural or geotechnical test. The results from these works indicated that ANNs can be incorporated into the finite element method as alternative constitutive models. It was also shown that the trained ANNs incorporated in the finite element analysis provide better predictions of the behaviour of materials in comparison to the conventional/empirical models. In spite of all advantages, ANNs are also known to suffer from some shortcomings. One of the main disadvantages of the neural network-based constitutive models (NNCM) is that the optimum structure of the ANN (such as number of inputs, hidden layers, transfer functions, etc.) must be identified a priori which is usually obtained using time consuming trial and error procedures (Giustolisi and Savic, 2006). Another main drawback of the ANN approach is about the complexity of the network structure as ANN represents the knowledge in terms of weight matrices together with biases which are not accessible to the user. In other words ANN models do not provide any information on the way the inputs affect the output and therefore are considered as a black box class of models. The lack of interpretability of ANN models has stopped them from achieving their full potential in real world problems ((Lu, AbouRizk and Hermann, 2001) and (Javadi and Rezania, 2009a)).

In this thesis, a recently developed technique, named evolutionary polynomial regression (EPR), is considered as a powerful alternative to ANN. The proposed technique expresses the behaviour of the material being studied in terms of structured mathematical expressions. Giustolisi & Savic (2006) first introduced the use of EPR in modelling of hydroinformatics and environmental related problems. EPR is a two-stage technique: in the first step EPR attempts to find symbolic structures using a genetic algorithm and in the second stage it estimates the constants using a linear least square technique. In this thesis the EPR is used to model constitutive behaviour of complex civil enginnering systems including geomaterials and particularly unsaturated soils.

1.2 Aims

This thesis aims at:

- Introducing a new approach to modelling constitutive behaviour of complicated civil engineering materials.
- Presenting important applications of the proposed methodology in modelling complicated civil/geotechnical engineering problems relating saturated and unsaturated soils and rubber concrete.
- Discussing the advantages of the proposed methodology and the shortcomings/cautions that need to be considered in applying it.

1.3 Objectives

In this thesis EPR is employed, as an effective data mining and pattern recognition technique, to model some of the most complicated materials in civil and geotechnical engineering. The objectives of this thesis can be defined as:

- Presenting most recent developments in using data mining techniques for material modelling.
- Describing the model development procedure using the proposed evolutionary-based data mining technique.
- Modelling various aspects of the complex behaviour of unsaturated soils including (i) stress-strain and volume change behaviour; (ii) soil water characteristic curve (SWCC) and (iii) thermo-mechanical behaviour.
- Identification of coupling parameters between shear strength behaviour and chemical's effects in compacted soils.
- Constitutive modelling of coarse grained soils.
- Modelling permeability and compaction characteristics of soils and stability analysis of soil and rock slopes.
- Modelling the mechanical behaviour of rubber concrete.

1.4 Contribution to the knowledge

Applications presented and discussed in this thesis are amongst the most important geotechnical and civil engineering systems and material modelling problems with very little knowledge about their erratic nature and complicated mechanical behaviour. In this research a novel methodology is presented to develop models to represent this complicated behaviour in the shape of a unique, explicit and easy to understand mathematical expression with the capability of predicting the real behaviour of the system based on the data acquired from experiments or field measurements with very high accuracy levels. Pros and cons of the proposed methodology and its advantages over the existing techniques used in civil engineering modelling and also any concerns relating to the use of the proposed method in practical engineering problems are discussed.

1.5 Layout of the thesis

The thesis includes six chapters. In what follows a short description of the contents for every chapter is presented.
Chapter one (current chapter) provides a general description and objectives of the thesis. It gives an overall insight into the thesis and describes the order in which the materials are arranged in the thesis.

The second chapter presents a review of the literature on the most important and up-to-date developments in using data mining techniques in material modelling. In this chapter a background on the conventional constitutive material modelling techniques as well as developments in using data mining techniques (in particular artificial neural networks) in material modelling are presented.

In chapter three the new data mining technique, evolutionary polynomial regression (EPR), is described in detail. A general introduction is given to the most popular data mining techniques, including artificial neural network (ANN) and genetic programming (GP), and a detailed description of the evolutionary polynomial regression (EPR) technique is provided. The key features and important advantages of the proposed EPR technique are highlighted in this chapter.

In chapter four, EPR based modelling of constitutive stress-strain and volume change behaviour, thermo-mechanical behaviour and the soil-water characteristic curve in unsaturated soils, and also the constitutive stress-strain and volume change behaviour of granular soils are presented. EPR is also used to identify the coupling parameters between shear strength behaviour and chemicals' effects in compacted soils. After validation and verification, comparison of the predictions of the proposed models with experimental data as well as conventional models and artificial neural network results are presented. The results of sensitivity analyses of the proposed models are then presented to provide an understanding of the contributions of the involved parameters.

In chapter five some other applications for EPR are presented including modelling the compaction and permeability of soils, predicting stability status of soil and rock slopes and also the mechanical behaviour of rubber concrete. Model verification results, comparison of the predictions of the proposed models with experimental data and conventional models as well as artificial neural network results (where available) are presented. Effects of different contributing parameters on the proposed models are also investigated.

The concluding chapter, chapter 6, includes the main conclusions based on the contents of the present thesis and makes recommendations for further research.

Chapter 2

CONSTITUTIVE MODELLING BASED ON DATA MINING TECHNIQUES

2.1 Introduction

In the past few decades, numerical modelling techniques, in particular the finite element method, have been used to analyse a wide range of engineering problems. These problems span over a range of different disciplines including civil and structural engineering, aerospace, biomedical engineering, automotive and geotechnical engineering, among others. The finite element method is considered as a very robust tool for analysis of complex engineering problems. In this method, the behaviour of the actual material is approximated with that of an idealised material that behaves according to predefined constitutive relationships. As a result, the choice of an appropriate constitutive model that adequately and accurately describes the behaviour of the actual material is a crucial step in the finite element analysis and affects the accuracy and reliability of finite element predictions (Faramarzi, Javadi and Ahangar-Asr, 2012).
A wide range of different models have been presented to describe the constitutive behaviour of different materials including soils. The constitutive models for soils vary from simple elastic models (Hooke, 1675) to elasto-plastic models (e.g., Drucker and Prager (1952)), models created based on the critical state theory (Schofield and Worth, 1968) and strain hardening models (Lade and Jakobsen, 2002; Lade, 1977), among many others. In these models determination of the model (material) parameters is one of the important stages of model development process and many of these parameters have very little or no physical meanings (Shin and Pande, 2000). In recent years data mining techniques are introduced as alternatives to conventional methods for constitutive modelling of complex systems.
In this chapter, a history of the applications of the data mining-based constitutive modelling approaches is included. Advantages and disadvantages of the presented methodologies are also discussed.

2.2 Conventional approach to constitutive modelling

In developing conventional constitutive models, first a mathematical model is selected based on the understanding of the behaviour of the material or trends of the available data. In the next step, some appropriate physical tests are conducted on the samples of

the material in order to capture the behaviour of the material and to define the parameters of the model (model/material parameters). Accurate determination of these parameters is very important when these constitutive models are implemented into numerical models (such as FEM), as the accuracy of the numerical model predictions greatly depends on the accuracy with which the selected constitutive model describes the real behaviour of the material. Despite the considerable complexity of the existing constitutive theories and the fact that these theories encompass most of the characteristics of the material behaviour, due to the unpredictable and complex nature of some materials including soils and rocks, the existing constitutive models are not able to accurately describe the behaviour of such materials under various stress paths and loading conditions (Javadi and Rezania, 2008).

2.3 Data mining techniques and constitutive modelling

With the rapid development in information technology and computational software and hardware in the past few years, the use of computer-aided pattern recognition techniques has been introduced as an alternative approach to constitutive modelling of materials. Pattern recognition techniques, such as artificial neural network, fuzzy logic and genetic programming, can learn adaptively from data and generalise the captured behaviour.

2.3.1 Artificial neural networks (ANN)

Artificial neural networks (ANNs) are the most common pattern recognition procedures that have been widely used in constitutive modelling of materials. The use of ANN for material modelling was first introduced by Ghaboussi et al. (1991) for modelling the behaviour of concrete. This continued by the works of Ellis et al. (1992) and Ghaboussi et al. (1994) who applied the methodology to model the behaviour of geotechnical materials. The results of these and similar research works showed that the neural networks are able to capture and represent the nonlinear material behaviour with a good degree of accuracy.

ANN models have the ability to work with large quantities of data. They can learn complex behaviour of systems by training with input and output sets of data. The most outstanding advantage of ANNs over conventional material models is their ability to capture complex relationships between parameters contributing to the system without the need to assume the form of the relations between input and output variables.

The neural network assigns a given set of output vectors to a given set of input vectors. When applied to the constitutive description, the physical nature of these input-output data is determined by the measured quantities like stresses, strains, pore pressure, temperature, etc (Javadi, Tan and Elkassas, 2009). A typical representation of an ANN based model is shown in Figure 2.1.

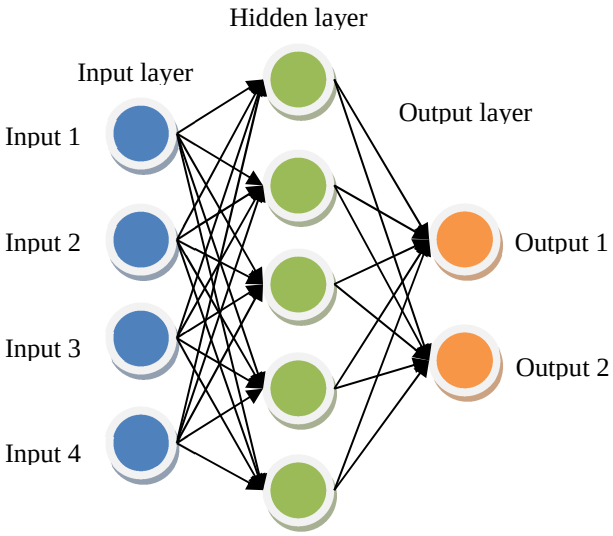

Figure 2.1: Typical neural network model

In the above network, one input layer, one hidden layer, and one output layer are used to represent the neural network model. All neurons in each layer (e.g. input layer) are individually connected to the neurons in the next layer (e.g. hidden layer) with a "connection weight". The knowledge stored in the developed network is hidden in the sets of connection weights and is used to make predictions of the output parameters.
Training of the neural network is done by modifying its connection weights in an appropriate manner through the data set used for "training" of the network. Training continues until the predicted output variables agree satisfactorily with the target values in the training data set. Networks trained in this way are generally termed back-propagation neural networks. The "back-propagation" term refers to the algorithm through which the error observed in the predicted output variables is used to modify the connection weights and repeat the training until the most suitable network is obtained.
However, ANNs also suffer from some shortcomings with the most important one being their back-box nature that prevents them from giving the user a clear insight and understanding to the model and the way that the involved parameters affect the model predictions.

2.3.2 Nested adaptive neural network

Nested adaptive neural network (NANN) was introduced by Ghaboussi and Sidarta (1998) and was applied to develop models to represent the constitutive behaviour of geotechnical materials. Ghaboussi and Sidarta (1998) applied this new type of neural network to develop models for drained and undrained behaviour of sands in triaxial tests. Nested adaptive neural network takes advantage of the nested structure of the material test data, and represents it in the layout of the neural network. Although the proposed new type of networks suggests the advantage of the nested structure; but, they show very little improvement towards removing the down sides of using ANNs in material modelling.

2.3.3 Application of neural network-based methods in material modelling

Penumadu & Zhao (1999) modelled the stress-strain and volume change behaviour of sand and gravel under drained triaxial compression test conditions using neural network. Data from a large number of tests (around 250 triaxial test data) were used to train the neural network. The optimum structure of the neural network was found by trial and error. The proposed neural network had 3 hidden layers with 15 neurons in each layer, eleven neurons in the input layer and two outputs. The input and output parameters of the model were as follows:

Inputs parameters: $D_{50}, C_u, C_c, h, n_s, e, \varepsilon^i, \Delta\varepsilon^i, \acute{\sigma}_3, \sigma_d^i, \varepsilon_v^i$
Output parameters: σ_d^{i+1}, ε_v^{i+1}

where D_{50}, C_u, C_c represent equivalent particle size and their distribution, h is an indicator of hardness of the material, n_s is the shape factor, e is the void ratio, and $\acute{\sigma}_3$ is the effective confining pressure. The current state of stress and strain was also represented with deviator stress σ_d^i, axial strain ε^i and volumetric strain ε_v^i. For a specimen with given current state of stress and strain, the developed ANN model aimed to predict two outputs, deviator stress σ_d^{i+1} and volumetric strain ε_v^{i+1} for the next stress-strain state corresponding to an axial strain increment of $\Delta\varepsilon^i$. The results showed that the developed neural network model was able to capture the stress-strain behaviour of granular soil with an acceptable level of accuracy considering both non-linear stress-strain relationship and volume change behaviours.
In case of isotropic materials, or when isotropy can be assumed, a strategy was proposed by Shin and Pande (2002) to generate additional data from limited number of general homogeneous material test results to be used in training of neural network-based constitutive models. In this strategy, by assuming that the material is isotropic, the stress-strain pairs of data are transformed. This is done by rotating the datum axes (X, Y and Z) from the axes with respect to which the material tests are done (1-2-3). This strategy increases the amount of training data so that there will be enough data lines for proper training of the neural network model. Shin and Pande (2002) solved a boundary value problem to evaluate their proposed methodology. In this problem a circular cavity in a plane stress plate was analysed using a finite element method in which the neural network-based constitutive model (NNCM) trained using their proposed strategy was used as the constitutive relationship. The results were compared to the ones from standard finite element analysis using conventional constitutive models and acceptable agreement was observed. The only limitation with this strategy, according to the developers, is that it cannot be used for anisotropic materials.
Penumadu & Zhao (1999) and Shin and Pande (2002) presented some important examples of applications of ANNs by suggesting methods of creating comprehensive input data for better training of the networks. Although the proposed technique to generate additional data helped improving the training experience of ANNs; however, no amendments to the actual methodology was suggested to improve the performance.

2.3.4 Neural network-based finite element and discrete element models

Javadi and colleagues investigated the application of neural networks in constitutive modelling of complex materials including soils. They developed a neural network based

finite element method (NeuroFEM) based on the incorporation of a back-propagation neural network (BPNN) in finite element analysis. The proposed model was validated and applied to solve different boundary value problems, mostly involving geotechnical engineering applications (e.g., (Javadi, Zhang and Tan, 2002); (Javadi and Zhang, 2003); (Javadi, Tan and Elkassas, 2004a); (Javadi and Zhang, 2004b); (Javadi, Tan and Elkassas, 2005); (Javadi, Tan and Elkassas, 2009)). The results showed that neural network is very efficient in capturing the behaviour of complex materials and generalising the behaviour to unseen conditions.

A closed-form solution for constructing material stiffness matrix using a neural network-based constitutive model was proposed by Hashash et al. (2004a). They also explained some of the problems concerning the numerical implementation of a neural network based constitutive model in finite element analysis. They proposed a procedure to establish the Jacobian (stiffness) matrix using neural network material models and implemented the matrix in ABAQUS through the user defined material subroutine (UMAT) and analysed some numerical examples including analysis of a beam bending problem and also the behaviour of a deep excavation.

Furukawa and Hoffman (2004) used a neural network for modelling of material behaviour under monotonic and cyclic plastic deformation and implemented it in finite element analysis. Two neural networks were trained and developed; one was used to learn the back stress and the other network was trained with the drag stress. The back and drag stresses represented kinematic hardening Y, and isotropic hardening R respectively. A more detailed illustration of these networks is presented in the figure below.

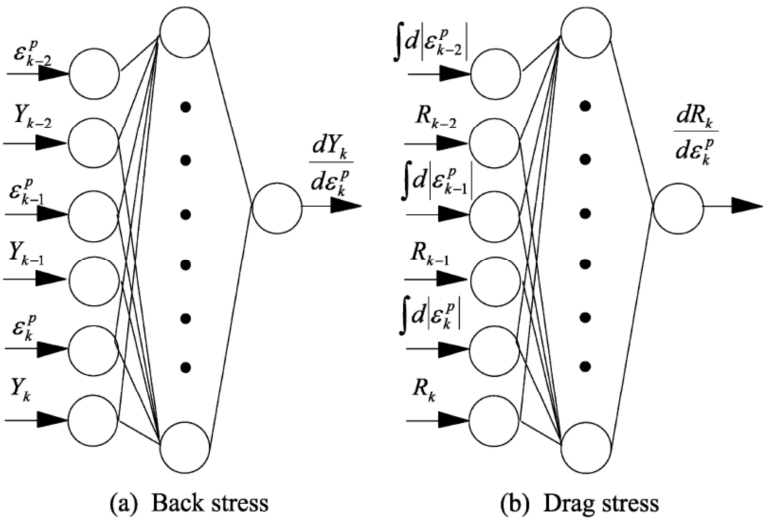

Figure 2.2: Neural network material models for back and drag stresses (Furukawa and Hoffman, 2004)

In the above figure Y and R show the kinematic and isotropic hardenings respectively and ε^p represents the plastic strain. The subscripts k, k-1 and k-2 represent current and two previous states of variables. Furukawa & Hoffman (2004) trained and validated the neural networks and then implemented the neural network based constitutive models in the commercial finite element software, MARC, using its user subroutine feature for external material models. To make this possible, they defined the stiffness (Jacobian) matrix, D, to describe the stress and strain relationship.

$$\boldsymbol{\sigma} = \boldsymbol{D\varepsilon} \qquad 2\text{-}1$$

D matrix was defined as the sum of the elastic ($\mathbf{D}^e$) and plastic ($\mathbf{D}^p$) matrices:

$$\mathbf{D} = \mathbf{D}^e + \mathbf{D}^p \qquad 2\text{-}2$$

The elastic matrix was derived using the Young's modulus and Poisson's ratio and only the plastic matrix was updated using the trained neural networks. To validate the performance of the proposed approach, two material models similar to Figure 2.2 were developed using real material data with monotonic plastic deformations. The results were compared with those of a conventional material model (Chaboche model) as well as experimental data. The same procedure was also followed for the case of cyclic plastic deformation and an acceptable agreement of results was reported. As the final stage, the proposed neural network based models representing the behaviour of the central part of a tensile specimen under cyclic loading were implemented in the finite element analysis package (MARC). Figure 2.3 illustrates the results.

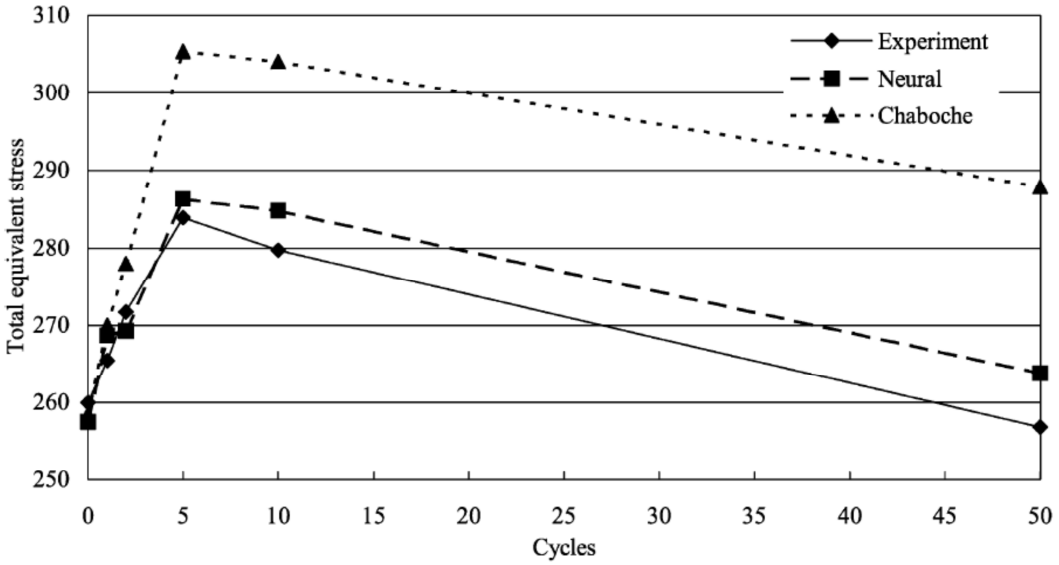

Figure 2.3: Comparison of experimental, FEA, ANN, best-fit Chaboche model and experimental results (Furukawa and Hoffman, 2004)

A better prediction of the results is presented by the proposed neural network-based finite element model in comparison to the conventional Chaboche model.
Nezami et al. (2006) used discrete element method (DEM) to generate stress-strain data in order to train neural network models for soils. The developed models were then implemented into the Real Time Simulation Method (RTSM) within which the model training process is done in a non-real time scale which is several times faster than the reality. This approach resulted in a much faster simulation process compared to the actual discrete element method simulation. Nezami et al (2006) used 2D and 3D examples to validate their proposed approach. They showed that the results of the neural network based models in RTSM framework provide more reasonable predictions in comparison to the DEM and can be obtained considerably faster.

2.3.5 Rate-dependent neural network-based finite element material modelling

A rate-dependent neural network-based material model with its implementation into finite element software was presented by Jung and Ghaboussi (2006a). In rate dependant material models, the material behaviour is considered to be dependent on both strains/stresses and the rate of strains/stresses. This assumption led to the development of a neural network model with the following structure:

$$\dot{\boldsymbol{\sigma}}^n = \dot{\boldsymbol{\sigma}}^n \mathbf{NN}(\boldsymbol{\varepsilon}^n, \boldsymbol{\varepsilon}^{n-1}, \boldsymbol{\sigma}^{n-1}, \boldsymbol{\sigma}^n, \dot{\boldsymbol{\varepsilon}}^n, \dot{\boldsymbol{\varepsilon}}^{n-1}, \dot{\boldsymbol{\sigma}}^{n-1}) \quad 2\text{-}3$$

The following equations were used to define stress and strain rates:

$$\dot{\sigma}^n = \frac{1}{\Delta t}(\sigma^n - \sigma^{n-1}) \quad 2\text{-}4$$

$$\dot{\varepsilon}^n = \frac{1}{\Delta t}(\varepsilon^n - \varepsilon^{n-1}) \quad 2\text{-}5$$

The developed neural network model was implemented into the commercial finite element software ABAQUS through its user material (UMAT) feature. A hypothetical material and structure was considered to verify the proposed methodology. Laboratory test data obtained by previous researchers were also used as an example of application of the proposed rate-dependent neural network-based material model. The structure used for testing was scaled by the factor of 1 to 8 with respect to the real bridge, and the time dependent strain variations were measured in mid span using three strain gauges located at the top, bottom, and middle of the bridge cross section as shown in Figure 2.4.

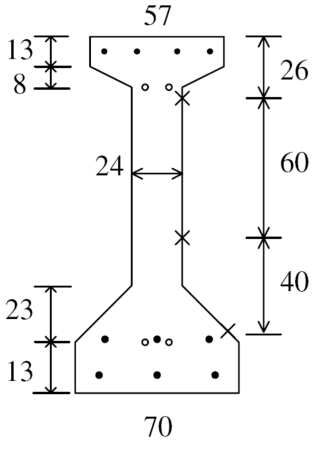

(Unit: mm)

Figure 2.4: Test specimen – Physical geometry (Jung and Ghaboussi, 2006a)

To construct the beam for the experiment, concrete cylinders with diameter of 10 cm and height of 20 cm were made. Loading was applied to these samples and the corresponding time dependant strains were measured. The obtained stress-strain data were used to train the neural network-based material model. UMAT subroutine of ABAQUS was used to implement the developed neural network model to be used in the finite element analysis of the beam structure. The results of the analysis along with the measured strains are shown in the following figure.

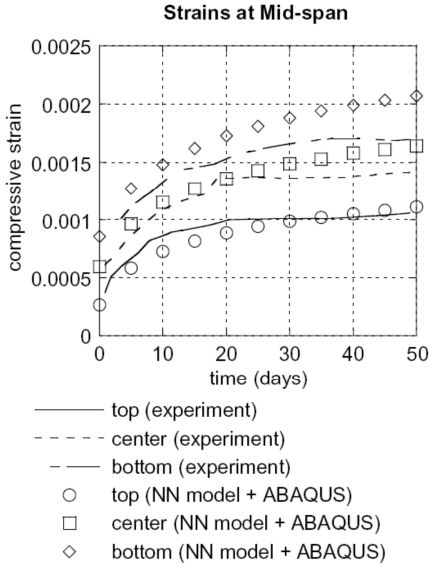

Figure 2.5: Measured and predicted strains at mid-span (Jung and Ghaboussi, 2006a)

The results (Figure 2.5) show that in spite of the considerable differences between the experimental measurements and neural network-based finite element predictions concerning the bottom gauge, an overall reasonable agreement was obtained.
Kessler et al. (2007) presented an implementation of a neural network (ANN) material model in the finite element software, ABAQUS, through its user subroutine VUMAT. They developed a neural network model using a database for 6061 Aluminium under compression and in different temperature conditions. They tried different neural network structures and different input parameters and finally used the following inputs for training of the neural network:

$$\ln(\varepsilon), \ln(\dot{\varepsilon}), \ln(\sigma), \frac{1}{T}, tabular\ data\ of\ flow\ stresses\ and\ strains$$

where ε and $\dot{\varepsilon}$ are strain and strain rate parameters respectively, σ is stress, and T is temperature. VUMAT was used to implement the developed neural network model in ABAQUS to conduct the finite element analysis and the results were compared with those from two conventional material models embedded in ABAQUS: power law model and tabular data. The results showed that the neural network-based finite element model provided more accurate predictions than the others. Besides, some parameters needed to be defined a priori in the case of conventional models, while no parameter identification was required in the neural network modelling technique. No explanation of the procedure through which the models were implemented in the finite element analysis using ABAQUS is provided in Kessler et al. (2007).
Utilizing numerical techniques including finite element and discrete element methods for numerical modelling of neural network-based constitutive models and developing rate-dependent ANN models with the capability of jointing with commercial finite element analysis software (ABAQUS) using UMAT and VUMAT subroutines has been a remarkable improvement to numerical artificial intelligence modelling. However, the black box nature of neural network-based constitutive modelling still limits its applications in engineering practice.

2.3.6 Neural network-based constitutive modelling of FRPs

A neural network based constitutive model for fibre reinforced polymeric (FRP) composites was proposed by Haj-Ali and Kim (2007). Four different combinations of neural network models were considered in this study. Off-axis compression and tension tests were conducted with coupons cut from a monolithic composite plate manufactured by pultrusion process to obtain the required data for training the neural network models. The parameters considered as inputs of the neural network were σ_{11}, σ_{22}, τ_{12} and the outputs were inelastic or total strains; which created the four different combinations. Good agreement was reported between the experimental results and the neural network predictions. A notched composite plate with an open hole was tested to evaluate the developed finite element model using the created neural network model. ABAQUS user subroutine was used to implement the neural network model in the finite element analysis. Comparison of the finite element analysis result with the experimental data for an arbitrary point where the response of the structure was linear revealed that the model was able to predict the linear behaviour of the composite; however, a small diversion of predicted results from the experimental data was observed as the strains increased. The results were not compared at any point around the hole where the behaviour was expected to show nonlinearity. A parametric study could also be useful to show contributions of involved input parameters; however, this is not very practical due to black-box nature of neural networks.

2.3.7 Recurrent neural network-based models

Najjar and Huang (2007) used a recurrent neural network to develop a model to simulate the behaviour of clay under plane strain loading conditions. The results showed that the developed model was capable of assessing the effect of strain rate and stress history on the behaviour of the clay being studied. However, according to the authors, the model cannot be used to solve boundary value problems directly. This problem could be addressed if the authors could have more clear insight into the developed constitutive model. A sensitivity analysis could help find the most and least effective parameters and removing the ineffective parameters and emphasizing on the key ones could lead to development of better models, but the black box nature of ANNs limits the user access to only the weight matrices and biases which are not easily interpretable.

2.3.8 Neural network-based models for materials under cyclic loading

Yun et al. (2008a) and Yun et al. (2006a) used a neural network approach for modelling the cyclic behaviour of materials including hysteresis. In the investigation of the hysteric behaviour of materials, one strain value may correspond to more than one stress and this could potentially prevent neural network from learning the hysteretic and/or cyclic behaviour of materials properly. Yun et al. (2008a) and Yun et al. (2006a) introduced two new internal variables (additional input parameters) to the neural network based material model to help ANN learn the hysteretic and/or cyclic behaviour of materials. The structure of the neural network was as follows:

$$\sigma_n = \hat{\sigma}_{NN}(\varepsilon_n, \varepsilon_{n-1}, \sigma_{n-1}, \xi_{\varepsilon,n}, \Delta\eta_{\varepsilon,n}) \qquad 2\text{-}6$$

where ε_n, is the current strain; ε_{n-1}, is the previous state of strain, σ_{n-1}, is the previous state of stress, σ_n is the current stress, and $\xi_{\varepsilon,n}$, and $\Delta\eta_{\varepsilon,n}$ are additional internal parameters defined as:

$$\xi_{\varepsilon,n} = \sigma_{n-1}\varepsilon_{n-1} \text{ and } \Delta\eta_{\varepsilon,n} = \sigma_{n-1}\Delta\varepsilon_n \qquad 2\text{-}7$$

The developed constitutive model was implemented into the ABAQUS software using the UMAT subroutine. The material tangent stiffness matrix was defined as:

$$\boldsymbol{D}^{ep} = \frac{\partial({}^{n+1}\Delta\sigma)}{\partial({}^{n+1}\Delta\varepsilon)} \qquad 2\text{-}8$$

where ${}^{n+1}\Delta\sigma = {}^{n+1}\Delta\sigma - {}^{n}\Delta\sigma$ and ${}^{n+1}\Delta\varepsilon = {}^{n+1}\Delta\varepsilon - {}^{n}\Delta\varepsilon$. Three sets of data were used to evaluate the neural network-based material model two of which were real experimental data and the third one was a simulated data set. Data from a cyclic test on a plain concrete sample were first used to train a neural network-based material model (Equation 2-6). The neural network model predictions, experimental data as well as the results from an analytical model are presented in the following figure:

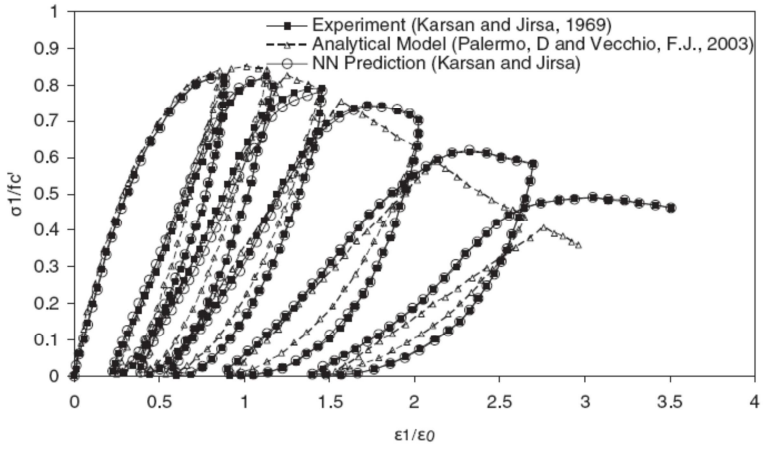

Figure 2.6: Neural network model simulation results against analytical model predictions and experimental data (Yun, Ghaboussi and Elnashai, 2008a)

The developed neural network model was also exposed to a new (previously unseen) series of data in order to evaluate the generalisation capabilities of the model. The results are presented in Figure 2.7.

As the second example, two experimental data sets from two different steel beam-column connections were used to train and validate another neural network based model to predict the cyclic behaviour of the material. In none of the above examples the neural network-based material models were implemented into finite element analysis. The third example was a three-floor building modelled using the finite element software ABAQUS. In this example, the Lemaitre-Chaboche model was used as the material model. Data were extracted and used to train another neural network model the structure of which was presented as:

$$\left\{{}^{n+1}\sigma_{11};\ {}^{n+1}\sigma_{22};\ {}^{n+1}\sigma_{12}\right\} = \hat{\sigma}_{NN}({}^{n+1}\varepsilon_{11};\ {}^{n+1}\varepsilon_{22};\ {}^{n+1}\varepsilon_{12};\ {}^{n}\varepsilon_{11};\ {}^{n}\varepsilon_{22};\ {}^{n}\varepsilon_{12};\ {}^{n}\sigma_{11};\ {}^{n}\sigma_{22};\ {}^{n}\sigma_{12};\ {}^{n+1}\varsigma_{\varepsilon,11};\ {}^{n+1}\varsigma_{\varepsilon,22};\ {}^{n+1}\varsigma_{\varepsilon,12}) \qquad 2\text{-}9$$

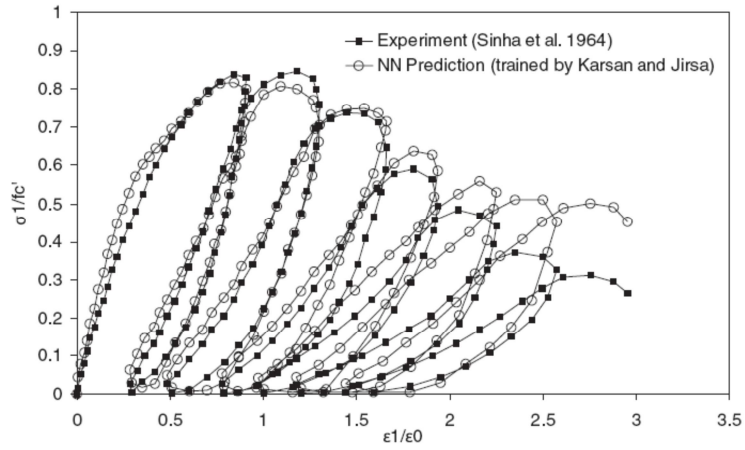

Figure 2.7: Neural network model predictions on an unseen data set (Yun, Ghaboussi and Elnashai, 2008a)

where $\varsigma_{\varepsilon,n} = \xi_n + \Delta\eta_{\varepsilon,\mathrm{n}}$ is an additional input parameter (similar to and a combination of the two previously introduced internal variables in previous examples). The developed neural network model was incorporated into a non-linear finite element analysis code and was used as the constitutive model to make predictions on the cyclic behaviour of the beam sections. Comparison of the results revealed an acceptable agreement of the neural network-based finite element analysis predictions with the original data despite minor differences at some points where comparisons were made.

The neural network model developed by Yun et al. (2008a) and Yun et al. (2006a) to predict the behaviour of materials under cyclic loadings for beam-column connections was extended by Yun et al. (2008b) by adding some other mechanical and design input parameters. The structure of this neural network model is:

$$M_n = \widehat{M}_{NN}(\theta_n, \theta_{n-1}, M_{n-1}, \xi_{\theta,n}, \Delta\eta_{\theta,n}, \mathcal{G}_i(DV_1, \dots, DV_j)) \qquad 2\text{-}10$$

where n represents the nth loading (or time) step, θ and M represent the rotational displacement and moment respectively and $\xi_{\theta,n}$=$M_{n-1} \times \theta_{n-1}$ and $\Delta\eta_{\theta,n} = M_{n-1} \times \Delta\theta_n$ are the two additional internal variables used to accelerate the learning of neural network of hysteretic behaviour. $\mathcal{G}$(DV$_1$... DV$_j$) is also the ith mechanical parameter which is a function of design variables (DV).
In order to validate the proposed neural network model, two different types of connections including extended-end-plate (EEP) and top-and-seat-angle with double web-angle (TSADWA) connections, were considered and exposed to cyclic and earthquake loading conditions. ABAQUS was used for the numerical simulation. The developed synthetic data were then used to develop a neural network model for the extended-end-plate connection. Depth of the beam (d_b), thickness of the end plate (t_p) and diameter of the connecting bolt (f_b) were used as design variables.

$$M_n = \widehat{M}_{NN}(\theta_n, \theta_{n-1}, M_{n-1}, \xi_{\theta,n}, \Delta\eta_{\theta,n}, \mathcal{G}(d_b, t_p, f_b)) \qquad 2\text{-}11$$

In case of the top-and-seat-angle with double web-angle connection type, real experimental data were available and employed to train and validate the neural network material model. In spite of some discrepancies, in both cases good agreement between the neural network model predictions and actual data was observed.

Kim et al. (2010) presented a comparison between two different approaches for modelling of steel beam-to-column connections. The first approach investigated was a component-based model where all components of connection were idealized by assuming one-dimensional springs. Constitutive relationships defining the behaviour of every spring were defined in to represent the actual and comprehensive response of a joint (Figure 2.8).

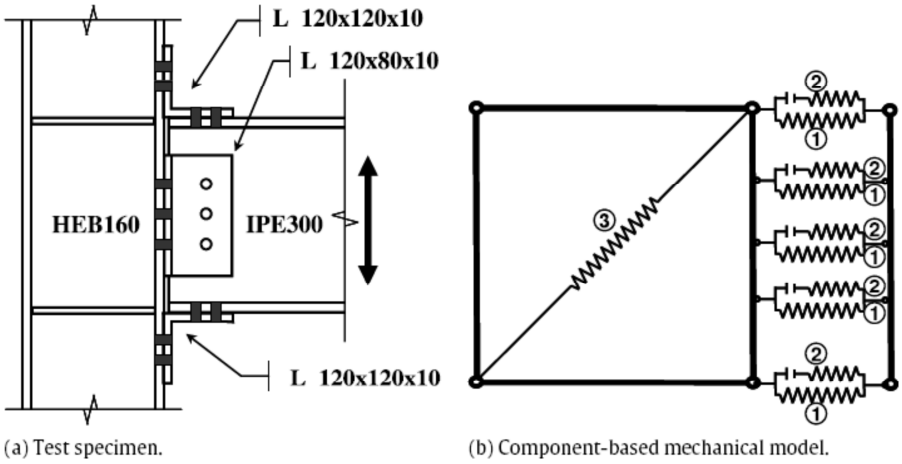

Figure 2.8: A top-and-seat angle connection with double web angles, actual and idealized (Kim, Ghaboussi and Elnashai, 2010)

Two experimental data sets from literature, (Calado et al. (2000) and Kukreti and Abolmali (1999)), were used to validate the proposed component-based modelling approach. Comparison of the experimental and component-based model results for both examples are shown in the following figures (Figures 2.9 and 2.10).

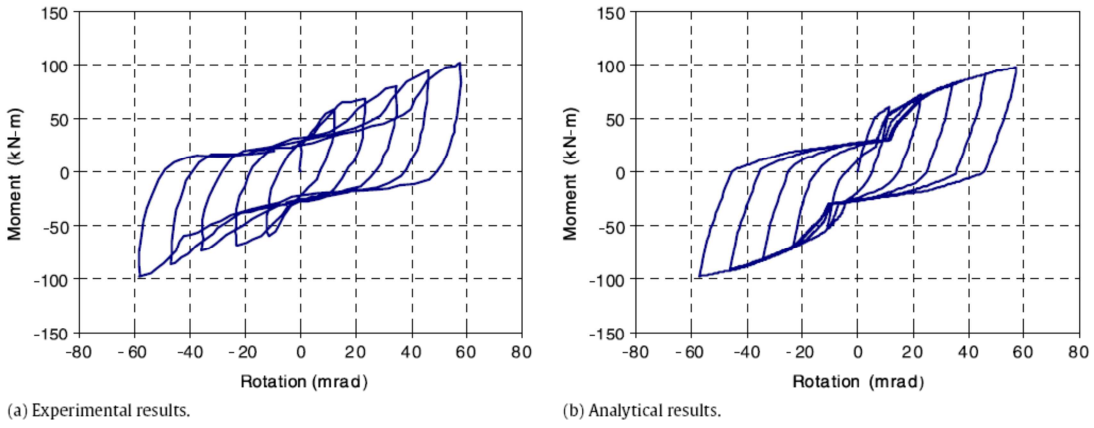

Figure 2.9: Experimental and analytical hysteretic responses for the case suggested by Calado et al. (2000)

It can be seen that the component-based model has been capable of predicting the general behaviour of the connection; however, predicting every detail does not seem to be possible using this methodology.

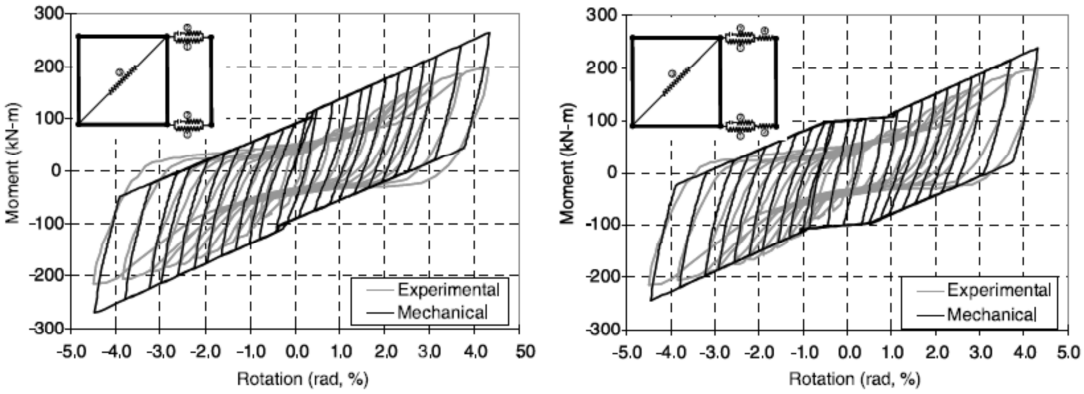

Figure 2.10: **Comparisons of experimental and analytical results for the case suggested by Kukreti and Abolmali (1999)**

As the second approach, the nonlinear hysteretic neural network model proposed by Yun et al. (2008a) was employed to model the stress-strain behaviour of the connections. The neural network-based model was first verified using the synthetic data which were generated using the Ramberg-Osgood model. The proposed neural network-based approach was also applied to two experimental data cases to provide further verification to the component-based model.

Comparison of the results of the proposed neural network based model with the experimental data showed that the neural network model is able to predict the overall pinched hysteretic loops with a better accuracy than the component-based model. A third approach which was a combination of the two approaches proposed earlier in their study was proposed by the authors for future investigation. The third suggested approach would involve the most effective mechanical and informational aspects of the complex behaviour of connections.

Neural networks were used to develop models for materials and connections under cyclic and hysteretic loading; however the problem with the proposed neural network models for connections was that the models were limited to prediction of the global responses of the joints and were not able to represent the contribution of individual components and therefore could not provide the user with an insight into the underlying mechanics of the components.

2.4 Auto-progressive and self-learning neural network and its application in constitutive modelling

2.4.1 Auto-progressive approach

Ghaboussi et al. (1998) proposed a methodology, called auto-progressive approach, for training neural network material models. In this approach the acquired information from a global load-deflection response of a structural test was used as data for training the neural network model. Neural networks require large number of data lines to be able to capture and learn the material behaviour and model the material response. It is usually not possible to obtained comprehensive data from a single test on one sample of the material. The proposed approach was based on the fact that a structural test contains a large and diverse amount of data (e.g., different patterns of stresses and strains) that can be used for training of the neural network. In this methodology an iterative non-linear finite element analysis of the test specimen was implemented to extract and gradually improve the stress-strain data for training of the neural network. This approach needs

data from structural tests to be defined a priori which may not be available in some practical cases.
Sidarta and Ghaboussi (1998) used the auto-progressive training technique to develop a neural network-based constitutive model for modelling geotechnical materials. They used a non-uniform material test, a triaxial test with end friction, which provides non-uniform distribution of stresses and strains. The measured boundary forces and displacements obtained from this test were implemented into a finite element model of the test in order to generate the input and output data for training the neural network material model using the auto-progressive methodology.

2.4.2 Self-learning finite element method

Shin and Pande (2000) also presented a self-learning finite element code with an implemented neural network based constitutive model which was considered to replace the conventional material models. The proposed methodology was similar to the auto-progressive approach proposed by Ghaboussi and his co-workers (Ghaboussi et al., 1998). Two boundary value problems were considered including a two-bar structure in which one of the bars was constructed from an ideally plastic or a strain softening material and the other was linear elastic. For the non-linear bar, the load-deformation data was generated artificially using analytical relationships and were used for training of the neural network-based constitutive model. In the second example a plane stress panel of linear elastic material under vertical point loading from top was simulated. The displacements at a number of points were extracted from the analysis and used to train a neural network-based constitutive model. It was shown that the positions of monitoring points could affect the training of the neural network and consequently the convergence of the predictions of the developed neural network model towards the standard solutions. The position of the loading was also changed in order to show that the neural network-based model has been trained enough to be used in analysis of any boundary value problem in which the material law corresponds to the trained neural network model.
Another approach was suggested by Shin and Pande (2001) to construct the tangential stiffness matrix of the material. This methodology used partial derivatives of the neural network-based constitutive model which was developed based on total stress and strain data. The developed stiffness matrix was incorporated into a self-learning finite element code developed by the authors and the developed finite element model was validated by application to analysis of a rock specimen with fixed ends under uniaxial cylindrical compression.
Shin and Pande (2003) also used the self-learning neural network-based finite element code to identify elastic constants for orthotropic materials from a structural test. They proposed a two-step methodology. In the first step, the measured data from analysis of a structure were used to train a neural network model which was implemented into a finite element code. In the next step, the trained neural network-based constitutive model was used to construct the constitutive stiffness matrix using the following equation to obtain the material elastic parameters.

$$D_{NN} = DNN_{ik}(\varepsilon_i, \sigma_k) = \frac{\partial \sigma_k}{\partial \varepsilon_i} \qquad 2\text{-}12$$

Figure 2.11 shows the inputs and outputs of the developed neural network model and its optimal structure. Strain vectors were considered as the inputs of the developed model and the stress vectors were the outputs.

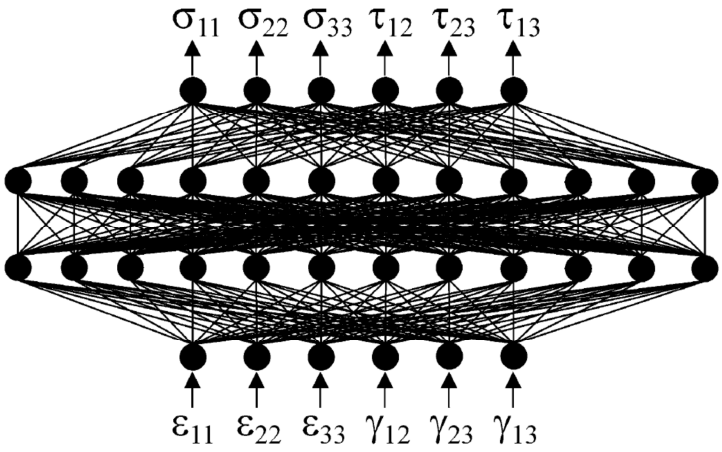

Figure 2.11: Structure of the neural network based constitutive model (Shin and Pande, 2003)

The same methodology was then applied to the case of a plane stress problem involving a panel with a circular hole located in its centre subjected to compression. Synthetic structural test data, including displacements obtained from 66 nodes at 5 loading stages from finite element analysis of the panel with assumed values for the nine independent orthotropic elastic constants, were used as the training data. The material showed linear elastic behaviour and after 3cycles of self-learning a good agreement was obtained with target results used as reference. The predicted orthotropic elastic constants were also in good agreement with the reference values. The nine elastic constants were:

$$E_x, E_y, E_z, G_{xy}, G_{yz}, G_{xz}, \nu_{xy}, \nu_{yz}, \nu_{xz}$$

The neural network-based stiffness matrices were not symmetric and altogether 36 elastic constants were achieved. The off diagonal terms were averaged to symmetrise these matrices. A relatively large number of nodes were needed to monitor the displacements of a structure with a relatively simple geometry and simple linear elastic behaviour. This could mean that in the case of more complicated and nonlinear problems using this method could suggest some limitations.

Hashash et al. (2003) considered a braced excavation and used measured lateral deflections of the walls and settlements of the surface of the structure in different construction stages to extract and capture the constitutive behaviour of the soil using the auto-progressive approach. They obtained synthetic data for training of the neural network model by simulating the excavation problem using the finite element method. The constitutive model used for the soil in the simulation stage in the finite element analysis was the modified cam clay model. Two finite element models of the problem were prepared in order to start the auto-progressive procedure. The first one was used to simulate soil removal and installation of the bracing at n^{th} stage of excavation and the second one was implemented to apply monitored deformations of the same excavation stage. The first finite element model and the second one were used to obtain stresses and strains respectively and the stress-strain pairs were used to train a neural network based soil model. At the very beginning of the model development procedure the material behaviour was totally unknown and the two finite element models were used to initialise with developing the neural network-based model representing the linear elastic

behaviour. The procedure was repeated until the entire excavation stages were simulated. At the end of the process, a neural network-based material model, which was trained with a comprehensive set of data, was created through the iterative process. Comparison of the results showed that the methodology proposed in this paper was capable of capturing the behaviour of the material from a series of finite element analyses of the excavation model and the incrementally learning from field observations.

Hashash et al. (2004b) proposed a general and systematic procedure for probing constitutive models. The following general strain probe equation, composed of all six independent components of the strain tensor, was implemented to explore the constitutive model behaviour:

$$\sqrt{(\Delta\varepsilon_{11})^2 + (\Delta\varepsilon_{22})^2 + (\Delta\varepsilon_{33})^2 + (\Delta\varepsilon_{12})^2 + (\Delta\varepsilon_{23})^2 + (\Delta\varepsilon_{31})^2} = r_{\Delta\varepsilon} \qquad 2\text{-}13$$

True triaxial strain probe (TTSP) and plane-strain strain probe (PSSP) were considered as two specific cases of probing to investigate the application of the above equation in studying material behaviour. Von Mises, Modified Cam Clay, and MIT-E3 (an elasto-plastic constitutive model for overconsolidated clays) were used as three different models to demonstrate the true triaxial probing procedure. In case of the plane strain probing an artificial neural network model was considered. The proposed neural network model was trained using the auto-progressive algorithm in a braced excavation problem using MIT-E3 constitutive model. The neural network based model showed a good performance and provided good predictions of the surface settlements and lateral displacements concerning the excavation problem. But, at the time of implementing the probing procedure to find the yield loci of the neural network model, it was revealed that the neural network model had not been able to capture the correct shape of the loci; however, the overall size of the response surface was similar to MIT-E3 model. Although the data were generated synthetically using the results of FE analysis the authors claimed that the reason for this (model not capturing the correct shape of the loci) can be the lack of training data available for neural network model development.

2.4.3 Self-Sim methodology

Hashash et al. (2006a) introduced Self-Sim (self-learning simulation) methodology. They described the newly suggested procedure as a software analysis framework to implement and extend the auto-progressive algorithm. The modelling procedure and steps of the suggested Self-Sim methodology were the same as the auto-progressive method introduced by Ghaboussi et al. (1998) and Hashash et al (2003). The performance of the Self-Sim technique was validated using a simulated excavation case history. Synthetic data (including lateral wall deflections and surface settlements) obtained using a finite element model employing the MIT-E3 as soil constitutive model were used to train the neural network. Results from five example problems, including three numerical examples and two actual case histories, were used to validate the capabilities and performance of Self-Sim in predicting the behaviour of a deep excavation. The results showed that the proposed methodology was able to help obtain sufficient data on behaviour of the soil and the models developed using this methodology were able to predict the soil behaviour with acceptable accuracy.

Hashash et al. (2006b) used load-displacement measurements along with their suggested Self-Sim methodology to characterize the constitutive behaviour of granular materials in general and a particular case of extra-terrestrial soil. The steps suggested for Self-Sim

presented in this work (Hashash, Ghaboussi and Jung, 2006b) are the same as Hashash et al (2006a). They assumed an in-situ test being conducted on an extra-terrestrial soil in which the applied load and resultant deformation were being recorded. Two finite element models were created for the considered domain and the measured loads and displacements in each case were applied to the models in an incremental manner. Stresses were obtained from the first model where measured loads were applied. Measured displacements and the compatibility principal were used to obtain strains using the second finite element model. As all the measurements could be taken in situ, the acquiring and transferring process of extra-terrestrial soils, which would be an expensive process, was avoided. Additionally, as in the Self-Sim methodology no priori assumptions are needed for developing constitutive relationship for materials, this methodology can be considered as a strong alternative that can be used to investigate the behaviour of unknown and new materials like extra-terrestrial soils.

2.4.4 Auto-progressive algorithm for rate dependant material models

Jung and Ghaboussi (2006b) presented an extended version of the auto-progressive algorithm which included rate dependant material models. In the new auto-progressive algorithm, rates of stresses and strains were also measured from finite element simulation models. To validate the proposed methodology a hypothetical cylinder with variable diameter, made of a visco-elastic material was considered (Figure 2.12).

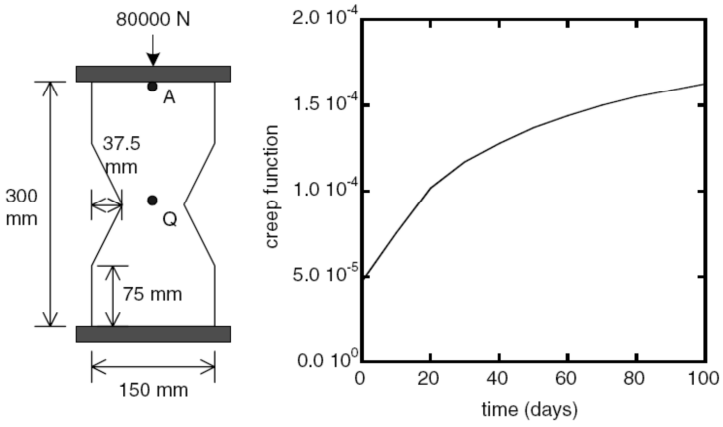

Figure 2.12: Structure of the simulated experiment and the implemented creep function (Jung and Ghaboussi, 2006b)

The structural test shown in **Error! Reference source not found.** and its global response was used to develop a neural network-based rate dependant material model which was then employed to solve a new boundary value problem. An important aspect of the neural network-based model was that it was capable of learning the effects of time step. If the neural network based model was trained using only one time step, its predictions for other time steps would be poor ((Jung and Ghaboussi, 2006a); (Jung and Ghaboussi, 2006b)). Considering this fact Jung and Ghaboussi (2006b) suggested the model to be trained using different time step data. The methodology was applied to the results from actual experiments with the aim of capturing the non-linear creep behaviour of a super alloy.

Aquino and Brigham (2006) also employed the auto-progressive or self-learning finite element methodology to develop a neural network-based thermal constitutive model. Similar to the previous applications of this methodology, the main steps followed were

pre-training or initialising of the neural network model, developing and using two simulated finite element models, and training the neural network material model.
In order to verify the capabilities of the proposed methodology a steel plate with a prescribed heat flux on one side and 100 ˚C temperature as boundary condition on the other three sides was simulated (Figure 2.13).

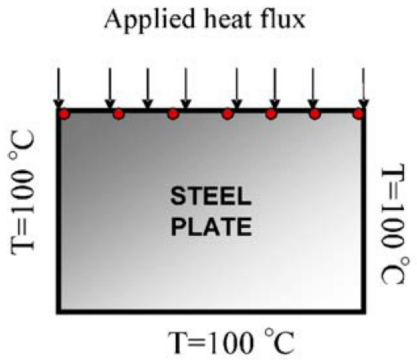

Figure 2.13: Simulated steel plate experiment (Aquino and Brigham, 2006)

This experiment was simulated numerically to generate synthetic data. A random noise was introduced into the simulated data to evaluate the stability of the self-learning finite element-based methodology. Three test cases were considered. The self-learning algorithm started with pre-training of a neural network model by generating random temperature, temperature gradient, and also their corresponding heat flux data using the Fourier law. Two finite element models were eventually created. The temperature and temperature gradient data were extracted from the second finite element model and were used as inputs, and the heat flux vectors were extracted from the first finite element analysis and were used as outputs. The neural network model was trained using the generated data and the inputs and outputs of the model were:
Inputs: $\frac{\partial T}{\partial x}$, $\frac{\partial T}{\partial y}$, $and\ T$
Outputs: J_x, J_y
where: $\frac{\partial T}{\partial x}$, $\frac{\partial T}{\partial y}$ are gradients in x and y directions respectively and T represents temperature. J_x, and J_y are heat flux vectors in x and y directions.
The results showed that the self-learning methodology was able to help develop neural network thermal constitutive models using noisy data.
Modelling time-dependant behaviour of concrete at the time of construction of a segmental bridge was investigated by Jung et al. (2007) using the previously introduced Self-Sim methodology. They used Self-Sim to develop neural network models using stresses, strains, and their corresponding rates from early stages of construction to predict future stress-strain states of the structure as the construction continued. The proposed methodology was used to analyse Pipiral Bridge, a concrete segmental bridge that was built employing the balanced cantilever method in Colombia. The neural network model used in this application had 2 hidden layers, each layer made of 14 nodes, 7 inputs and 1 output parameter (Figure 2.14).

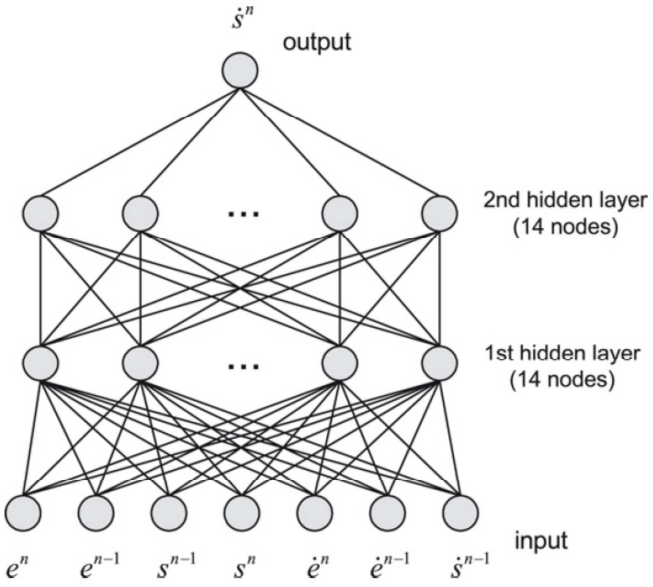

Figure 2.14: Rate-dependent neural network material model (Jung, Ghaboussi and Marulanda, 2007)

The input and output parameters for the neural network model were considered to be:

$$\dot{s}^n = \dot{s}^n NN(e^n, e^{n-1}, s^{n-1}, s^n, \dot{e}^n, \dot{e}^{n-1}, \dot{s}^{n-1}) \qquad 2\text{-}14$$

where $s = \sigma - \delta\ \sigma_v/3$, $e = \varepsilon - \delta\ \varepsilon_v/3$. The superscripts *n* and *n-1* represent the current and the previous time steps.
The proposed constitutive equation was iteratively solved using the following equation:

$$s^n = s^{n-1} + \Delta t \times NN(e^n, e^{n-1}, s^{n-1}, s^n, \dot{e}^n, \dot{e}^{n-1}, \dot{s}^{n-1}) \qquad 2\text{-}15$$

The current strain state together with previous states of other parameters, were obtained from the results of finite element analyses and the rate-dependent neural network model was used to predict the creep of concrete.
Two different implementations of the Self-Sim methodology were proposed to predict the deflection of a segmental bridge (Figure 2.15). In the first approach, when a construction case had a repetition of many cantilevers, the first two cantilevers were used to calibrate the neural network model and the remaining ones were predicted using the calibrated neural network model. In the second approach the neural network-based model had already been trained using data from earlier segments and was used to predict the deflections of the remaining segments in the same cantilever. However it should be noted that data mining based models like the ones developed using neural networks cannot be relied on 100% when they are used to make predictions beyond the range of data that they have experienced during the training phase. The authors (Jung, Ghaboussi and Marulanda, 2007) suggested adding previously obtained data from other resources like data from laboratory tests, field measurements and synthetic data generated using conventional constitutive models to their current database in order to improve the prediction capabilities of the proposed Self-Sim methodology and possibly predicting the deflections of the remaining segments.

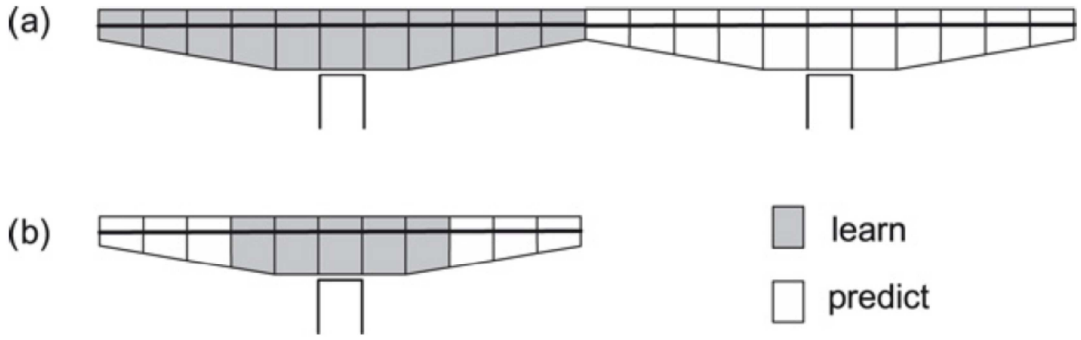

Figure 2.15: (a) learn from the current cantilever and predict deflections of the remaining cantilevers (b) learn from the earlier segments and predict the deflections of the remaining segments (Jung, Ghaboussi and Marulanda, 2007)

Fu et al. (2007) and Hashash et al. (2006c) implemented the Self-Sim methodology to develop constitutive models for soils based on laboratory test data. They applied the methodology to two simulated laboratory tests including a triaxial compression test and a triaxial torsional shear test. A neural network-based constitutive model was developed using the extracted soil data from the laboratory test simulations to represent the behaviour of the soil. The developed model was then used to predict the load-settlement behaviour of a simulated strip footing.

Yun et al. (2008c) and Yun et al. (2006b) used self-learning simulation to model the cyclic behaviour of beam-column connections in steel frames. They used a similar neural network model to the one presented by Yun et al. (2008a) and (2008b) for predicting the cyclic and hysteretic behaviour of beam-column connections. The structure and input and output parameters of the neural network model were as:

$$M_n = \widehat{M}_{NN}(\theta_n, \theta_{n-1}, M_{n-1}, \xi_{\theta,n}, \Delta\eta_{\theta,n}) \qquad 2\text{-}16$$

where $\xi_{\theta,n} = M_{n-1}\theta_{n-1}$ and $\Delta\eta_{\theta,n} = M_{n-1}\Delta\theta_n$ are two internal variables, M=moment, θ=rotation, $\widehat{M}_{NN}$: $R^5 \rightarrow R$ is the functional mapping to be established through neural networks. n indicates n^{th} time (or loading) step. An intuitive description of the two internal variables is presented in the following figure.

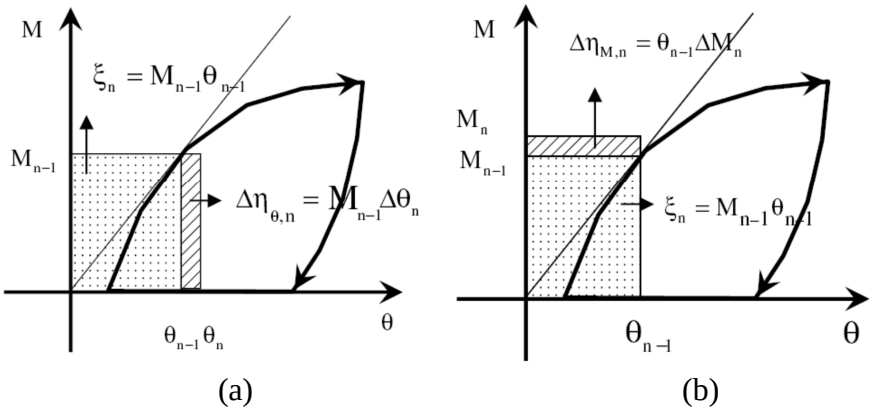

Figure 2.16: Internal variables defined for the neural network based cyclic connection model: (a) displacement control form and (b) stress resultant control form (Yun, Ghaboussi and Elnashai, 2008c)

The following equation was used to obtain tangential stiffness from the neural network-based model for the connection.

$$\mathbf{K} = \frac{\partial \Delta \mathbf{M}}{\partial \Delta \boldsymbol{\theta}} \qquad 2\text{-}17$$

where $\Delta \mathbf{M} = {}^{n+1}\Delta \mathbf{M} - {}^{n}\Delta \mathbf{M}$ and $\Delta \boldsymbol{\theta} = {}^{n+1}\Delta \boldsymbol{\theta} - {}^{n}\Delta \boldsymbol{\theta}$

The self-learning simulation methodology presented by Yun et al. (2008c) was enhanced with a new algorithmic formulation suggested for the neural network-based cyclic material model. Numerically simulated data as well as actual data were used to validate the improved self-learning simulation method presented for prediction of cyclic behaviour of connections. As mentioned above, in the Self-Sim methodology, in the second step of the modelling procedure, two finite element models (A, B) run parallel to each other to update and improve the neural network based material model. From models A and B, force and displacement values are obtained respectively and are applied as stress strain pairs to train the neural network model. At each load step (or time step), two FE analyses (FEM-A and FEM-B) are performed: in the FEM-A, the measured forces are applied; and, in the FEM-B, the measured displacements are enforced. The local stress resultant vector at the connections from FEM-A represents acceptable approximation of the actual stress resultant vector. The local displacement vector from FEM-B is considered to be a good approximation of the actual displacement vector. Two different cases were considered to construct the stiffness matrices based on the FEM-A and FEM-B as shown in Figures 2.17 and 2.18.

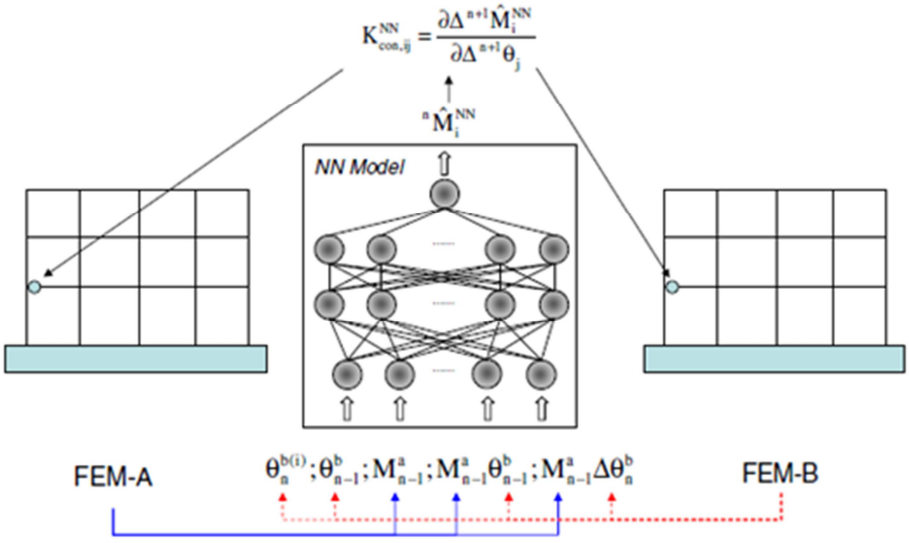

Figure 2.17: Case I: Algorithmic tangential stiffness formulation during the self-learning simulation process (Yun, Ghaboussi and Elnashai, 2008c)

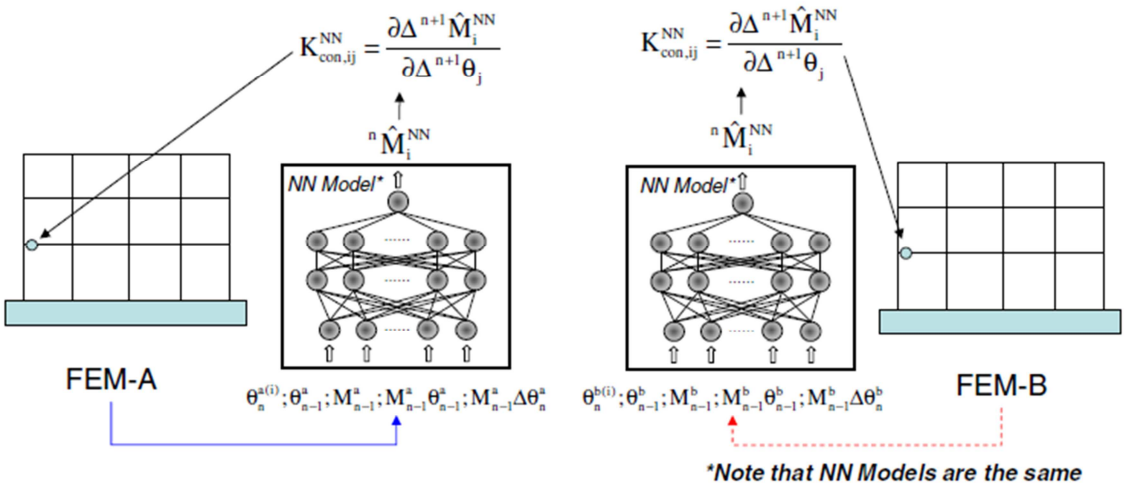

Figure 2.18: Case II: Algorithmic tangential stiffness formulation during the self-learning simulation process (Yun, Ghaboussi and Elnashai, 2008c)

Yun et al (Yun, Ghaboussi and Elnashai, 2008c) showed that the neural network-based model from case I provides a better prediction in comparison to case II for the examples presented in their paper.

Hashash and Song (2008) implemented the self-learning simulation (Self-Sim) technique to capture and predict behaviour of soils through neural network models. They presented three different examples including a triaxial test with frictional loading plates, deformation due to deep excavations and site response as a result of horizontal shaking. Hashash and Song (2008) showed that the developed model is capable of predicting the soil behaviour with a good accuracy, but as the authors stated, selecting parameters of Self-Sim and neural network is an empirical and important process and requires personal experience. This can be considered as a drawback for the neural network models.

Another application of the Self-Sim methodology in analysis of dynamical behaviour of soils was suggested by Tsai and Hashash (2008). They described the implementation of the Self-Sim methodology and the process of integrating field data measurements and numerical simulations of seismic site responses with the aim of obtaining the underlying cyclic response of soils. They applied the Self-Sim methodology to study one-dimensional seismic site response in steps.

Step 1: The ground responses corresponding to shaking of the base were measured in selected points in different depths in the soil. Base shaking and the obtained measurements were used to make sets of field measurement data. Initially a neural network-based soil model was pre-trained using stress-strain data concerning the linear elastic behaviour over a limited range of strains.

Step 2(a): The initial neural network model was implemented in a FE model and was used to simulate the site response and the acceleration from the deepest point in a downhole array was measured and was applied at the bottom of the soil column. By conducting a dynamic equilibrium analysis, the stresses and strains were computed all along the soil column. Because the base acceleration and the applied boundary forces are accurate, in the Self-Sim approach it was assumed that the computed equilibrium stresses corresponding to the applied boundary forces provide an acceptable approximation of the actual stresses experienced by the soil, but computed strains were discarded because they may not match the expected results.

Step 2(b): In a similar site response analysis approach and using the same neural network model, the measured displacements from a downhole array were applied as additional boundary conditions and stresses and strains were also computed in the soil

column. It was assumed that the applied displacements were accurate and therefore the corresponding computed strains were considered to be an acceptable approximation of the true field strain experienced by the soil.
Stresses and strains obtained from steps 2(a) and 2(b) respectively formed stress-strain pairs that approximate the soil constitutive response. The obtained stress-strain pairs were used to update the neural network based material model through retraining. The entire process was repeated several times using the full ground motion time series until the ground responses similar to the measured ones were acquired. An illustration of the process is presented in the following figure.

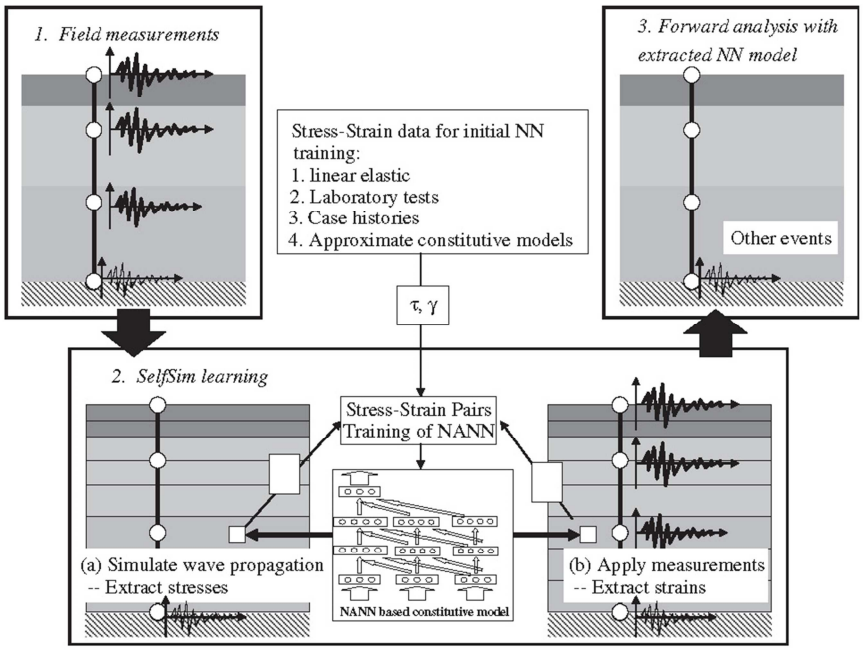

Figure 2.19: Self-Sim algorithm applied to a downhole array (Tsai and Hashash, 2008)

Tsai and Hashash (2008) also applied this procedure to a synthetically generated downhole array data to create models. In order to evaluate the capability of the model in capturing the dynamic behaviour of soils the proposed methodology was applied to three different synthetically created case examples including a single soil layer under a sinusolidal motion, a uniform but multilayer soil profile under seismic motion, and a non-uniform multilayer soil profile under seismic motion. The results from application of the proposed modelling approach revealed that the Self-Sim was able to provide acceptable predictions of the site response in all considered cases. To evaluate the predictive capabilities of the material model created based on individual events, it was assumed that there were two more recordings available. Site response analyses (with FE incorporated NN material model obtained from a given event) were performed using input motions of the other two events. The results showed that in some cases the prediction of surface response is not accurate. The difference between the predated and expected results was because the site response analyses had been experiencing a different range of strains which had not been introduced to the neural network model development procedure at the training stage, as mentioned by Tsai and Hashash (2008). Further to this, the three different individually extracted stress-strain behaviour regarding three different events were combined to create a more comprehensive database to be used to train a new neural network material model with the aim of increasing the accuracy of the predicted results. Comparison of the results revealed that despite the significant difference in one case between the predicted response spectra and

the expected one, the prediction of the new NN material model was improved compared to the previous results (Tsai and Hashash, 2008).

Self-Sim methodology was also used to capture the drained behaviour of sand based on data from triaxial test with fully frictional loading platens (Hashash et al., 2009). Three series of isotropic drained triaxial tests were conducted on different loose, medium, and dense specimens. The triaxial tests were simulated using the finite element method and the Self-Sim approach was used to extract the non-uniform stress-strain behaviour of the material considering external load and displacement measurements. The results of this study showed that the Self-Sim methodology was able to capture the behaviour of the soil specimens accurately. Hashash et al. (2009) mentioned that integration of Self-Sim methodology and laboratory testing can make it possible to use a single laboratory test to generate multiple stress paths, instead of applying the current practice of using a laboratory test for creating only one stress path.

Two different methodologies used for learning the behaviour of deep excavations in urban environment were compared by Hashash et al. (2010). They implemented the genetic algorithm (GA) and Self-Sim methodology to help the neural network learn the behaviour of the soil in a deep excavation. In the first approach a genetic algorithm was implemented to optimise the material parameters of an existing material model, which was the hardening soil model of PLAXIS, and the second approach was including a combination of the finite element method and artificial neural network (ANN) and was employed to capture the behaviour of soil. In this proposed procedure no predefined constitutive models were required. The above mentioned two approaches were used to analyse a case study in Lurie Centre excavation in Chicago, USA. It was observed that GA and Self-Sim were able to reproduce the deformations of the wall reasonably well; however it came out that the hardening soil model implemented into the FE model in the GA approach was not capable of reproducing the magnitude or the shape of the settlement profile behind the wall (Figure 2.20). The graph on the right hand side of the figure shows the settlement of the surface. In this graph the difference between the results of the GA-based approach and the measured values can be easily seen. This difference for results related to Self-Sim seems to be negligible. This can be an indication of the fact that the GA-based approach highly depends on the constitutive model selected and the results would be different if a different soil constitutive model was used in implementing the genetic algorithm approach. Although, considering the left side of the figure both approaches have provided acceptable predictions, it can be easily observed that none of the methods have been able to predict the exact deformations of the wall.

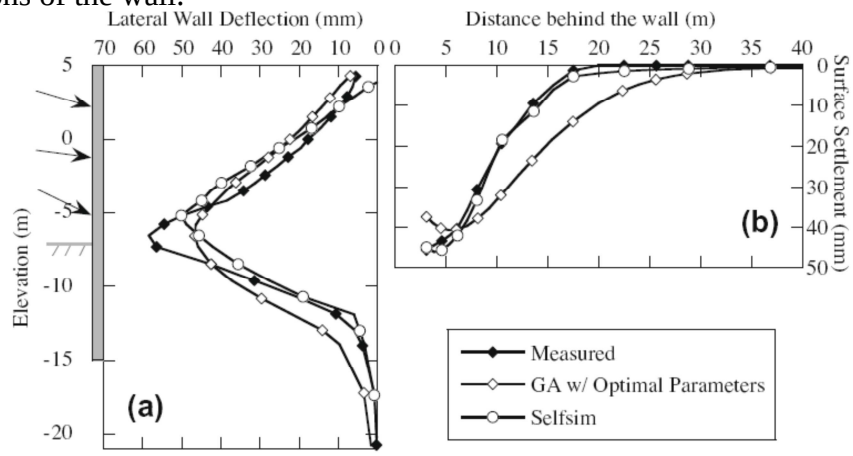

Figure 2.20: Comparison of the computed (a) lateral wall deformations and (b) surface settlements using GA and Self-Sim of the excavation (Hashash et al., 2010)

Jung and Ghaboussi (2010) used the auto-progressive method to train neural network-based constitutive models considering the load-displacement measurements from structural monitoring. After pre-training the neural network model, the method was applied to inverse identification of creep in a concrete beam. The results of the auto-progressive model were then compared to the experimental results (Figure 2.21).

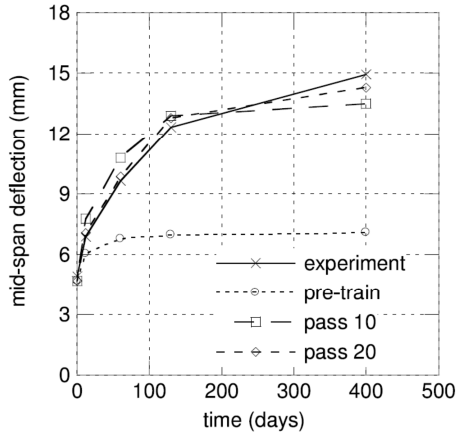

Figure 2.21: Representation of the convergence of mid-span deflections during the auto-progressive training (Jung and Ghaboussi, 2010)

In order to improve the prediction capabilities of the proposed methodology Jung and Ghaboussi (2010) added the shrinkage effect to the neural network model parameters. The results showed that considering shrinkage had an improving effect on the predictions made by the neural network model but this improvement does not seem to be very noticeable (Figure 2.22).

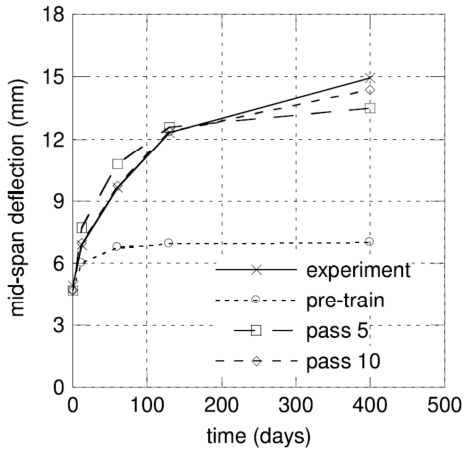

Figure 2.22: Representation of the convergence of mid-span deflections during the auto-progressive training (Jung and Ghaboussi, 2010)

Predicting the long-term behaviour of concrete structures based on their short-term behaviour was also investigated by Jung and Ghaboussi (2010). They used the auto-progressive methodology to conduct this study with not very satisfactory results.

2.4.5 Mathematics and information-based hybrid modelling framework

Ghaboussi et al. (2010) considered the suggestions made by Kim et al. (2010), and developed a hybrid modelling framework utilizing mathematics and information-based methodologies (HMIM). The proposed method combines the mathematical models of engineered systems, which were developed considering physics and mechanical laws, with artificial neural network-based models created using auto-progressive and Self-learning Simulation procedures. In the HMIM, neural networks only keep the information that is presented in the experimental data and the mathematical models are not able to capture them because of their complex nature. The proposed HMIM methodology was applied to modelling of a steel beam-to-column connection. In this example the components of the connection were divided into two parts: (i) Mathematical-based components and (ii) Information-based components. The components in which the underlying mechanics are well-developed are very suitable for the mathematical modelling and these types of models can provide accurate predictions. The remaining components with more complicated behaviour or where there has not been enough investigation to model their behaviour mathematically will lay into the informational modelling category. Kukreti and Abolmaali (1999) conducted an experiment on top-and-seat-angle connection which was exposed to the methodology proposed by Ghaboussi et al. (2010) to evaluate its capabilities. In this connection, the angles and column panel zones were considered as mathematical-based and the slip and ovalisations were assumed to be information-based components. For the calculation purposes, the mathematical-based components were idealized as one-dimensional springs with reliable constitutive equations for every component. In case of the information-based components, the auto-progressive methodology was used to generate neural network-based model. The predictions of the behaviour of the connection under cyclic loading by the presented hybrid model were compared with the ones from an analytical model as well as the experimental results (Figure 2.23). This comparison revealed that the hybrid model was able to predict the behaviour of the considered type of connection better than the analytical method. In this case, in contrary to the normal procedure, the whole data set was used to train the model and it was not divided into training and testing data cases.

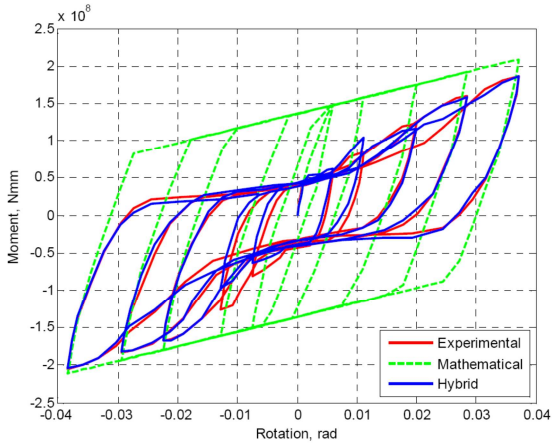

Figure 2.23: Comparison of the predictions of the hybrid and analytical models with the experimental data (Ghaboussi, Kim and Elnashai, 2010)

The effect of different measurement and monitoring instrumentations and their considered locations in an excavation project and also the impact of the quality of

information being extracted for modelling the behaviour of the excavation using the self-learning simulation technique was investigated by Osouli et al (2010). Synthetic data were generated using finite element analysis considering the MIT-E3 constitutive model. The generated data represented measurements from different locations of an excavation project including surface settlement, wall deflection and other data and were used to study the relationship between selecting the suitable field instrumentations and the quality of the material behaviour captured during the learning (training) process. The results showed that considering inclinometers placed behind the wall and also measuring forces in the struts in addition to the measurements of lateral wall deflections and surface settlement can improve the quality of extracted soil behaviour to a great extent. A real case of a deep excavation project in Taiwan was considered to verify the results of this study.

2.4.6 Self-Sim approach for analysing a 3D problem

Hashash et al. (2011) also considered the Self-Sim approach for analysing a three-dimensional deep excavation. They provided a description of the numerical issues concerning the problem, including the problems faced in developing the proposed three-dimensional model. The capabilities of the proposed method in capturing the behaviour of soil using the measured wall deformation and surface settlement from a 3D problem were highlighted.

The new auto-progressive, Self-Sim and mathematics and information-based hybrid modelling framework self-learning methodologies for 2 and 3D problems suggested by Ghaboussi et al. (1998) and (2010), Sidarta and Ghaboussi (1998), Hashash et al. (2006a) and (2011) and Jung and Ghaboussi (2006b), presented in section 2.4, are efficient ways of training neural networks with very little data available and were successfully applied to practical examples. Although these works are major contributions to development of NNCM approach, the main shortcomings of ANN remain unresolved.

2.5 Conclusions

Many researchers have used ANNs as a useful tool for developing constitutive models for different materials as well as models to describe the behaviour of complex engineering systems.

Despite the great capabilities and advantages of the neural network in constitutive modelling of materials and its successful implementation in the finite element and discrete element analysis of different problems, this technique is also known to suffer from a number of shortcomings. One of the negative points that can be considered in a neural network-based modelling system is that the optimum structure of the neural network including number of input layers, hidden layers and transfer functions need to be identified a priori through a time consuming trial and error procedure. Another main drawback of the neural network approach is the large complexity of the structure of the proposed network. This is because the neural network stores and represents the knowledge in the form of weights and biases which are not easily accessible to the user. The lack of interpretability of ANN models has inhibited them from achieving their full potential in real world problems ((Lu, AbouRizk and Hermann, 2001); (Javadi and Rezania, 2009a)). As a matter of fact, neural network-based models do not provide clear and easily accessible information on the way that input parameters affect the output(s) and are considered as a black-box class of modelling methodologies.

In this thesis, a new data mining technique, evolutionary polynomial regression (EPR), is proposed for modelling the complex constitutive behaviour of geomaterials and a number of civil engineering systems. The proposed method overcomes most of the issues and drawbacks associated with neural networks and other previously mentioned material modelling procedures. EPR provides a transparent representation of models in terms of mathematical (polynomial) expressions to describe the complex behaviour of materials / systems and there is no need to provide any prior information to develop the models. A detailed description of the technique is provided and its application in modelling different important aspects of saturated and unsaturated soils and also a number of other geotechnical and civil engineering problems is presented.

Chapter 3

EVOLUTIONARY POLYNOMIAL REGRESSION (EPR)

3.1 Introduction

Developing material models using data mining techniques (and particularly the artificial neural networks) was discussed in the previous chapter. It was shown that these techniques have been able to be trained using experimental and/or numerical simulation data and/or the field measurements to capture and reproduce the material behaviour. It was also shown that these developed models can be implemented in numerical analysis techniques like the finite element method.

Amongst all data mining techniques the artificial neural networks (ANN) and genetic programming (GP) techniques are the most popular and widely used methods. The artificial neural networks make use of many processing elements called neurons. These neurons are connected to each other by links of different weights and all together form a "black box" system called artificial neural network. When large amounts of data exist, artificial neural networks can easily learn and capture very complicated relations between contributing parameters through training with the provided data. A suitably trained network can accurately represent the behaviour of the system. Artificial neural networks are able to model highly complex and nonlinear processes without the need to assume any pre-specified structure for the relationships between considered input and output parameters. Although the artificial neural networks can be considered a robust and capable modelling technique; they also suffer from some drawbacks. The main drawback of ANNs is that the structure of a neural network including model inputs, transfer functions, number of hidden layers and their neurons should be identified a priori. Another disadvantage is that the structure of ANN is generally very complex and the acquired knowledge is represented in the form of weight matrices and biases which are not easily accessible to the user and any engineering judgment on the developed models remains very difficult. Over-fitting problem is also another issue with artificial neural network-based modelling techniques (Giustolisi and Savic, 2006; Giustolisi and Laucelli, 2005).

Genetic programming (GP), another popular and extensively used modelling approach, is also an evolutionary based computing method and generates structured representation of the considered system. Koza (1992) proposed a symbolic regression based genetic

programming methodology which has been used very frequently with interested researchers since then. GP develops mathematical expressions with the aim of fitting a set of data points using the evolutionary process which is the nature of genetic programming. Similar to most other evolutionary modelling techniques, populations of solutions, which are mathematical expressions in case of genetic programming, are manipulated by symbolic regression using operations very much like the evolutionary processes that are already on operation in nature. The genetic programming methodology imitates the natural selection at the time that the 'fitness' of the solutions in the available population improves through successive generations. Due to the nature of the genetic programming technique global explorations is possible and the user is able to obtain more information on the behaviour of the system. In other words by using this technique the user is able to gain an insight into the way that the input and output parameters are related. Despite very distinct advantages, the genetic programming technique is also known to suffer from some shortcomings and limitations. Previous research works have proven that this technique is not very powerful in finding constant values and it also tends to produce functions that grow in length over time (Giustolisi and Savic, 2006).
The Evolutionary Polynomial Regression (EPR), a new data mining technique, is introduced in this chapter with the advantage of overcoming some problems associated with artificial neural networks and genetic programming. EPR is a two-stage process that uses a combination of Genetic Algorithm (GA) and Least Square (LS) regression. In EPR an evolutionary searching method is used to find the exponents of polynomial expressions using a genetic algorithm engine and the parameters of the model are determined using the least squares method (Giustolisi and Savic, 2006).

3.2 Evolutionary algorithms

In artificial intelligence-based methodologies optimal solutions are searched for and found from among a finite set of solutions by implementing evolutionary algorithms (EAs). The main idea behind evolutionary algorithms / techniques is to mimic natural evolutions and their corresponding aspects like mutation, selection, and crossover in generating solutions to optimization problems (Faramarzi, 2011). Two most commonly used evolutionary algorithms are genetic algorithm (GA) and genetic programming (GP). A brief description of genetic algorithm is presented below as it is a part of the suggested evolutionary technique in this thesis.

3.3 Genetic algorithm (GA)

Genetic algorithms are search algorithms based on the mechanics of natural selection and natural genetics. Genetic algorithms are combination of the survival of the fittest between string structures together with a randomized (but controlled and structured) information exchange to create a search algorithm with some of the innovative styles of human search (Doglioni, 2004). Genetic algorithms seek to maximize the fitness of the population by selecting the fittest individuals, based on Darwin's theory of survival of the fittest, and using their genetic information in mating and mutation operations to create a new population of solutions. Although the process involves randomized operations, however genetic algorithms are not simple random walk. Genetic algorithms utilize historical information in an efficient way to find new search points with expected

improved performance. Genetic algorithms have been developed by John Holland and his co-workers in the University of Michigan (Goldberg, 1989).
Genetic algorithm is a global optimization technique and can be implemented to a wide variety of problems with large and complex search spaces. Because of their high capabilities and potential, they have received a lot of attention and have been used by many researchers. The most distinct advantage of the genetic algorithm over other traditional optimization methods is that it does not need derivatives of the function and works on the function evaluations only to search for optimums. Genetic algorithm searches among a population of available points rather than focusing on a single point. It can consider design spaces consisting of a mix of continuous and discrete variables and therefore, it has a better chance of finding global optimums (Doglioni, 2004).
In spite of all the advantages, genetic algorithms also suffer from some limitations. One of the main disadvantages of genetic algorithm techniques is that although as global optimization techniques they have good initial convergence characteristics, but they may slow down considerably once the region of optimal solutions has been identified (Javadi et al (2005b), Abramson and Abela (1992)).
Many research works have used genetic algorithm as an effective optimization tool to solve various engineering problems. The results of these studies have proven that the genetic algorithm can be successfully employed as a strong optimization tool to engineering optimization problems.

3.4 Evolutionary polynomial regression

3.4.1 Introduction

In order to simplify the understanding of the differences between mathematical modelling approaches, colours are used to group these modelling techniques considering their required level of prior information. In this type of categorization, models are considered to be white-box, black-box, or grey-box models. Brief descriptions of these types of models are presented below (Giustolisi and Savic, 2006):

- A white-box model is a model with known variables, parameters, and underlying physical laws. It explains the relationship of the system in form of a set of mathematical equations or a single one.
- Black-box models are systems for which there is no prior information available. These are data-driven or regressive models, for which the functional form of relationships between variables and the numerical parameters in those functions are unknown and need to be estimated.
- Grey-box models are conceptual models whose mathematical structure can be derived through conceptualisation of physical phenomena or through simplification of differential equations describing the phenomena under consideration. These models usually need parameter estimation by means of input/output data analysis, though the range of parameter values is normally known.

White-box models have the ability to describe the underlying relationships between the contributing parameters of the desired systems considering only the physics principles which can be considered as a great positive point. On the other hand developing white-box models can be difficult due to the fact that the underlying mechanisms are not always totally understood by the users or the samples that are used in the lab to conduct

experiments providing the required understanding of the phenomenon, may not be an entirely perfect representation of the real environment being considered.
If one wants to contextualize the evolutionary polynomial data mining technique into one of the categories defined above, EPR is classified as a symbolic grey box technique which is able to identify and construct structured model expressions for a given data (Giustolisi and Savic, 2006). Table 3.1 shows the classification of the most commonly used modelling techniques.

Table 3.1: Classification of EPR and other modelling techniques (Doglioni, 2004)

	Artificial Neural Networks (ANN)	**Genetic Programming (GP)**	**Evolutionary polynomial regression (EPR)**	**Mathematical Equations derived based on Physical principles**
Black-box modelling	iiiiiiiiiiiiiiiiiiii			
Grey-box Models		iiiiiiiiiiiiiiiiiiii	iiiiiiiiiiiiiiiiiiii	
White-box Models				iiiiiiiiiiiiiiiiiiii

3.4.2 EPR procedure

The evolutionary polynomial regression works as a two-stage technique. Firstly it searches for symbolic structures using a specific but simple genetic algorithm and in the second stage EPR estimates the constant values for the model by solving a linear Least Square (LS) problem.

3.4.2.1 Evolutionary structural identification

General formulation of the EPR expression is given as (Giustolisi and Savic, 2006):

$$y = \sum_{j=1}^{m} F(\mathbf{X}, f(\mathbf{X}), a_j) + a_0 \qquad 3\text{-}1$$

where y is the estimated output of the system; a_j is a constant value; F is a function constructed by the process; $\mathbf{X}$ is the matrix of input variables; f is a function defined by the user; and m is the number of terms of the expression excluding bias a_0.

At the first stage of the modelling process, EPR identifies the structure of the model. To do this the equation 3-1 is transformed into the following form (vector form):

$$\mathbf{Y}_{N\times 1}(\boldsymbol{\theta}, \mathbf{Z}) = \left[\mathbf{I}_N \quad \mathbf{Z}^j_{N\times m}\right] \times [a_0 \quad a_1 \quad \dots \quad a_m]^T = \mathbf{Z}_{N\times d} \times \boldsymbol{\theta}^T_{d\times 1} \qquad 3\text{-}2$$

where

$\mathbf{Y}_{N\times 1}(\boldsymbol{\theta}, \mathbf{Z})$ is the least square estimate vector of N target values

$\boldsymbol{\theta}_{1\times \mathrm{d}}$ is the vector of $d = m + 1$ parameters $a_j, j = 1{:}\, m, and\ a_0$

$\mathbf{Z}_{N\times d}$ is a matrix formed by **I**, for bias a_0, and m vectors of variables $\boldsymbol{Z}^j$ that for a fixed j are a product of the independent predictor vectors of variables/inputs, $\mathbf{X} = \langle \mathbf{X}_1 \ \ \mathbf{X}_2 \ \ ... \ \ \mathbf{X}_k \rangle$.

Initially EPR starts from Equation **Error! Reference source not found.** and searches for the best structure which is meant to be a combination of vectors of independent variables (inputs parameters) $\mathbf{X}_{S=1:k}$. The matrix of inputs **X** is:

$$\mathbf{X} = \begin{bmatrix} x_{11} & x_{12} & x_{13} & ... & x_{1k} \\ x_{21} & x_{22} & x_{23} & ... & x_{2k} \\ x_{31} & x_{32} & x_{33} & ... & x_{3k} \\ ... & ... & ... & ... & ... \\ x_{N1} & x_{N1} & x_{N1} & ... & x_{Nk} \end{bmatrix} = [\mathbf{X}_1 \quad \mathbf{X}_2 \quad \mathbf{X}_3 \quad ... \quad \mathbf{X}_k] \qquad 3\text{-}3$$

where the k^{th} column of **X** represents the candidate variable for the j^{th} term of Equation **Error! Reference source not found.**. Therefore the j^{th} term of Equation **Error! Reference source not found.** can be written as

$$\mathbf{Z}^j_{N\times 1} = \left[(\mathbf{X}_1)^{\mathbf{ES}(j,1)} \cdot (\mathbf{X}_2)^{\mathbf{ES}(j,2)} \cdot (\mathbf{X}_3)^{\mathbf{ES}(j,3)} \cdot \ldots \cdot (\mathbf{X}_k)^{\mathbf{ES}(j,k)}\right] \qquad 3\text{-}4$$

where, $\mathbf{Z}^j$ is the j^{th} column vector in which its elements are products of candidate independent inputs and **ES** is a matrix of exponents. Therefore, the problem is to find the matrix $\mathbf{ES}_{k\times m}$ of exponents whose elements can be values within user-defined bounds. For example, if a vector of candidate exponents for inputs, **X**, **(**chosen by user) is $\mathbf{EX} = [0, \quad 1, \quad 2]$ and number of terms (m) (excluding bias) is 4, and the number of independent variables (k) is 3, then the polynomial regression problem is to find a matrix of exponents $\mathbf{ES}_{4\times 3}$. An example of the ES matrix can be seen in Equation 3-5:

$$\mathbf{ES} = \begin{bmatrix} 0 & 1 & 2 \\ 0 & 1 & 1 \\ 1 & 2 & 0 \\ 1 & 1 & 0 \end{bmatrix} \qquad 3\text{-}5$$

Substituting the above matrix into Equation 3-4 will give the following set of mathematical expressions:

$$\begin{aligned} \mathbf{Z}_1 &= (\mathbf{X}_1)^0 \cdot (\mathbf{X}_2)^1 \cdot (\mathbf{X}_3)^2 = \mathbf{X}_2 \cdot \mathbf{X}_3^2 \\ \mathbf{Z}_2 &= (\mathbf{X}_1)^0 \cdot (\mathbf{X}_2)^1 \cdot (\mathbf{X}_3)^1 = \mathbf{X}_2 \cdot \mathbf{X}_3 \\ \mathbf{Z}_3 &= (\mathbf{X}_1)^1 \cdot (\mathbf{X}_2)^2 \cdot (\mathbf{X}_3)^0 = \mathbf{X}_1 \cdot \mathbf{X}_2^2 \\ \mathbf{Z}_4 &= (\mathbf{X}_1)^1 \cdot (\mathbf{X}_2)^1 \cdot (\mathbf{X}_3)^0 = \mathbf{X}_1 \cdot \mathbf{X}_2 \end{aligned} \qquad 3\text{-}6$$

And the expression of Equation **Error! Reference source not found.**3-2 would be:

$$\begin{aligned} \mathbf{Y} &= a_0 + a_1 \cdot \mathbf{Z}_1 + a_2 \cdot \mathbf{Z}_2 + a_3 \cdot \mathbf{Z}_3 + a_4 \cdot \mathbf{Z}_4 \\ &= a_0 + a_1 \cdot \mathbf{X}_2 \cdot \mathbf{X}_3^2 + a_2 \cdot \mathbf{X}_2 \cdot \mathbf{X}_3 + a_3 \cdot \mathbf{X}_1 \cdot \mathbf{X}_2^2 + a_4 \cdot \mathbf{X}_1 \cdot \mathbf{X}_2 \end{aligned} \qquad 3\text{-}7$$

Each row in the **ES** matrix expresses the exponents of the candidate variable of the j^{th} term in Equations **Error! Reference source not found.**3-1 and **Error! Reference source not found.**3-2. Each exponent in matrix **ES** corresponds to a value in the **EX** vector. This allows the transformation of the symbolic regression problem into the problem of finding the best **ES**, which is the best structure of the EPR equation.

It is noteworthy that the EPR can also construct non-polynomial mathematical expressions. There is a possibility of assuming the function f to be the natural logarithm, hyperbolic tangent, hyperbolic secant, exponential or have a structure similar to one of the following expressions (Doglioni, 2004):

$$\mathbf{Y} = a_0 + \sum_{j=1}^{m} a_j \cdot (\mathbf{X}_1)^{\mathbf{ES}(j,1)} \cdot \ldots \cdot (\mathbf{X}_k)^{\mathbf{ES}(j,k)} \cdot f\left((\mathbf{X}_1)^{\mathbf{ES}(j,k+1)}\right) \cdot \ldots \cdot f\left((\mathbf{X}_k)^{\mathbf{ES}(j,2k)}\right) \quad \text{case 1}$$

$$\mathbf{Y} = a_0 + \sum_{j=1}^{m} a_j \cdot f\left((\mathbf{X}_1)^{\mathbf{ES}(j,1)} \cdot \ldots \cdot (\mathbf{X}_k)^{\mathbf{ES}(j,k)}\right) \quad \text{case 2}$$

$$\mathbf{Y} = a_0 + \sum_{j=1}^{m} a_j \cdot (\mathbf{X}_1)^{\mathbf{ES}(j,1)} \cdot \ldots \cdot (\mathbf{X}_k)^{\mathbf{ES}(j,k)} \cdot f\left((\mathbf{X}_1)^{\mathbf{ES}(j,k+1)} \cdot \ldots \cdot (\mathbf{X}_k)^{\mathbf{ES}(j,2k)}\right) \quad \text{case 3} \qquad 3\text{-}8$$

$$\mathbf{Y} = g\left(a_0 + \sum_{j=1}^{m} a_j \cdot (\mathbf{X}_1)^{\mathbf{ES}(j,1)} \cdot \ldots \cdot (\mathbf{X}_k)^{\mathbf{ES}(j,k)}\right) \quad \text{case 4}$$

Standard genetic algorithm is used as the global search tool to find the best form for the Equation 3-7 . Chromosomes, which are sets of character strings, similar to the ones that can be found in Deoxyribonucleic acid (DNA) in the bodies of the living creatures, are used to code the parameters needing to be optimised. In standard genetic algorithm binary codes, which are 0 and 1 characters, are implemented to form the chromosomes. Integer GA coding is used here to determine the location of the candidate exponents of the **EX** matrix in the matrix **ES** (Doglioni, 2004).
Values of the adjustable parameters a_j are also computed by the EPR after the evolutionary identification of the structure, by implementing the linear Least Square (LS) method and minimising the sum of squared errors (SSE) considered as the cost function (Giustolisi and Savic, 2006).

3.4.2.2 Least square solution

Calculation of the values of a_j in Equation 3-7 is an inverse problem that corresponds to solving an over-determined linear system in form of a least square problem. This

problem can normally be solved using Gaussian elimination technique (Giustolisi and Savic, 2006).
A random population of exponent vectors is first created and assigned to the columns of the input matrix. A population of structures for equations is then created. The least square technique is subsequently used to develop a set of equations to be exposed to the fitness criteria. If the considered complexity and fitness criteria are met, then the results will be shown and otherwise, the creation of another exponents pool will be passed to GA and this procedure will be repeated until the defined criteria for developing the models are satisfactorily met. A typical flow diagram representing EPR procedure is shown in Figure 3.1.

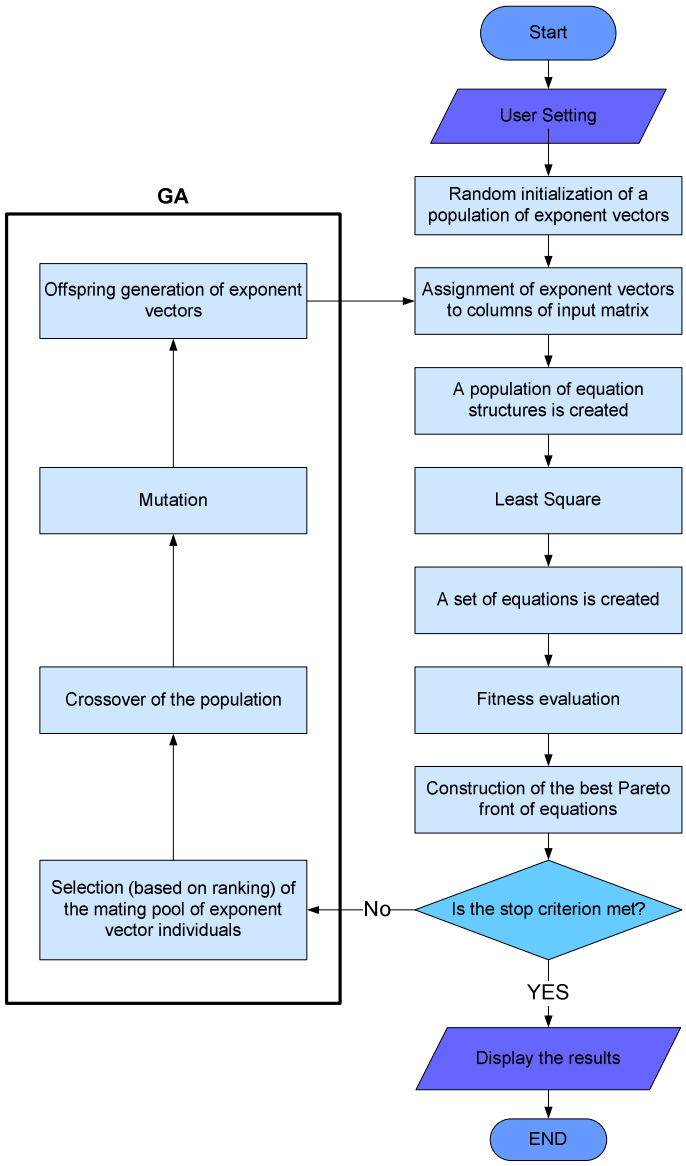

Figure 3.1: Flow diagram for representing the evolutionary polynomial regression procedure (Doglioni, 2004)

3.4.3 Objective functions used in the evolutionary polynomial regression

During the modelling process, different objective functions are provided for EPR to be optimised. This is done with the aim of developing the best symbolic model representing the system being modelled. EPR has the ability to operate in single and multi-objective configurations. Figure 3.2 depicts a summary of main available objective functions in the proposed EPR technique.
Multidimensional strategies are introduced in EPR modelling technique for selecting models considering a comprehensive complexity analysis including number of terms, number of inputs and also the fitness of the models. The best modelling approach is obviously the one that can provide the simplest model fitting the application purpose. The "principle of parsimony" also states that in case of availability of multiple and equivalent models describing one system, the simplest model should be chosen to explain the available set of data. Considering this, one can conclude that the fitness in regression-based models should also include a measure of trade-off between the complexity of the model and the quality of fit. This could be achieved in the following ways (Doglioni, 2004):

I. In single-objective configuration, an objective function must be used to control the fitness of the models preventing unnecessary complexities from entering into the models.

II. At least two objective functions should be introduced if the multi-objective configuration is used. In this case one of the objective functions is aimed to control the fitness of the models, while at least another one is needed to control the model complexity. The advantage of the multi objective approach is that it returns a set of non-dominated models, each one presenting fitness and complexity features. There is no need for the user to assume the number of building blocks a priori. The user will only need to set the maximum number of terms and the control on the complexity will let the number of building blocks vary considering the fitness of the model (Giustolisi and Savic, 2006).

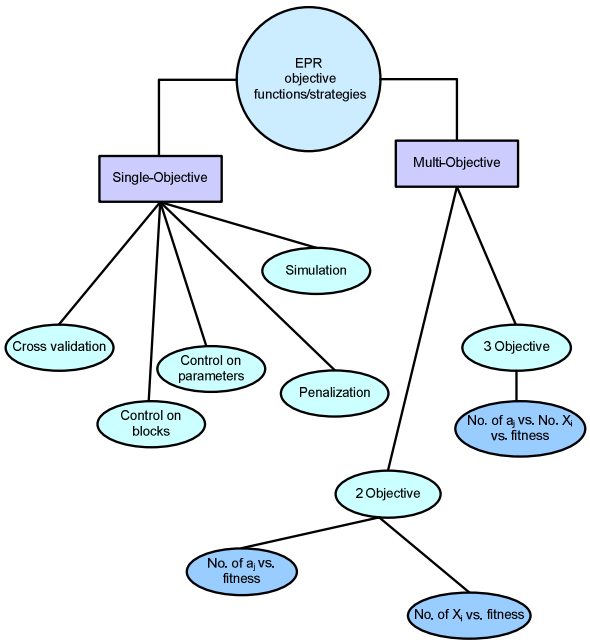

Figure 3.2: Main objective functions/strategies available in EPR methodology (Doglioni, 2004)

3.4.3.1 Single-objective strategy

Once experimental, field or simulation-based data is available; a regression-based technique being used to model the desired phenomena needs to search among a large or infinite number of possible models to be able to find an explanation for those data. The EPR technique does the search among all possible models by changing the exponents for the columns of matrix **X** and searching for the best-fit set of parameters **θ**. However, in order to avoid complexity, there is a need for an objective function ensuring the best fit. Unwanted unnecessary complexity can be defined as "bringing additional terms into the model or combinations of input parameters that introduce noise to the raw data" and is not the real representative of the target system.
An important aim of this methodology is finding ways of avoiding the over-fitting problem. Following strategies are introduced to help face this problem (Giustolisi and Savic, 2006):

1. Penalising the complexity of the expression by minimising the number of terms
2. Controlling the variance of a_j constants (the variance of estimates) with respect to their values
3. Controlling the variance of $a_j \cdot \mathbf{Z}_j$ terms with respect to the variance of residuals
4. Cross-validation of the models
5. Optimisation of the SSE evaluated on the simulation (off-line prediction) of the phenomenon performed by the models

Detailed explanation of these strategies can be found in Doglioni (2004)

3.4.3.2 Multi-objective strategy

Earlier editions of EPR used single-objective genetic algorithm (SOGA) strategy to explore the formulae space. This exploration is achieved by first assuming the maximum number of terms m in the pseudo-polynomial expressions shown in Equation **Error! Reference source not found.** and then sequentially exploring the formulae space having one, two … and m terms. However, the SOGA-based EPR methodology has the following disadvantages (Giustolisi and Savic, 2009):

a) As the number of polynomial terms m increases, the performance of the SOGA-based EPR methodology decreases exponentially. More terms means more GA runs.
b) Interpretation of the results of SOGA-based EPR is very difficult in some occasions. The identified models can either be ranked based on their fitness to data or considering their structural complexity. Ranking the models chosen based on structural complexity requires some subjective judgment, and therefore this process can be biased by the analyst's experience rather than being only based on some mathematical criteria.
c) During the searching process for the formulae with j terms, the ones with fewer terms are not presented; however, these formulas could have a better accuracy than the previously found ones with $j-1$ terms (Giustolisi and Savic, 2009).

To overcome the above mentioned shortcomings, multi-objective genetic algorithm strategy (MOGA) was introduced to the evolutionary polynomial regression methodology with the aim of searching for the best model structures that comply with the fitness and include limited structural complexity (Giustolisi and Savic, 2009). Two different objective functions are defined to control the fitness and complexity. The objectives represented by the functions are mutually conflicting, and then their

optimisation returns a trade-off surface of models. The multi-objective strategy in hybrid evolutionary computing helps the user with:

a) Finding a set of feasible symbolic models
b) Making a robust choice
c) Having a set of models with variable parsimony levels in an efficient computational time

Multi objective genetic algorithm-based evolutionary polynomial regression (MOGA-EPR) takes advantage of a multi-model strategy by varying the structural parsimony, which is the number of constant values in the equation, and working on the objective function used in single-objective EPR. Then, MOGA-EPR finds the set of symbolic expressions that perform well according to two (or more) conflicting criteria considered simultaneously; the level of agreement between simulated and observed measurements and structural parsimony of the expressions obtained. The implemented objective functions are:

a) Maximizing the fitness
b) Minimizing the total number of input parameters selected by the modelling strategy
c) Minimizing the length of the model expression (decreasing the number of terms in the developed model)

Ranking of the developed models is done considering the Pareto dominance criterion. By using the MOGA-EPR the computational time needed by the multiple executions of EPR reduces. In the case of SOGA-EPR this time would only be enough for one of the objective functions introduced in the model development process. The best possible models from among all developed models are chosen and presented to the user based on the MOGA-EPR methodology. The Pareto set of solutions seems to be the best set of expressions required for the analysis of the problem (Giustolisi and Savic, 2009).

The most commonly used objective functions implemented to measure the fitness of the symbolic structures are based on the Sum of Squared Errors (SSE) or on the Penalisation of Complex Structures (PCS). The result of the single-objective EPR optimization is normally made of a set of models that all are good in an equal manner. It is normally easier to rank these models considering their sum of squared errors, rather than according to their structural complexity. As a matter of fact, putting the models in order according to their structural complexity can be quite complicated (Giustolisi and Savic, 2009). The multi-objective strategy is implemented to improve both the post-processing and the general modelling framework of the basic evolutionary polynomial regression. MOGA strategy allows ranking the developed models considering both the Coefficient of Determination (CoD) and the structural complexity. Objective functions implemented in multi objective genetic algorithm-based evolutionary polynomial regression are (Giustolisi and Savic, 2009):

a) (1-CoD), which is equal to the SSE,

$$\mathrm{CoD} = 1 - \frac{N-1}{N}\frac{\sum_N\left[(\mathbf{Y}_\mathrm{p} - \mathbf{Y}_\mathrm{a})^2\right]}{\sum_N\left[\left(\mathbf{Y}_\mathrm{a} - \frac{1}{N}\sum_N \mathbf{Y}_a\right)^2\right]} = 1 - k \cdot \mathrm{SSE}$$
$$k = \frac{2(N-1)}{\sum_N\left[\left(\mathbf{Y}_a - \frac{1}{N}\sum_N \mathbf{Y}_a\right)^2\right]} \qquad 3\text{-}9$$

where $\mathbf{Y}_a$ is the vector of actual (measured or experimental) data, $\mathbf{Y}_\mathrm{p}$ values are the corresponding predicted ones and N is the number of data lines based on which the coefficient of determination is obtained.

b) The number of constant values a_j (# of a_j) and
c) The total number of input parameters involved in the symbolic expression (% of $\mathbf{X}_i$).

It is noteworthy that the total number of input parameters corresponds to the number of times that each input is involved in the symbolic expression. The user must set the maximum number of constant values, which puts an upper limit on the maximum number of the symbolic expression inputs. MOGA-EPR tries to find the best non-dominated models with respect to both structural complexity and fitness performance which is placed on the best Pareto front. In other words, a direct multi-model methodology is provided where the post-processing phase is improved using MOGA-EPR returning models ranked considering both their fitness and structural complexity.

Another outstanding feature of the new MOGA-EPR is that, this strategy applies extra pressure on achieving structural parsimony. The reason for this is that a large number of a_j values or a large total number of inputs can only be introduced in case that there is a justification by the fitness of the model. It must be noted that the Pareto dominance criterion and the function need to be minimised. Objective functions can be used in a double-objective configuration or all together (Giustolisi and Savic, 2009):

a) Coefficient of Determination versus % of $\mathbf{X}_i$
b) Coefficient of Determination versus % of a_j
c) Coefficient of Determination versus [(% of $\mathbf{X}_i$) and (% of a_j)]

By choosing the Pareto dominance criterion for the multi-objective optimisation the following advantages can be obtained:

a) Less searching time is required: It is reasonably fast for few objective functions in comparison with the total amount of time required by multiple single-objective sessions.
b) Simultaneous action: It deals simultaneously with multiple solutions.
c) Uniformity of the suggested solutions: It is able to provide a uniformly distributed range of Pareto solutions.

Figure 3.3 shows a typical outlook of the MOGA-EPR on operation.

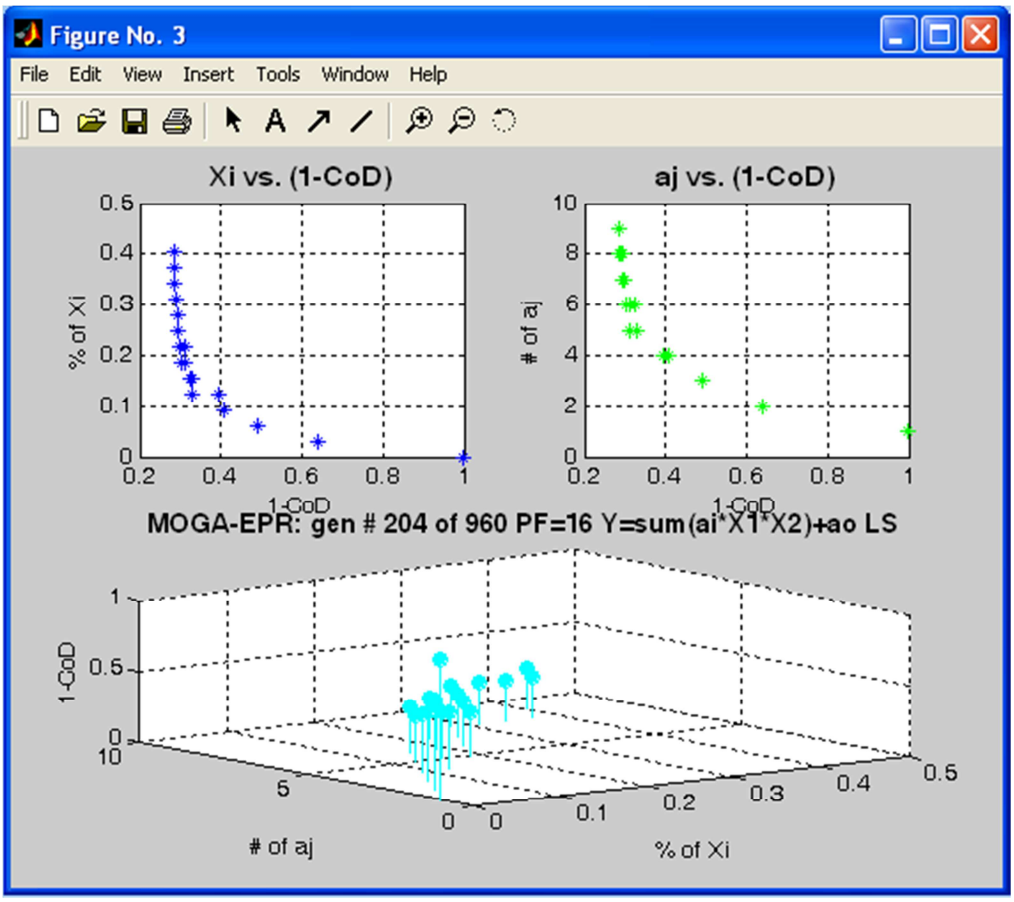

Figure 3.1: A typical outlook of multi-objective EPR on operation

3.4.4 EPR user interface

EPR has been coded using MATLAB® in POLITECNICO DI BARI University, Italy, by Professor Giustolisi and his co-workers in collaboration with Professor Savic in University of Exeter, UK. EPR is provided with a user-friendly interface, (following figure):

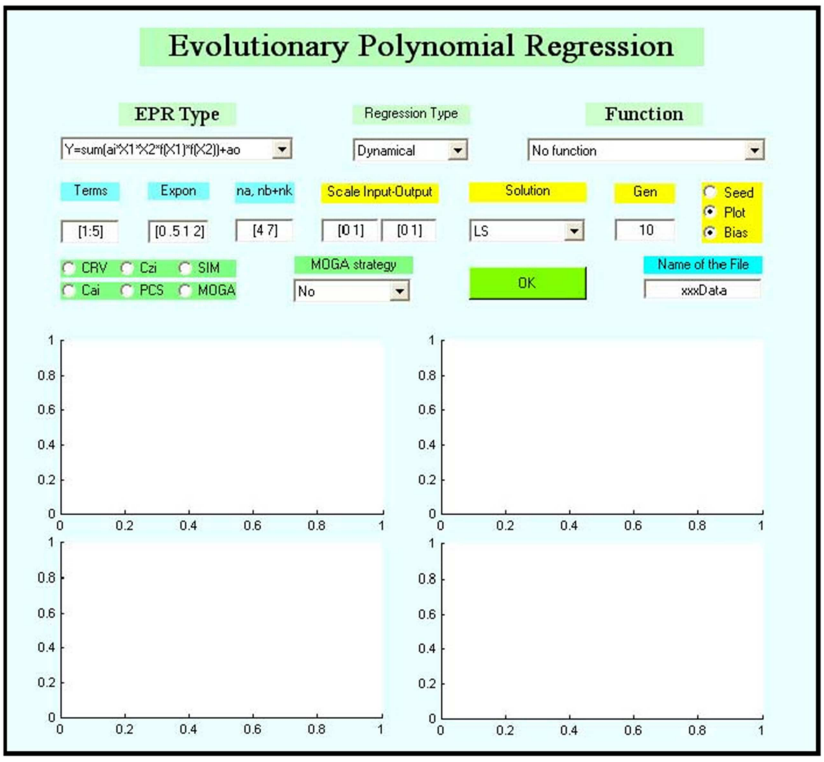

Figure 3.2: User interface of the evolutionary polynomial regressioncode

Within this graphical user interface (GUI), the user can set up the modelling phase according to the features described in the previous sections. Moreover, the user can decide on the number of generations of the GA by setting the proper value in the "Gen" box. This value corresponds to a proportionality factor which will be multiplied for the maximum length of the expression (maximum number m of monomial building blocks) and for the total number of inputs. Another option is about the possibility of seeding the population with random elements from the previous parental set. This option efficiently works when large data sets are available and in single-objective configuration. In multi-objective search the seed option does not seem to add any advantage in the GA phase (Giustolisi and Savic, 2009). Finally, the option "bias" refers to the possibility of looking for symbolic expression containing the term a_0. If the bias option is not selected, EPR will automatically exclude all those expressions containing a_0, otherwise EPR will search for both types of expression with and without a_0 term (Doglioni, 2004).

3.4.5 Application of the evolutionary polynomial regression technique in modelling engineering problems

EPR is successfully employed to model various problems and systems in many engineering disciplines including structural, environmental and geotechnical engineering. Rezania et al (Rezania, Faramarzi and Javadi, 2011) used EPR to predict the earthquake-induced soil liquefaction and lateral displacement. A 3D surface was developed discriminating between the cases of occurrence and non-occurrence of liquefaction using the evolutionary polynomial regression. Faramarzi et al (2011) employed EPR to model and predict the behaviour of steel plate shear walls (SPSW) under cyclic behaviour. The results of a number of actual experiments on cyclic

behaviour of SPSW structures were used to develop EPR models with the aim of predicting lateral deformations of SPSWs under cyclic loading. Some other research works were also published including the ones from the author of this thesis (e.g.; (Ahangar-Asr et al (2012); (2011a); (2011b); (2010)); (Faramarzi, Javadi and Ahangar-Asr, 2013); (Cuisinier et al., 2013)).

3.5 Conclusions

In this chapter the Evolutionary Polynomial Regression (EPR) methodology was introduced as a new data mining technique. EPR is a two-stage process that uses a Genetic Algorithm (GA) and Least Squares (LS) regression to develop models representing data. Both single-objective and multi-objective modelling strategies were explained with sufficient details. The advantages of EPR in overcoming some problems associated with artificial neural networks and genetic programming were represented along with detailed explanation of the related formulations. The user interface of the programme and past applications of the methodology were also presented in this chapter.

In the next two chapters important applications of EPR in geotechnical and civil engineering problems will be presented.

Chapter 4

APPLICATION OF EPR FOR CONSTITUTIVE MODELLING OF SOILS

4.1 Introduction

Constitutive modelling is an important element of finite element analysis. In conventional constitutive modelling, initially a suitable constitutive model is selected from a range of available models and then the parameters of the model are identified from suitable physical tests on representative samples of the material. Therefore, the accuracy with which the selected constitutive model describes the real behaviour of the material has significant effect on the accuracy and reliability of the numerical predictions. In the past few decades a number of constitutive models have been developed to describe the complex behaviour of geomaterials. Due to erratic and complex nature of soils, none of the existing constitutive models can completely describe the real behaviour of these materials under various stress paths and loading conditions.

In this chapter the evolutionary polynomial regression technique is applied to constitutive modelling of different soils. Five different applications are considered including (i) modelling of mechanical behaviour of unsaturated soils, (ii) modelling of soil-water characteristic curve for unsaturated soils, (iii) thermo-mechanical behaviour of unsaturated soils, (iv) stress-strain and volume change behaviour of granular soils and (v) identification of coupling parameters between shear strength behaviour and chemical's effects in compacted soils.

Comparisons of the results of the proposed EPR models with experimental data, and conventional models and also artificial neural network model results in some cases are presented. Sensitivity analyses of the proposed models are presented with the aim of understanding the level of contribution of the involved parameters in the EPR models.

In what follows a review of the relevant literature, development of the EPR models, comparison of the results with previous models and the sensitivity analysis are presented for modelling the mechanical stress-strain behaviour of unsaturated soils (Section 4.2), soil-water characteristic curve in unsaturated soils (Section 4.3), thermo-

mechanical behaviour of unsaturated soils (Section 4.4), stress-strain and volume change behaviour of granular soils (Section 4.5) and coupling parameters between shear strength behaviour and chemical's effects in compacted soils of unsaturated soils (Section 4.6).

4.2 Constitutive modelling of unsaturated soils

4.2.1 Introduction

The mechanical behaviour of unsaturated soils has been the subject of numerous investigations over the past few decades. Some notable contributions are presented here. Toll (1990) proposed a framework to describe the shear behaviour of an unsaturated soil in terms of total stresses and suctions in the soil. His proposed model was based on the critical state model for saturated soils incorporating additional variables needed to formulate the behaviour of unsaturated soil. The effects of total stress and suction were considered separately to avoid the possibility of treating the two stress components as equivalent. The framework was based on coupling of volumetric and shearing behaviour. It incorporated separate stress state variables and included degree of saturation as a controlling variable.

Alonso et al (1990) presented a constitutive model to describe the stress-strain behaviour of partially saturated soils. The model was formulated within the framework of hardening plasticity using two independent stress variables: the excess of total stress over air pressure and the suction. The mode1 was able to represent the fundamental features of the behaviour of partially saturated soils which had been treated separately by previously proposed models. On reaching saturation, this mode1 becomes a conventional critical state model. However, as the experimental evidence was lacking at the time, the model was kept simple in order to provide a basic framework from which extensions could be possible. The mode1 was intended for slightly or moderately expansive partially saturated soils.

Wheeler and Sivakumar (1995) used data collected from a series of controlled suction triaxial tests on samples of compacted white kaolin to develop an elasto-plastic critical state framework for unsaturated soil. The framework was defined in terms of four state variables: mean net stress, deviator stress, suction and specific volume. An isotropic normal compression hyperline, a critical state byperline and a state boundary hypersurface were included within the proposed framework. For states situated inside the state boundary hypersurface the soil behaviour was assumed to be elastic with movement over the state boundary hypersurface corresponding to expansion of the yield surface in stress space. The proposed critical state model for unsaturated soil would have possible applications at three different levels, as described by Wheeler & Sivakumar (1995): (i) in providing a qualitative framework that would enhance fundamental understanding of the mechanical behaviour of unsaturated soil, (ii) in guiding the choice of drained and undrained strength or stiffness parameters to be used in conventional calculations of collapse load or deformation and (iii) in providing a formalized elasto-plastic constitutive model that could be incorporated within numerical formulations, such as the finite element method, for the solution of boundary value problems. However, in this model, similar to some other sophisticated constitutive models for unsaturated soils, within a numerical formulation for the solution of real boundary value problems, it is difficult to measure all the relevant soil parameters such as elastic constants, the suction-dependent parameters, etc.

Kogho et al (1993) discussed several theoretical aspects for preparation of constitutive equations governing the behaviour of unsaturated soils. They described possible pore water states including insular air, fuzzy and pendular saturation which were considered to examine the mechanical behaviour of unsaturated soils. They also classified the suction effects into two categories: (i) increase in suction that induces an increase in effective stress values and (ii) increase in suction that causes both the yield stress and stiffness of the soil skeleton to increase. According to this research, taking the three saturation conditions (insular air saturation, fuzzy saturation and pendular saturation) into account in modelling the behaviour of unsaturated soils is practical.

Bolzon et al. (1996) extended the elasto-plastic constitutive model developed by Pastor et al. (1990), which has been extensively validated for fully saturated soil behaviour, to include partially saturated soil behaviour. They particularly investigated soil stiffness changes induced by suction together with the process of collapse (i.e. irreversible compressive volumetric strains) of soil on wetting. They introduced Bishop's stress and suction as the stress parameters to describe the behaviour of partially saturated soils under isotropic conditions. For full saturation, when suction is equal to zero, Bishop's stress reduces to total stress in excess of pore water pressure, which is the stress measure considered in the original saturated model. Stress paths different from the isotropic one can also be dealt with in the general framework established by Pastor et al. (1990). Bolzon et al. (1996) introduced a few additional parameters to Pastor et al (1990) saturated soil model with the aim of characterizing the material response to suction changes.

Loret and Khalili (2000) proposed a framework to define the constitutive behaviour of unsaturated soils which was developed within the theory of mixtures applied to three-phase porous media. Each of the three phases is endowed with its own strains and stresses. Elastic and elastic-plastic constitutive equations were developed. Particular emphasis was put on the interactions between the phases both in the elastic and plastic regimes. Nevertheless, the clear structure of the constitutive equations required a minimum number of material parameters and the soil-water characteristic curve was directly used to identify these parameters. Following this work which was an extension of the elasto–plastic models of saturated soils to unsaturated states within a three-phase framework, Loret and Khalili (2000) stated their main concern to be on the behaviour of the solid skeleton. They described a model for the elasto–plastic behaviour of unsaturated soils requiring minimal number of material parameters to define the effect of desaturation. These material parameters were identified and the application of the model was demonstrated using the data reported by Wheeler and Sivakumar (1995) that included results from first wetting, followed by consolidation and finally triaxial compression tests. They aimed to develop an elasto-plastic model for unsaturated soils with the least possible deviation from the classic saturated soil models and therefore, they chose the modified Cam-Clay model as the plastic driver.

Gallipoli et al. (2003) presented an elasto-plastic model for unsaturated soils that took explicitly into account the mechanisms with which suction affects mechanical behaviour of soil, as well as their dependence on degree of saturation. The proposed model was formulated in terms of constitutive variables directly related to suction mechanisms. The analysis of experimental data on isotropic compression tests suggested that the quotient between the void ratio of an unsaturated soil and the void ratio corresponding to the saturated state at the same average soil skeleton stress is a unique function of the bonding effect due to water menisci at the inter-particle contacts. The same result was obtained when examining critical states at different suctions. Based on these observations, an elasto-plastic constitutive model was developed using a single yield

surface, the size of which was controlled by volumetric hardening. It was shown that the model could reproduce many important features of unsaturated soil behaviour.

Wheeler et al. (2003) developed an anisotropic elasto-plastic model for soft clays. Experimental data from multistage drained triaxial stress path tests on Otaniemi clay from Finland supported their proposed shape of the yield curve and the proposed relationship describing the change of yield curve inclination with plastic straining. They also suggested procedures for determining the initial inclination of the yield curve and the values of the two additional soil constants within their model. They compared their model simulations with experimental data and the Modified Cam Clay model. They attributed the discrepancies observed in comparison of the results to the role of destructuration in the sensitive Otaniemi clay.

Borja (2004) presented a mathematical framework for analysis of deformation and strain localization of partially saturated granular media using three-phase continuum mixture theory. He developed conservation laws governing a three-phase mixture to identify energy-conjugate expressions for constitutive modelling. Energy conjugate expressions identified relate a certain measure of effective stress to the deformation of the solid matrix, the degree of saturation to the matrix suction, the pressure in each phase to the corresponding intrinsic volume change of this phase and the seepage forces to the corresponding pressure gradients. He used the second law of thermodynamics to obtain the dissipation inequality; from the principle of maximum plastic dissipation a condition for the convexity of the yield function was driven. Then, he formulated expressions describing conditions for the onset of tabular deformation bands under locally drained and locally undrained conditions. His proposed model changes to the classical modified Cam-Clay model in saturated conditions. He also presented numerical examples to demonstrate the performance of the return mapping algorithm and illustrated the localization properties of the model as functions of imposed deformation and matrix suction histories.

Ehlers et al. (2004) investigated the deformation and the localization behaviour of unsaturated soil and exhibited the influence of the solid–fluid coupling on the localization analysis. In the framework of a triphasic formulation, unsaturated soil was considered as a materially incompressible elasto-plastic or elasto-viscoplastic skeleton saturated by two viscous pore-fluids, a materially incompressible pore-liquid and a materially compressible pore-gas. Assuming quasi-static situations, the numerical computations proceed from weak formulations of the momentum balance of the overall triphasic material together with the mass balance equations of the pore-fluids and Darcy-like relations for the seepage velocities. As a result, a system of coupled differential-algebraic equations (DAE) occurred, which was solved using the finite element method. They also studied the influence of the pore-gas constituent on the material behaviour of partially saturated soil with respect to fluid-flow simulations and embankment and slope failure problems.

Khalili et al (2008) presented a fully coupled constitutive model for describing the flow and deformation behaviour of unsaturated soils. The elastic–plastic behaviour due to loading and unloading was captured using the bounding surface plasticity. The hydraulic hysteresis was accounted for through the soil water characteristic curve. The coupling between fluid flow and deformation fields was also established using the effective stress parameters. They paid special attention to the interrelations between the effective stress and wetting and drying paths, and the shift in the soil water characteristic curve with the matrix deformation. They also introduced a single set of material parameters for characterization of the coupled constitutive model.

These contributions constitute major steps forward in constitutive modelling of unsaturated soils. However many of these models have proven to be incapable of dealing with different complex aspects of unsaturated soils behaviour in a consistent and unified manner. Indeed, currently there exist no constitutive models of unsaturated soils in which a point-by-point matching of test data as observed in the laboratory can be achieved.

In recent years, the use of artificial neural network (ANN) has been introduced as an effective alternative to constitutive modelling of complex materials. As mentioned in the previous chapters, ANN is a computer-based modelling technique for computation and knowledge representation inspired by the neural architecture and operation of the human brain. Habibagahi ad Bamdad (2003) presented a neural network approach to describe the mechanical behaviour of unsaturated soils. A sequential architecture (that is, a multilayer perceptron network with feedback capability) was chosen for the network. The input layer consisted of nine neurons, where six of them represented the initial soil conditions and the remaining three neurons were continuously updated for each increment of axial strain based on outputs from the previous increment. The output layer consisted of three neurons representing values of deviatoric stress, volumetric strain, and change in suction at the end of each increment. A database of triaxial test results from literature was used to train and test the network.

The use of artificial neural networks that are constructed directly from the experimental data, offers a fundamentally different approach to modelling of the material behaviour. Because of their ability to learn and generalize interactions among many variables, ANNs have the potential to model various aspects of material behaviour.

Although neural networks have shown to be very efficient in modelling the behaviour of materials they do have shortcomings. One of the drawbacks of neural network is that the optimum structure of ANN (e.g., number of inputs, hidden layers, and transfer functions) must be identified a priori. This is usually done through a trial and error procedure. The other major shortcoming is the black box nature of ANN models as described in Chapter 2.

In this section the evolutionary polynomial regression is implemented for modelling the behaviour of unsaturated soils. The capabilities of the technique are demonstrated by application to a comprehensive set of unsaturated soil triaxial data for a range of stresses and drainage conditions. It is shown that the EPR can capture various aspects of the behaviour of unsaturated soils effectively.

4.2.2 Database

Results from a set of constant water content triaxial tests on Lateritic gravel reported by Toll (1988) were adopted for the analysis. Table 4.1 indicates the range of basic soil properties. Table 4.2 shows the initial conditions of soil specimens adopted for this study and also indicates whether the results of a particular test were used for training or testing of the EPR models. This database consists of the results from 23 different unsaturated samples prepared using static or dynamic compression. However, for the sake of consistency, only 14 specimens prepared with static compression were considered in this investigation. The experimental results (graphs) presented by Toll (1988) were digitized. Digitization resulted in a database including a total of 5153 patterns that were used for training and testing of the EPR models.

Table 4.1: Range of basic soil properties of the specimens

Properties	Range
Initial water content (%)	17,26.3
Dry density (Mg/m3)	1.442,1.716
Suction (kPa)	-9.5,545.4
Axial strain (%)	0,11.52
Deviator stress (kPa)	0,930
Volumetric strain (%)	-7.5,0.35
Mean net stress (kPa)	23.9,237.6

Table 4.2: Initial conditions of soil specimens

Sample	Water content (%)	Dry density (Mg/m^3)	Initial suction (kPa)	σ_3 (kPa)	EPR status
MGU1	19.6	1.442	384	552	Train
MGU2	25.5	1.632	4	302	Train
MGU3	20.8	1.531	149	350	Train
MGU4	21.4	1.551	22	300	Train
MGU5	20.7	1.646	105	353	Train
MGU6	21	1.489	256	500	Test
MGU7	17	1.474	450	500	Train
MGU8	21.1	1.587	186	352	Test
MGU10	25.1	1.508	11	350	Test
MGU11	24.9	1.506	26	350	Train
MGU14	26	1.706	5	350	Train
MGU15	25	1.702	12	399	Train
MGU22	24.3	1.708	78	473	Train
MGU23	25.8	1.705	54	324	Train

4.2.3 Data preparation

From among 14 tests, 11 were used for model construction and 3 for validation. It was checked to make sure that all parameter values in the testing data sets were within the range of data chosen to be used for training EPR and developing the models. Overall, 20 possibilities were available for choosing 3 sets of data to be used as the testing datasets to meet the above criterion.

To select the most robust combination of the training and testing data sets, a statistical analysis was performed on the input and output parameter values (Table 4.3) of the selected training and validation sets (all 20 possible combinations were considered). The aim of the analysis was to ensure that the statistical properties of the data in each of the subsets were as close to the others as possible and thus represented the same statistical population. The mean and standard deviation values were calculated for every single contributing parameter and for the training and testing datasets for each combination and the one for which these statistical values were the closest in the training and testing data sets was chosen to be used in training and testing stages in the EPR model development process (Rezania, Javadi and Giustolisi, 2008).

Table 4.3: Parameters involved in the developed incremental EPR models*

Contributing parameters	Model output
w , ρ_d , ε_a , $(p-u_a)$, s_i , $\varepsilon_{v,i}$, q_i , $\Delta\varepsilon_a$	q_{i+1}
	s_{i+1}
	$\varepsilon_{v,i+1}$

* w = initial water content; ρ_d = dry density; ε_a = axial strain; $(p-u_a)$ = mean net stress; s = suction; ε_v = volumetric strain; q = deviator stress; $\Delta\varepsilon_a$ = axial strain increment

4.2.4 EPR modelling procedure

As mentioned in chapter 3, before starting the evolutionary procedure a number of constraints can be implemented to control the structure of the models to be constructed in terms of length of the equations, type of functions used, number of terms, range of exponents, number of generations, etc. It can be seen that there is great potential in achieving different models for a particular problem which enables the user to gain additional information. Applying the EPR procedure, the evolutionary process starts from a constant mean of output values. By increasing the number of evolutions it gradually picks up the different participating parameters in order to form equations representing the constitutive relationships. Each model is trained using the training data and validated using the testing data provided by the user (Rezania, Faramarzi and Javadi, 2011). The level of accuracy at each stage is evaluated based on the coefficient of determination (CoD) i.e., the fitness function as

$$CoD = 1 - \frac{\sum_N \left(Y_a - Y_p\right)^2}{\sum_N \left(Y_a - \frac{1}{N}\sum_N Y_a\right)^2} \qquad 4\text{-}1$$

where $\mathbf{Y}_a$ is the actual output value; $\mathbf{Y}_p$ is the EPR predicted value and N is the number of data points on which the CoD is computed. If the model fitness is not acceptable or the other termination criteria (in terms of maximum number of generations and maximum number of terms) are not satisfied, the current model should go through another evolution in order to obtain a new model.

To examine the efficiency of the proposed EPR approach in capturing the behaviour of unsaturated soils, the database was used to train three different EPR models for deviator stress (q), suction (s) and volume strain (ε_v) in terms of the contributing parameters listed in Table (4.1).

4.2.5 EPR models for unsaturated soils

A typical scheme to train most of the neural network-based material models for soils includes an input set providing the network with information relating to the current state units (e.g., current stresses and strains) and then a forward pass through the network that yields the prediction of the next expected state of stress or strain relevant to an input strain or stress increment (Ghaboussi et al., 1998). Due to the incremental nature of soil stress–strain modelling in practical applications, this scheme has been utilized in this research. The EPR models have eight input parameters as summarized in Table 4.3. The first two input parameters namely, gravimetric water content, and dry density represent

the initial conditions of the soil specimens and the other parameters, namely; axial strain, net mean stress, suction, volumetric strain, and deviator stress are being updated incrementally during the training and testing based on the outputs relating to the previous increment of the axial strain. The output parameters are deviator stress, suction and volumetric strain corresponding to the end of the incremental step for the three EPR models.

The data was divided into training and testing sets (Table 4.2). One set was used for training to develop the models and the other one was used for validation to appraise the generalization capabilities of the trained models. Three separate models were developed for deviator stress (q), suction (s) and volumetric strain (ε_v). After development of the EPR models, from the 15 resultant equations for deviator stress, 6 equations did not include the effect of all contributing parameters. Among the remaining equations the shortest one possible, with the highest coefficient of determination value was selected as the final model. The same procedure was followed to choose the best fit equations for volumetric strain and suction. Equations 4-2, 4-3 and 4-4 represent the incremental EPR models for deviator stress, volumetric strain, and suction respectively. It should be noted that the proposed models are unit dependent.

$$q_{i+1} = \frac{3.33}{w.\varepsilon_a} + \frac{53.89\times10^{3}\Delta\varepsilon_a - 5.04\varepsilon_{v,i}}{\rho_d^3} + \frac{2.91\times10^{-5}(p-u_a)^2\varepsilon_a^2}{s_i} + 1.0032q_i + 1.14\times10^{-5}(p-u_a)^2\varepsilon_a\cdot\varepsilon_{v,i} - \frac{1.52\times10^{5}\Delta\varepsilon_a}{w.\rho_d^2}$$
$$+ \frac{12.4\times10^{3}\Delta\varepsilon_a\cdot\rho_d^3}{w} - \frac{32.31\times10^{3}\Delta\varepsilon_a + 1.43\Delta\varepsilon_a\cdot w(p-u_a)}{\rho_d^2} + 4.84\times10^{-6}\Delta\varepsilon_a\cdot q_i^3 + \frac{137.8\Delta\varepsilon_a\cdot\rho_d\cdot\varepsilon_{v_i}}{\varepsilon_a} + 7.9\Delta\varepsilon_a.\rho_d(p-u_a) \quad 4\text{-}2$$
$$+ \frac{6.18\Delta\varepsilon_a.\rho_d^2.q_i}{\varepsilon_a(p-u_a)} - \frac{187.64\Delta\varepsilon_a^2}{\varepsilon_a} - 1.868$$

$$\varepsilon_{v,i+1} = -\frac{4.18\times10^{-3}}{s_i} + 1.0042\varepsilon_{v,i} + 7.69\times10^{-4}\varepsilon_{v,i}^2 + \frac{542.51\Delta\varepsilon_a\cdot\rho_d^2\cdot\varepsilon_{v,i}}{w\cdot\varepsilon_a(p-u_a)} + 0.2\Delta\varepsilon_a - 4.11\times10^{-3}\Delta\varepsilon_a\cdot q_i \quad 4\text{-}3$$
$$+ 0.09\Delta\varepsilon_a.\varepsilon_a - 6.27\times10^{-3}\Delta\varepsilon_a\cdot\varepsilon_a^2 + 2.07\times10^{-5}\Delta\varepsilon_a(p-u_a)^2 + 0.0027$$

$$s_{i+1} = \frac{8.83\times10^{-3}q_i}{\rho_d^2} + \frac{79.11q_i}{(p-u_a)^2} - \frac{2.93s_i}{(p-u_a)} + \frac{0.37s_i^2}{(p-u_a)^2} + \frac{5.29\times10^{-6}w^3\cdot\varepsilon_{v,i}}{\varepsilon_a^2} - \frac{3.97\times10^{3}\Delta\varepsilon_a}{w^2\cdot\rho_d^2\cdot\varepsilon_a} + 1.01s_i - 1.706 \quad 4\text{-}4$$

Figure 4.1 shows typical deviator stress-axial strain, volumetric strain-axial strain, and suction-axial strain curves predicted by the (incremental) EPR models in Equations 4-2, 4-3 and 4-4 (dashed lines) against the experimental results for a test that was used in training of the models (sample MGU22). ANN simulation results after Habibagahi and Bamdad (2003) are also presented.

After training, the performance of the trained EPR models was verified using 3 sets of validation data which had not been introduced to the EPR models during training. The purpose of validation was to examine the capabilities of the trained models to generalise the training to conditions that have not been seen by the model during the training phase. Figure 4.2 shows predictions made by the developed EPR models against the experimental data which were not previously seen by EPR and were used as validation data (MGU 6). The CoD values of the EPR models (Equations 4-2, 4-3 and 4-4) are given in Table (4-4).

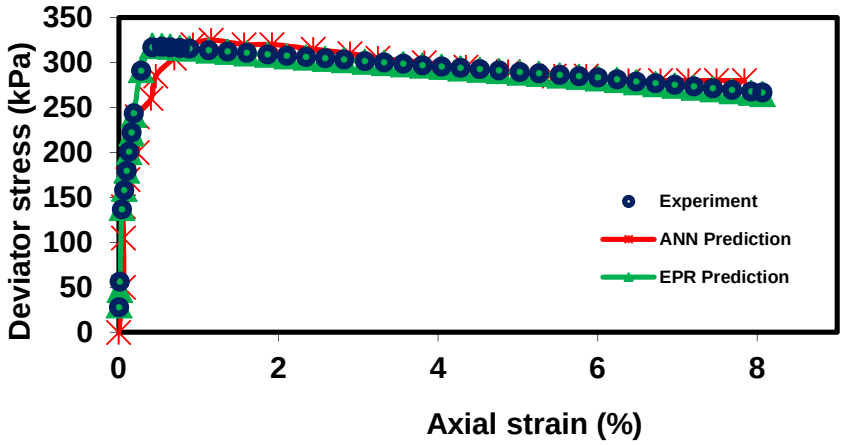

(a)

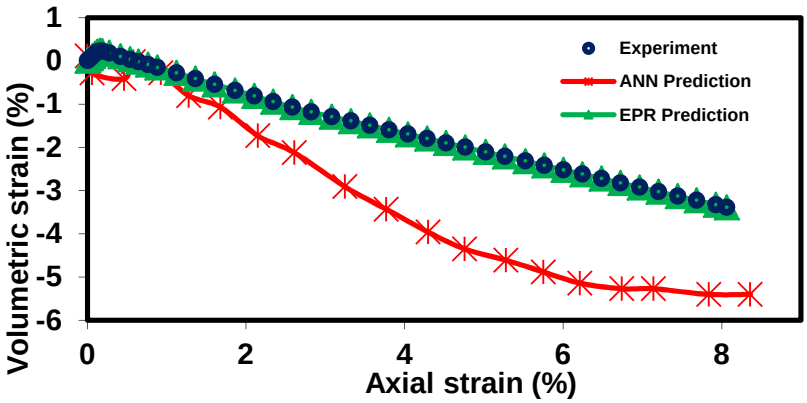

(b)

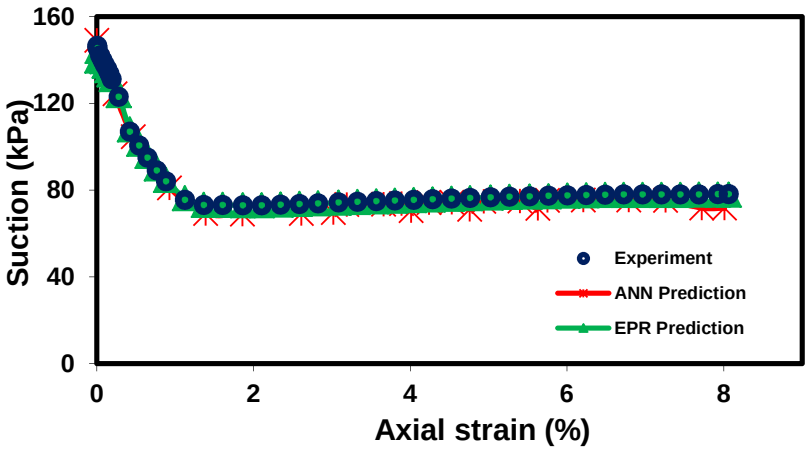

(c)

Figure 4.1: Comparing the EPR model predictions with experimental training data (MGU 22) and ANN predictions for deviator stress, volumetric strain, and suction

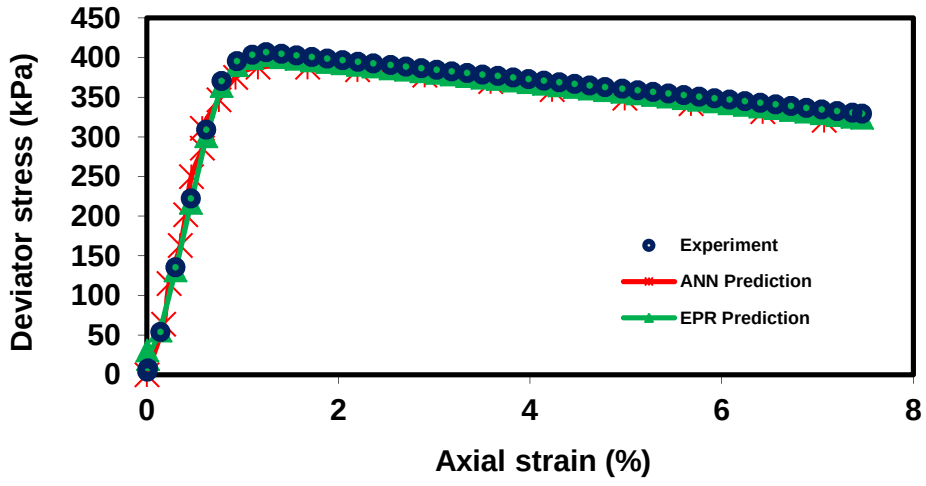

(a)

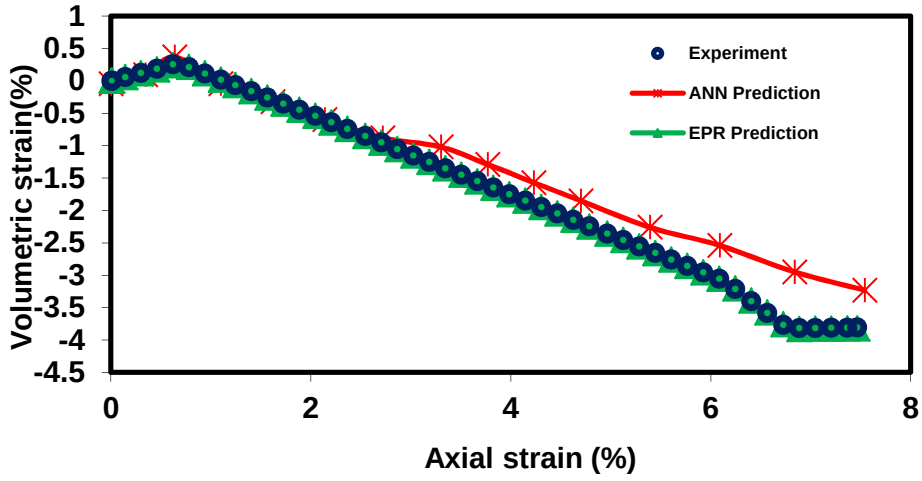

(b)

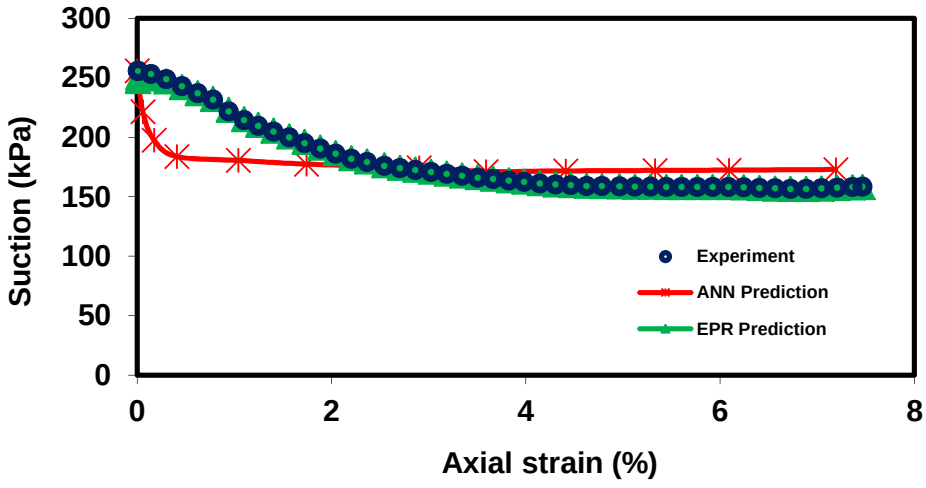

(c)

Figure 4.2: Comparing the EPR model predictions with experimental testing data and ANN predictions (MGU 6) for deviator stress, volumetric strain, and suction

Table 4.4: CoD values for EPR models

Equation	CoD values for training (%)	CoD values for testing (%)
Deviator stress (Equation 4.2.2)	99.96	99.85
Volumetric strain (Equation 4.2.3)	99.99	99.99
Suction (Equation 4.2.4)	99.99	99.98

Comparison of the results and the high CoD values for the EPR models indicate the excellent performance of these models in capturing the underlying relationships between contributing parameters and response of unsaturated soils and also in generalizing the training to predict the behaviour of the soils under unseen conditions. The results also show that EPR outperforms ANN and its results are a closer match to the actual experimental data.

4.2.6 Predicting entire stress paths using the EPR models

In this section, the EPR models (Equations 4-2, 4-3 and 4-4) are used to predict the entire stress paths, incrementally, point by point, in $q:\varepsilon_a$; $s:\varepsilon_a$ and $\varepsilon_v:\varepsilon_a$ spaces. Results from three different sets of (testing) data (MGU6, 8, and 10) are used to evaluate the ability of the incremental EPR models to predict the complete behaviour of unsaturated soil during the entire stress paths. The values of water content and dry density represent the initial conditions of the soil and are constant throughout the tests. Other contributing parameters are updated in each incremental step, considering the values from the previous increment and the EPR models' outputs in response to an axial strain increment. Figure 4.3 illustrates the procedure followed for updating of the input parameters and building the entire stress path for a shearing stage of a triaxial test.

At the start of the shearing stage in a conventional triaxial experiment, the values of all parameters are known. For example in a test on a sample of unsaturated soil, the values of $(p-u_a)_i, s_i, \varepsilon_{a,i}, q_i$ and $\varepsilon_{v,i}$ are known from values of applied cell pressure, air pressure, water pressure and volume change at the end of the previous stage (e.g., $\varepsilon_{a,i}=0$ and $q_i=0$). Then, for a prescribed increment of axial strain, $\Delta\varepsilon_a$, the values of q_{i+1}, $\varepsilon_{v,i+1}$ and s_{i+1} are calculated from the EPR models (Equations 4-2, 4-3 and 4-4 respectively). For the next increment, the values of $(p-u_a)_i, s_i, \varepsilon_{a,i}, q_i$ and $\varepsilon_{v,i}$ are updated as:

$$s_i = s_{i+1}$$

$$q_i = q_{i+1}$$

$$\varepsilon_{v,i} = \varepsilon_{v,i+1}$$

$$(p-u_a)_i = (p-u_a)_i + \left(\frac{q_{i+1}-q_i}{3}\right)$$

$$\varepsilon_{a,i} = \varepsilon_{a,i} + \Delta\varepsilon_a$$

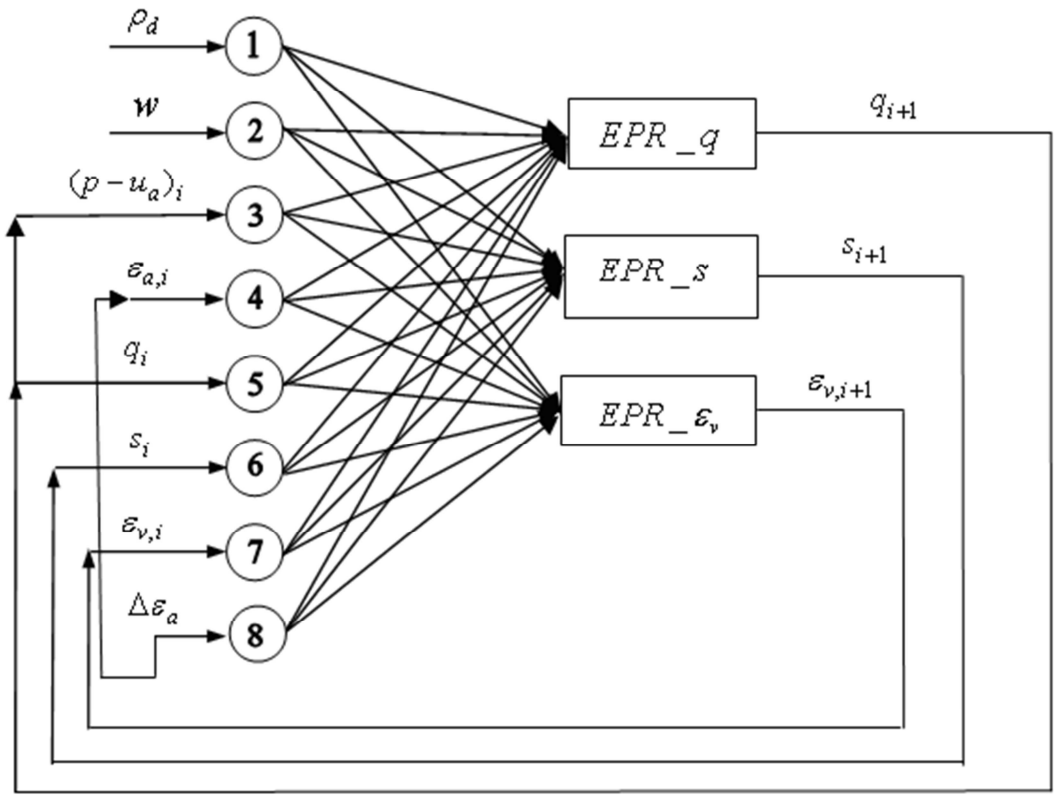

Figure 4.3: Incremental procedure for predicting the entire stress path

In this way the second points on the curves are predicted. The incremental procedure is continued until all the points on the three curves are predicted and the curves are established. Figures 4.4, 4.5 and 4.6 show the comparisons between the three complete curves predicted using the EPR models following the above incremental procedure and the actual experimental data as well as ANN simulation results (Habibagahi and Bamdad, 2003) for three tests. It should be noted that the data for these tests have not been introduced to the EPR during the model building process. The predicted stress paths are in excellent agreement with the experimental results. Despite the facts that (i) the entire curves have been predicted point by point and; (ii) the errors of prediction of the individual points are accumulated in this prediction, the EPR models are able to predict the complete stress paths with a very high degree of accuracy. These are testaments to the robustness of the developed EPR framework for modelling of unsaturated soils.

4.2.7 Sensitivity analysis

A parametric study was carried out for further examination of the prediction capabilities of the proposed EPR models and the extent to which they represent the physical relationships and the effects of different input parameters on the model output. In a typical testing data set (MGU6, with basic soil properties given in Table 4.2, which was not used in the model construction stage) all the input parameters but the one being examined were kept constant and the model predictions for three different values (within the maximum and minimum values of the parameter in the database within the available range of data) of the parameter under study were investigated.

The effect of dry density was examined by applying the models (Equations 4-2, 4-3 and 4-4) to predict the changes in the $q:\varepsilon_a$, $\varepsilon_v:\varepsilon_a$ and $s:\varepsilon_a$ curves for three different values of dry density (1.5, 1.6 and 1.7 Mg/m^3). The results are shown in Figure 4.7. Figure 4.7a shows the influence of dry density on stress-strain behaviour, while other parameters are kept constant. As expected, with an increase in dry density the stress-strain curve shifts upwards, indicating that a sample with higher density has a higher failure point and also a larger elastic modulus. Figure 4.7c shows the influence of dry density on variation of soil suction with axial straining. For a soil sample, increasing dry density increases the tendency for dilation of the sample which in turn results in an increase in the suction during constant water content shearing, as correctly predicted by the model. Figure 4.7b shows the influence of ρ_d on variation of volumetric strain.

The effect of water content of soil is evaluated by applying the models to predict the changes in the deviator stress-axial strain, suction-axial strain, and volumetric strain-axial strain curves for 3 different values of water content (18%, 21% and 24%). Figure 4.8a shows the effect of change in water content on the stress-strain behaviour of unsaturated soil. As expected, increasing the water content causes the curve to move downwards indicating that a dryer sample has a higher failure stress and a greater stiffness (elastic modulus). Figure 4.8c shows that generally for a soil sample increasing water content decreases soil suction. Figure 4.8b shows that, for the soil used in this analysis, effect of water content on volumetric strain is negligible.

4.2.8 Discussion and conclusions

A number of EPR models were developed to model various aspects of unsaturated soil behaviour. Incremental relationships were presented. It was shown that the EPR models can capture the underlying relationships between various parameters directly from experimental triaxial data and predict the unsaturated soil behaviour with a very high accuracy. The EPR models were also tested using data that were not used in the training stage of the model development process; in this way, an unbiased performance indicator was obtained on the real prediction capability of the models.

The results showed the excellent ability of the EPR models in generalizing the training to predict the behaviour of unsaturated soils under unseen conditions. The proposed EPR models outperformed the ANN model and provided closer results to the experiments. The results of the sensitivity analysis conducted based on the EPR models were also consistent with the expected behaviour of unsaturated soils.

It was shown that the incremental EPR models can be used to predict the complete stress paths in the $q:\varepsilon_a$, $\varepsilon_v:\varepsilon_a$ and $s:\varepsilon_a$ spaces incrementally and point-by-point. The errors of prediction of the individual points were accumulated in this approach and still the EPR models were able to predict the complete stress paths with a very good degree of accuracy. This is another indication of the robustness of the developed EPR framework for modelling of unsaturated soils.

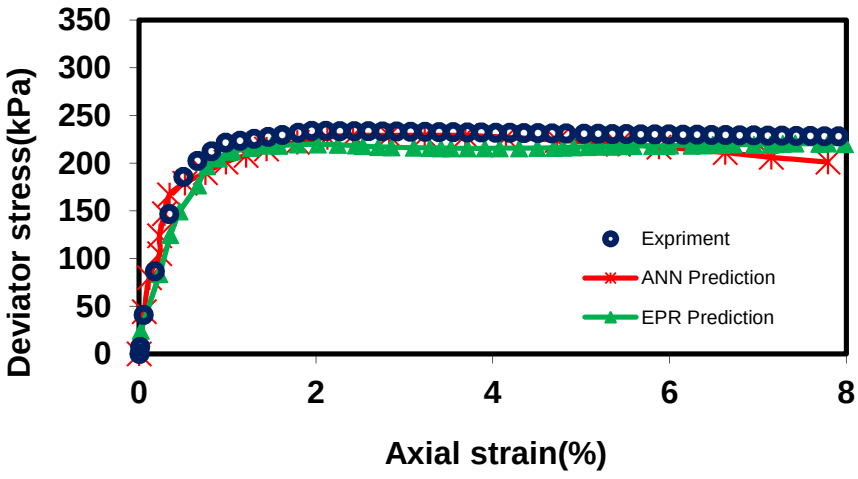

(a)

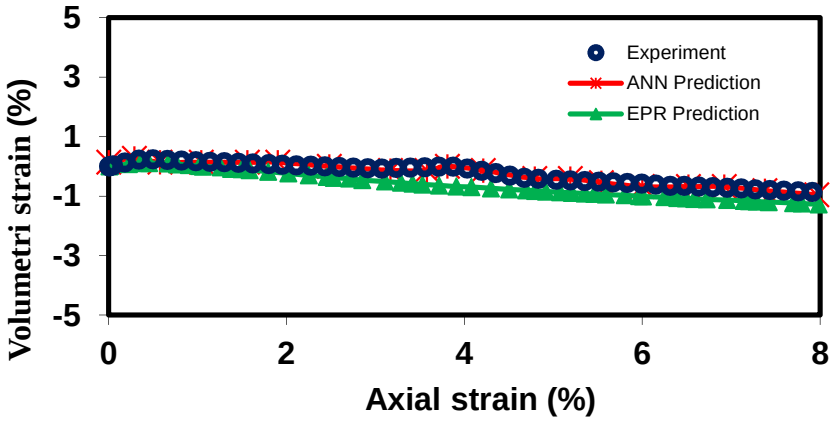

(b)

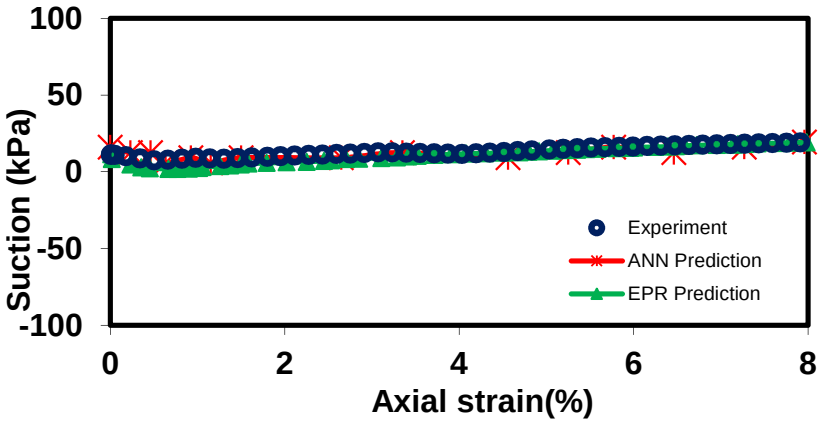

(c)

Figure 4.4: Comparison between the incremental EPR model predictions of an unseen data set with experimental data and ANN predictions for deviator stress, volumetric strain, and suction (MGU 10)

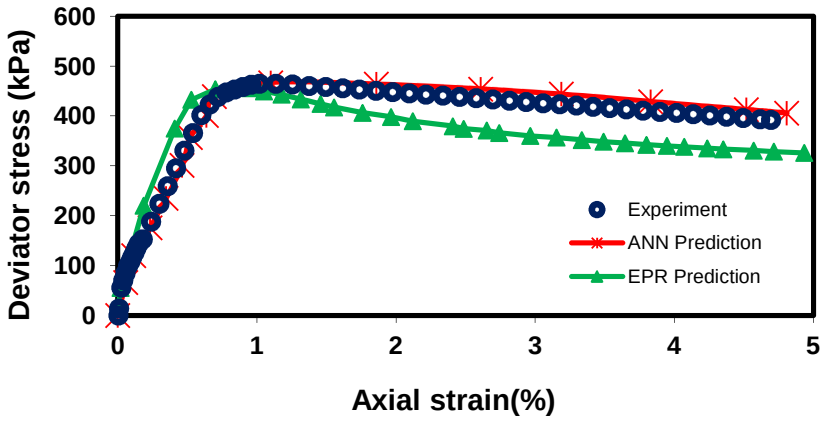

(a)

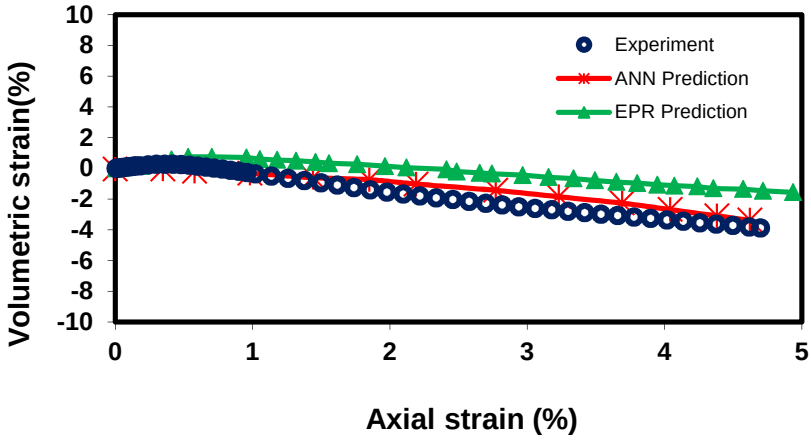

(b)

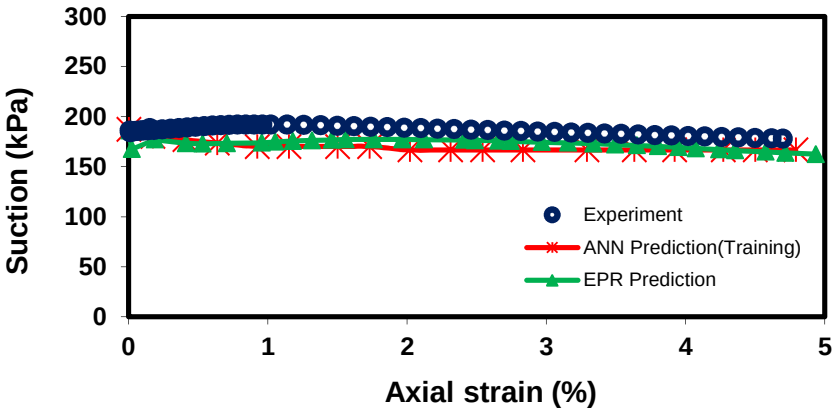

(c)

Figure 4.5: Comparison between the incremental EPR model predictions of an unseen data set with experimental data and ANN predictions for deviator stress, volumetric strain, and suction (MGU 8)

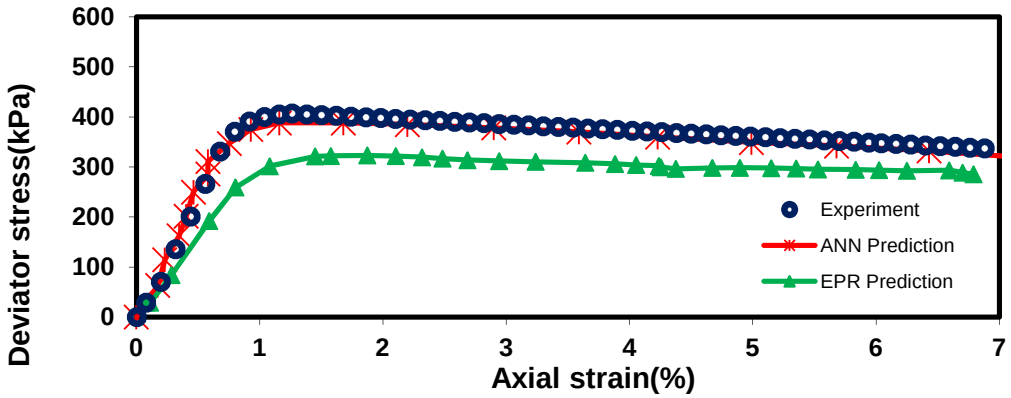

(a)

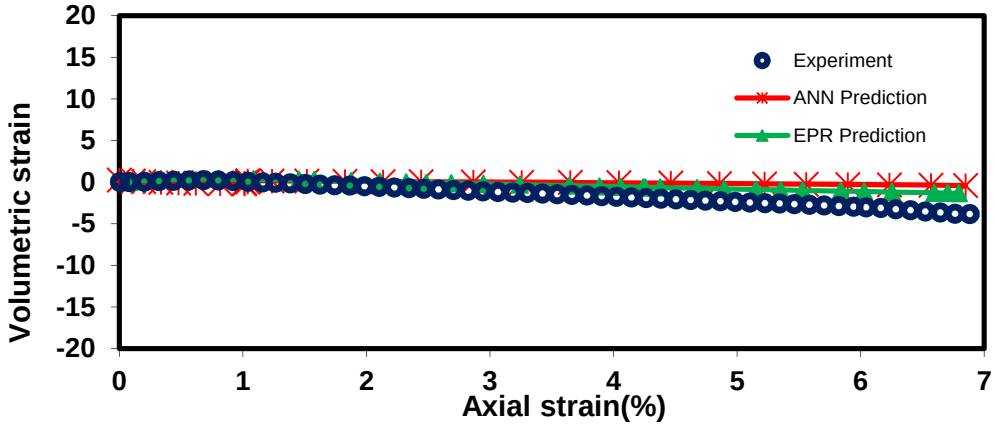

(b)

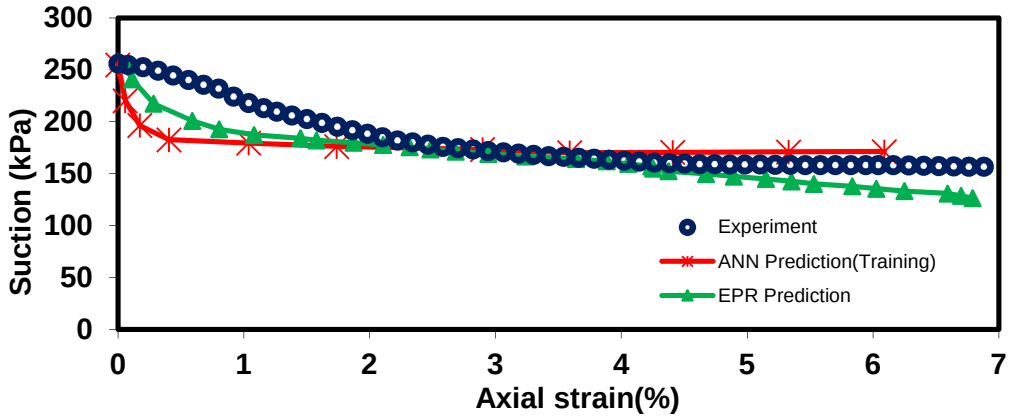

(c)

Figure 4.6: Comparison between the incremental EPR model predictions of an unseen data set with experimental data and ANN predictions for deviator stress, volumetric strain, and suction (MGU 6)

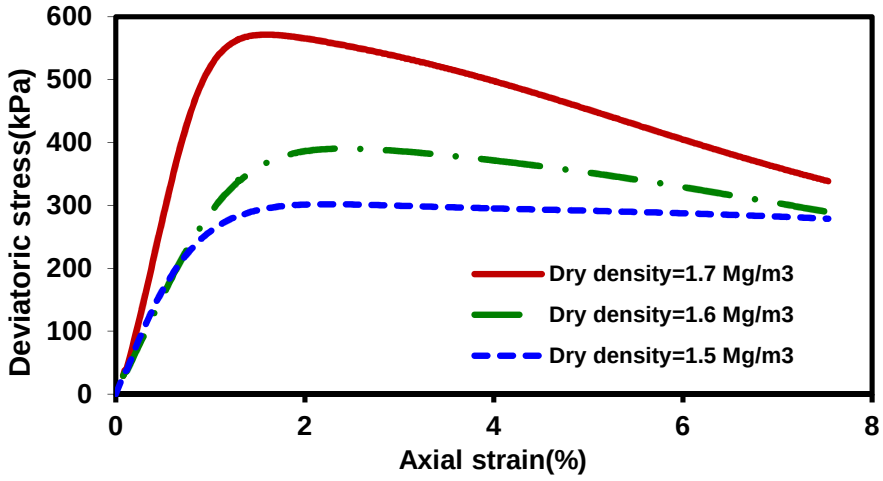

(a)

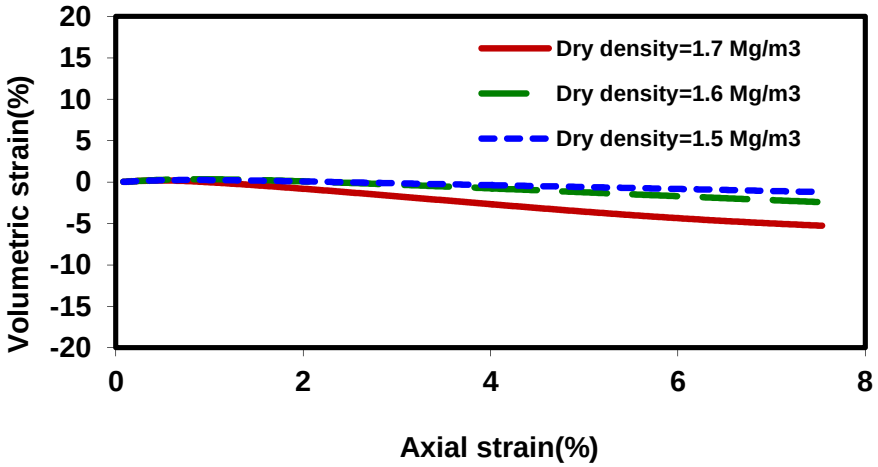

(b)

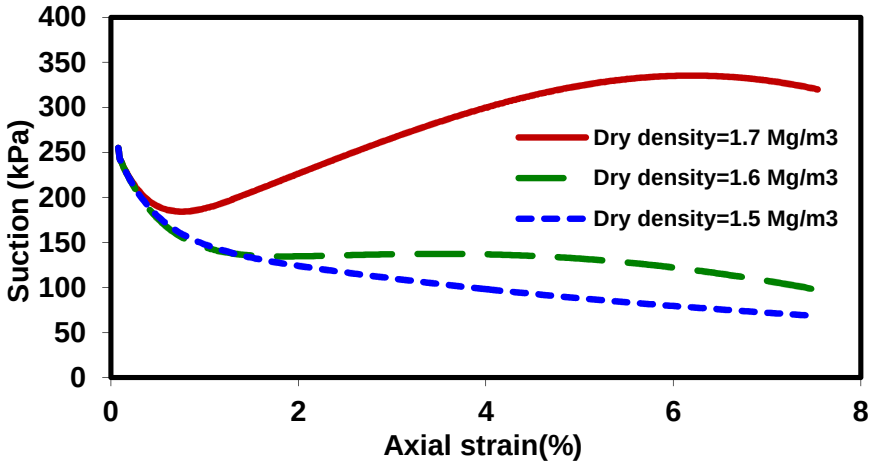

(c)

Figure 4.7: Influence of dry density on predicted parameters

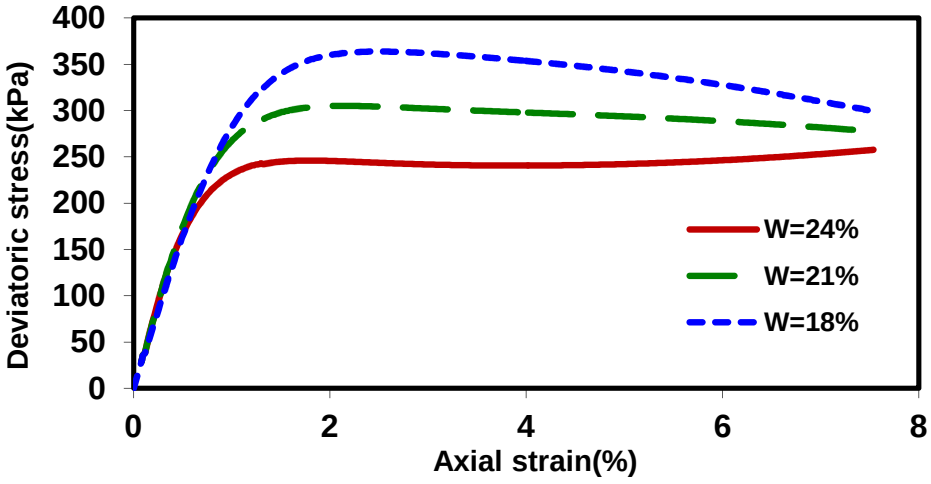

(a)

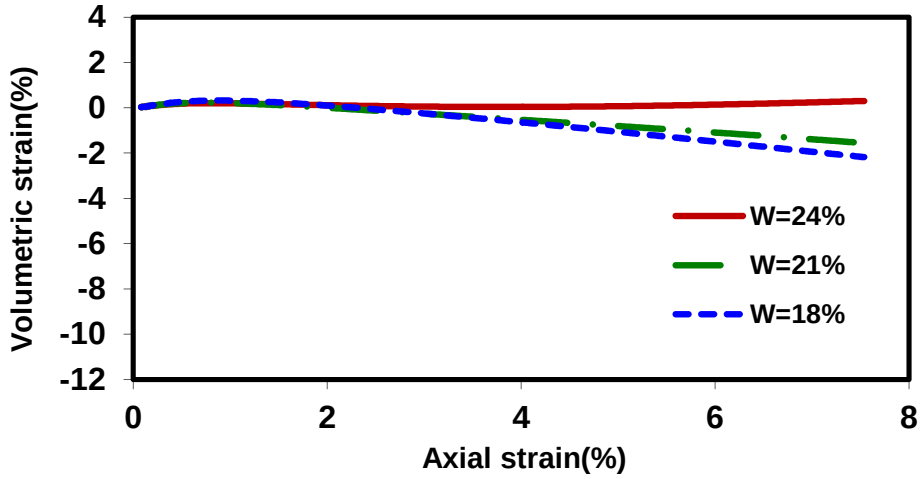

(b)

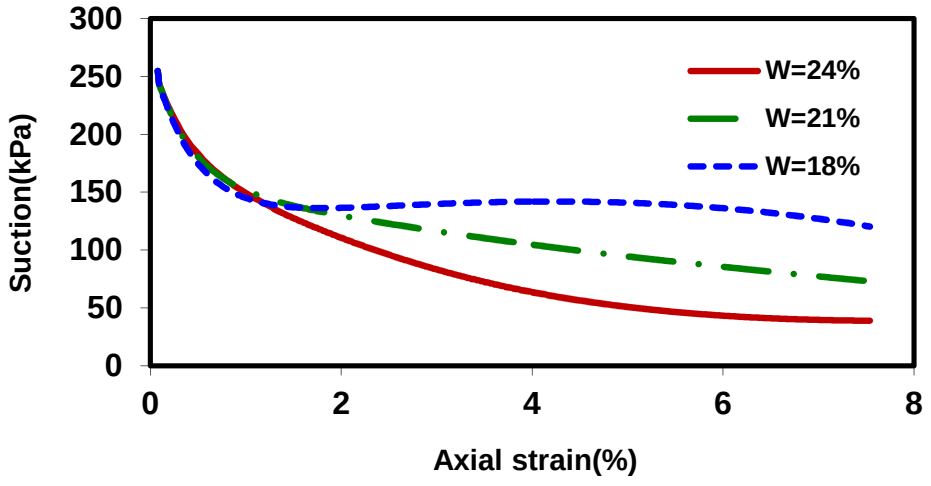

(c)

Figure 4.8: Influence of water content on predicted parameters

4.3 Modelling of soil-water characteristic curve in unsaturated soils

4.3.1 Introduction

Soil-water characteristic curve (SWCC) contains important information regarding the amount of water contained in the pores at a given soil suction and the pore size distribution corresponding to the stress state in the soil. SWCC can be viewed as a function that describes the water storage capacity of a soil as it is subjected to various suctions. Different aspects of unsaturated soil behaviour such as shear strength, volume change, diffusivity, and adsorption are related to soil-water characteristic curve. A number of researchers have studied the relation between the soil-water characteristic curve and the shear strength of soils (e.g., (Fredlund et al., 1995); (Vanapalli et al., 1996)).
There are different methods available to obtain the SWCC for a particular soil. SWCC may be determined directly or indirectly in the laboratory. Direct methods include pressure plate, Buchner funnel, tensiometers, and pressure membranes. These methods measure the pore-water pressure in the soil or impose a known air pressure to the soil and allow the water content to come to equilibrium with the imposed air pressure. Among these methods, conventional pressure plate test (ASTM D 6836) is the most common method. Indirect methods include filter paper and heat dissipation sensors. These methods use measurements or indicators of water content or a physical property that is sensitive to changes in water content; however, these experiments are costly and time consuming and therefore several methods have been proposed in the literature to determine SWCC values of unsaturated soils. These methods can be classified into five major groups described below ((Johari, Habibagahi and Ghahramani, 2006a)):

1. Fitting type equations for SWCC. In this group of equations simple mathematical equations are fitted to the experimental data and the unknown parameters are determined ((Brooks and Corey, 1964); (Van Genuchten, 1980); (Pedroso and Williams, 2010)).
2. Correlating parameters of an analytical equation with basic soil properties such as grain size distribution, porosity and dry density using regression analyses ((Cresswell and Paydar, 1996); (Tomasella and Hodnett, 1998); (Hutson and Cass, 1987); (Aubertin, Ricard and Chapuis, 1998)).
3. Physico-empirical modelling of SWCC. This approach converts the grain size distribution into a pore size distribution, which is in turn related to a distribution of water content and associated pore pressure ((Fredlund and Pham, 2006); (Zapata, Houston and Walsh, 2003); (Fredlund, Wilson and Fredlund, 2002); (Pereira and Fredlund, 2000)).
4. Artificial Intelligence (AI) methods such as neural networks, genetic programming and other machine learning techniques have been used in various disciplines of civil engineering ((Xie et al., 2006); (Muttil and Chau, 2006); (Cheng, Ou and Chau, 2002)). Predicting SWCC using artificial intelligence also falls into this group ((Johari and Javadi, 2010); (Johari, Habibagahi and Ghahramani, 2006a); (Johari, Habibagahi and Ghahramani, 2006b)).

In this research a new data mining technique, the Evolutionary Polynomial Regression (EPR), is applied to modelling of soil-characteristic curve in unsaturated soils. It is

shown that EPR may effectively be utilized to capture and represent the soil-water characteristic curve in unsaturated soils.

4.3.2 Database

Results from pressure plate tests performed on clay, silty clay, sandy loam, and loam reported by various researchers were adopted for the analysis. Table 4.5 indicates the range of the properties of the soil used in this study. Five parameters namely void ratio, saturated water content, logarithm of suction normalized with respect to atmospheric air pressure, clay content, and silt content were selected as the input. The output parameter was the gravimetric water content corresponding to the assigned input suction (Table 4.6). This database consists of the results from 130 pressure plate tests together with their grain size distributions. The experimental results (graphs) were digitized. Digitization resulted in a database including a total of 1890 patterns that were used for training and testing of the developed EPR model.

4.3.3 Data preparation

To select the most suitable combination of the training and testing data, a similar procedure detailed in section 4-2-3 was implemented. In this way, the most statistically consistent combination was used for construction and validation of the EPR model. Results from 104 tests, 80% of the total data base, were used for model construction and the remaining 20% (26 tests) were utilized to validate the developed EPR model.

Table 4.5: Range of soil properties used in the experiments

Properties	Range
Void ratio	0.458–2.846
Suction (kPa)	0.2–104,857.6
Specific gravity	2.28–2.92
Water content (%)	0.18–98.27
Dry density (kg/m3)	702–1,811
Saturated water content (%)	17.34–105.41
Clay content - <0.002mm - (%)	4.4–76.7
Silt content - 0.002mm to 0.075mm - (%)	10.3–87.5

Table 4.6: Parameters involved in the developed EPR model of SWCC *

Contributing parameters	Model output
e, w , Su , Cc , Sc	GWC

* e = void ratio; w = saturated water content; $S_u = \log(Suction / 100)$; C_C = clay content; S_C = silt content; GWC = Gravimetric water content

4.3.4 Modelling procedure

The data was divided into training and testing sets. One set was used for training to develop the model and the other one was used for validation to appraise the generalisation capabilities of the trained model. The maximum number of terms in the EPR equation was set to 15. Among developed EPR models, the one with the highest coefficient of determination value was selected to represent the soil-water characteristic curve:

$$GWC = \frac{1.48\times10^{-6}Su^3}{e^3\cdot Cc\cdot Sc} + \frac{1.8Su\cdot Cc^3 - 1.79e\cdot Su^2\cdot Cc\cdot Sc}{w} - \frac{4.07\times10^{-3}Su\cdot Sc + 0.25e\cdot Cc^2}{Cc} - 1.7\times10^{-3}w\cdot Su$$
$$+ 2.25\times10^{-3}w^2 - 0.17e\cdot w + 3.11e^2 - \frac{2.15e^2\cdot w^3}{Cc\cdot Sc^2} + 0.10214 \qquad 4\text{-}5$$

In this equation *e*, *w*, *Su*, *Cc* and *Sc* are void ratio, saturated water content, logarithm of suction normalized with respect to atmospheric air pressure, clay content, and silt content respectively. After training, the performance of the trained EPR model was examined using the validation dataset which had not been introduced to EPR during training. The purpose of validation was to examine the capabilities of the trained model in generalizing the training to conditions that have not been seen by the model in the training phase. Figure 4.9 compares the predicted values of gravimetric water content with the actual data for training and validation stages. The figure shows a very good correlation between the predictions of the EPR model and the actual data both for modelling and validation datasets. Figures 4.10 and 4.11 compare gravimetric water contents predicted using the Genetic Programming (GP) model presented by Johari et al (2006a) and the approach proposed by Fredlund et al (1997) against the actual data for the same training and validation datasets. Table 4.7 also shows the values of the coefficient of determination for EPR, GP, and Fredlund et al (1997) methods for both training and validation stages. Comparing Figures 4.9, 4.10 and 4.11 and the coefficients of determination for all three methods in Table 4.7 shows the robustness and high capabilities of the proposed EPR model in predicting the soil-water characteristic curve in unsaturated soils.

Figures 4.12 and 4.13 show typical soil water characteristic curves predicted using the proposed EPR model in comparison to the actual curves from the database for training and unseen validation data cases respectively. Figure 4.14 compares the SWCC curves predicted using of the EPR model with the ones from the GP and Fredlund et al (1997) methods and the experimental data. Comparison of the results highlights the capabilities of the proposed EPR model in providing accurate predictions of the soil-water characteristic curve in unsaturated soils.

Table 4.7: CoD values for SWCC models

Equation	CoD values for training (%)	CoD values for testing (%)
EPR Model	95.76	98.38
Genetic programming (Johari et al, 2006a)	94	93
Fredlund et al (1997)	85	89

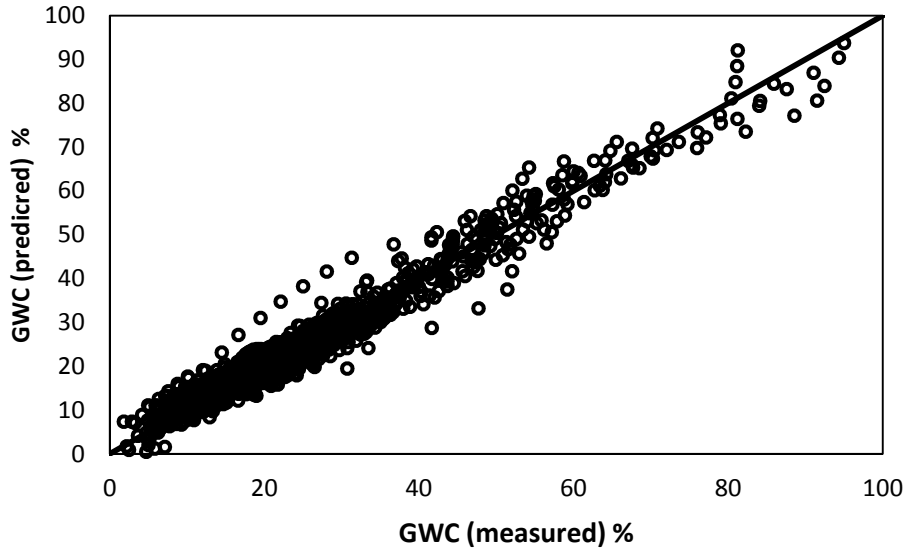

(a)

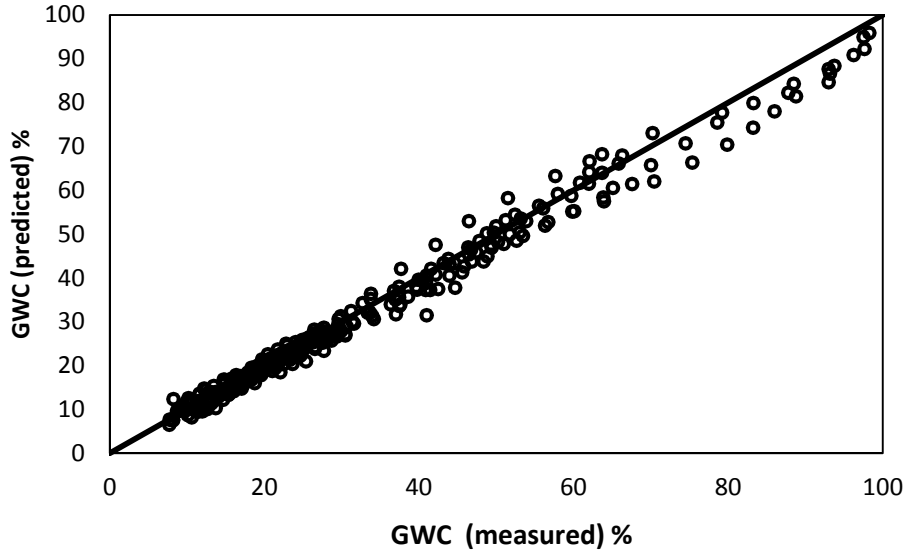

(b)

Figure 4.9: Actual versus predicted GWC for (a) training (CoD=95.76%) and (b) validation (CoD=98.38%) data for EPR model

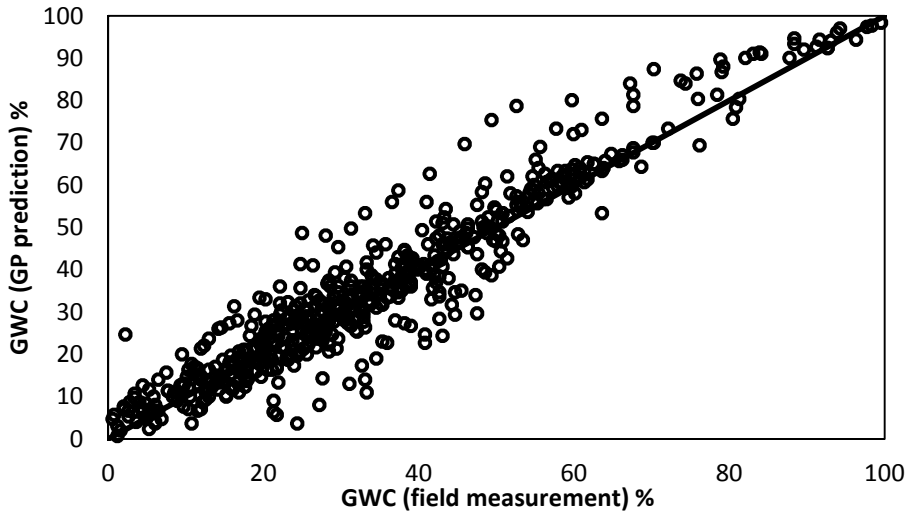

(a)

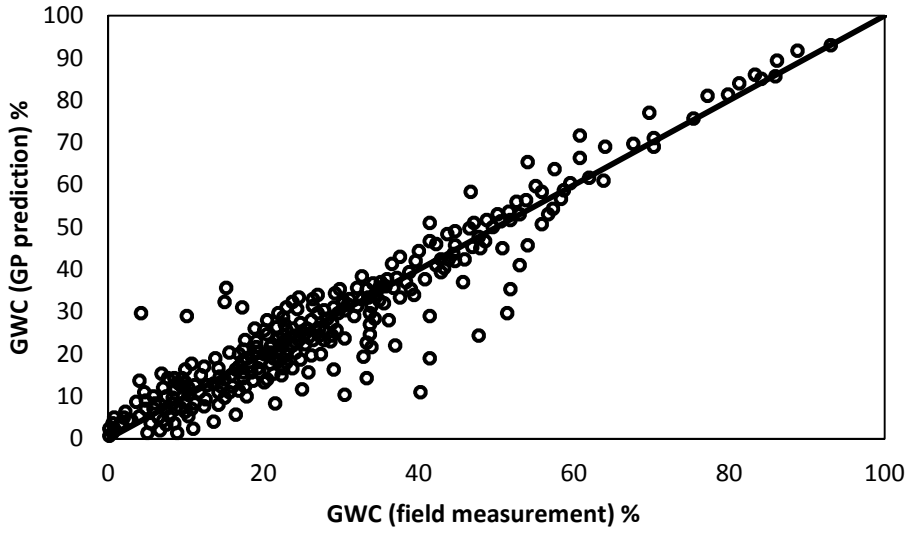

(b)

Figure 4.10: Actual versus predicted GWC for (a) training (CoD=94%) and (b) validation (CoD=93%) data for GP model (Johari, Habibagahi and Ghahramani, 2006a)

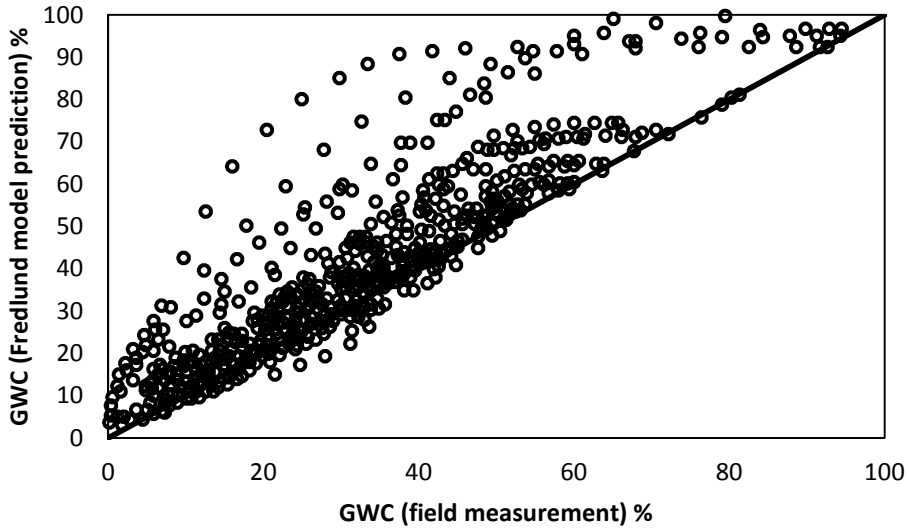

(a)

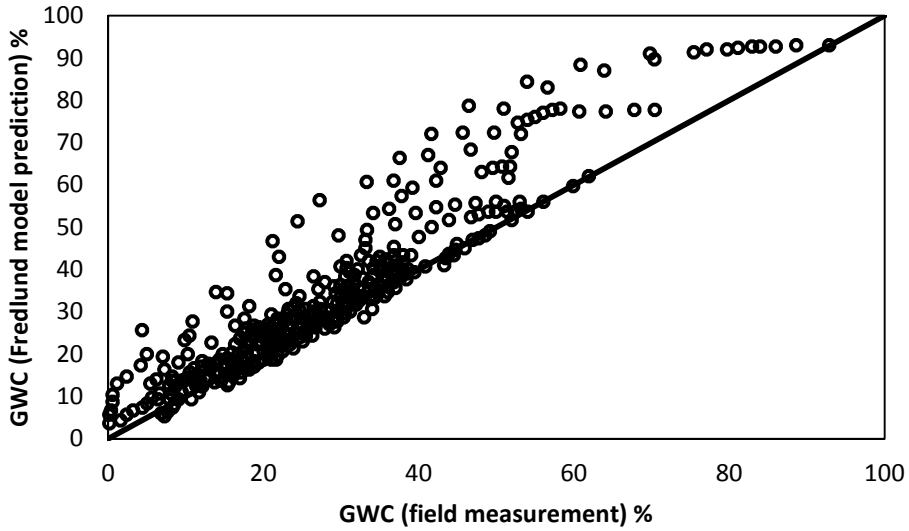

(b)

Figure 4.11: Actual versus predicted GWC for (a) training (CoD=85%) and (b) validation (CoD=89%) data for the model of Fredlund et al (Fredlund, Fredlund and Wilson, 1997)

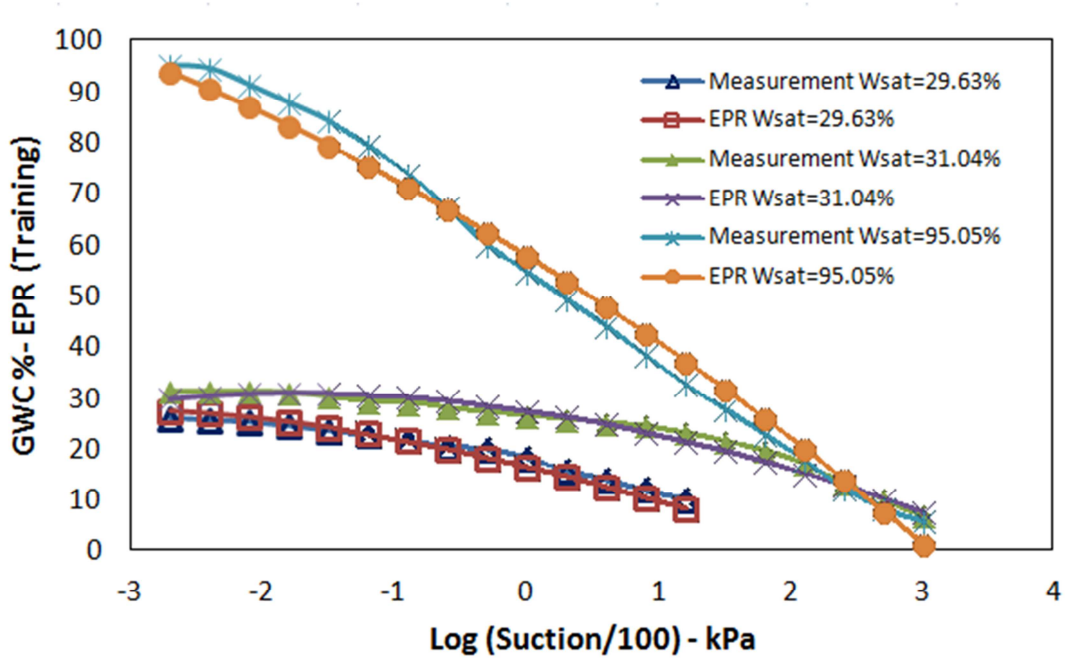

Figure 4.12: Typical prediction results of the EPR model for training data cases with saturated water contents of 29.63%, 31.04% and 95.05%

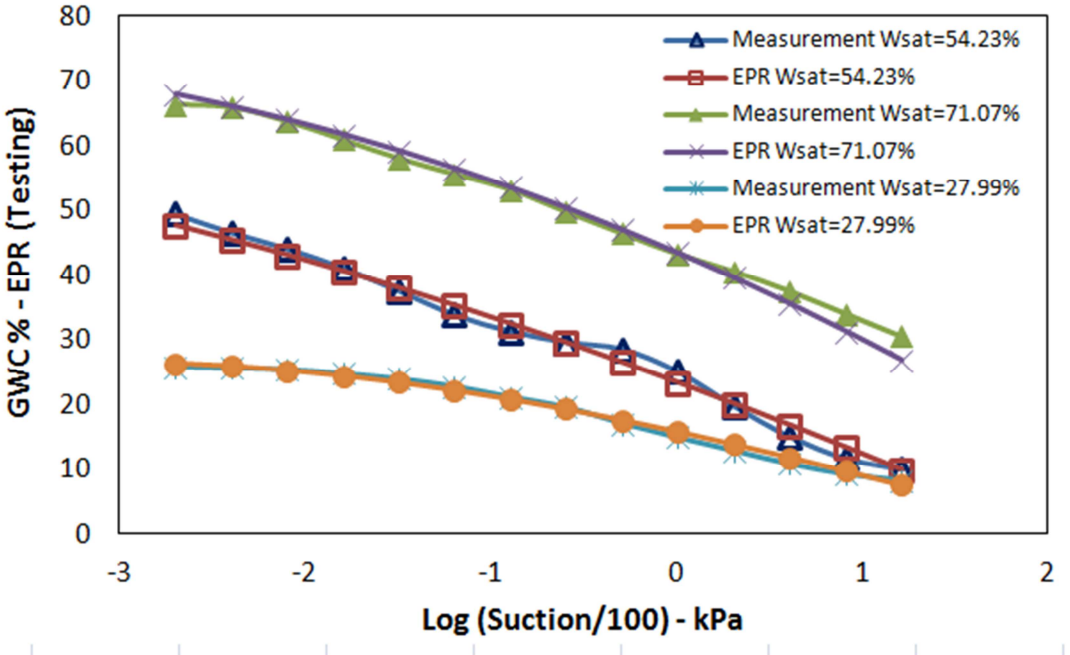

Figure 4.13: Typical prediction results of the EPR model for validation data cases with saturated water contents of 54.23%, 71.07% and 27.99%

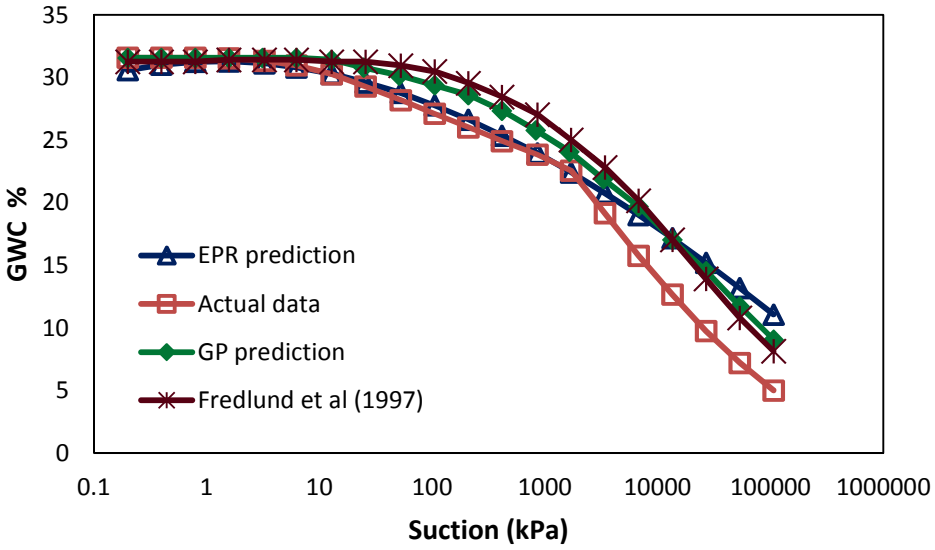

(a)

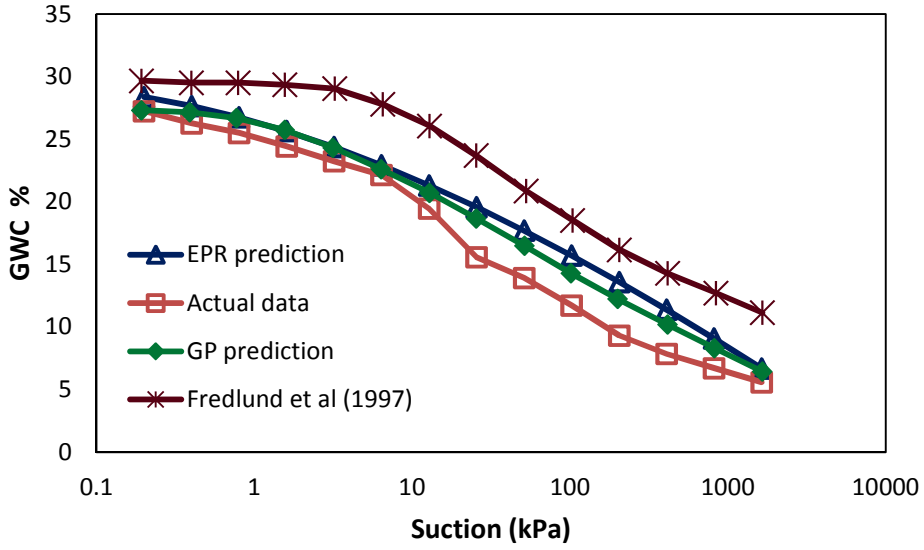

(b)

Figure 4.14: Comparison of the SWCCs predicted by the EPR, GP and Fredlund et al (1997) models and the actual data for two cases with saturated water contents of (a) 31.57% and (b) 29.63%

Table 4.8 and Figure 4.15 are also generated based on the measured data and the EPR based equation. They show that the developed EPR model reaches the saturated water content when suction tends to zero and also approaches zero as suction tends to infinity. It can be seen that the proposed EPR model satisfactorily meets the SWCC limits within the range of data used to develop and validate the model.

Table 4.8: SWCC limits

Sample	Suction (kPa)	e	Silt content %	Clay content %	Wsat %	GWC(EPR) %
Train	0	0.8	62	20	29.63	27.15
Train	0	0.869	31	66	31.04	28.84
Train	0	2.69	29	63	95.05	96.83
Test	0	1.415	62	18	54.23	55.61
Test	0	1.919	51	48	71.07	73.30
Test	0	0.736	70	20	27.99	25.36

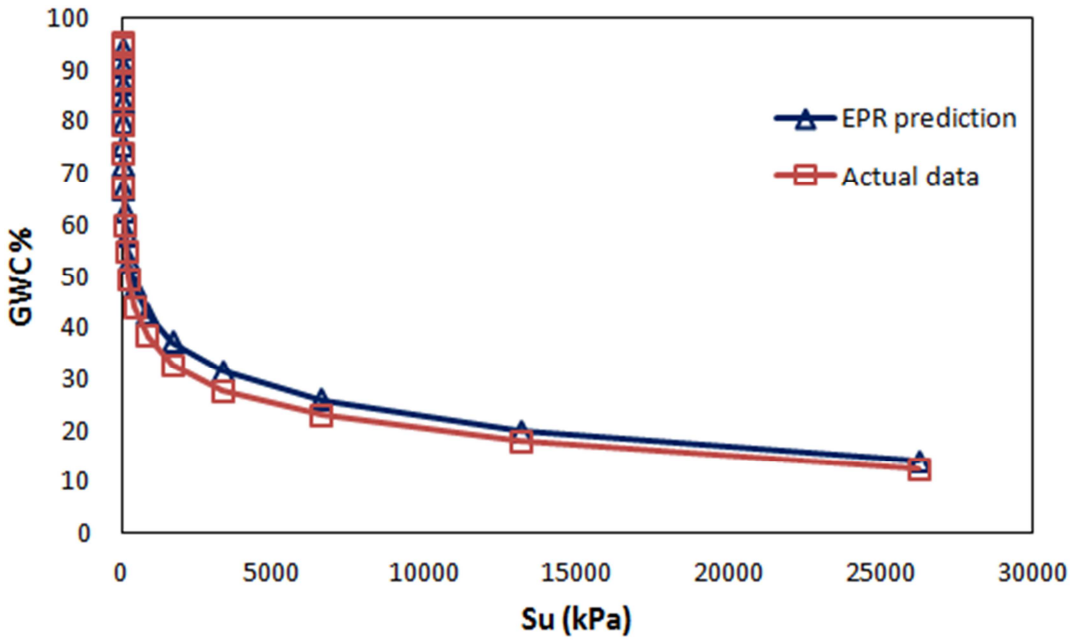

Figure 4.15: Soil-water characteristic curve limits

4.3.5 Parametric study

Figure 4.16 shows the results of the parametric study conducted based on the procedure detailed in section 4.2.7, to investigate the effect of changes in clay and silt contents on the EPR model output. The results show an upward shift of the SWCC by increasing the clay and silt contents of the soil. This behaviour of the model is consistent with the results from previous studies (Johari, Habibagahi and Ghahramani, 2006a). Increasing fine grained particles (silt and clay) caused the specific surface of the soil mixture to increase leading to higher values of the gravimetric water content at a constant suction. The effect of increasing clay content on gravimetric water content at higher suction values seemed to be more significant than its effect at lower soil suctions; whereas, the effect of increasing silt content on the gravimetric water content was almost similar for different suction values. The sensitivity of the EPR model to void ratio (e) and initial water content parameters are also presented in Figures 4.17a and 4.17b. Figure 4.17a shows that all parameters being the same, at a given suction, a soil with a higher void ratio will have lower water content as the suction would be more effective in draining the soil with higher void ratio. Figure 4.17b also shows that all parameters (void ratio, clay content and silt content) being the same, for a given suction change, the amount of

water drained will be more or less similar. So, if hypothetically, soil "A" has a higher initial water content than soil "B", it will also have a higher water content at the end of application of suction increment as the amount of change is almost the same and mainly dependent on the void ratio.
A study was also conducted to investigate the interdependencies between different contributing parameters to the proposed model. Figure 4.18 represents the effect of change in saturated water content on predicted GWC-suction relationship for three different values of silt content. Similar results for three different values of clay content are shown in Figure 4.19. It can be seen that for a given saturated water content and a given suction, increasing clay or silt (fines) content increases water retention capacity of the soil.
Figure 4.20 shows the combined effects of void ratio and silt content on the GWC-suction relationships. It is shown that, as expected, for a given silt content value and at a given suction, a higher void ratio will result in a lower water content in the soil. Similar results can be observed for the effects of void ratio and clay content (Fig. 4.21). Figure 4.22 shows the combined effects of void ratio and saturated water content on the GWC-suction relationships. It is shown that, as expected, for a given saturated water content value and at a given suction, a higher void ratio will result in a lower water content in the soil. The results of sensitivity analysis showed that the EPR model has been able to capture and represent different aspects of behaviour of unsaturated soil correctly.

4.3.6 Discussion and conclusions

Soil–water characteristic curve (SWCC) is one of the most important components of any model for describing unsaturated soil behaviour. It describes the variation of soil suction with changes in water content. SWCC can be viewed as a function describing the water storage capacity of the soil as it is subjected to various soil suctions.
An EPR model was developed and validated using a database from pressure plate tests performed on clay, silty clay, sandy loam, and loam soils. The results of model predictions were compared with actual data as well as two other models.
A parametric study was conducted to evaluate the effect of the contributing parameters on the predictions of the proposed EPR model. Combined effects of the parameters were also considered in the sensitivity analysis to investigate the interdependencies of parameters and their effect on the soil-water characteristic curve and the extent to which the developed models can represent the physical relationships between involved parameters.
Comparison of the results showed that the developed EPR model provides very accurate predictions for SWCC. The developed model presents a structured and transparent representation of SWCC, allowing a physical interpretation of the problem that gives the user insight into the relationship between the soil-water characteristic curve and various contributing parameters and is capable of predicting the unsaturated behaviour of soils with reasonable accuracy. From the practical point of view, the EPR model presented in this research is easy to use and provides results that are more accurate than or as accurate as the existing models.
The presented results show the robustness of the proposed EPR approach in modelling of soil-water characteristic curve in unsaturated soils and that the developed model is capable of providing a better understanding of the problem and is easily interpretable by the user.

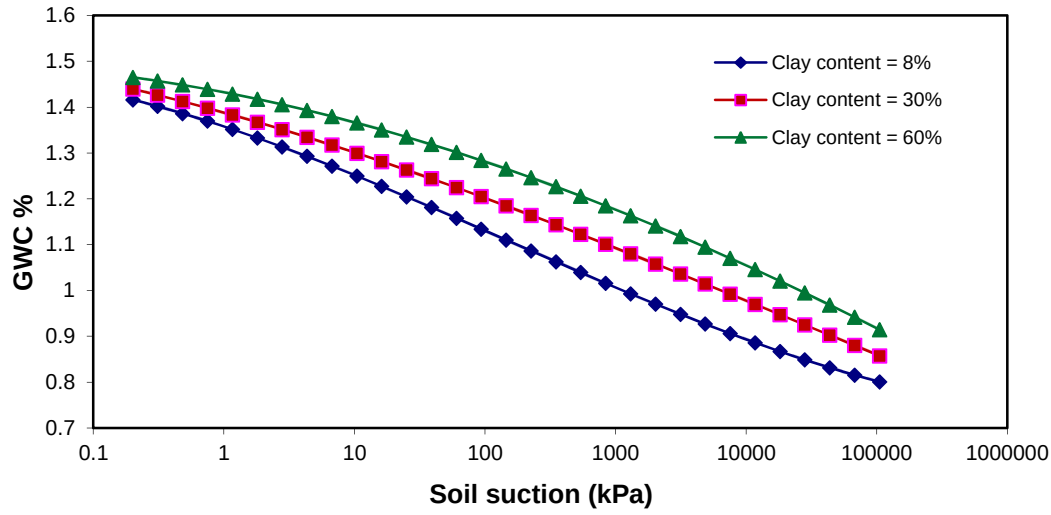

(a)

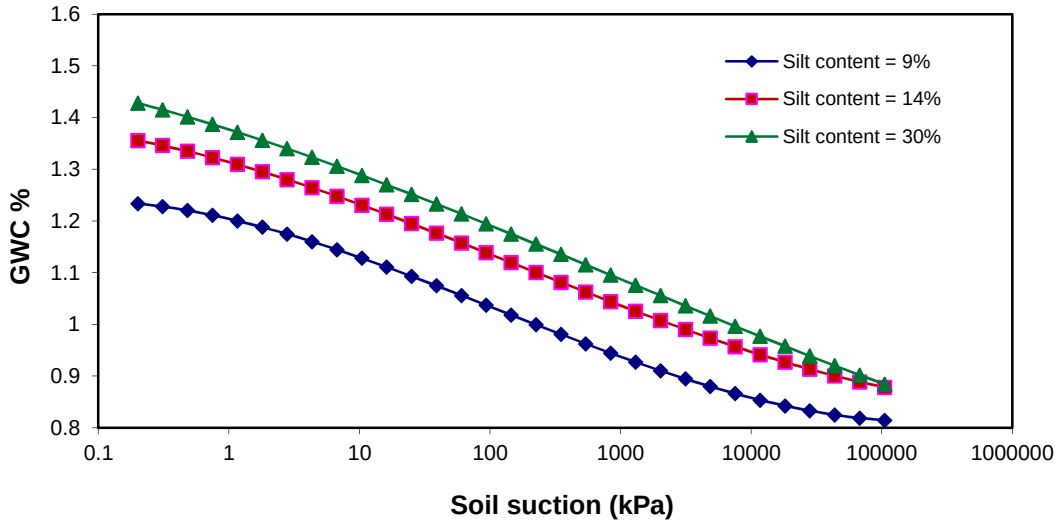

(b)

Figure 4.16: Changes in SWCC with (a) clay content and (b) silt content

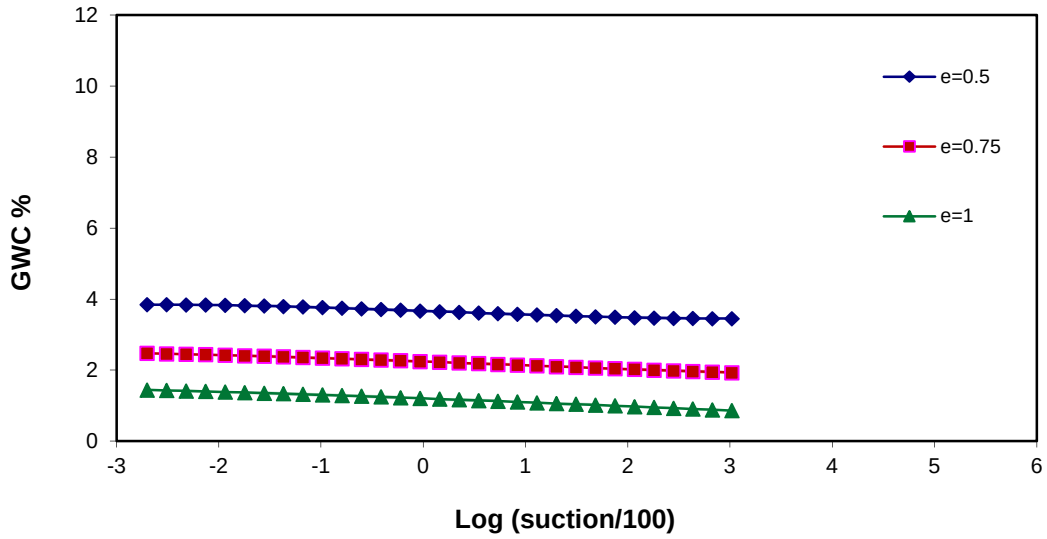

(a)

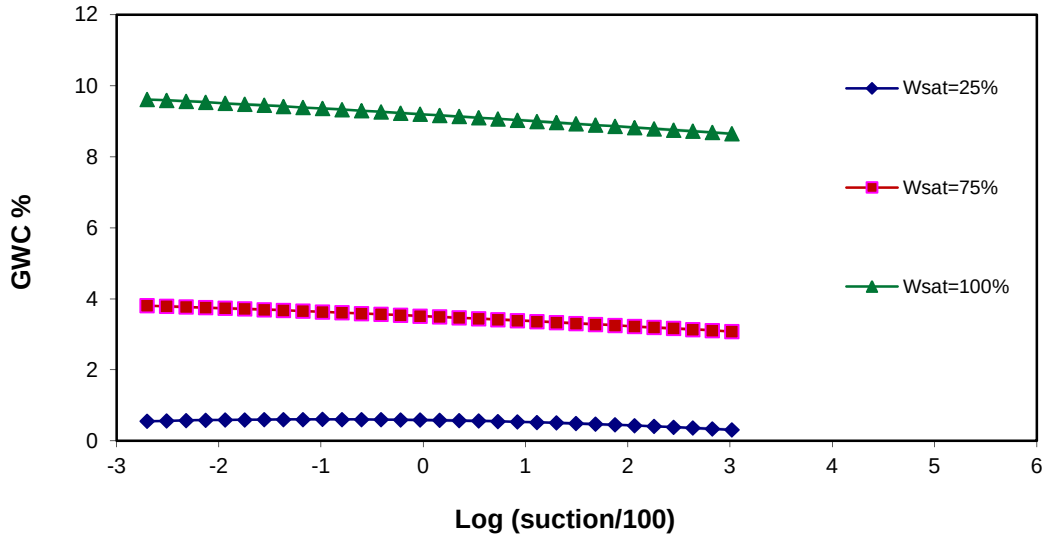

(b)

Figure 4.17: Sensitivity analysis results of SWCC model considering (a) void ratio and (b) water content

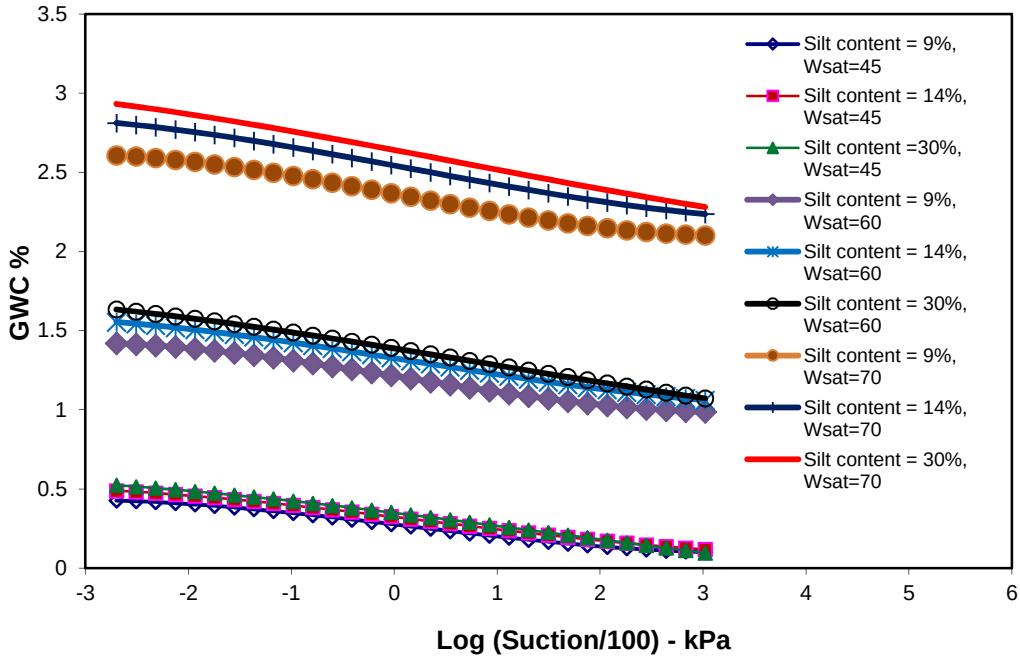

Figure 4.18: Effect of change in saturated water content on predicted GWC-suction relationship for different silt contents

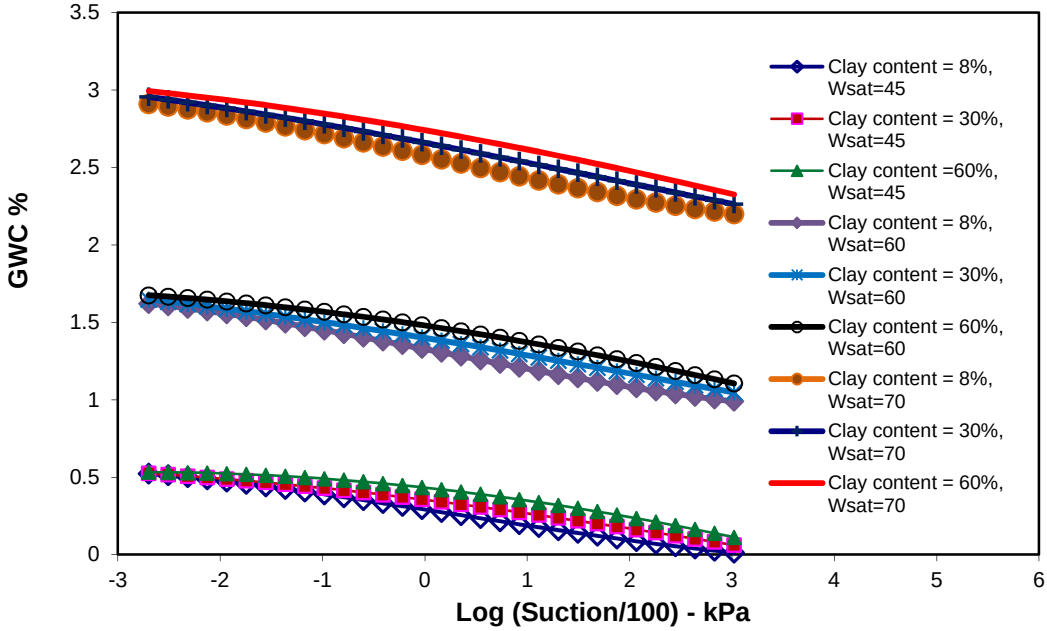

Figure 4.19: Effect of change in saturated water content on predicted GWC-suction relationship for different clay contents

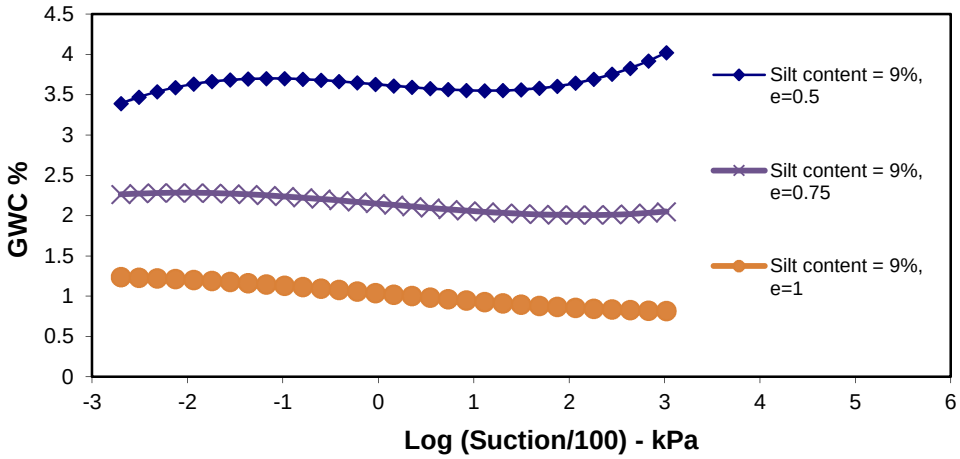

(a)

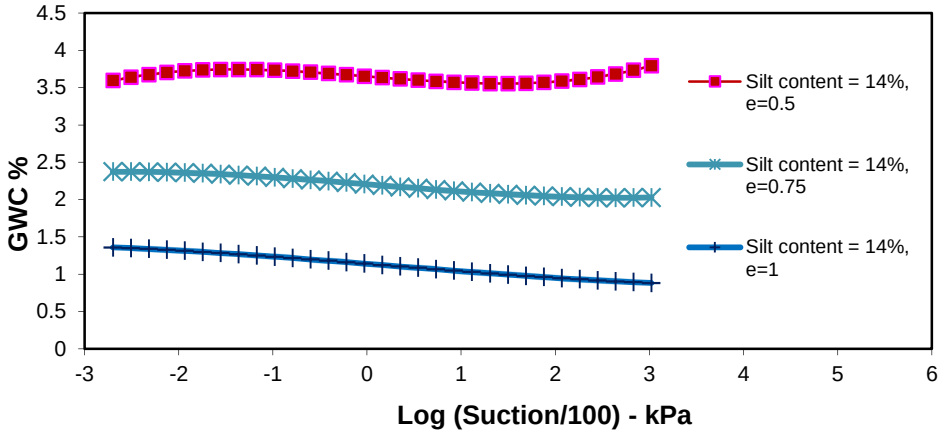

(b)

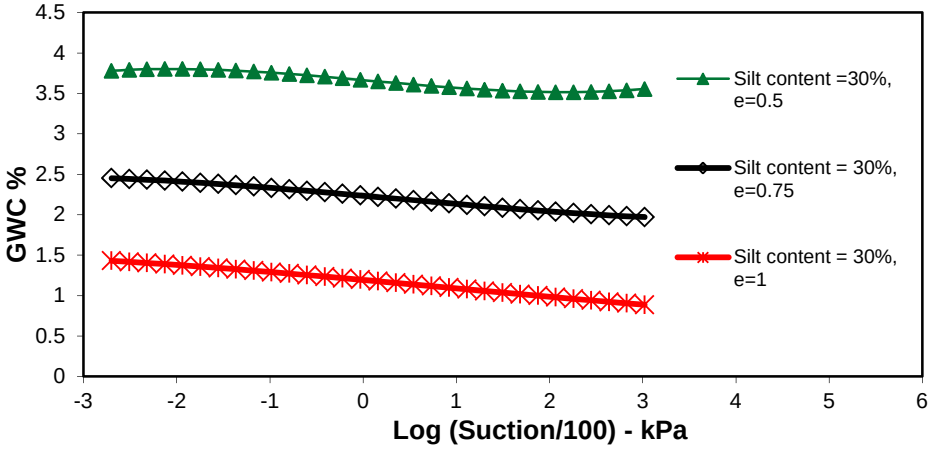

(c)

Figure 4.20: Combined effects of void ratio and silt content on GWC-suction relationship

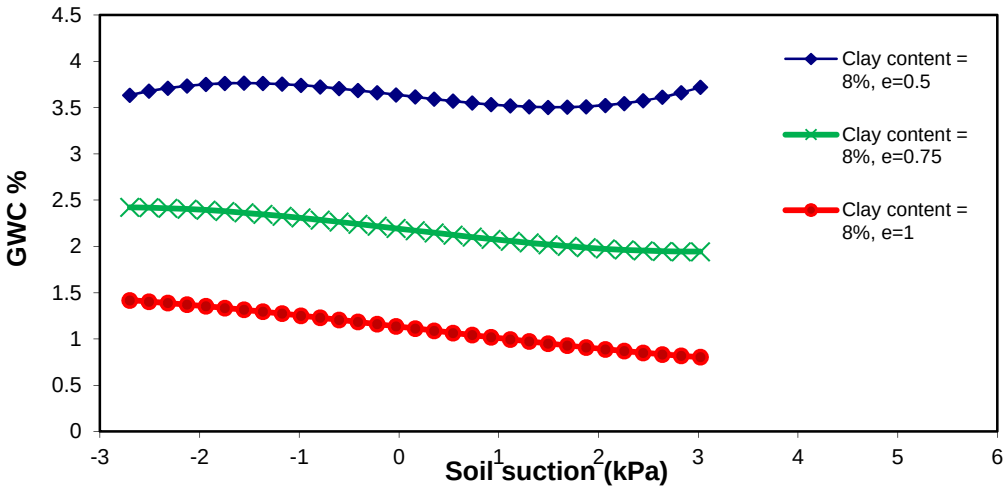

(a)

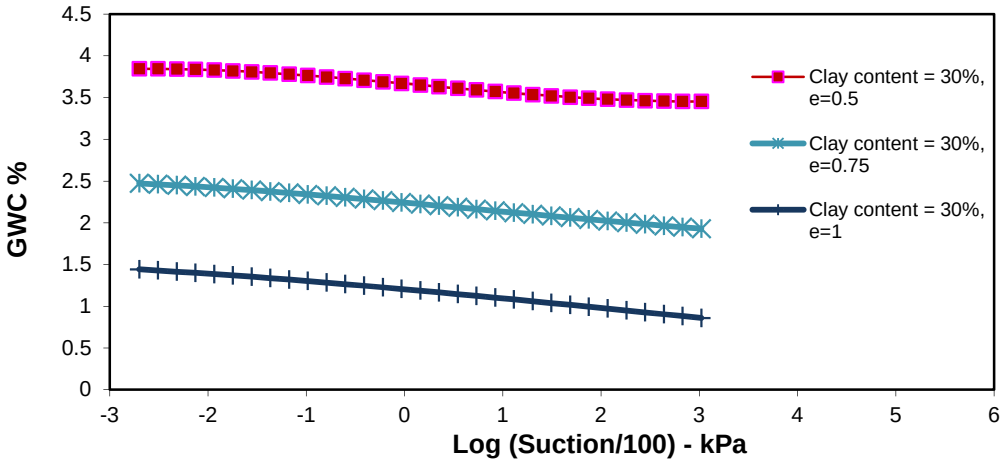

(b)

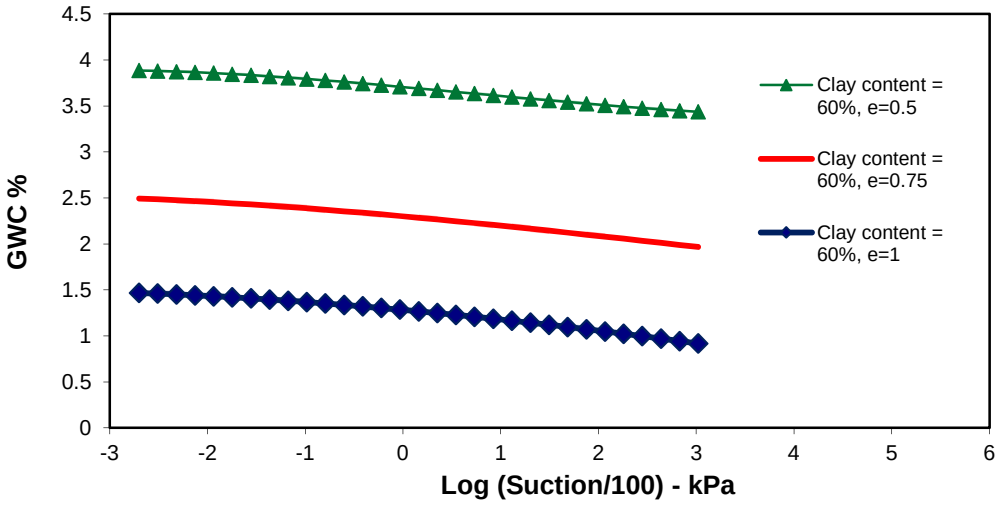

(c)

Figure 4.21: Combined effects of void ratio and clay content on GWC-suction relationship

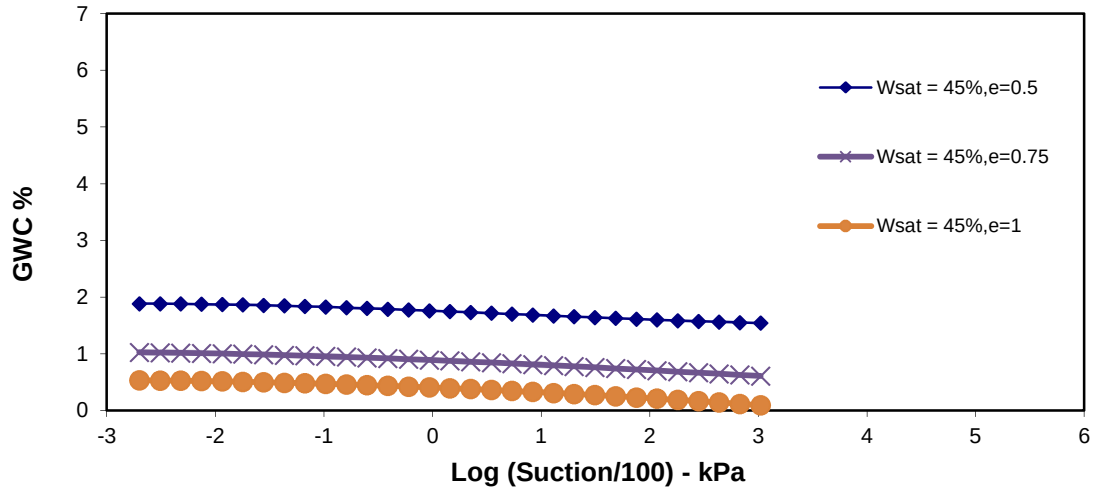

(a)

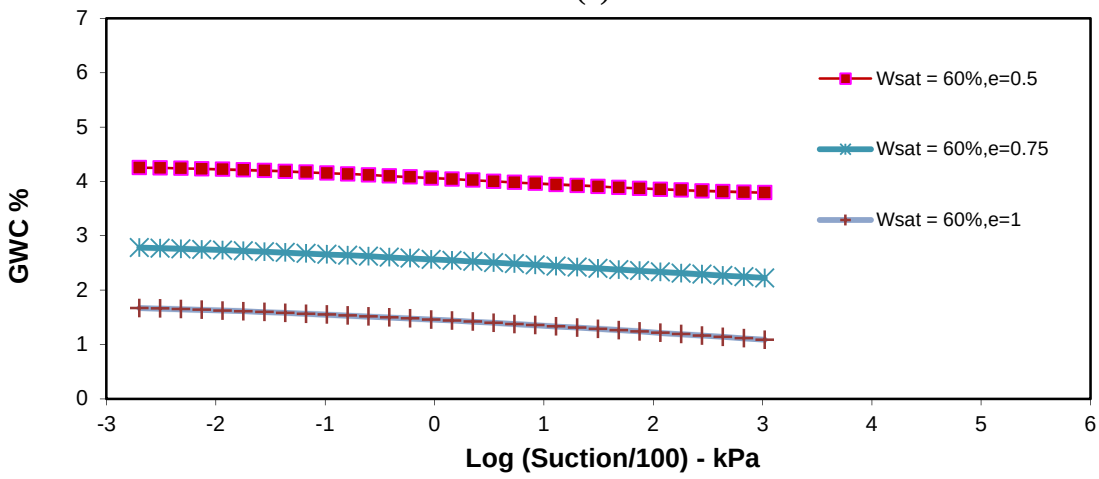

(b)

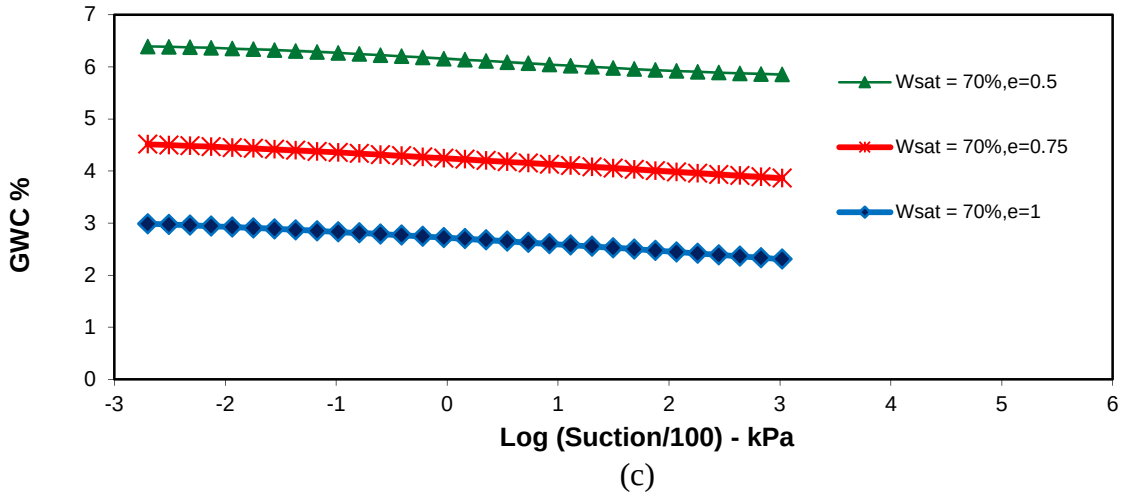

(c)

Figure 4.22: Combined effects of void ratio and saturated water content on GWC-suction relationship

4.4 EPR modelling of thermo-mechanical behaviour of unsaturated soils

4.4.1 Introduction

Extensive research has been done in the past decades to investigate the effects of temperature on different aspects of unsaturated soil behaviour. A literature review of the recent works is presented below.

4.4.1.1 Thermal effects on basic soil parameters

Over the past decades thermal effects in saturated soils have been centre of attention of researchers. The basic parameters of soils like liquid limit, plastic limit, specific gravity, and compaction characteristics are mainly considered to be affected by temperature variations. Temperature effects on liquid and plastic limits were first investigated by Youssef et al (1961). They conducted a series of tests on compacted clay samples and showed that increasing temperature caused reduction in both liquid limit and plastic limit at temperatures between 14^{o}C and 35^{o}C. Lagurous (1969) performed similar tests on kaolinite, illite, monmorillonitic and monmorillonitic-illite clays at temperatures ranging from 1.7^{o}C to 40.6^{o}C and found that an increase in temperature caused a reduction in liquid limit and plastic limit. He also showed that the effects were most significant on the monmorillonitic clays. Wang et al (1990) also reported that there were no thermal effects on the Atterberg limits over temperatures ranging from 20^{o}C to 400^{o}C for kaolinite and 20^{o}C to 500^{o}C for bentonite. They also observed that the specific gravity of kaolinite and bentonite were not sensitive to temperature in the range between 20^{o}C and 400^{o}C. Towhata et al (1994) also reported that there were no significant effects of preheating up to 200^{o}C on the liquid and plastic limits of the kaolin and bentonite clay. Effect of temperature on soil (specifically with a high clay content) compaction was investigated by Hogentogler (1936). He performed compaction tests in the laboratory on several predominantly clay soils and reported that as the temperature increases and causes the optimum moisture content to decrease, the maximum dry unit weight increases accordingly. Burmister (1964) also reported similar results.

4.4.1.2 Effects of temperature on volume change behaviour

The effects of temperature on the volume change behaviour of saturated soils have also been investigated by many researchers e.g. Campanella and Mitchell (1968), Plum and Esrig (1969), Habibagahi (1973), Demars and Charles (1982), Houston et al (1985), Eriksson (1989), Hueckel and Baldi (1990), Towhata et al (1993), Boudali et al (1994), Tanaka (1995), Crilly (1996), Fox and Edil (1996), Delage et al (2000) and Graham et al (2001).

Campanella and Mitchell (1968) conducted a series of isotropic triaxial consolidation tests on a saturated illite (remoulded) at different temperatures. The results showed that the compressibility index was independent of temperature, but the preconsolidation pressure decreased with increasing temperature. Investigation of the variation of the compressibility index with temperature was also conducted by Plum and Esrig (1969). They carried out one-dimensional consolidation tests on illite and Newfield clay and showed that the compressibility index of the material varied with temperature. Their

finding was not in agreement with the observations of Campanella and Mitchell (1968). However, the changes in the compressibility index with temperature were not remarkable at high stresses. Eriksson (1989) and Boudali et al (1994) repeated the tests that were performed with Plum and Esrig (1969) and the results revealed that temperature had no affect on the compressibility indices. Graham et al (2001) also presented similar results for the case of isotropic consolidation.

Decrease in the preconsolidation pressure with temperature was also investigated by Habibagahi (1973), Eriksson (1989), Boudali et al (1994), and Graham et al (2001) and led to similar results to the ones reported by Campanella and Mitchell (1968). This effect causes the entire compression curve to move towards smaller effective stresses with increasing temperature. Some research works have also shown that as temperature increases, the soil becomes more compressible in unloading-reloading regions (e.g. Eriksson (1989); Takaka (1995)). However, results to the contrary have also been reported by Campanella and Mitchell (1968) and Crilly (1996).

Researchers have also shown that heating normally consolidated and lightly overconsolidated soils under constant effective stress induces volume contraction; whereas, cooling the same type of soil causes swelling; (e.g. see Paaswell (1967); Campanella and Mitchell (1968); Plum and Esrig (1969); Baldi et al (1988); Hueckel and Baldi (1990); Towhata et al (1993); Boudali et al (1994); Delage et al (2000)). The experimental results have also indicated that the rate of consolidation of clays increases with the increasing temperature (e.g. Paaswell (1967); and Towhata et al (1993)). Paaswell (1967) showed that in a given effective stress condition, the greater the increase in temperature, the greater the volumetric contraction. He showed that the volumetric contraction decreases with increasing overconsolidation ratio and turns into expansion at large overconsolidation ratios. Similar results were also reported from other researchers (e.g. Plum and Esrig (1969); Baldi et al (1988); Hueckel and Baldi (1990); Towhata et al (1993); Delage et al (2000)). Delage et al (2000) showed that, in an increasing temperature condition, heavily overconsolidated soils dilate at low temperatures but contract at high temperatures.

The behaviour of normally consolidated soils under cycles of heating and cooling was investigated by a number of researchers such as Campanella and Mitchell (1968), Plum and Esrig (1969), Demars and Charles (1982), Hueckel and Baldi (1990) and Towhata et al (1993). The experimental results showed that the volume contraction of normally consolidated soils caused by heating under constant effective stress could not be recovered by later cooling. The results also showed that normally consolidated soils become overconsolidated when subjected to cyclic thermal loading. Additionally, Demars and Charles (1982) found that irreversible volume contraction due to cyclic thermal loading does not depend on effective confining pressure for normally consolidated soils; however, it is a function of overconsolidation ratio in case of overconsolidated soils. Plum and Esrig (1969) and Hueckel and Baldi (1990) indicated that after heating, soils continue to behave as they are normally consolidated. Towhata et al (1993) also found that heating creates a quasi-overconsolidated behaviour.

Investigations by Campanella and Mitchell (1968), Plum and Esrig (1969), Houston et al (1985), Towhata et al (1993), and Fox and Edil (1996) showed that temperature affects the primary consolidation as well as the secondary compression. Campanella and Mitchell (1968) showed that the larger the increase in temperature, the greater the rate of secondary compression. They also found that if the specimens cooled before heating, the change in the rate of secondary compression would be small in case that the initial temperature of the sample was not exceeded. Fox and Edil (1996), Plum and Esrig (1969), Houston et al (1985) and Towhata et al (1993) revealed that the rate of

secondary compression exponentially varies with temperature variations. They also observed that cooling causes a decrease in the rate of secondary compression.

4.4.1.3 Effects of temperature on pore water pressure

Change in temperature may induce significant change in pore water pressure and as this causes a change in effective stress, it can lead to failure in a specimen under constant deviator stress.
Temperature-induced pore water pressure has been investigated by a number of researchers (e.g. Campanella and Mitchell (1968); Plum and Esrig (1969); Hueckel and Baldi (1990); Hueckel and Pellegrini (1992); Tanaka (1995) and Graham et al (2001)). General results have shown that the pore water pressure increases with increase in temperature and decreases when the temperature drops. Test results presented by Campanella and Mitchell (1968) also showed that the cyclic temperature change results in a hysteretic change in pore water pressure. The pore water pressure developed in saturated soils during heating-cooling cycles involves a rise in pore water pressure during heating, while the subsequent cooling causes a substantial decrease in pore water pressure. The drop observed in pore water pressure during cooling was more than twice the increase during heating. They also observed that a large pore-water pressure increase induced by heating may cause a large irreversible strain and a possible mechanical failure. Tanaka (1995) and Graham et al (2001) showed that temperature induced pore water pressure could be normalised by the initial effective confining pressure but not by the pre-consolidation pressure.
Heating induced failure in saturated soils was also investigated by Hueckel and Baldi (1990). They conducted a series of undrained triaxial tests at constant deviator stress and showed that a rise in pore water pressure due to monotonic heating causes the sample to fail.

4.4.1.4 Effects of temperature on shear strength and stress/strain characteristics

Investigators have been conducted to study the effects of temperature on the shear strength and the stress/strain characteristics of saturated soils. Experimental results reported by Hueckel and Baldi (1990), and Graham et al (2001) showed that temperature had no effect on the critical state line in the deviator stress/ mean effective stress plane. Lingnua (1993) and Houston et al (1985) studied the uniqueness of the critical state line in the deviator stress/ mean effective stress plane. They found a small shift in the critical state line with changes in temperature. The shrinkage of yield locus with increasing temperature was also observed in the experimental results of Hueckel and Baldi (1990), Tanaka et al (1997), Cui et al (2000) and Graham et al (2001).
Sherif and Burrous (1969) and Maruyama (1969) studied the effects of temperature on shear strength by conducting unconfined compression tests on normally consolidated saturated clays. The results showed that increase in temperature causes the pore water pressure to increase and reduces the undrained shear strength of the soil. Lagurous (1969) carried out unconfined compression tests at different temperatures on compacted soil specimens at optimum moisture content. Before testing, the compacted specimens were kept in a chamber to achieve the testing temperature. The results revealed that unconfined compressive strength increases with increasing temperature. The increase in the unconfined compressive strength was attributed to the evaporation of water from the soil specimens in the testing chamber. Water evaporation caused the degree of saturation to drop and the suction in the specimen to increase. An increase in suction

resulted in an increase in the effective stress, and thus unconfined compressive strength increased with elevating temperature.
Hueckel and Baldi (1990) conducted drained triaxial tests on overconsolidated Pontida silty clay samples, which had been heated under drained condition. The results showed that an increase in temperature lowered the peak shear strength and reduced the dilation of the samples towards the critical state. Since the excess pore-water pressure was allowed to dissipate during heating, the effective stress of the samples remained constant. However, the size of the yield locus decreased with increasing temperature, so the peak shear strength decreased as the temperature increased. Similarly, the reduction in the size of the yield locus reduced the over consolidation ratio of the samples, and thus less dilation was observed during shearing towards the critical state.
Lingnau et al (1995) performed consolidated undrained triaxial compression tests on lightly overconsolidated sand-bentonite specimens, by applying heat and cell pressure under drained conditions and then shearing the samples undrained at constant temperature. The results showed that the undrained shear strength reduced with increasing initial temperature. Kuntiwattanakul et al (1995) also conducted several consolidated undrained triaxial tests along different heating and consolidation paths. It was revealed that, for normally consolidated clays, the undrained shear strength and stiffness of specimens were highly affected by heating under an initially drained condition. However, they remained unaffected for overconsolidated clay. It was argued that an increase in the temperature created compression in normally consolidated soils, which reduced with increasing overconsolidation ratio. Thus, the thermal effect on the undrained shear strength was more pronounced in normally consolidated soils as compared to overconsolidated soils.

4.4.1.5 Hydro-thermo-mechanical models for unsaturated soils

Hydro-thermo-mechanical models have been proposed by a number of researchers over the past decades to represent the behaviour of unsaturated soils. Philip and deVries (1957) introduced a model representing the coupled heat and moisture transfer in rigid porous media under the combined gradients of temperature and moisture. de Vries (1958) included moisture and latent heat storage in the vapour phase, and the advection of sensible heat by water in their previous model. Sophocleous (1978), Milly (1982), Thomas and King (1991) and Thomas and Sansom (1995) modified the Philip and deVries model using matric suction rather than volumetric moisture content as the model's primary variable. Ewen and Thomas (1989) and Thomas and Li (1997) validated the theory presented by Philip and de Vries (1957) both in the laboratory and in the field revealing reasonable agreement between the theoretical analyses and the laboratory/field results.
Geraminegad and Saxena (1986) developed a model considering the effect of matrix deformation on moisture, heat and gas flow through the porous media. Mechanical behaviour of the soil in their model was defined in terms of "stress state surface" and "independent stress state variables". The total stress tensor in excess of air pressure (net stress) and suction were considered to be independent in this model ((Matyas and Radhakrishna, 1968); (Fredlund and Morgenstern, 1977)). Later on, Thomas and He (1997) presented a coupled version of this formulation. Matrix displacement vector was considered as a primary variable in their model, and the coupling effects between the temperature and deformation and the energy balance equation was improved in this model by including moisture and latent heat storage in the vapour phase, in addition to the advection of heat by water previously accounted for by de Vries (1958). Similar

formulations were also presented by Gawin et al (1995), and Zhou et al (1998). Gawin et al (1995) introduced the constitutive laws of the solid phase using the effective stress concept. They used the degree of saturation as the effective stress parameter and also retained the degree of saturation as the main coupling element between the air and water flow fields.

Booker and Smith (1989) and Britto et al (1989) investigated simulating the consolidation and pore-water pressure around hot cylinders buried in saturated clay. These models consider only the reversible volume change of the soil due to a change in temperature.

Khalili and Loret (2001) presented an alternative theory for heat and mass transport through deformable unsaturated porous media. They extended their previous work (Loret and Khalili, 2000) on fully coupled isothermal flow and deformation in variably saturated porous media to include thermal coupling effects. The bases used to develop the governing equations included the equations of equilibrium, the effective stress concept, Darcy's law, Fourier's law and the conservation equations of mass and energy. The thermo-hydro-mechanical coupling processes considered in their model were: thermal expansion, thermal convection by moving fluid, fluid flux due to temperature gradient and phase exchange (vaporisation, condensation).

Wenhua et al (2004) presented a thermo-hydro-mechanical (THM) constitutive model for unsaturated soils. The influences of temperature on the hydro-mechanical behaviour in unsaturated soils were considered in this model. Particularly, the thermal softening phenomenon, i.e. decreases in value of pre-consolidation pressure and in critical value of the suction of the SI (suction increase) curve with heating process, was quantitatively modelled using experimental data. Francois and Laloui (2008) introduced an unconventional constitutive model for unsaturated soils. A generalized effective stress framework was adopted that included a number of intrinsic thermo-hydro-mechanical connections to represent the stress state in the soil. Two coupled constitutive aspects were used to fully describe the non-isothermal behaviour of unsaturated soils. The mechanical constitutive part was built on the concepts of bounding surface theory and multi-mechanism plasticity, but the water retention characteristics were described using elasto-plasticity.

Another thermo-hydro-mechanical (THM) constitutive model for unsaturated soils was proposed by Dumont et at (2010). In this research the effective stress concept was extended to unsaturated soils with the introduction of a capillary stress. This capillary stress was based on a micro-structural model and calculated from attraction forces due to water menisci. The effects of desaturation and the thermal softening phenomenon were modelled with the minimal number of material parameters.

A thermo-elastic-plastic model was also suggested by Uchaipichat (2005) for unsaturated soils based on the effective stress principle by taking the thermo-mechanical and suction coupling effects into account. The thermo-elastic-plastic constitutive equations for stress-strain relations and changes in fluid content were established in this model. Uchaipichat and Khalili (2009) published the results of an experimental investigation on thermo-hydro-mechanical behaviour of an unsaturated silt. They conducted an extensive array of isothermal and non-isothermal tests including temperature controlled soaking and desaturation, temperature and suction controlled isotropic consolidation, and suction controlled thermal loading and unloading tests.

In this thesis models are presented, based on evolutionary polynomial regression, to predict the complex thermo-mechanical behaviour of unsaturated soils. The results from the experimental investigations on compacted samples of silt using triaxial apparatus at different temperatures (Uchaipichat and Khalili, 2009) were used for developing and evaluating the EPR models. The input parameters of the model were considered to be

the over consolidation ratio, mean net stress, initial suction, temperature, initial degree of saturation, axial strain, deviator strain and volumetric strain and the models were developed to predict the stress-strain status of the soil corresponding to an increment in the axial strain and based on the current deviator stress and volumetric strain values. The EPR model predictions are compared with the experimental results. A sensitivity analysis is also conducted to investigate the effects of contributing parameters including temperature on the developed EPR models.

4.4.2 Database

The results from triaxial experiments on samples of an unsaturated soil reported by Uchaipichat and Khalili (2009) were used to develop the EPR-based models. These experiments were conducted at constant suction, constant temperature and constant water content stress paths including: i) temperature and suction controlled isotropic loading tests, ii) temperature controlled desaturation tests, iii) suction controlled thermal loading tests, iv) constant water content thermal loading tests, and v) temperature and suction controlled shear strength tests.
The tests were performed on silt samples compacted in the laboratory. The soil samples were obtained from the Bourke region of New South Wales, Australia. The index properties of the soil are presented in Table 4.9. Figures 4.23 and 4.24 show the soil water characteristic curve and the compaction curve for the soil respectively.

Table 4.9: Index properties of the silt used in the tests (Bourke silt)

Properties	Values
Liquid Limit (%)	20.5
Plastic Limit (%)	14.5
Specific Gravity	2.65
Air Entry Value (kPa)	18
Maximum dry unit weight from standard proctor test (kN/m^3)	18.8
Optimum moisture content from standard proctor test (%)	12.5

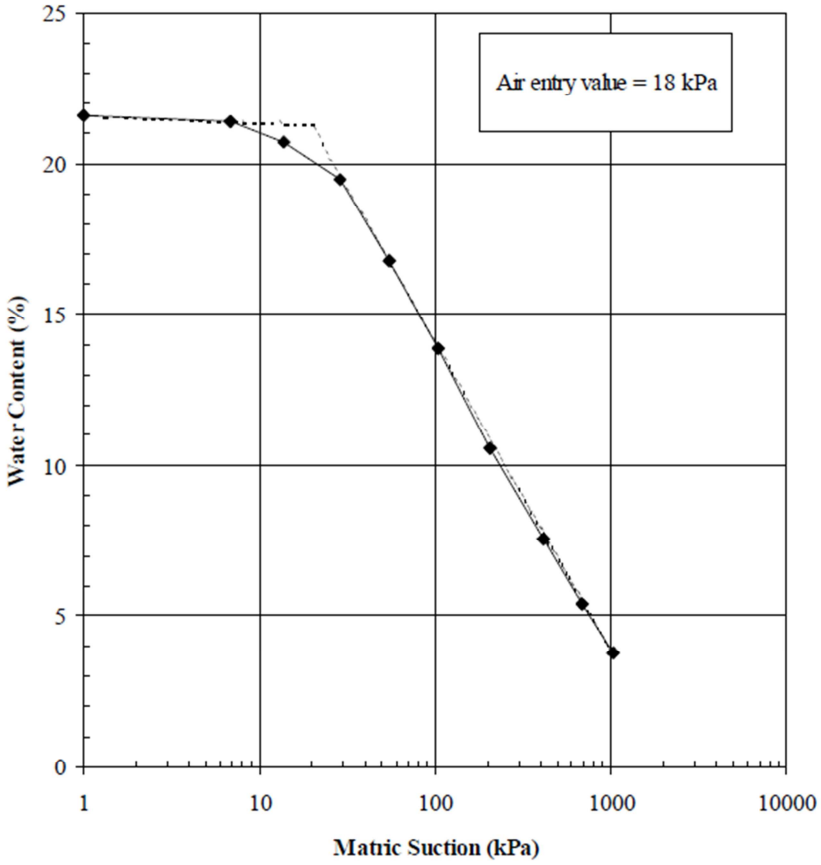

Figure 4.23: Soil-Water characteristic curve for the silt used in the tests (Uchaipichat, 2005)

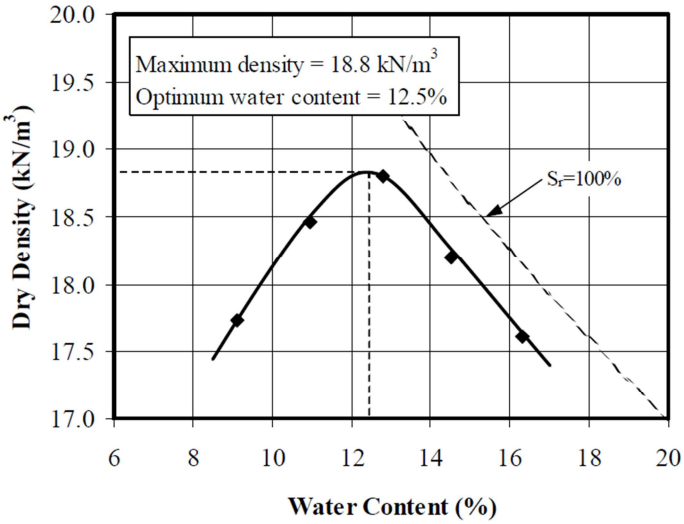

Figure 4.24: Compaction curve obtained from standard compaction test for the silt used in the tests (Uchaipichat, 2005)

4.4.3 Data preparation

Results from 27 temperature and suction-controlled shear tests were used to develop models to predict the shear strength and volumetric strain behaviour of unsaturated soil including the thermal effects. All the tests were conducted in a modified triaxial equipment depicted in figure 5.25 (Uchaipichat and Khalili, 2009). The temperature and

matric suction values varied from 25°C to 60°C and 0 to 300 kPa respectively. The effective cell pressures of 50, 100 and 150 kPa were used in the experiments. The implemented testing procedure was consolidated drained test and the deviatoric stress was applied by increasing the axial stress while the cell pressure was kept constant. Figures 4.26 to 4.28 show the experiment results used to develop and validate the EPR models.

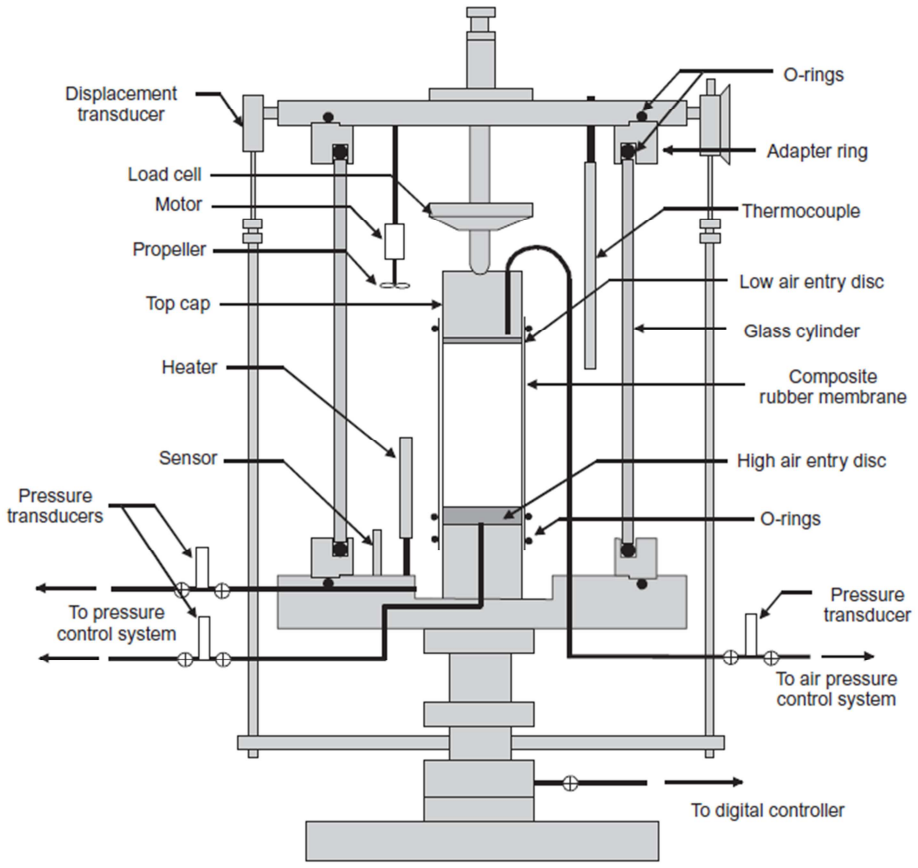

Figure 4.25: Modified triaxial equipment (Uchaipichat and Khalili, 2009)

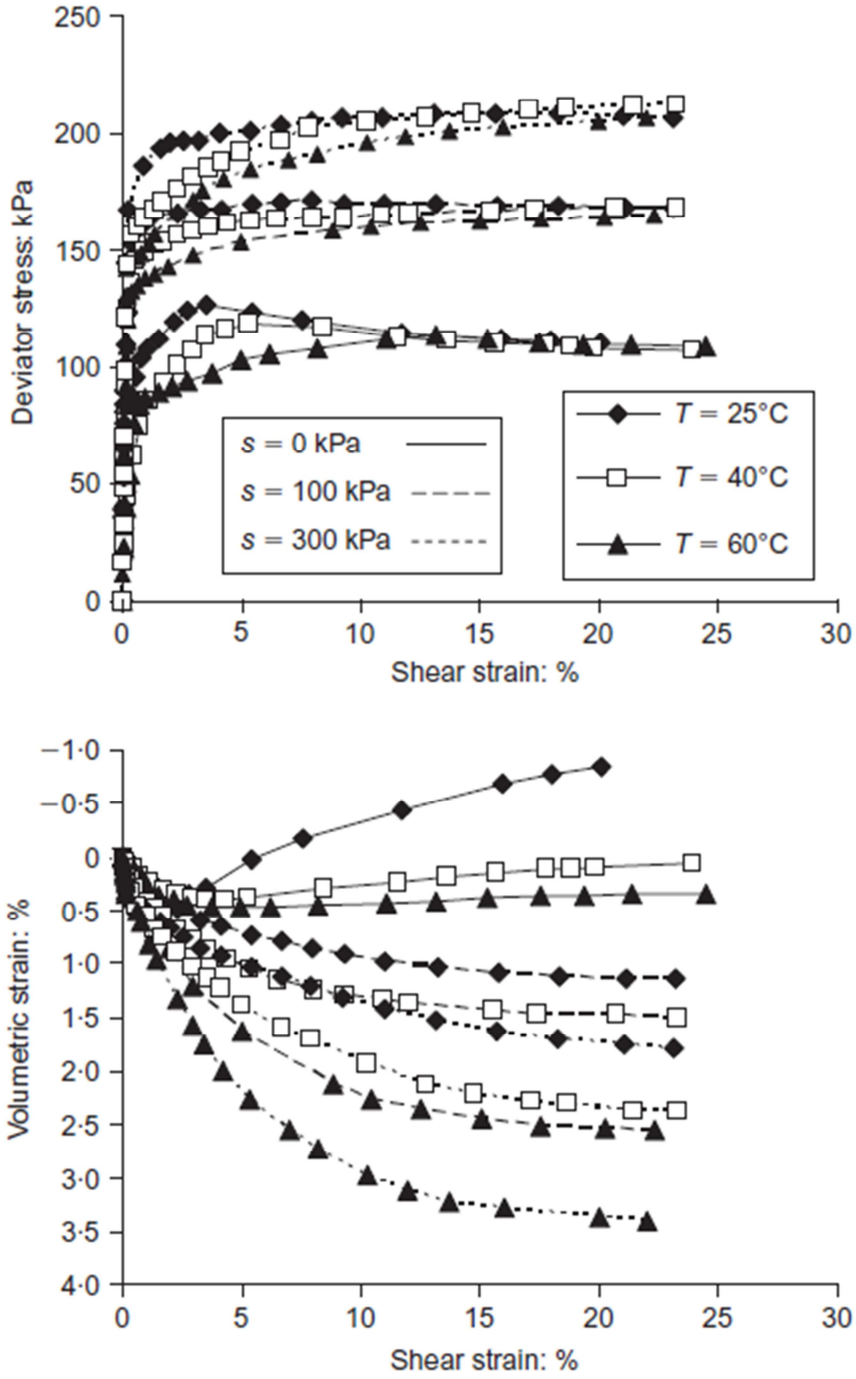

Figure 4.26: Suction and temperature controlled shear tests at initial mean effective stress of 50 kPa (Uchaipichat and Khalili, 2009)

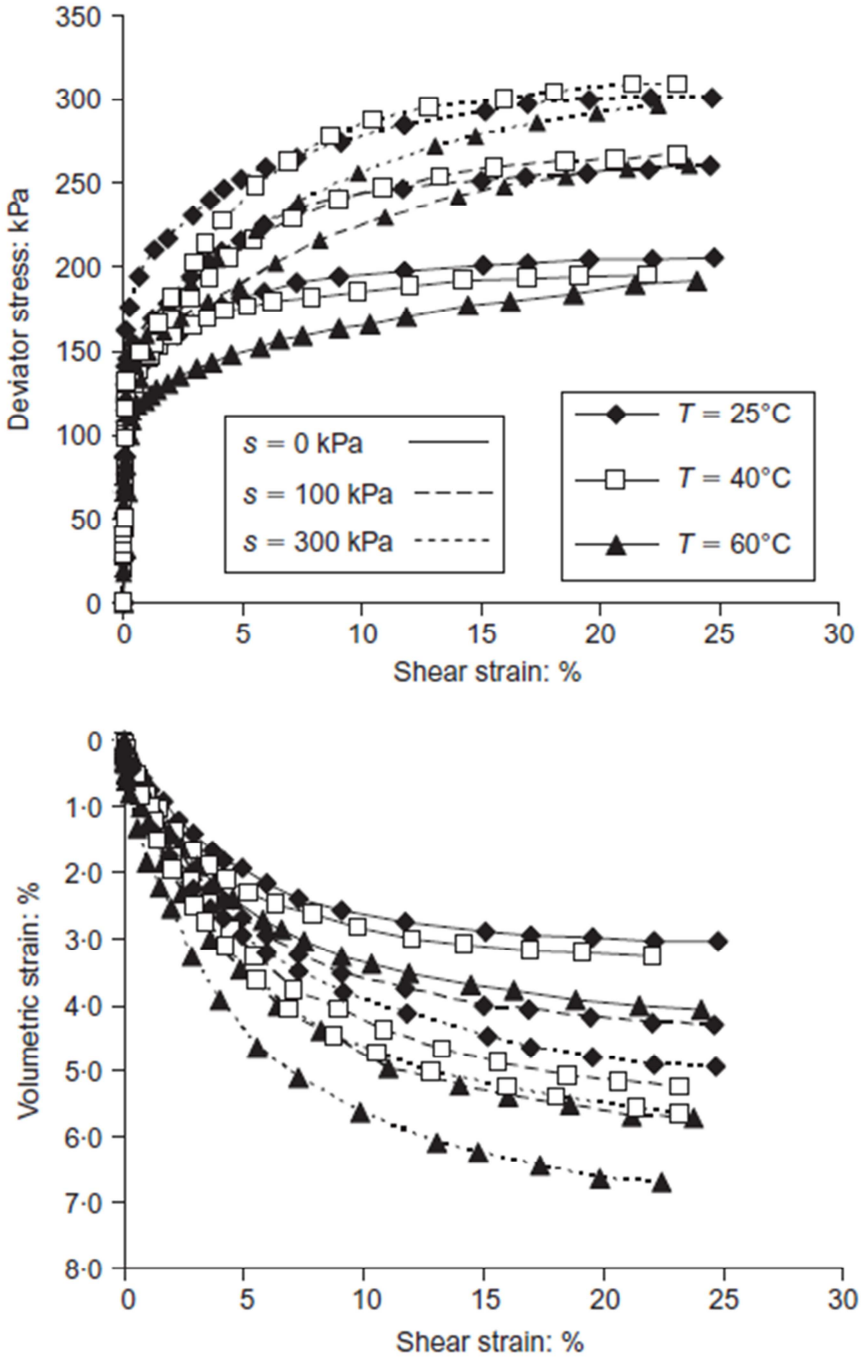

Figure 4.27: Suction and temperature controlled shear tests at initial mean effective stress of 100 kPa (Uchaipichat and Khalili, 2009)

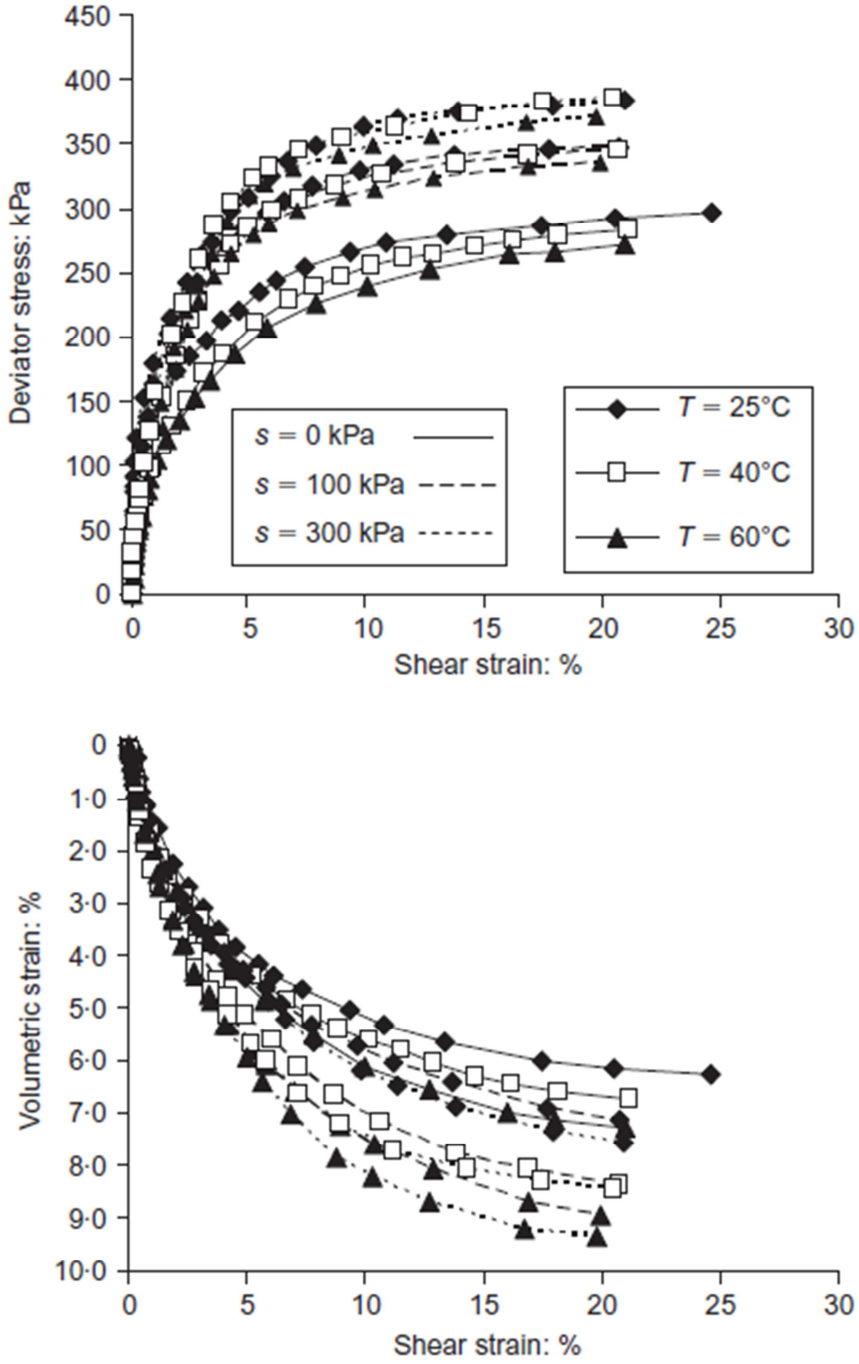

Figure 4.28: Suction and temperature controlled shear tests at initial mean effective stress of 150 kPa (Uchaipichat and Khalili, 2009)

The total number of cases in the database was divided into training and testing datasets. From the database 22 cases (approximately 80%) were used to train and develop the EPR models while the remaining 5 cases (about 20%) were kept unseen to the EPR during model construction and were used to validate the developed models. A similar procedure to that explained in section 4-2-3 was used to select the most statistically consistent training and testing sets to be utilized in the development of the presented models.

Table 4.10: Parameters involved in the developed incremental EPR models*

Contributing parameters	Model output
$OCR, P_{net}, Su_i, T, Sr_i, \varepsilon_a, q_i, \varepsilon_{vi}, \Delta\varepsilon_a$	q_{i+1} / $\varepsilon_{v,i+1}$

* OCR =overconsolidation ratio ; P_{net} =mean net stress (kPa); Su_i =initial suction (kPa); T =temperature (℃); Sr_i=initial degree of saturation; ε_a=axial strain; q_i=deviator stress (kPa); ε_{vi}=volumetric strain; $\Delta\varepsilon_a$=axial strain increment; q_{i+1}= deviator stress corresponding to the next increment of axial strain (kPa); $\varepsilon_{v,i+1}$ = volumetric strain corresponding to the next increment of axial strain.

4.4.4 EPR models for shear strength and volume change behaviour of unsaturated soils considering the temperature effects

The modelling procedure was similar to the one explained in case of modelling hydro-mechanical behaviour of unsaturated soils in the beginning of this chapter. Constraints were implemented to control the structure of the models to be constructed in terms of the length and complexity of the developed EPR models, type of implemented functions, number of terms, range of the exponents used and the number of generations to complete the evolutionary process. As the modelling process progressed the accuracy level at every stage was evaluated using the fitness equation (Equation 4-1).

Due to the incremental nature of soil stress–strain modelling in practical applications, the incremental procedure was utilized in this research. The developed EPR models include nine input parameters as summarized in Table 4.10.

Some input parameters including the overconsolidation ratio, initial mean net stress, initial suction, temperature and initial degree of saturation represented the initial conditions of the soil samples, but volumetric strain and deviator stress were updated incrementally as the training and testing stages progressed based on the predicted previous values (of deviator stress and volumetric strain) corresponding to the previous increment of axial strain. The output parameters were the deviator stress and volumetric strain corresponding to an increment of the axial strain.

After completion of the modelling process, 44 and 31 models were developed for deviatoric stress and volumetric strain respectively. From among the developed models some did not include all the defined parameters as inputs to the equations and were removed and the remaining were considered and compared in terms of the robustness of the equations based on the coefficient of determination, sensitivity analysis and also the length of the equations and the best models satisfying all these criteria were chosen as final models. Equations 4.6and 4.7 represent the EPR models for deviator stress and volumetric strain respectively. As noted above, these models are unit dependent.

$$q_{i+1} = \frac{0.06q_i^2 - 3.81 \times 10^{-4} Su_i \cdot T^2 \cdot Sr_i \cdot \varepsilon_a + 6.73 \cdot OCR^6 \cdot \varepsilon_a}{OCR^3 \times q_i} + \frac{1455.02 \cdot \varepsilon_a}{P_{net} \cdot Sr_i \cdot q_i} + \frac{23.11 Su_i \cdot Sr_i \cdot \Delta\varepsilon_a \cdot P_{net}^2 \cdot q_i - 8.67 \times 10^5 \cdot OCR^3 \cdot \varepsilon_a}{P_{net}^3 \cdot q_i} + \frac{378.26 \cdot \varepsilon_{v_i} \cdot \Delta\varepsilon_a - 0.07 \cdot OCR \cdot \varepsilon_a^2 \cdot q_i}{T \cdot q_i} + 48.87\Delta\varepsilon_a + 0.13{\varepsilon_{v_i}}^2 + 0.91q_i - 5.05Sr_i^3 - 0.1T - 0.12 \cdot OCR \cdot q_i \cdot \Delta\varepsilon_a + 19.81 \quad 4\text{-}6$$

$$\varepsilon_{v_{i+1}} = \frac{1.06 \times 10^{-3} Sr_i \cdot q_i \cdot \Delta\varepsilon_a}{OCR \cdot \varepsilon_a} + \frac{9.87 \times 10^{-7} Sr_i \cdot q_i^3 - 4.09}{P_{net}} + \frac{1.31 \times 10^{-7} Su_i^3 \cdot Sr_i^2 \cdot \varepsilon_a - 0.98T + 1.09 \times 10^{-3} T^3 - 9.15 \times 10^{-4} T^3 \cdot Sr_i}{T^2} + \frac{2.52 \times 10^{-4} {\varepsilon_{v_i}}^2 - 0.89 Sr_i^2 \cdot \Delta\varepsilon_a}{Sr_i} + 0.83\Delta\varepsilon_a + 0.98\varepsilon_{v_i} - 0.05\varepsilon_{v_i} \cdot \Delta\varepsilon_a - 2.24 \times 10^{-4} q_i - 4.44 \times 10^{-3} q_i \cdot \Delta\varepsilon_a + 0.01 P_{net} \cdot \Delta\varepsilon_a + 0.1 \quad 4\text{-}7$$

Figures 4.29, 4.30 and 4.31 show deviator stress-axial strain and volumetric strain-axial strain curves predicted using EPR models (Equations 4-6 and 4-7) against the experimental results for the tests used in the training of the model development process with figure 4.29 showing the worst predicted data case.

After training, the performance of the trained EPR models was verified using 5 sets of validation data which had not been introduced to EPR during training. The purpose of validation was to examine the generalisation capabilities of the developed models to conditions that were seen by the model during the training phase. Figures 4.32, 4.33 and 4.34 show predictions made by the developed EPR models against the experimental data for the testing dataset. The CoD values of the EPR models (Equations 4-6, 4-7) are given in Table 4.11.

Table 4.11: Coefficient of determination values for the presented models

Equation	COD values for training (%)	COD values for testing (%)
Deviator stress	99.85	99.44
Volumetric strain	99.99	99.86

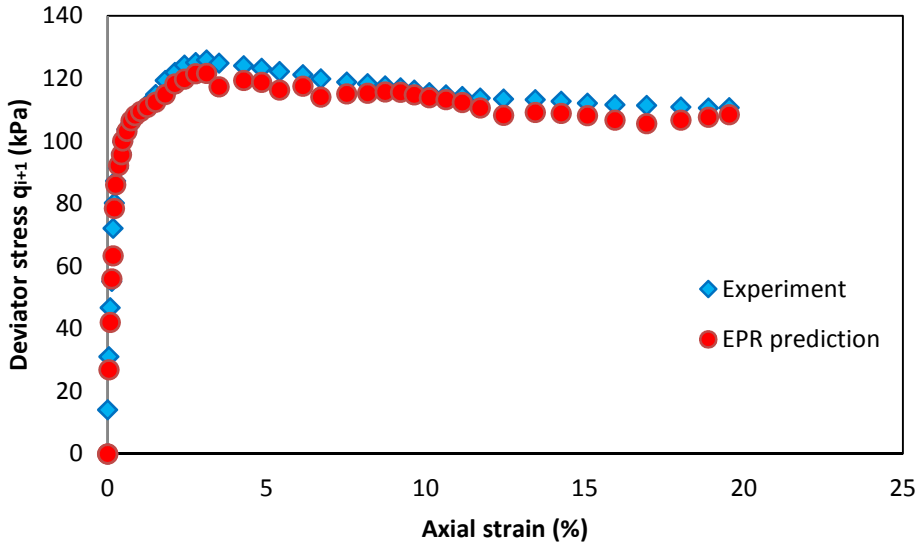

(a)

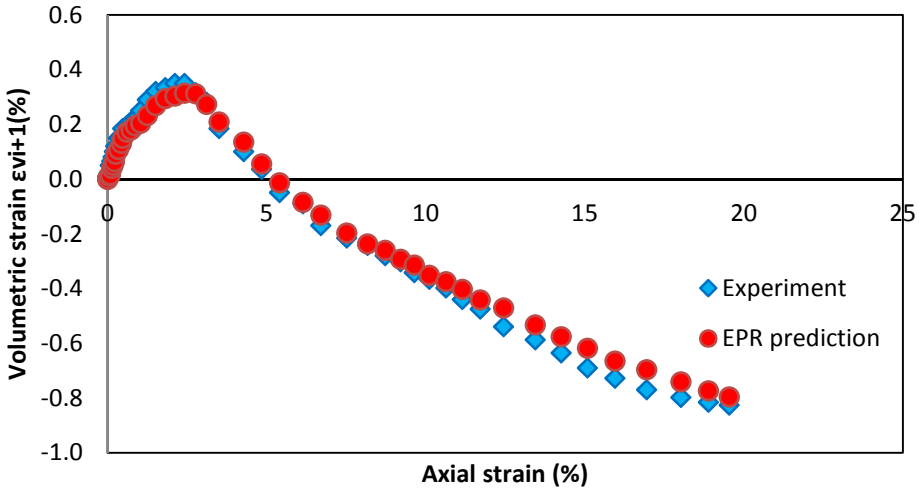

(b)

Figure 4.29: Comparison between the EPR model predictions with experimental data for deviator stress (a) and volumetric strain (b) – (OCR=4, Mean net stress=50 kPa, T=25°C)

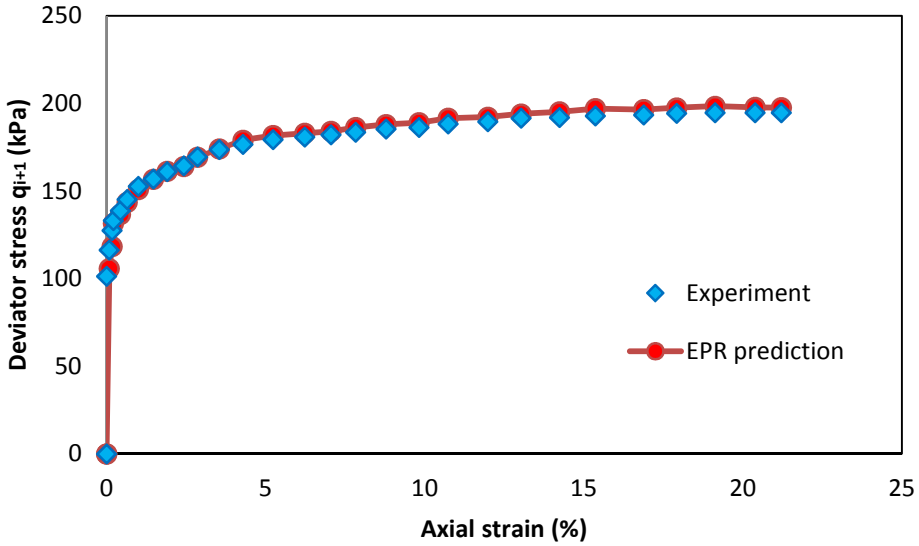

(a)

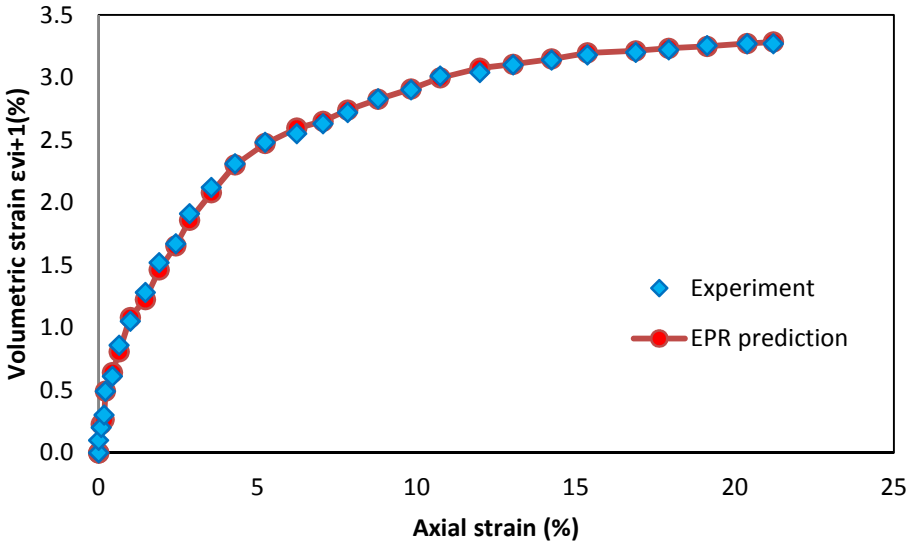

(b)

Figure 4.30: Comparison between the EPR model predictions with experimental data for deviator stress (a) and volumetric strain (b) – (OCR=2, Mean net stress=100 kPa, T=40°C)

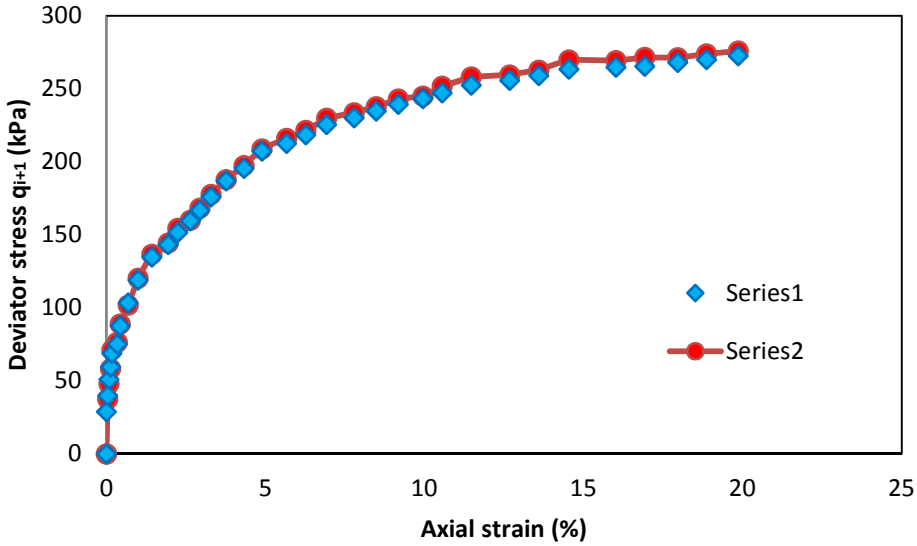

(a)

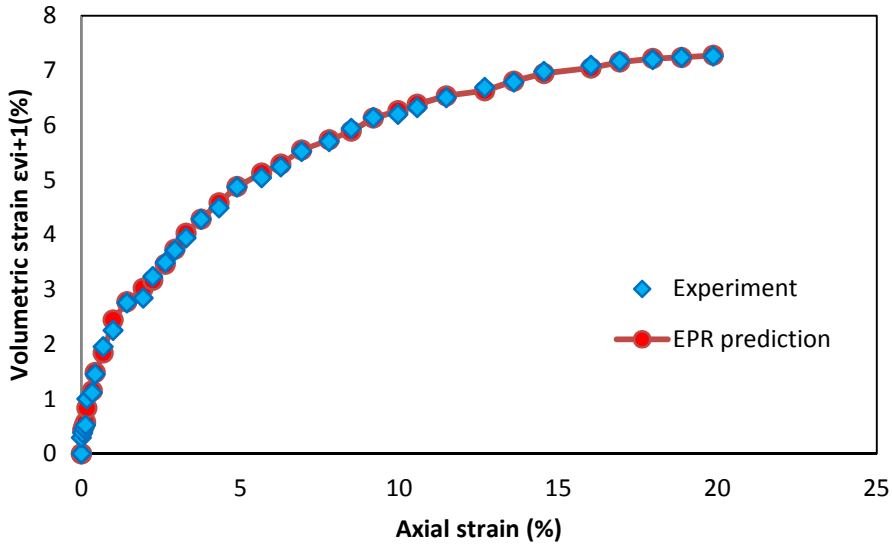

(b)

Figure 4.31: Comparison between the EPR model predictions with experimental data for deviator stress (a) and volumetric strain (b) – (OCR=1.33, Mean net stress=150 kPa, T=60°C)

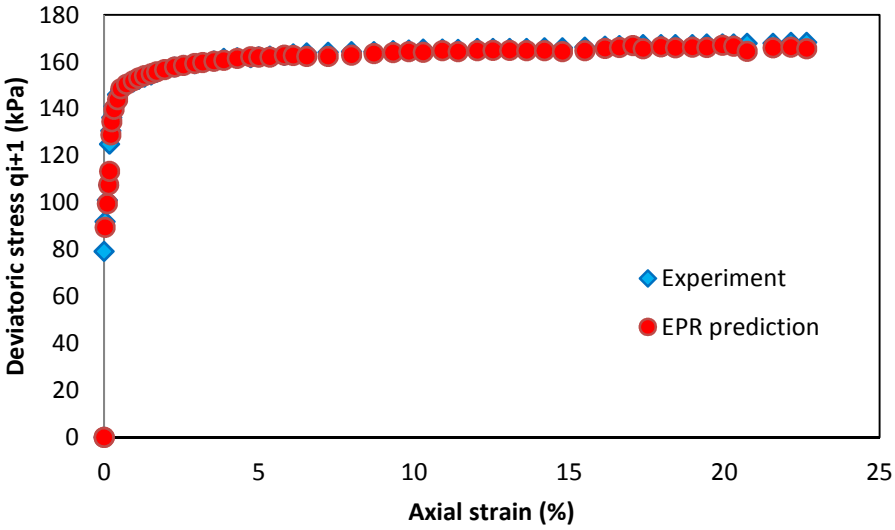

(a)

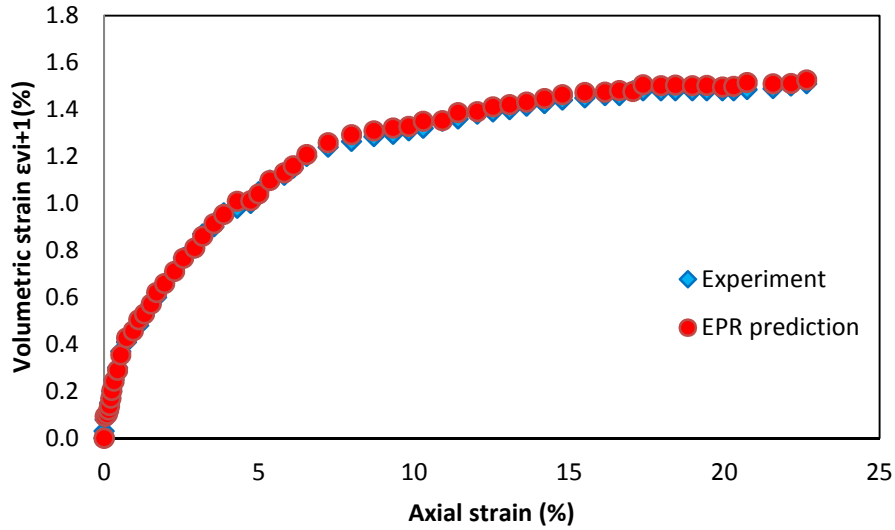

(b)

Figure 4.32: Comparison between the EPR model validation predictions with experimental data for deviator stress (a) and volumetric strain (b) – (OCR=4, Mean net stress=50 kPa, T=40°C)

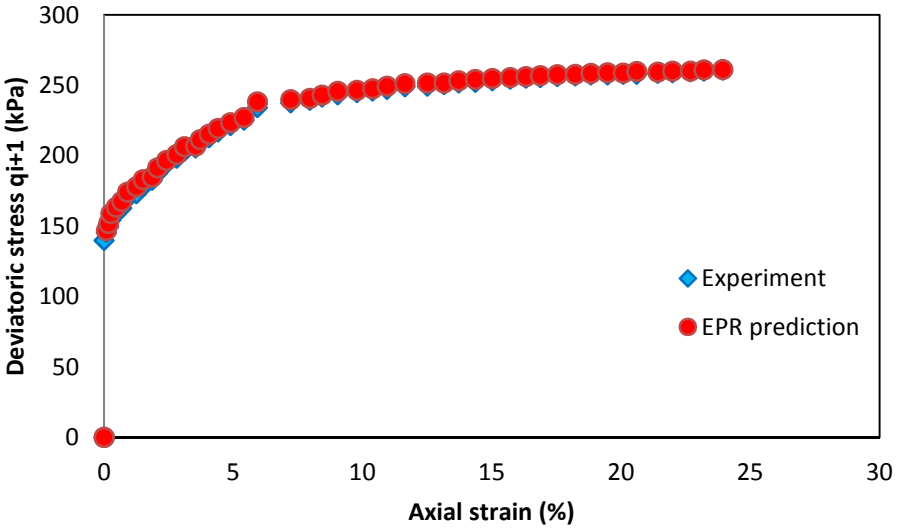

(a)

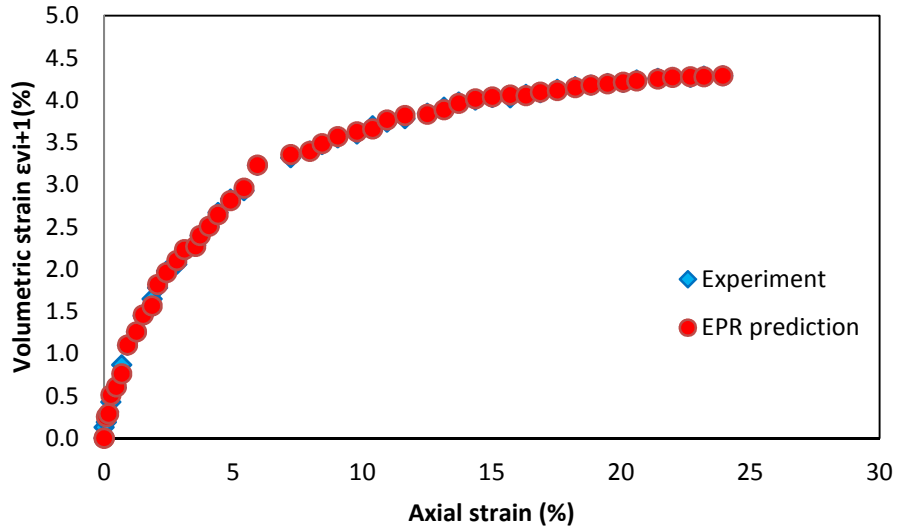

(b)

Figure 4.33: Comparison between the EPR model validation predictions with experimental data for deviator stress (a) and volumetric strain (b) – (OCR=2, Mean net stress=100 kPa, T=25°C)

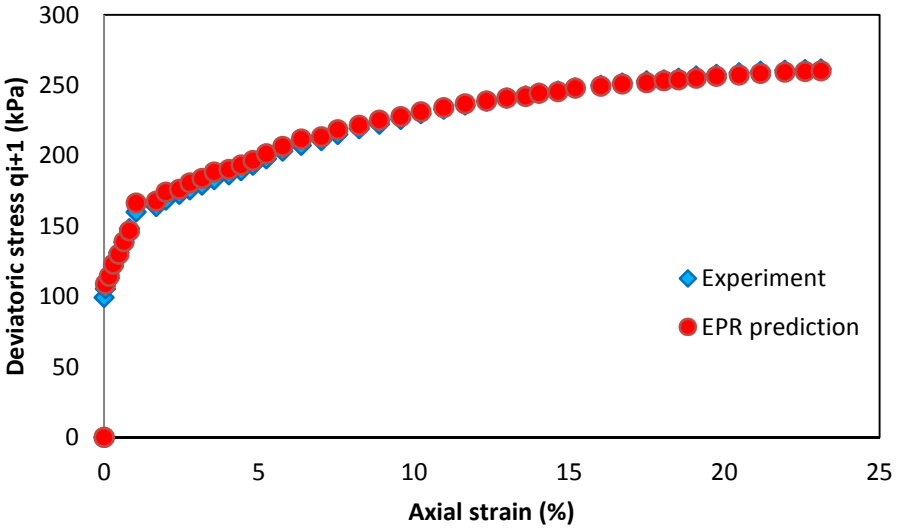

(a)

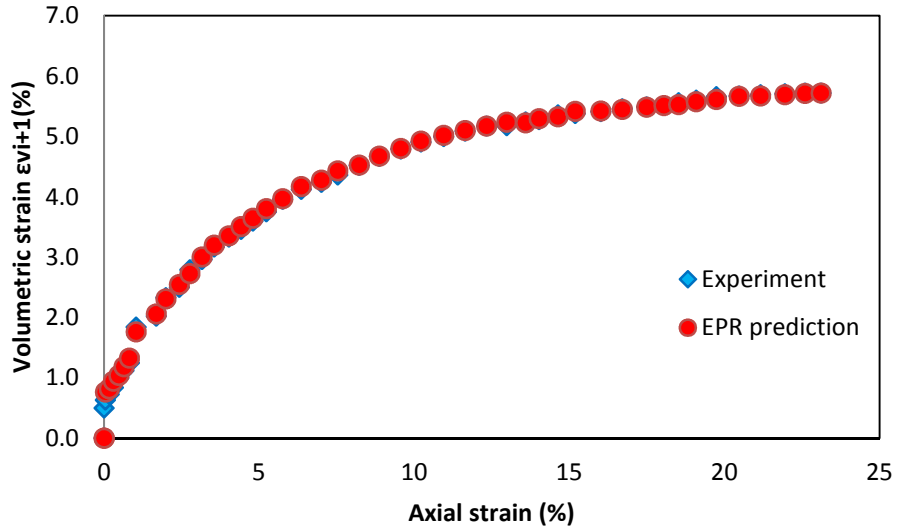

(b)

Figure 4.34: Comparison between the EPR model validation predictions with experimental data for deviator stress (a) and volumetric strain (b) – (OCR=2, Mean net stress=100 kPa, T=60°C)

Comparison of the results showed the exceptional capabilities of the developed models in capturing the shearing and volume change behaviour of unsaturated soils considering the temperature effects and generalising the behaviour to unseen cases.

4.4.5 Predicting entire stress paths using the developed EPR models

The EPR models represented as Equations 4-6 and 4-7 were used to predict the entire stress paths, incrementally, point by point, in $q:\varepsilon_a$ and $\varepsilon_v:\varepsilon_a$ spaces. The results from three different sets of (testing) data were utilized to evaluate the ability of the incremental EPR models to predict the complete thermo-mechanical behaviour of unsaturated soil during the entire stress paths. The values of overconsolidation ratio,

confining stress, initial suction, temperature and initial degree of saturation were kept constant throughout the test. Other contributing parameters were updated in each incremental step of axial strain considering values corresponding to the previous increment and the EPR models outputs in response to an axial strain increment. Figure (4.35) illustrates the procedure followed for updating of the input parameters and building the entire stress path for the shearing stage of a triaxial test. For a prescribed increment of axial strain, $\Delta\varepsilon_a$, the values of q_{i+1}, $\varepsilon_{v,i+1}$ are calculated using the EPR models. For the next increment, the values of $\varepsilon_{a,i}$, q_i and $\varepsilon_{v,i}$ are updated as:

$$q_i = q_{i+1}$$

$$\varepsilon_{v,i} = \varepsilon_{v,i+1}$$

$$\varepsilon_{a,i} = \varepsilon_{a,i} + \Delta\varepsilon_a$$

In this way the second points on the curves are predicted. The incremental procedure is continued until all the points on the curves are predicted and the curves are established.
Figures 4.36, 4.37 and 4.38 show the comparison between the three complete curves predicted using the EPR models following the above incremental procedure and the actual experimental data. It should be noted that the data for these tests were not introduced to the EPR during the model development process.
The predicted results are in a very close agreement with the experimental results and considering the fact that the entire curves have been predicted point by point and the errors of prediction of the individual points are accumulated, it can be easily seen that EPR models were able to predict the complete stress paths with a high degree of accuracy which can be an indication of the robustness of the developed EPR framework for modelling thermo-mechanical behaviour of unsaturated soils.

4.4.6 Sensitivity analysis

Similar to the previously represented EPR models in earlier sections of this chapter, a parametric study was carried out on a validation set of data to evaluate the response of the models to changes in input parameters. This was done through a basic approach to sensitivity analysis by fixing all but one input variable to their mean values and varying the remaining one within the range of its maximum and minimum values.
Figures 4.39 to 4.42 show the results of the parametric study conducted to investigate the effect of changes in confining pressure (joint effect of the mean net stress and the overconsolidation ratio), suction, degree of saturation and temperature on the developed models.
As expected, any increase in the values of the confining pressure and suction in the soil sample causes the shear strength of the soil and also the volumetric strain to increase (Figures 4.39 and 4.40). Any increase in the degree of saturation of the soil will cause the soil suction to drop and will result in lower shear strength and also expansion in the soil sample. This effect was also correctly predicted by the presented EPR models (Figure 4.41). The developed model for deviator stress also correctly predicts drop in the shear strength as the temperature increases; however the increasing effect of temperature on the volumetric strain is negligible (Figure 4.42).
The results of the parametric study indicated that the developed EPR models have been able to capture the underlying physical patterns between the contributing parameters

and the shear and volumetric behaviour of unsaturated soils under various temperatures correctly.

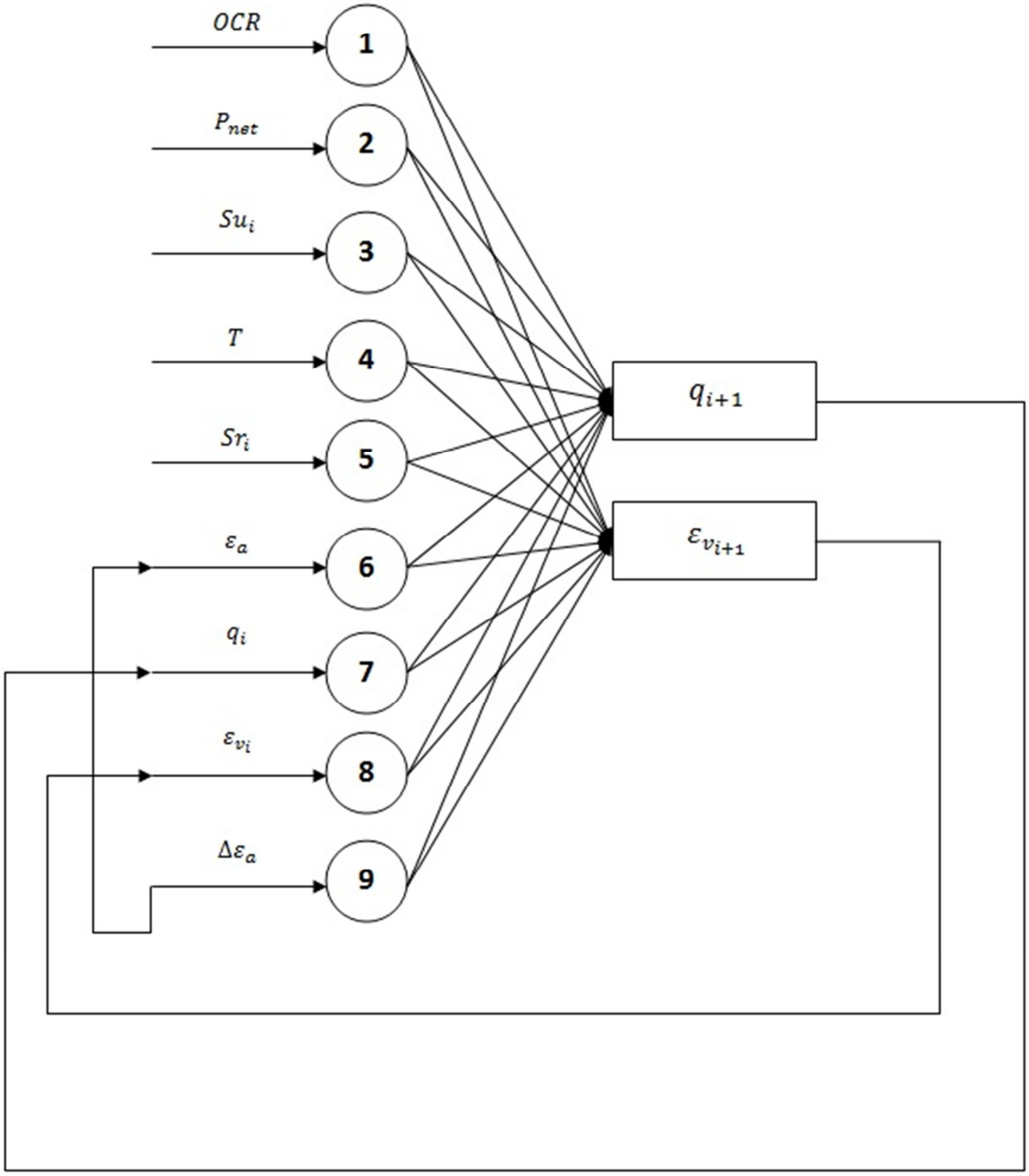

Figure 4.35: Incremental procedure for predicting the entire stress path

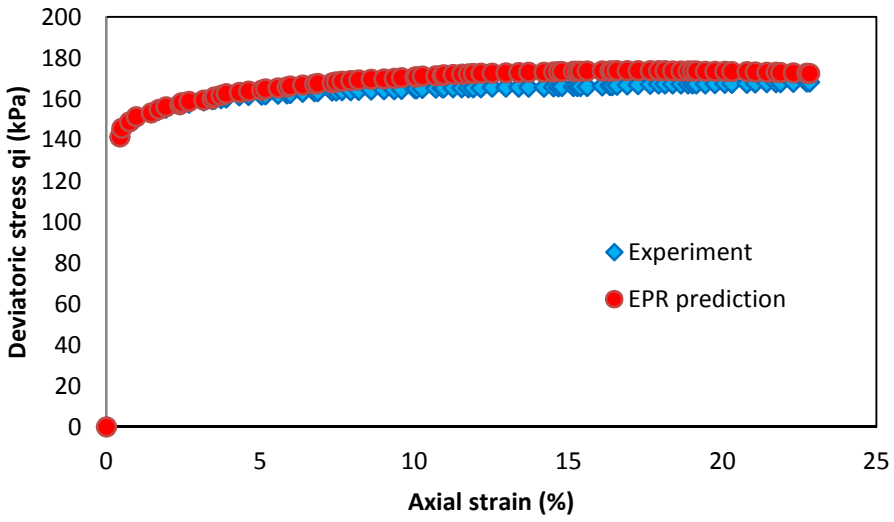

(a)

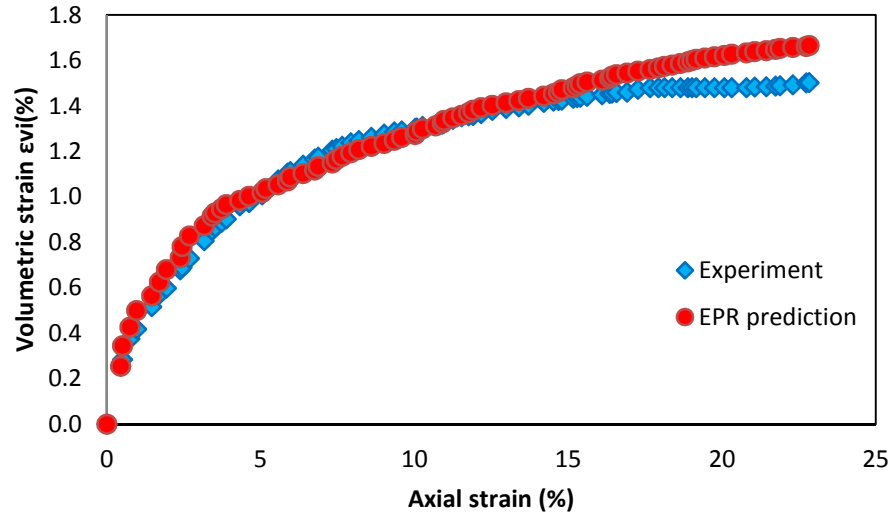

(b)

Figure 4.36: Comparison between the EPR model predictions (point-by-point predictions of entire stress paths) with experimental data for deviator stress (a) and volumetric strain (b) – (OCR=4, Mean net stress=50 kPa, T=40°C)

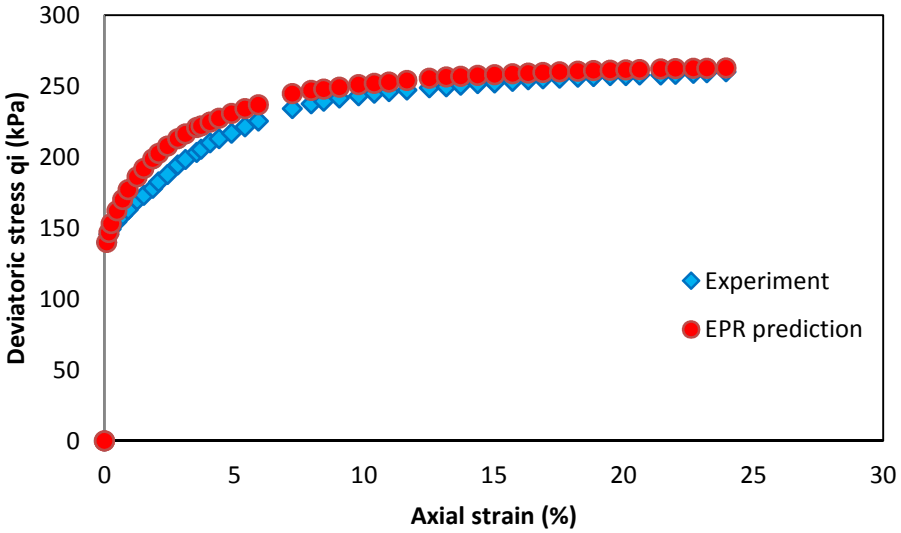

(a)

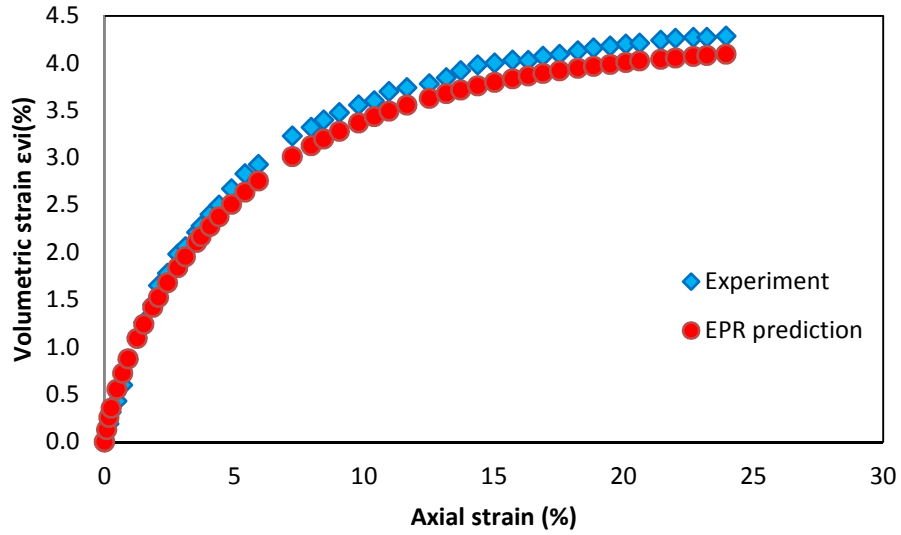

(b)

Figure 4.37: Comparison between the EPR model predictions (point-by-point predictions of entire stress paths) with experimental data for deviator stress (a) and volumetric strain (b) – (OCR=2, Mean net stress=100 kPa, T=25°C)

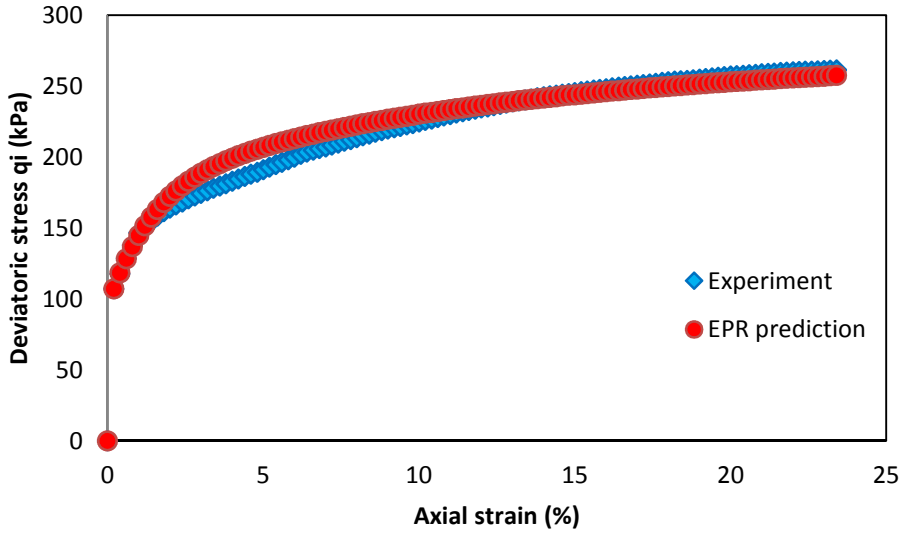

(a)

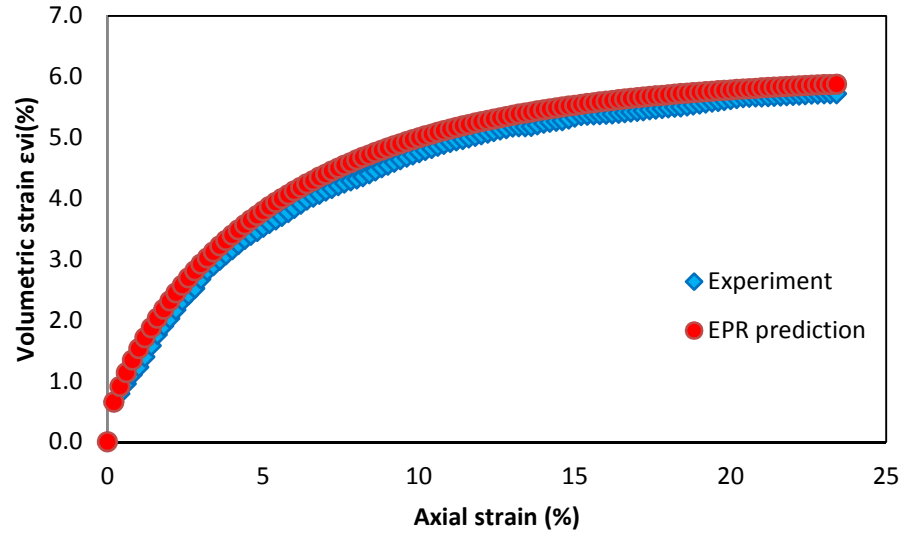

(a)

Figure 4.38: Comparison between the EPR model predictions (point-by-point predictions of entire stress paths) with experimental data for deviator stress (a) and volumetric strain (b) – (OCR=2, Mean net stress=100 kPa, T=60°C)

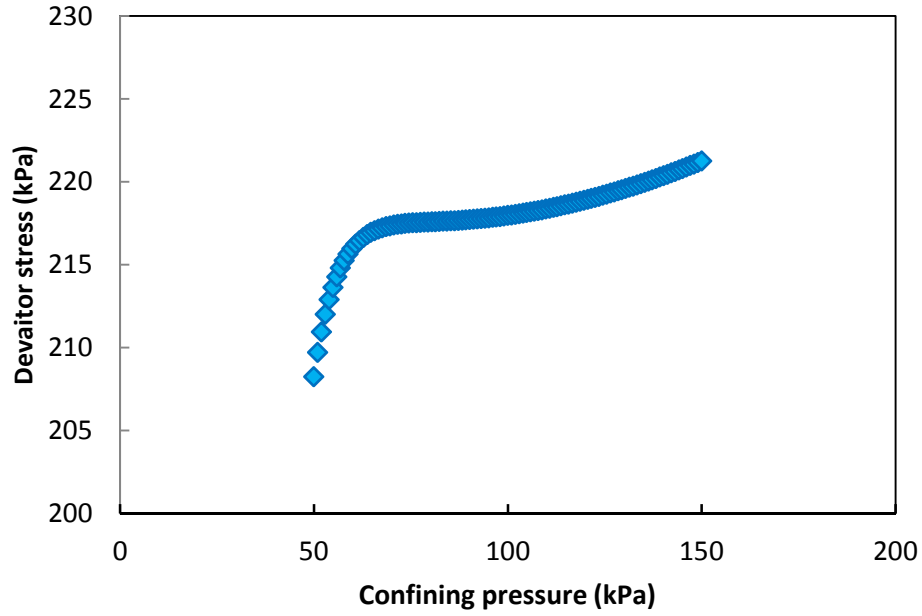

(a)

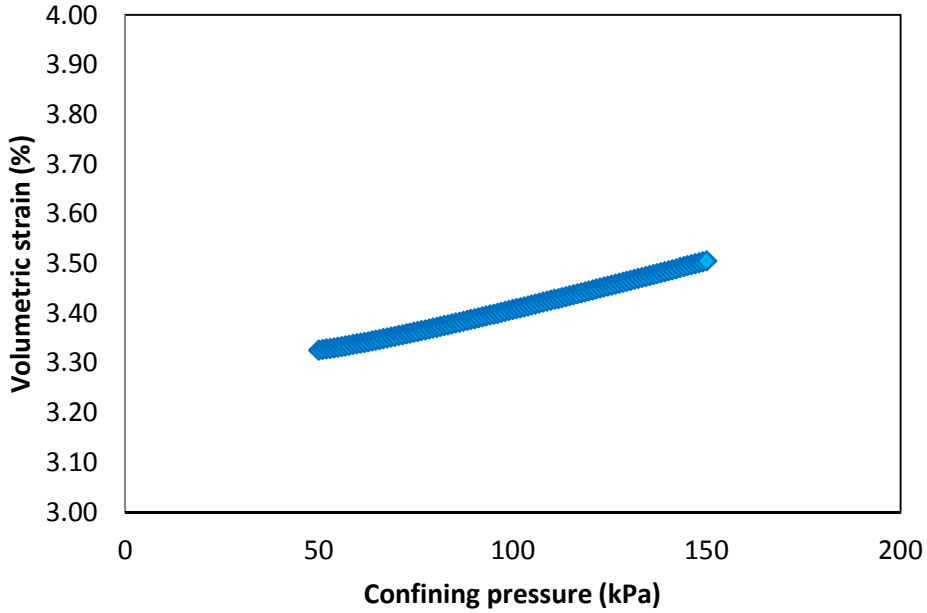

(b)

Figure 4.39: Effect of changes in confining pressure on (a) deviatoric stress and (b) volumetric strain model predictions

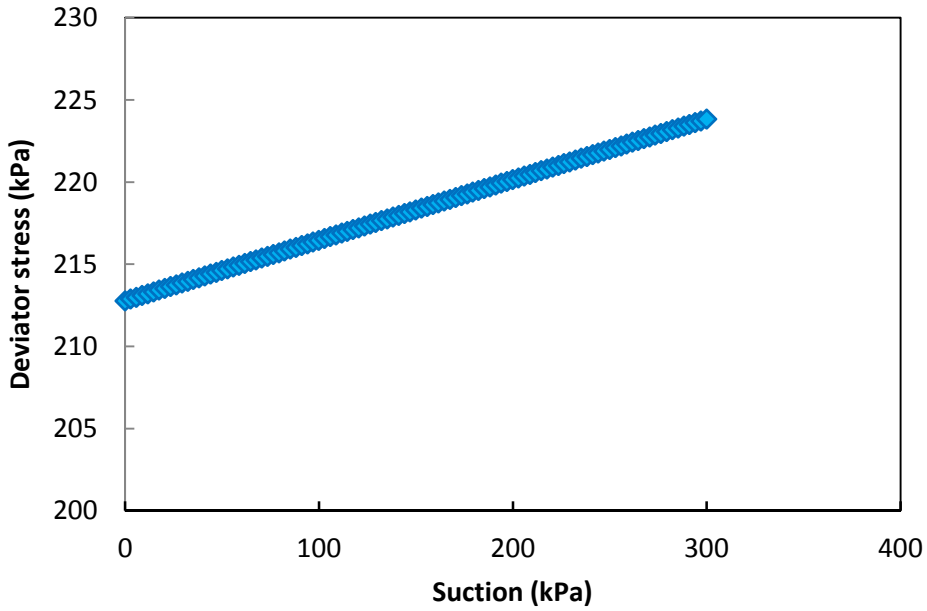

(a)

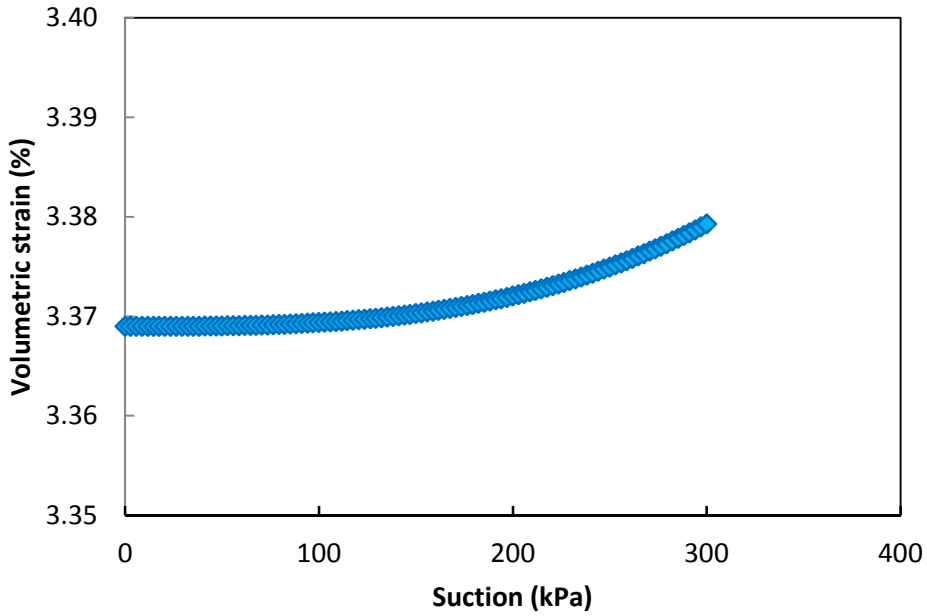

(b)

Figure 4.40: Effect of changes in suction on (a) deviatoric stress and (b) volumetric strain model predictions

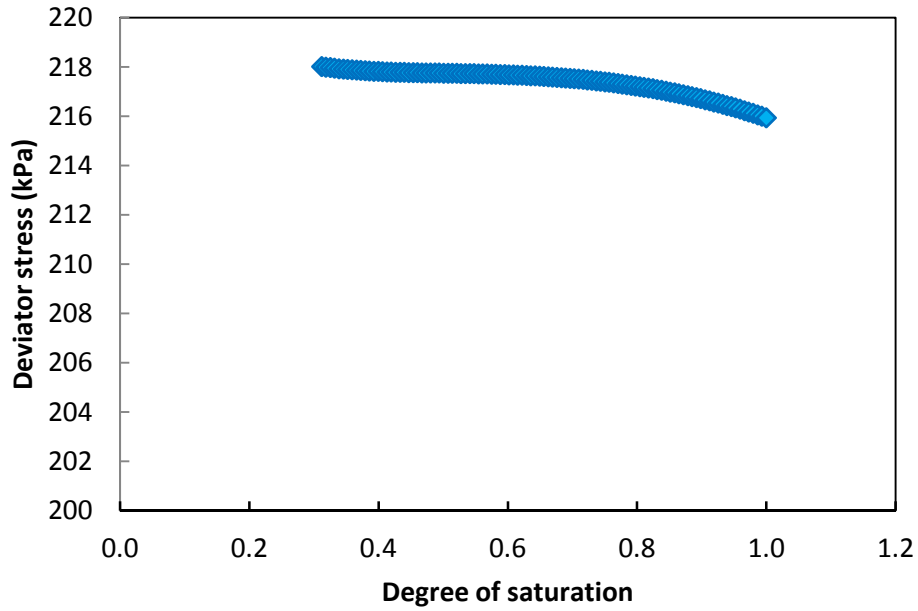

(a)

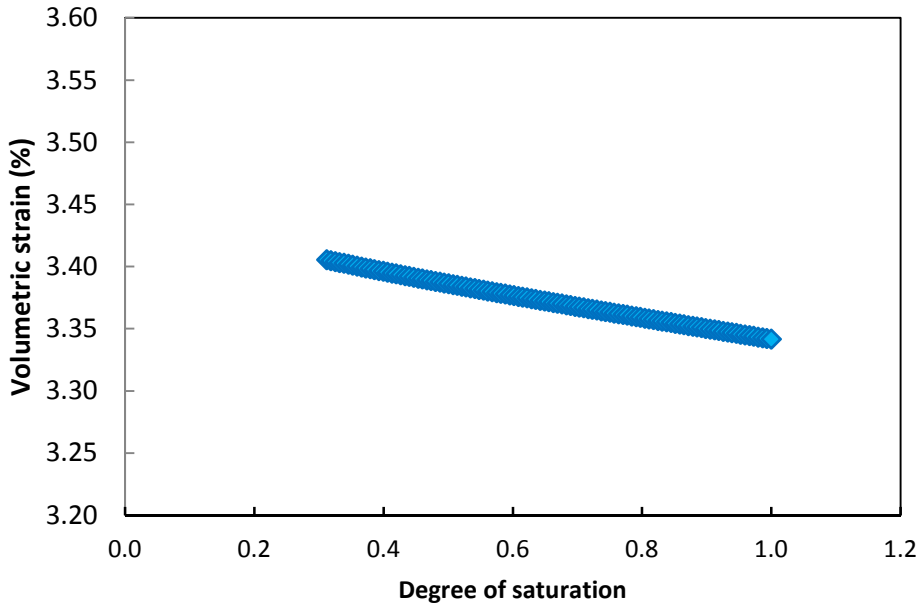

(b)

Figure 4.41: Effect of changes in degree of saturation on (a) deviatoric stress and (b) volumetric strain model predictions

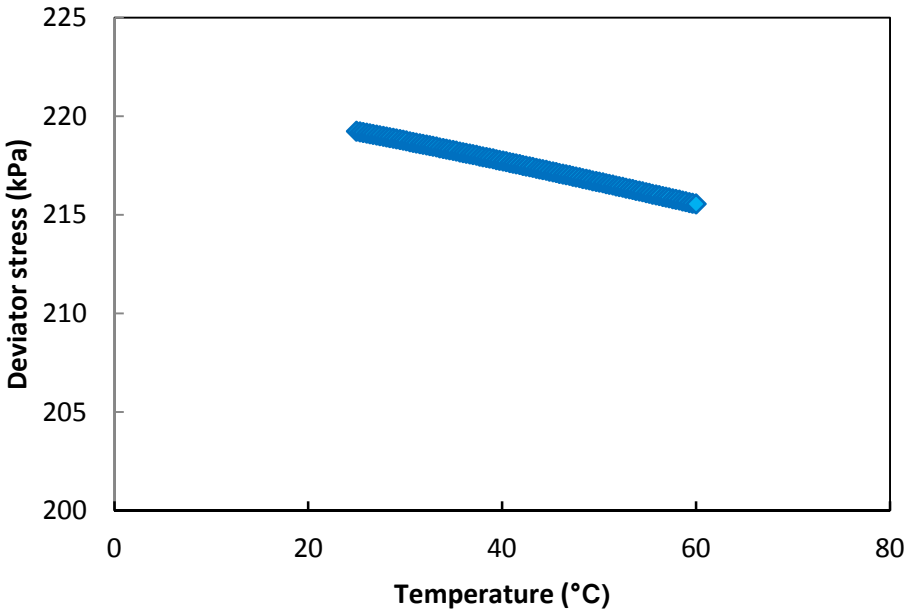

(a)

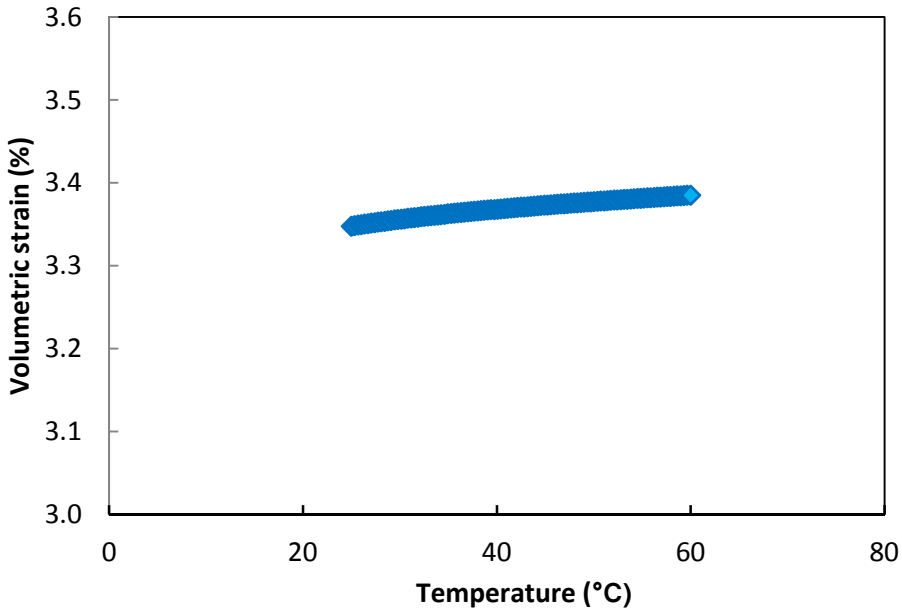

(b)

Figure 4.42: Effect of changes in temperature on (a) deviatoric stress and (b) volumetric strain model predictions

4.4.7 Discussion and conclusions

Evolutionary Polynomial Regression was used to develop two models to predict deviatoric (shear) stress and volumetric strain behaviour of unsaturated soil considering the temperature effects. It was shown that the presented models have the capability to predict the entire stress paths by implementing the incremental approach. The capability of the models in making accurate predictions of the behaviour of unsaturated soils was

shown using appropriate graphs and tables considering unseen validation data sets that were not introduced to EPR in the model development stage.

A parametric study was conducted to study the sensitivity of the models to variation of each of the contributing parameters. Using the resulted graphs, it was shown that the developed EPR models were capable of capturing the temperature effect as well as the effect of other parameters (confining pressure, suction and initial degree of saturation) correctly and accurately from the provided raw triaxial test data.

4.5 Stress-strain and volume change behaviour of granular soils

4.5.1 Introduction

The shear strength of cohesionless soil such as sand and gravel under varying drainage conditions has been a topic of significant interest for the last four decades. Many research works have contributed significantly to the understanding of the important factors that control the shear strength behaviour of sand and gravel for drained conditions. A comprehensive set of data from literature was collected and used to model stress-strain and volume change behaviour of cohesionless soils. This section presents the development of EPR models for granular soils using this database. Comparison is made between EPR model predictions and the Experimental data. Sensitivity analysis outcomes and the relevant discussions are presented in the following section.

Considerable amount of experimental data has been published in the literature contributing significantly to the understanding of the important factors that control the shear strength behaviour of granular soils in drained conditions. There has been tremendous interest in the research community to model the shear stress and volume change behaviour of cohesionless soil and because of its well defined conditions of stress and strain on the cylindrical specimens, many of the models developed to date are predominantly based on triaxial compression test data. The majority of the past research effort has been devoted to modelling of soil behaviour using the elasticity/plasticity based approach with some success (Rowe and Barden, 1964).

The EPR models developed in this study were produced based on a large database comprising data from 177 triaxial tests with the aim of providing comprehensive models that could be used to predict the behaviour of granular soils.

4.5.2 Database and the parameters involved in development of the models

Previous experimental research has shown that the important factors that govern the behaviour of cohesionless soil (sand and gravel) are its mineralogy, particle shape, particle size and its distribution, void ratio and also the effective confining stress level (Dayakar and Rongda, 1999). The experimental database from a large number of contributions from literature (shown in Table 4.12) was used to develop the models in this research. The database includes the effects of the above factors systematically in a comprehensive manner using a large number of drained triaxial compression tests.

Table 4.12: Data sources used to create the database (Dayakar and Rongda, 1999)

Reference	Experimental soil description
Lee and Seed (1967)	Sacramento river sand
Lee, Seed and Dunlop (1967)	Antioch sand
Leslie (1975)	Napa basalt New Hogan metavolcanic Carters Dam quartzite Cougar basalt Sonora dolomite Laurel sandstone Buchanan weathered granite
Lo and Roy (1973)	Back mine quartz sand St. Marc limestone sand Aluminum oxide sand
Marachi et al (1969)	Pyramid dam material Napa basalt
Miura and Yamanouchi (1975)	Toyoura sand
Miura and O-Hara (1979)	Ube decomposed granite
Ponce and Bell (1971)	Quartz sand
Ramamurthy et al (1974)	Badarpur sand
Raymond and Davies (1978)	Coteau dolomite Kenora granite Nouvelle igneous Sudburg slag
Raymond and Diyaljee (1979)	Grenville marble Kimberly float St. Isodore limestone Brandon gravel St. Bruno shale
Wu (1957)	Fluvioglacial sand
Erzin (2004)	Anatolian sands

The objective was to develop EPR-based models to represent the deviator stress-axial strain, and volumetric strain-axial strain relationships for granular soils with varying mineralogy, particle shape, uniformity coefficient, coefficient of curvature, effective particle size, void ratio, and effective confining pressure.

Data from a total of 177 triaxial compression tests were obtained from literature. Using the approach proposed by Hardin (1985), the mineralogy and grain shape were quantified in the database using crushing hardness, and average particle shape factor. The crushing hardness, $\boldsymbol{h}$ (a mineralogy factor) is approximately equal to the scratch hardness as defined by Moh's Scale. It takes a value of 7, 6, and 3 for quartz, feldspar, and calcite respectively (Dayakar and Rongda, 1999). The shape factor ($\boldsymbol{n_s}$) defines the degree of angularity or sphericity, and is equal to: 25 for angular, 20 for sub-angular, 17 for sub-round, and 15 for round shape (Dayakar and Rongda, 1999).

4.5.3 Data preparation

The data preparation process was similar to the procedure followed in section 4-2-3. 138 tests (80%) were used to train EPR and to construct the models and the remaining 39 tests were used for validation of the models.

Table 4.13: Parameters involved in the developed EPR models*

Contributing parameters	Model output
D_{50}, C_u, C_c, h, n_s, e, σ_3	q_{i+1}
ε_a , $\Delta\varepsilon_a$, q_i, $\varepsilon_{v,i}$	$\varepsilon_{v,i+1}$

* D_{50} (mm) = average grain size, Cu = coefficient of uniformity, C_c = coefficient of curvature; h= hardness of the mineral; ε_a = axial strain; n_s = shape factor; ε_v = volumetric strain; q = deviator stress; $\Delta\varepsilon_a$ = axial strain increment; e= void ratio; σ_3= effective confining pressure.

4.5.4 Developing the EPR models

As mentioned in the case of unsaturated soil modelling, a typical scheme to train most of the neural network based material models for soils includes an input set providing the network with information relating to the current state units (e.g., current stresses and strains) and then a forward pass through the network yields the prediction of the next expected state of stress or strain relevant to an input strain or stress increment ((Ghaboussi et al., 1998); (Dayakar and Rongda, 1999)). Due to the incremental nature of soil stress–strain modelling in practical applications, the same scheme was also used in this research to model the behaviour of granular materials.

The EPR models had 11 input parameters (Table 4.13). $\boldsymbol{D_{50}}$, $\boldsymbol{C_u}$, $\boldsymbol{C_c}$, $\boldsymbol{h}$, $\boldsymbol{n_s}$, $\boldsymbol{e}$ and $\boldsymbol{\sigma_3}$ represent the initial conditions of the soil specimens. The other three parameters, namely; axial strain, volumetric strain, and deviator stress are updated incrementally during the training and testing based on the outputs from the previous increment of the axial strain. The output parameters are the deviator stress and the volumetric strain corresponding to the end of the incremental step and are calculated using the two EPR models.
The training of the EPR resulted in development of few equations for deviator stress. Of these, 2 equations did not include the effect of all contributing parameters. Among the remaining equations the most appropriate and efficient one based on the model performance (fitness), complexity and also the sensitivity analysis results was selected as the final model. The same procedure was also followed to choose the best fit equation for the volumetric strain. Equations 4-8 and 4-9 represent the (unit dependent) incremental EPR models for deviator stress and volume strain respectively.

$$q_{i+1} = -\frac{1.3\times10^{-5}C_c^3\cdot\varepsilon_a\cdot\Delta\varepsilon_a\cdot\sigma_3\cdot\varepsilon_{v_i}}{D_{50}^2\cdot C_u^3} + \frac{1.14\times10^{-4}C_c^3\cdot h^3\cdot n_s^3\cdot\varepsilon_a\cdot\Delta\varepsilon_a}{D_{50}\cdot C_u\cdot e^3\cdot q_i} + \frac{0.08n_s^3\cdot\Delta\varepsilon_a}{C_u\cdot C_c^2\cdot h\cdot e^2} + \frac{0.2C_c\cdot h\cdot\Delta\varepsilon_a\cdot\sigma_3}{n_s} + \frac{60.86C_u\cdot\Delta\varepsilon_a\cdot\sigma_3\cdot\varepsilon_{v_i}}{C_c^2\cdot n_s^2\cdot q_i} + \frac{2.32\times10^{-9}C_u^3\cdot e^3\cdot\sigma_3^3\cdot\varepsilon_{v_i}}{C_c^2\cdot h^2\cdot n_s^3\cdot\Delta\varepsilon_a^2} + \frac{2.28\times10^{-4}C_u^3\cdot\Delta\varepsilon_a^2\cdot\sigma_3^2\cdot\varepsilon_{v_i}}{h^2\cdot n_s^2\cdot q_i} + \frac{5.85\times10^{-4}D_{50}\cdot C_c^3\cdot e^2\cdot\sigma_3^3\cdot\varepsilon_{v_i}^2}{C_u^2\cdot h\cdot n_s^3\cdot\Delta\varepsilon_a\cdot q_i} + \frac{8.34\times10^{-9}D_{50}\cdot h^3\cdot\varepsilon_a\cdot\Delta\varepsilon_a^2\cdot\sigma_3\cdot q_i}{C_u\cdot n_s} - 8.26\times10^{-4}C_c\cdot h\cdot\varepsilon_a\cdot\Delta\varepsilon_a\cdot\sigma_3 + 0.03\sigma_3 + 0.99q_i \quad (4\text{-}8)$$

$$\varepsilon_{v_{i+1}} = -\frac{0.06\varepsilon_a}{D_{50}\cdot C_c^2\cdot h^2\cdot n_s\cdot\Delta\varepsilon_a} + \frac{0.03h}{D_{50}\cdot C_c\cdot n_s} - \frac{1.53\times10^{-7}e\cdot\varepsilon_a\cdot\sigma_3\cdot\varepsilon_{v_i}}{C_u^3\cdot C_c^2\cdot h} - \frac{3.55\times10^{-9}\cdot h\cdot n_s\cdot\sigma_3}{C_u\cdot C_u^3\cdot e\cdot\Delta\varepsilon_a} - \frac{3.03\times10^{-5}}{C_u\cdot C_c\cdot\Delta\varepsilon_a^2} + \frac{0.13\varepsilon_a\cdot\Delta\varepsilon_a - 1.54\times10^{-4}D_{50}\cdot C_u^2\cdot C_c\cdot n_s\cdot\Delta\varepsilon_a^3\cdot h}{h^2} + \frac{0.51\Delta\varepsilon_a^3\cdot q_i\cdot n_s + 271.9h^2\cdot\Delta\varepsilon_a^3\cdot e}{n_s\cdot e\cdot\sigma_3} + \frac{0.16\varepsilon_{v_i}\cdot q_i\cdot\Delta\varepsilon_a - 0.34\varepsilon_a^2\cdot\Delta\varepsilon_a - 1.29\times10^{-8}C_u\cdot C_c\cdot\varepsilon_a^4\cdot q_i}{\varepsilon_a\cdot q_i\cdot\Delta\varepsilon_a} - \frac{2.13\times10^{-4}\cdot h^3\cdot\varepsilon_{v_i}}{n_s\cdot e^2\cdot\Delta\varepsilon_a^2\cdot\sigma_3} - 1.63\Delta\varepsilon_a^2 + \varepsilon_{v_i} + 0.05 \quad (4\text{-}9)$$

Figures 4.43 to 4.45 show deviator stress-axial strain and volumetric strain-axial strain curves predicted by the EPR models in Equations 4-8 and 4-9 against the experimental results for data sets that were used to train the models.

A comparison was also made between the predictions of the ANN models suggested by Dayakar and Rongda (1999) and EPR results for the training data cases. Typical results are presented in Figure 4.46.

After training, the performance of the trained EPR models was verified using 39 sets of validation data which had not been introduced to EPR during training. This was to evaluate the generalisation capabilities of the developed models to unseen cases. Figures 4.47 to 4.49 show predictions made by the developed EPR models against the experimental data which were not previously seen by EPR and were only used to validate the models. A comparison was also made with the predictions of the ANN models suggested by Dayakar and Rongda (1999).

Comparison of the results and the high CoD values for the EPR models indicate the excellent performance of these models in capturing the underlying relationships between the contributing parameters and deviator stress and volumetric strain response of granular soils and also in generalizing the training to predict the behaviour of these soils under unseen conditions. The results also show that EPR over performs ANN and its results are a closer match to the actual experimental data.

The incremental procedure was continued until all the points on the curves were predicted and the curves were established. Figures 4.51 to 4.54 show the comparison between the four complete curves predicted using the EPR models following the above incremental procedure and the actual experimental results for 4 data sets.

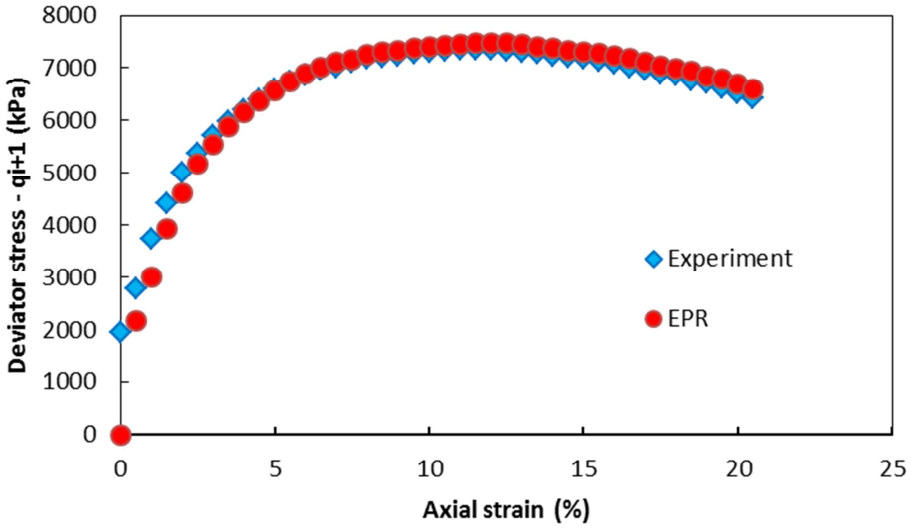

(a)

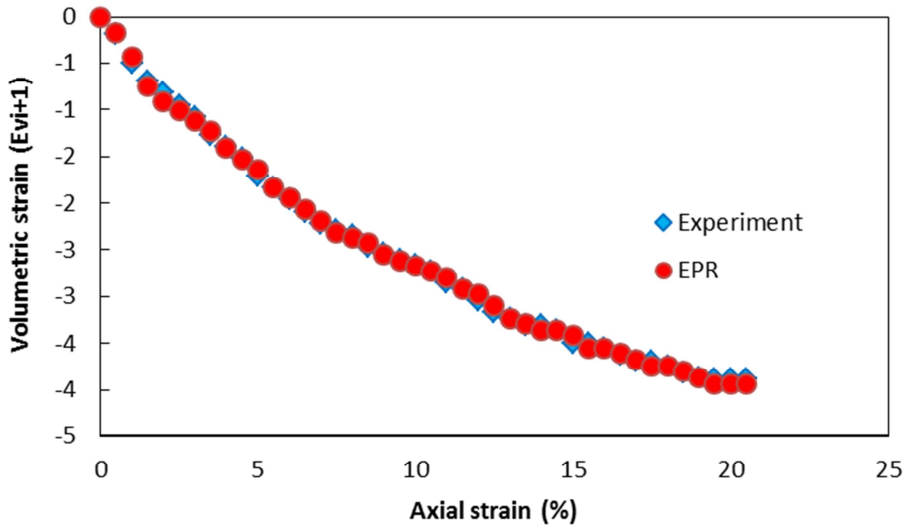

(b)

Figure 4.43: (a) Deviator stress-axial strain and (b) volumetric strain-axial strain curves predicted by the EPR models compared to experimental data ($\sigma_3 = 2932\ kPa$) – training data case

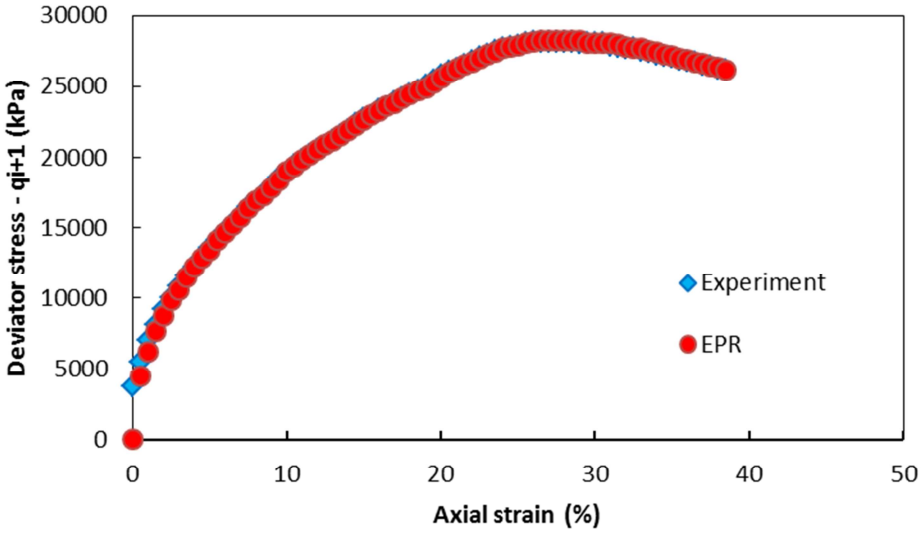

(a)

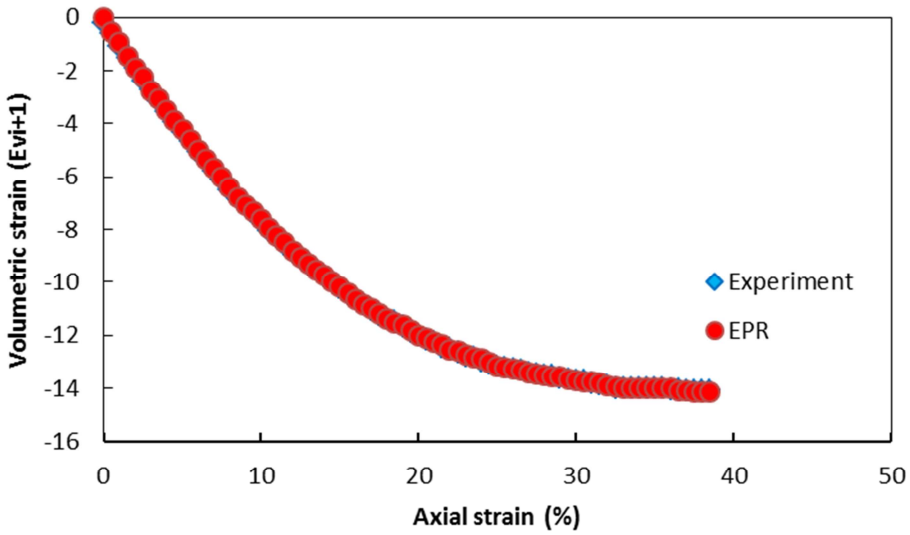

(b)

Figure 4.44: (a) Deviator stress-axial strain and (b) volumetric strain-axial strain curves predicted by the EPR models compared to experimental data ($\sigma_3 = 11767\ kPa$) – training data case

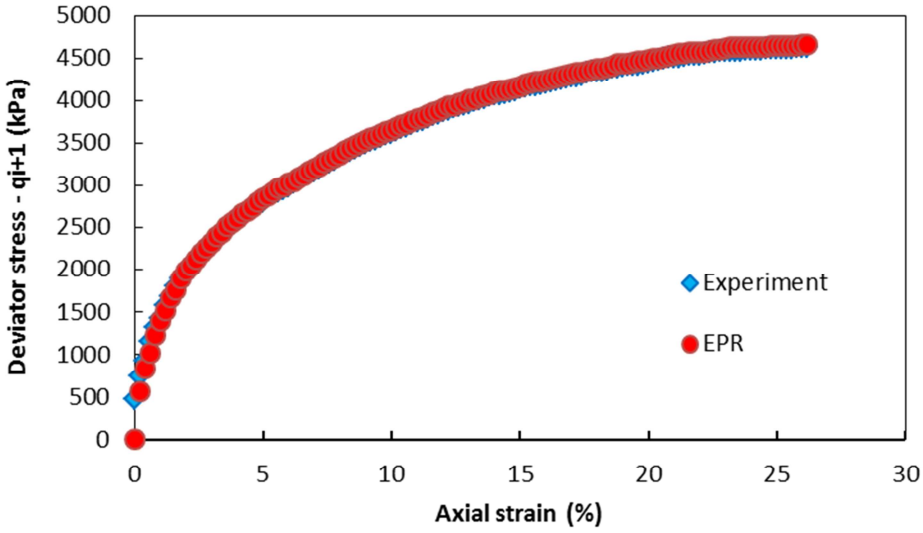

(a)

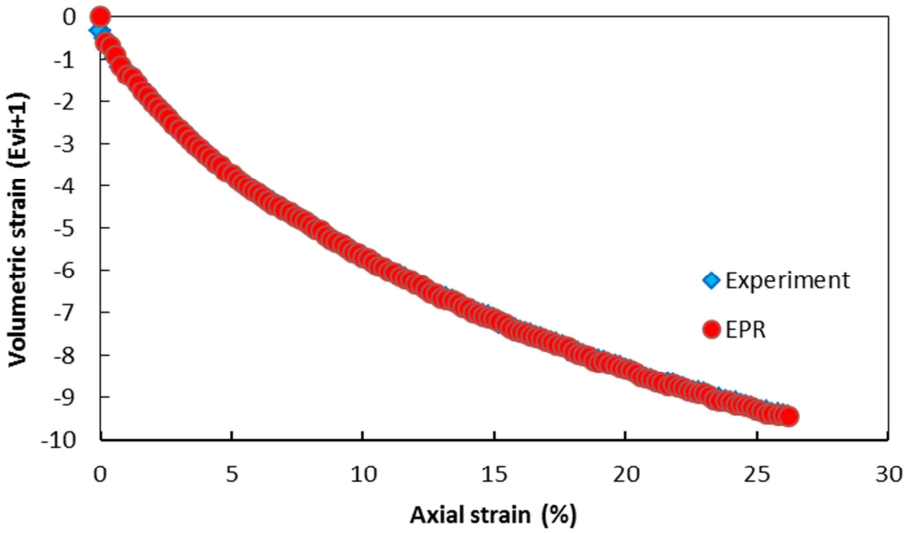

(b)

Figure 4.45: (a) Deviator stress-axial strain and (b) volumetric strain-axial strain curves predicted by the EPR models compared to experimental data ($\sigma_3 = 1961\ kPa$) – training data case

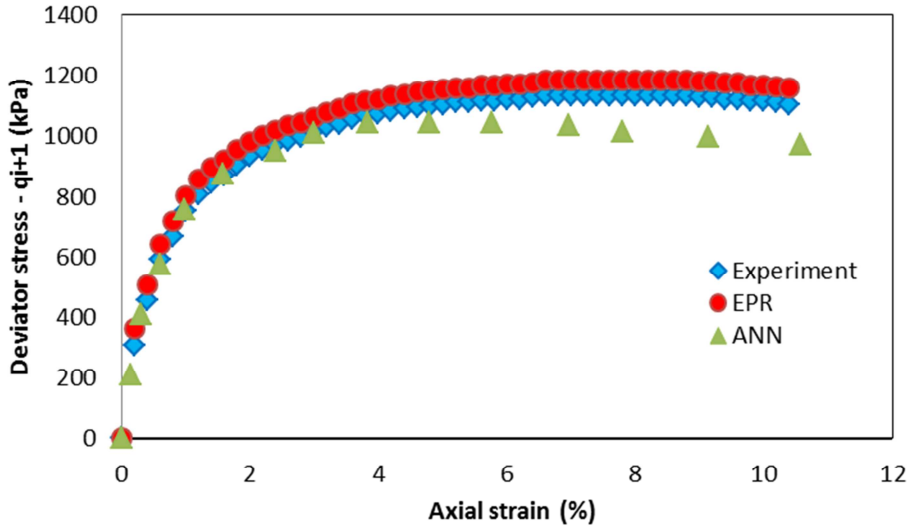

(a)

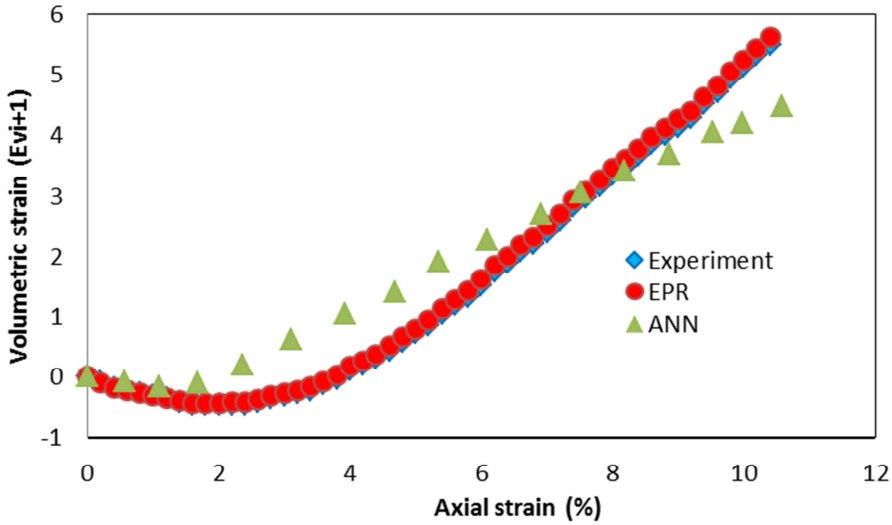

(b)

Figure 4.46: (a) Deviator stress-axial strain and (b) volumetric strain-axial strain curves predicted by the EPR models compared to experimental data and ANN model predictions ($\sigma_3 = 275\ kPa$) – training data case

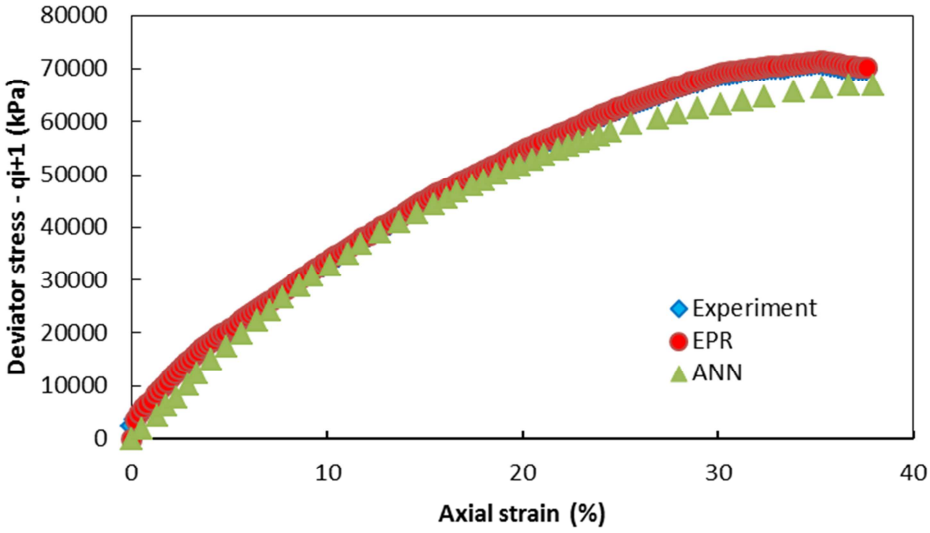

(a)

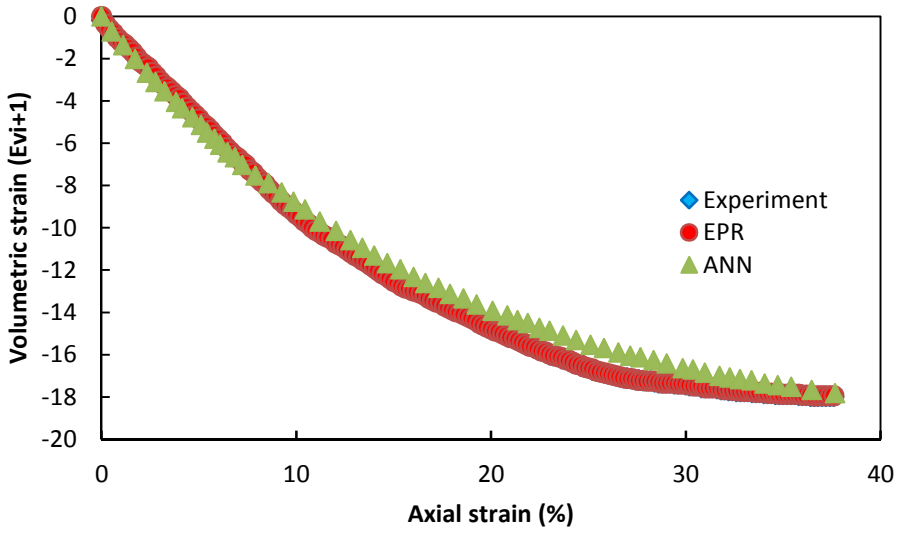

(b)

Figure 4.47: (a) Deviator stress-axial strain and (b) volumetric strain-axial strain curves predicted by the EPR models compared to experimental data and ANN model predictions ($\sigma_3 = 11767\ kPa$) – testing data case

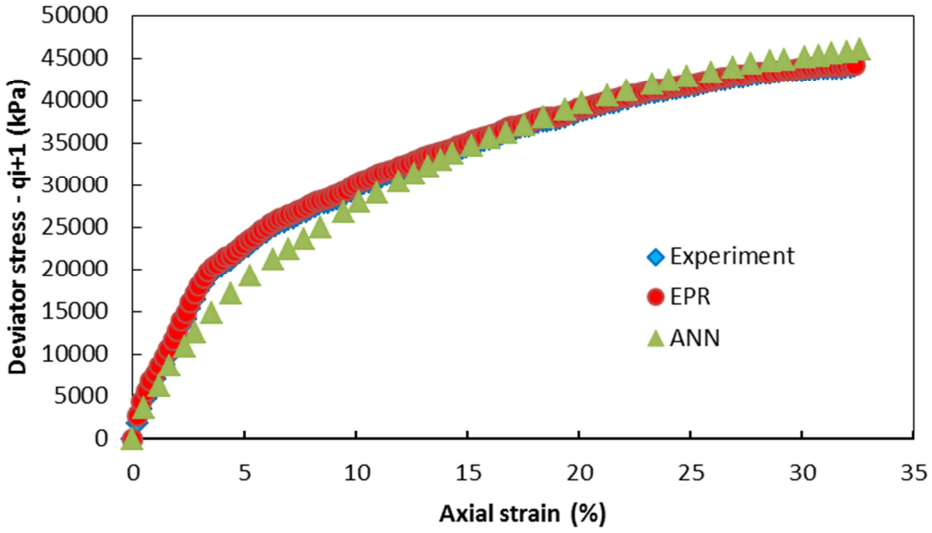

(a)

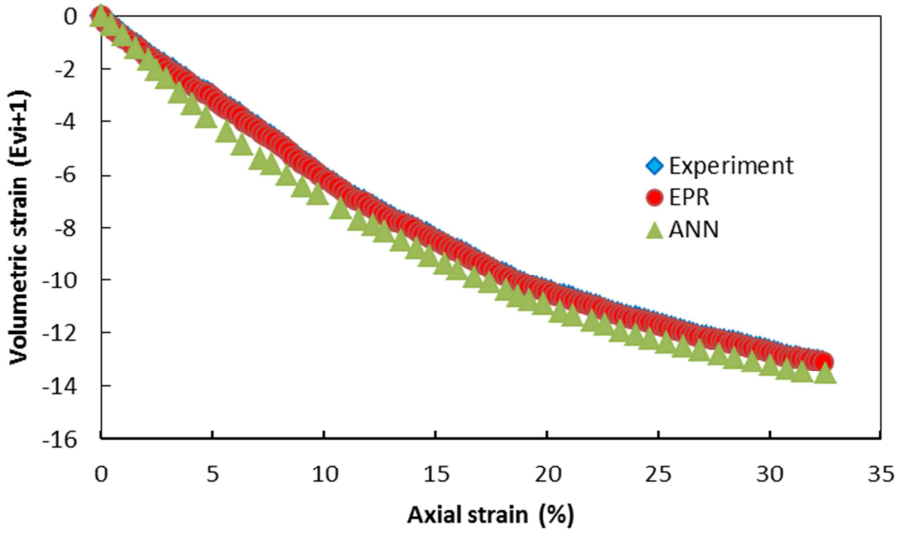

(b)

Figure 4.48: (a) Deviator stress-axial strain and (b) volumetric strain-axial strain curves predicted by the EPR models compared to experimental data and ANN model predictions ($\sigma_3 = 19613\ kPa$) – testing data case

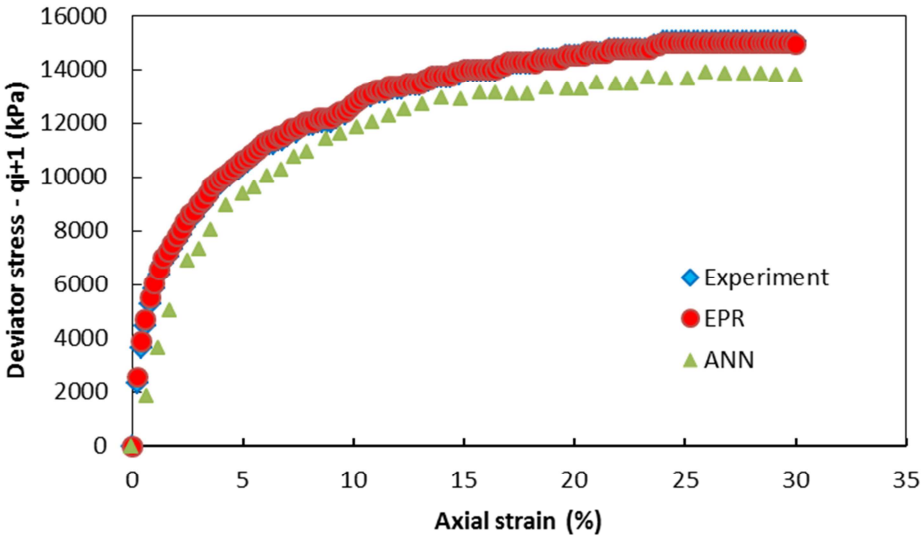

(a)

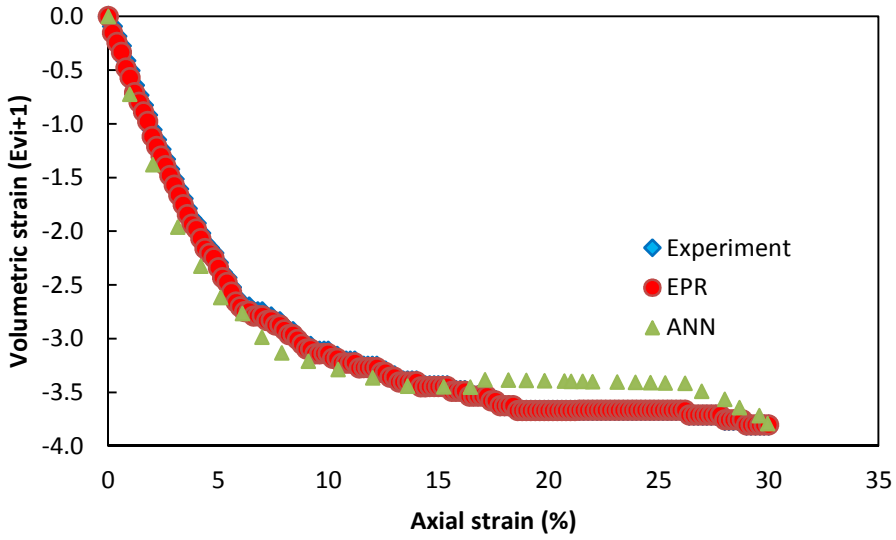

(b)

Figure 4.49: (a) Deviator stress-axial strain and (b) volumetric strain-axial strain curves predicted by the EPR models compared to experimental data and ANN model predictions ($\sigma_3 = 5515\ kPa$) – testing data case

The CoD values of the EPR models (Equations 4-8 and 4-9) are given in Table (4.14).

Table 4.14: COD values for EPR models

Equation	COD values for training (%)	COD values for testing (%)
Deviator stress (Equation 5.2.1)	99.99	99.98
Volumetric strain (Equation 5.2.2)	99.99	99.99

4.5.5 Predicting entire stress paths using the EPR models

In this section, the EPR models (Equations 4-8 and 4-9) are used to predict the entire stress paths, incrementally, point by point, in $q:\varepsilon_a$ and $\varepsilon_v:\varepsilon_a$ spaces. Results from four different sets of (testing) data were used to evaluate the ability of the incremental EPR models to predict the complete behaviour of granular soils during the entire stress paths. The values of average grain size, coefficients of uniformity and curvature, hardness, shape factor, void ratio and the confining pressure represented the initial conditions of the soil and were considered constant throughout the test. Other contributing parameters including axial strain and the current values of deviator stress and volumetric strain were updated in each incremental step, considering the values from the previous increment and the EPR models outputs in response to an axial strain increment. Figure 4.50 illustrates the procedure followed for updating of the input parameters and building the entire stress path for the shearing stage of a triaxial test.
At the start of the shearing stage in a conventional triaxial experiment, the values of all parameters are known. Then, for a prescribed increment of axial strain ($\Delta\varepsilon_a$) the values of q_{i+1}, $\varepsilon_{v,i+1}$ are calculated from the EPR models (Equations 4-8 and 4-9 respectively). For the next increment, the values of $\varepsilon_{a,i}$, q_i and $\varepsilon_{v,i}$ are updated as:

$$q_i = q_{i+1}$$

$$\varepsilon_{v,i} = \varepsilon_{v,i+1}$$

$$\varepsilon_{a,i} = \varepsilon_{a,i} + \Delta\varepsilon_a$$

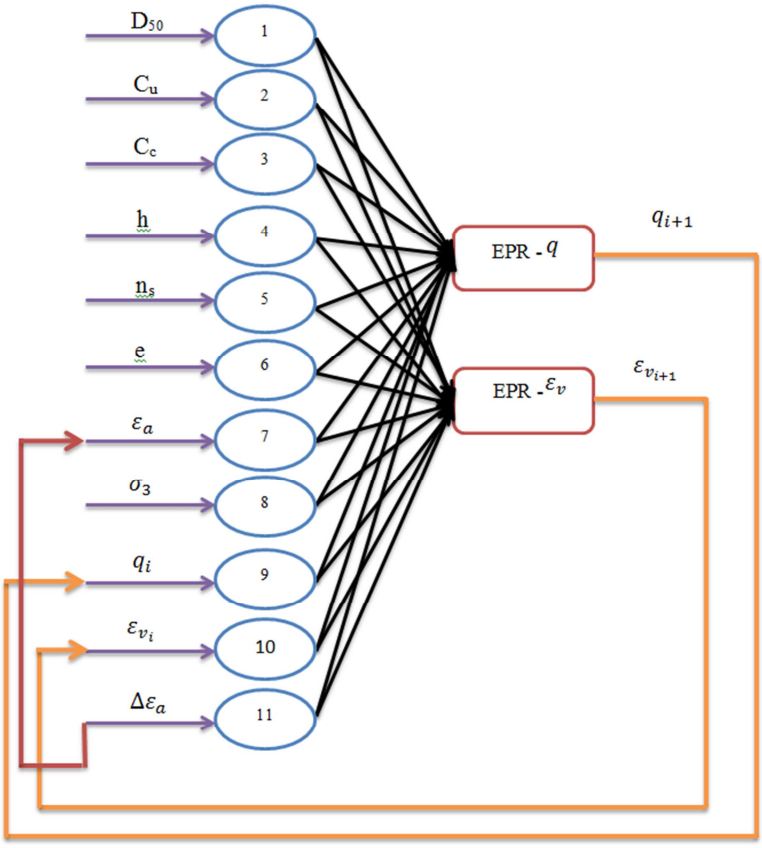

Figure 4.50: Incremental procedure for predicting the entire stress path

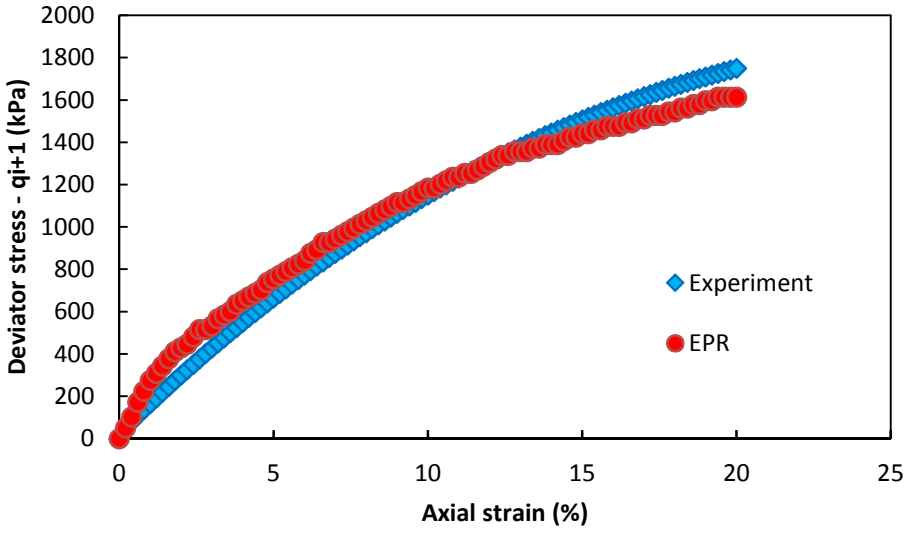

(a)

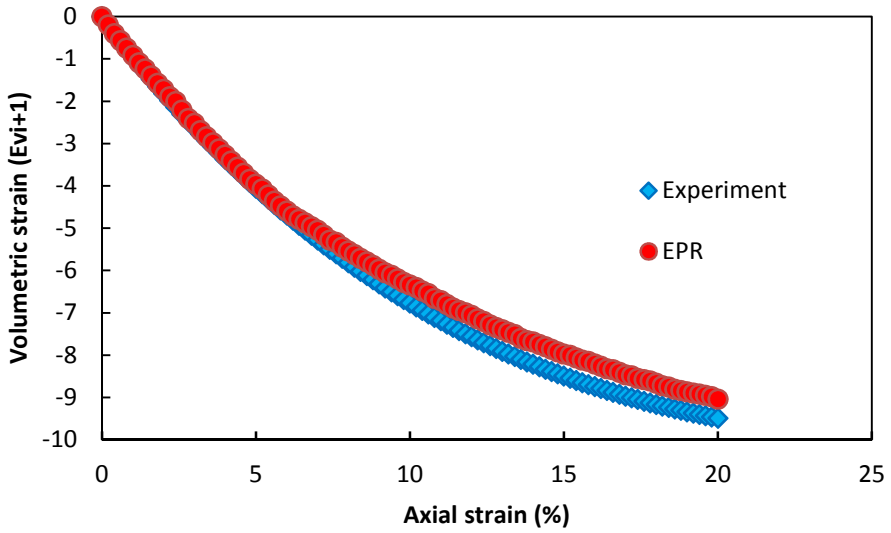

(b)

Figure 4.51: (a) Deviator stress-axial strain and (b) volumetric strain-axial strain curves predicted by the EPR models compared to experimental data ($\sigma_3 = 413\ kPa$) – testing data case, entire stress path prediction.

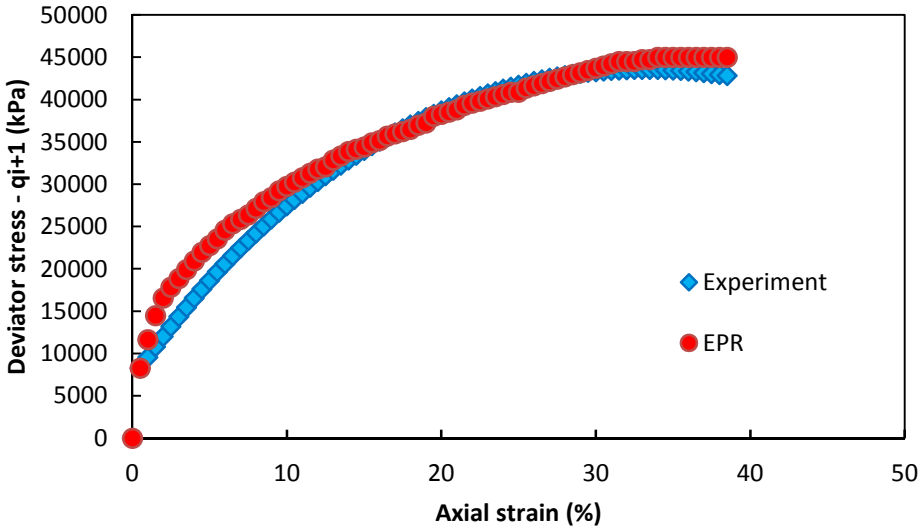

(a)

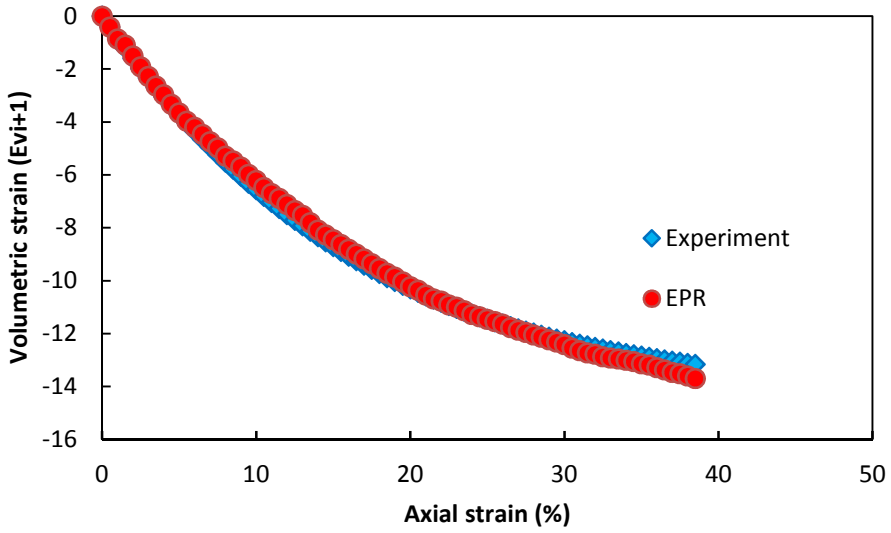

(b)

Figure 4.52: (a) Deviator stress-axial strain and (b) volumetric strain-axial strain curves predicted by the EPR models compared to experimental data ($\sigma_3 = 19613\ kPa$) – testing data case, entire stress path prediction.

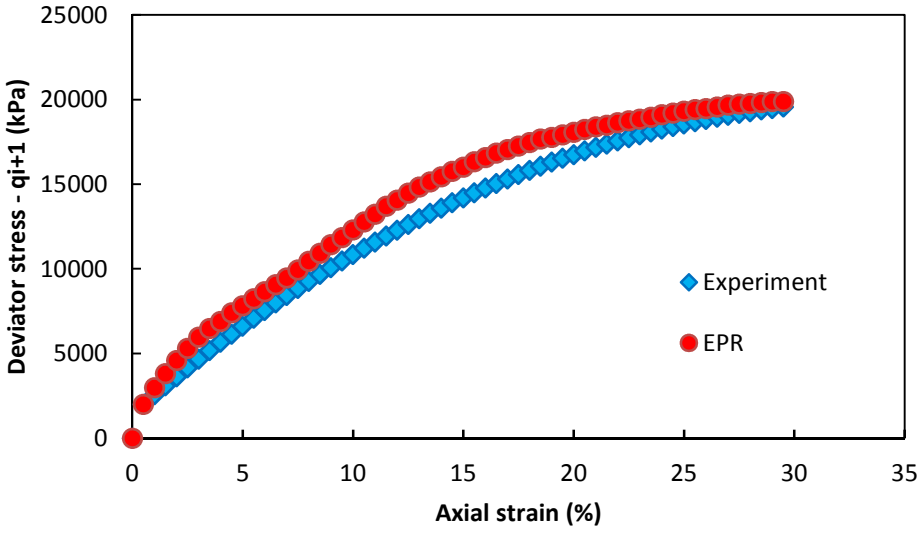

(a)

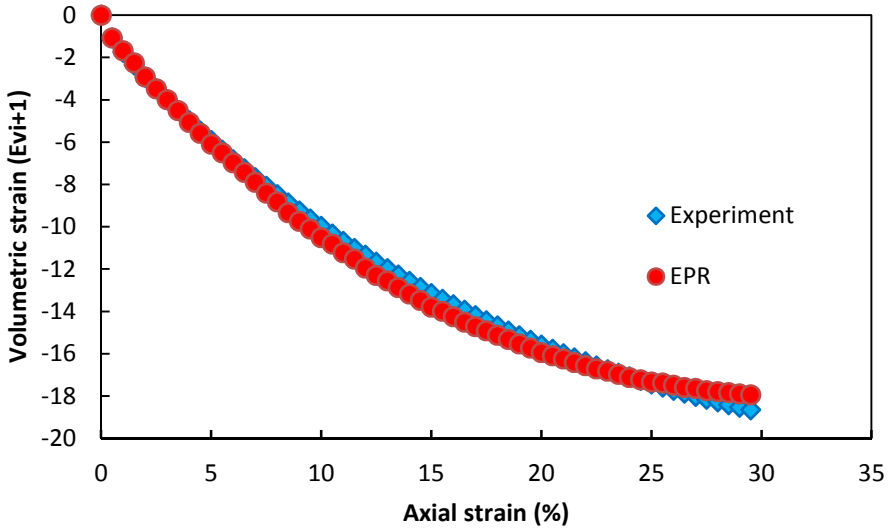

(b)

Figure 4.53: (a) Deviator stress-axial strain and (b) volumetric strain-axial strain curves predicted by the EPR models compared to experimental data ($\sigma_3 = 8276\ kPa$) – testing data case, entire stress path prediction.

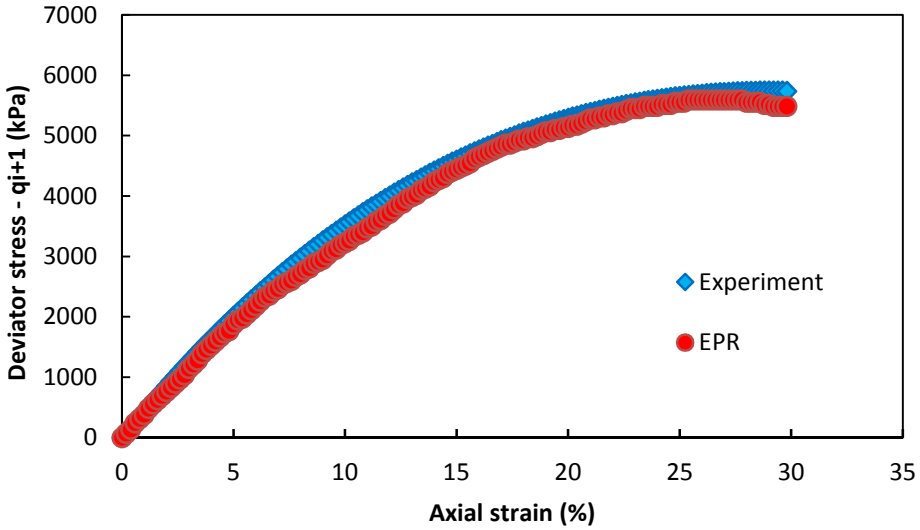

(a)

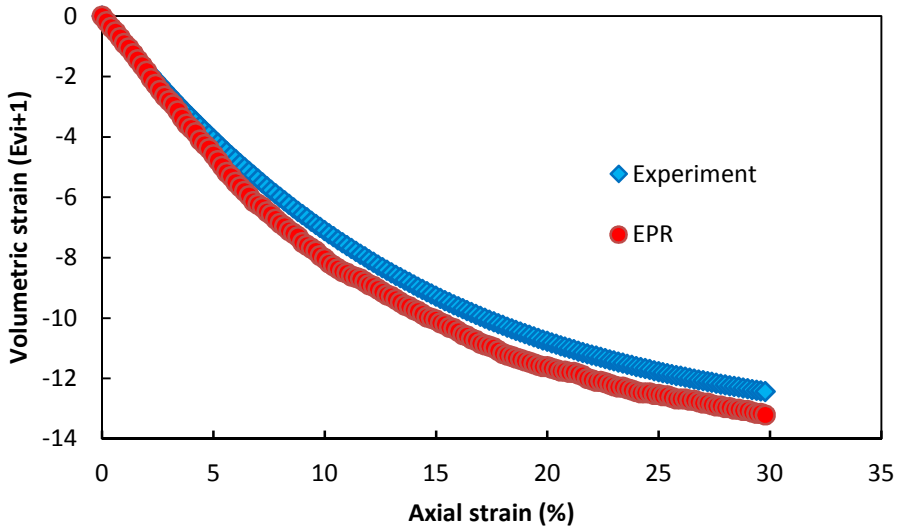

(b)

Figure 4.54: (a) Deviator stress-axial strain and (b) volumetric strain-axial strain curves predicted by the EPR models compared to experimental data ($\sigma_3 = 2068\ kPa$) – testing data case, entire stress path prediction.

The data for these tests have not been introduced to the EPR during the model building process. The predicted results are in very good agreement with the experimental results and, similar to the unsaturated soil models discusses before, in spite of the facts that the entire curves have been predicted point by point and also the errors of prediction of the individual points are accumulated in this prediction, still the EPR models are able to predict the complete stress paths. This shows that EPR framework is very effective and robust in modelling the behaviour of granular soils.

4.5.6 Sensitivity analysis

Results of the sensitivity analysis (conducted as described in section 4.4.6) are shown in Figures 4.55 to 4.57.

As expected increasing the average particle size (which indicates that the soil grains are getting coarser) causes the shear strength of the soil to increase (Figures 4.55a). In case

of granular soils the best way to compact a soil sample is vibration rather than compression. This is because of the friction between the coarse grains which increases under compression and makes it more difficult for the soil grains to move and fill up the voids. Figure 4.55b shows the negligible effect of increase in particle size on volumetric strain in granular soils.

Increasing the shape factor parameter shows that angularity of the soil increases resulting in higher friction and subsequently higher shear strength; however, as the soil grains gets more angular the possibility of crushing of the angular grains under stress also increases. Figure 4.56 shows that, due to the opposing effects of increase in friction and crushing of angular soil grains, the overall effect of increasing the shape factor, on shear strength and volumetric strain of granular soils is negligible.

Increasing void ratio causes the shear strength to drop and also the volumetric strain to increase under shearing. These effects are also correctly predicted by the proposed models (Figure 4.57).

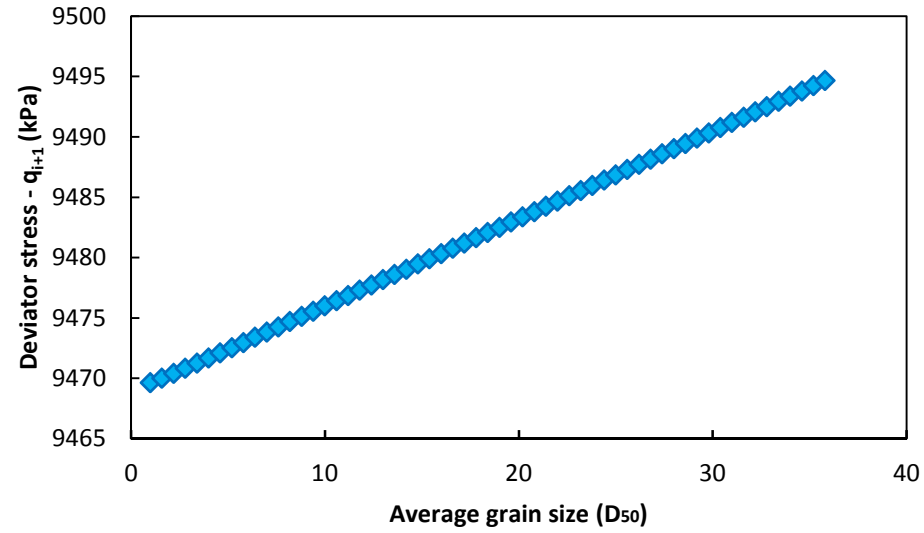

(a)

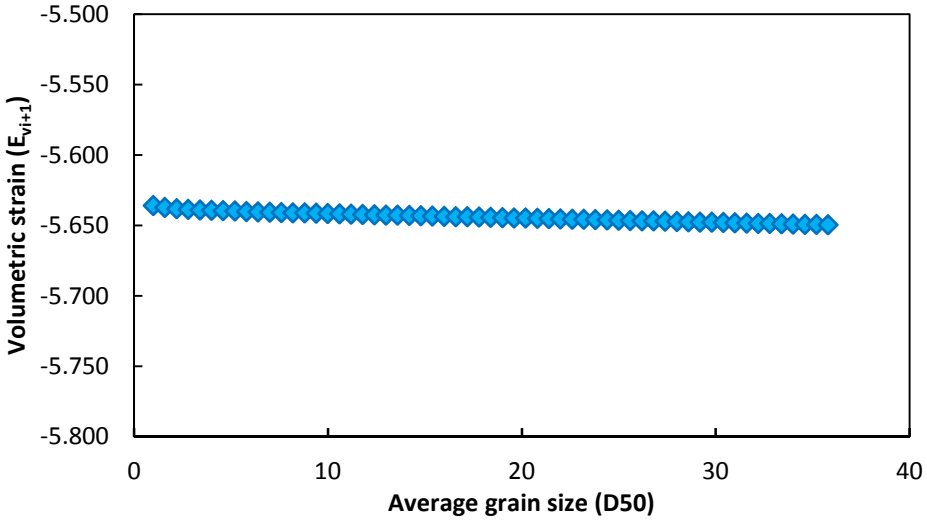

(b)

Figure 4.55: Sensitivity analysis results considering the effect of average grain size D_{50} on EPR model predictions for (a) deviator stress and (b) volumetric strain.

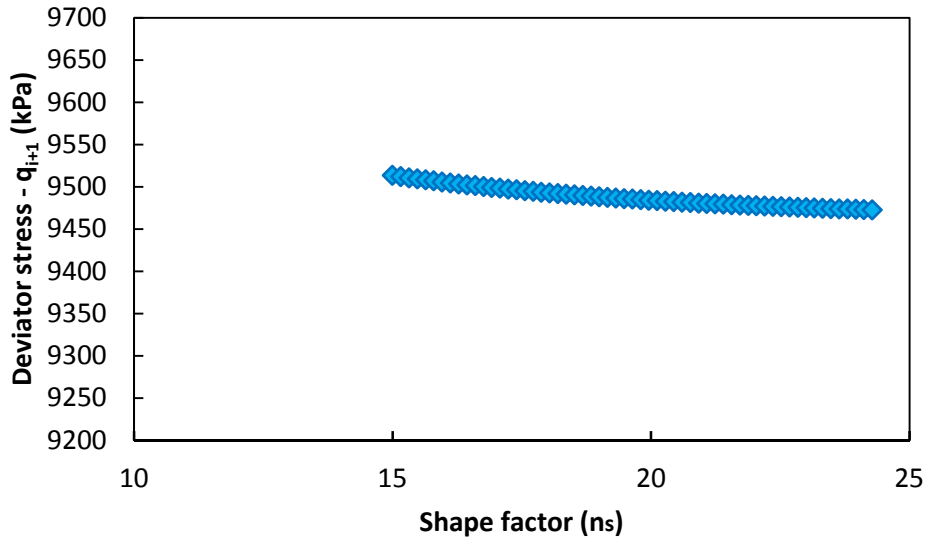

(a)

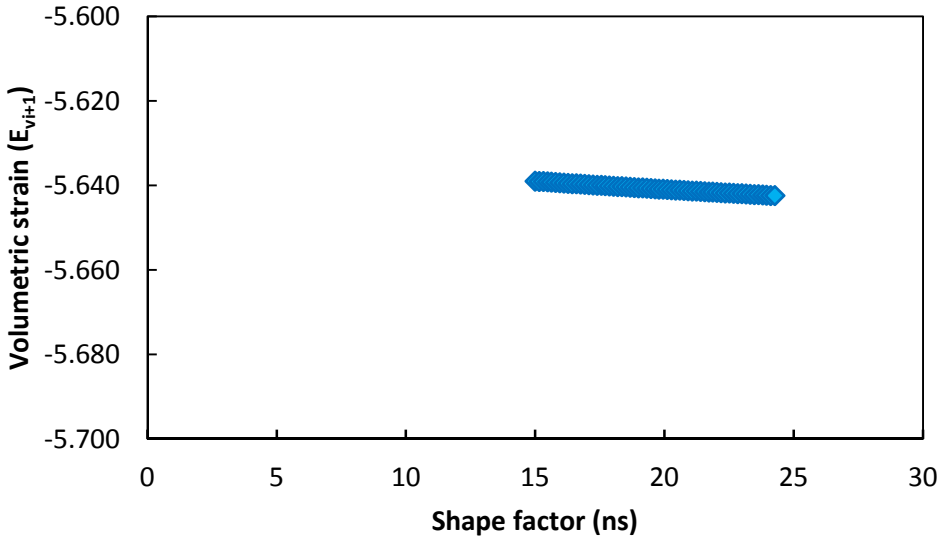

(b)

Figure 4.56: Sensitivity analysis results considering the effect of shape factor (n_s) parameter on EPR model predictions for (a) deviator stress and (b) volumetric strain.

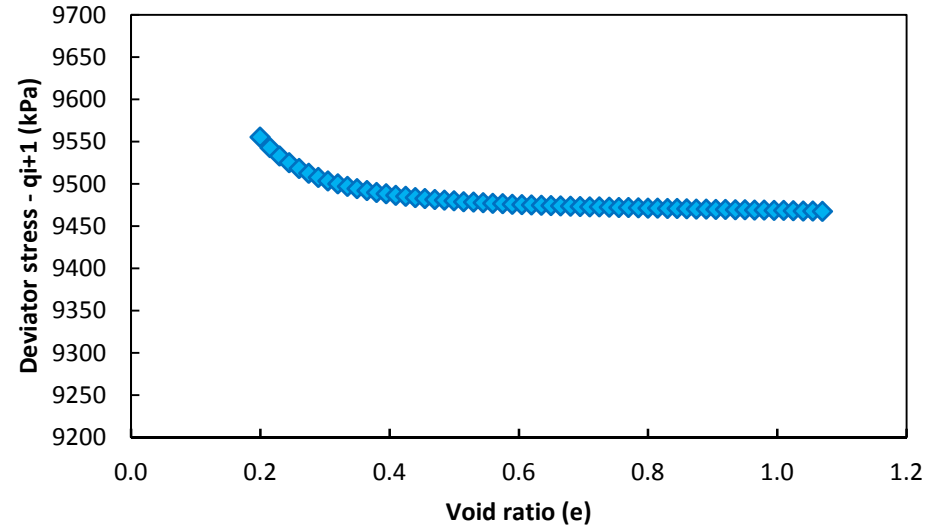

(a)

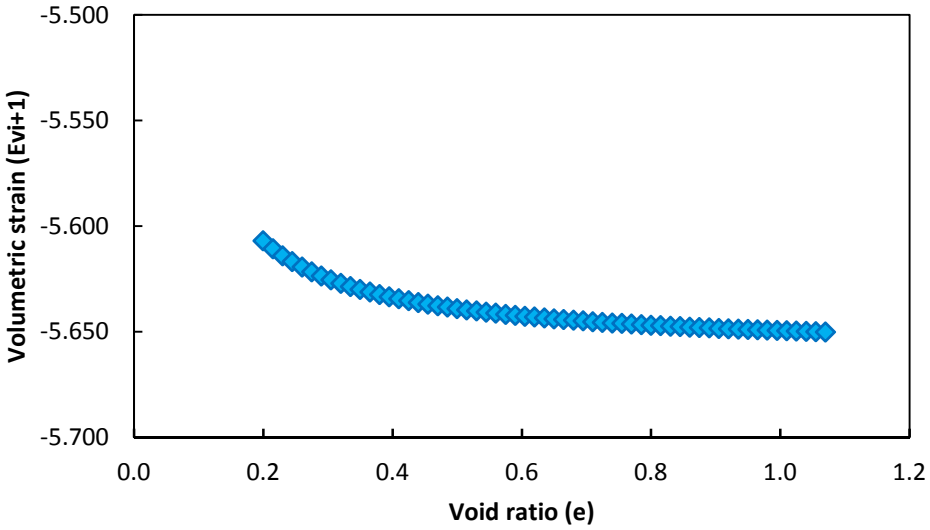

(b)

Figure 4.57: Sensitivity analysis results considering the effect of void ratio parameter (e) on EPR model predictions for (a) deviator stress and (b) volumetric strain.

4.5.7 Discussion and conclusions

Two models were developed based on the evolutionary polynomial regression to describe the deviator stress-axial strain and volumetric strain-axial strain behaviour of granular soils. It was shown that the EPR models can capture the underlying relationships between various parameters directly from experimental triaxial data and predict the granular soil behaviour with a very high accuracy. The EPR models were also tested using data that were not used in the training of the EPR models; in this way, an unbiased performance indicator was obtained on the real prediction capability of the models. The results revealed that the EPR-based models are capable of generalizing the training to predict the behaviour of granular soils under conditions have not previously seen by EPR in the training stage.

Through the comparison of the results it was shown that the proposed EPR models outperform ANN and provide closer results to the experiments.

The EPR models also successfully predicted the complete stress paths in $q:\varepsilon_a$ and $\varepsilon_v:\varepsilon_a$ spaces incrementally and point-by-point for unseen cases of data.

4.6 Identification of coupling parameters between shear strength behaviour and chemicals effects in compacted soils with EPR

4.6.1 Introduction

In the concept of nuclear waste storage, the stability of the galleries will be ensured with a concrete lining and this repository will be backfilled after use. Among other functions, this backfill will limit the convergence of the galleries after the concrete lining breaks (i.e. after thousands of years); it should also constrain the bentonite seals during their hydration. One key point is the degradation of the concrete lining of the galleries that will generate alkali-rich and high-pH solutes (Anderson et al., 1989) that will then diffuse into the backfill. This will give rise to a phenomenon called the hyperalkaline plume. Under extremely alkaline conditions, i.e. pH > 12, most of the usual soil minerals undergo extensive physicochemical transformations ((Huertas et al., 2000); (Boardman, Glendinning and Rogers, 2001)). Very high pH water causes the dissolution of the soil primary minerals accompanied by the formation of secondary minerals like calcium silicate hydrates (CSH) and calcium aluminate hydrates (CAH) (pozzolanic reactions) ((Bauer and Berger, 1998); (Bauer and Velde, 1999); (Chermak, 1993); (Ramírez et al., 2002); (Claret et al., 2002)). Many geochemical modelling studies have also been performed ((Savage, Noy and Mihara, 2002); (Gaucher et al., 2004)).
However, only very few studies have been carried out on these processes at the scale of compacted clay samples to characterise potential chemo-mechanical couplings between such high-pH water circulation and its impact on the geomechanical behaviour (shear strength, compressibility, permeability, etc.). Rodwell et al (2005) concluded that these physico-chemical reactions should alter the backfill physical properties, like porosity changes associated with permeability variation. Studying the interaction between Friedland Ton clay and low-pH cement water Pusch et al (2003) identified a slight drop in the clay hydraulic conductivity. Robinet (2005) showed that permeability of MX-80 bentonite was not sensitive to alkaline fluid circulation but to the temperature of the experiment. Karnland (2005) subjected MX-80 samples to several alkaline water types (NaOH and Ca(OH)2 solutions). Their results showed that the swelling pressure in bentonite is strongly reduced by exposure to NaOH solutions while little effect on swelling pressure was found in the samples exposed to Ca(OH)2 solutions.
Cuisinier et al ((2008) and (2009)) carried out a study to depict the influence of the circulation of very high-pH water on the hydro-mechanical behaviour of compacted argillite, pure or mixed with an additive (sand, bentonite or quicklime), that are the candidate materials to be used for backfilling. The geomechanical behaviour and the microstructure of the considered materials were studied over a period of alkaline water circulation of 12 months. The impact of the alkaline fluid on the geomechanical properties of the materials appeared to be a direct function of the nature of the additive. The geomechanical behaviour of the sand – argillite mixture remained almost stable over a period of 12 months of alkaline water circulation while, over the same period, dramatic modification of the lime – argillite mixture was observed. The subsequent step of this research would be to identify the key coupling parameter(s) between the

chemical stress imposed by the alkaline water circulation and the alteration of the hydro-mechanical behaviour of the tested mixtures. This is required to be able to assess the sensitivity of a given mixture, different from the one experimentally tested, to the circulation of alkaline water.
The large amount of tested configurations, the four different mixtures, and experimental conditions have rendered difficult the determination of such coupling parameter(s) and due to this the EPR was used to model the complex hydro-mechanical behaviour of the soil during alkaline fluid circulation.
An EPR model was developed and evaluated based on results from test data involving various additives circulation times (i.e. 0, 3, 6, and 12 month). Four cases of data, not employed for the training phase, were chosen to be used in the testing stage to evaluate the generalization capabilities of the developed model. In the last section, a parametric study was carried out where all parameters were set to their mean values except the one being monitored that was changed from its minimum to the maximum value in the training and testing data sets. The results of this analysis were used to identify coupling parameter(s) between chemical effects and shear strength behaviour alteration in order to assess the sensitivity of compacted soil to alkaline water circulation.

4.6.2 Experiments and data

Data used to develop the EPR models were acquired from the works of Cuisinier and his colleagues ((2008), (2009)). The selected material corresponds to the callovo-oxfordian argillite where the French underground laboratory has been built. After sampling, the Manois Argillite (MA) was carefully homogenised and crushed into a very fine grain powder. Chemical and XRD analyses indicated that the MA contains 26 to 32 % calcite, 22 to 27 % quartz, and 41 to 49 % clays. The clays were mainly illite, kaolinite and an interstratified illite-smectite. The specific surface determined with BET was 40.4 ± 1 $m^2.g^{-1}$.
For the study of the backfilling of deep galleries, three different additives intended to improve the hydro-mechanical properties of the argillite, were considered. The first was a 50 % sand and 50 % MA mixture on a dry-weight basis. The addition of sand increases the dry density and the frictional characteristics of the compacted argillite ((Dixon, Gray and Thomas, 1985); (Mollins, Stewart and Cousens, 1999)). The selected sand was calcareous sand produced in a quarry near the Meuse-Haute Marne site. It contained more than 95 % calcite, with the remaining minerals being quartz and ankerite. Its characteristics are given in Table 4.15.

Table 4.15: Properties of the tested materials

Material	Liquid limit (LL%)	Plasticity index (PI%)	Solid density (Mg/m^3)	Cation exchange capacity (meq/100g)
MHM argillite[a]	31	17.9	2.7	6-14
MA	51	11.2	2.68	23
Calcareous sand	Non-plastic	Non-plastic	2.71	-
MX-80[b]	520	458	2.65	97

[a] Data of MHM argillite from Deroo (Deroo, 2002)
[b] Data from Marcial et al (Marcial, Delage and Cui, 2002) and Neaman et al (Neaman, Pelletier and Villieras, 2003)

The second additive was MX-80 bentonite, which was selected to enhance the sealing properties of the backfill through improved swelling (Dixon, Gray and Thomas, 1985). The properties of MX-80 are also given in Table 4.15. This clay contains more than 80 % montmorillonite with sodium and calcium as exchangeable cations and 86.1 % of the particles are smaller than 2 μm. The mixture used was 20 % MX-80 and 80 % MA on a dry-weight basis.

The third additive considered was quicklime, which improves both the cohesion and the friction angle of clayey materials ((Fossberg, 1965); (Brandl, 1981)). When added to a soil, lime induces physico-chemical reactions that increase the mechanical characteristics of the soil ((Little, 1995); (Bell, 1996); (Le Runigo et al., 2009)). The quicklime used in that study was composed of more than 97 % of pure CaO. A lime content of 4 % with the remainder MA on a dry-weight basis was selected for the experimental program.

Results from 33 consolidated undrained triaxial tests conducted on samples of argillite (MA), lime-MA, sand-MA, bentonite-MA mixtures, subjected to different periods of exposure to alkaline water circulation, were used for development and validation of the EPR model. Of the total of 33 cases, 29 cases related to different circulation times (i.e. 0, 3, 6, 12 months) were used for training of the EPR model. Of these 29 cases, 11 cases were related to no circulation (0 month of circulation), 5 cases to 3 months, 2 cases to 6 months and 11 cases to 12 months of circulation of the alkaline water through the samples. The remaining 4 cases (each relating to a different soil and circulation time) were kept unseen during the model development process and used to evaluate the developed model.

4.6.3 EPR model

Eight parameters were used as input for the EPR model including dry density (ρ_d), alkaline water circulation time (t), axial strain (ε_a), pore pressure (u), effective confining pressure (σ_3'), porosity of macro-pores (e_M), porosity of micro-pores (e_m), and the specific surface of the soil particles (SS). The only output was considered to be the deviatoric stress ($\sigma_1'-\sigma_3'$). The following equation represents the (unit dependent) EPR model developed through the above mentioned procedure:

$$\sigma_1'-\sigma_3' = \frac{-2.95\times10^5\varepsilon_a^2}{\rho_d^3\cdot SS^2}+\frac{4.68}{\rho_d^2\cdot e_M^3}+\frac{0.01t}{e_M^3}+\frac{1.07\times10^5\varepsilon_a+5.97\times10^3 e_m^2\cdot u}{e_M\cdot SS^2}-\frac{136.56}{e_m^3}-\frac{5.65\times10^3\Delta u}{SS^3}+$$
$$2.99\times10^{-6}u\cdot\sigma_3'^2-3.23\times10^4 e_m^2-\frac{10^{-5}e_m^3\cdot t^3\cdot\varepsilon_a\cdot\sigma_3'^3}{SS^3}-1.22\times10^4 e_M+\frac{1.09\times10^5 e_M\cdot e_m^2\cdot\varepsilon_a}{SS}-2.18\times10^4\rho_d \quad \text{4-10}$$
$$+\frac{20.48\rho_d\cdot e_M\cdot\varepsilon_a^3\cdot\sigma_3'}{SS^2}-\frac{1.72\times10^{-3}\rho_d^2\cdot\varepsilon_a}{e_M^3\cdot e_m^3}+45633.1$$

Figure 4.58 shows typical results of the training of the EPR model for sand-argillite, lime-argillite and MX-80-argillite mixtures at slightly different confining pressures after 12 months of circulation. The results are compared with actual measurements and it is shown that the EPR model has been able to capture the behaviour of the mixtures with a good accuracy.

Figure 4.59 presents typical results of testing of the developed EPR model for pure argillite at confining pressure of 295kPa with no circulation, lime-argillite at confining pressure of 274kPa after 6 months of circulation and MX-80-argillite at confining pressure of 270kPa after 12 months circulation. It is shown that the developed model

has also been able to generalize the training to conditions that were not introduced to the model during the training process. The values of coefficient of determination for testing and training data are 93.2% and 94.24% respectively.

4.6.4 Sensitivity analysis

This sensitivity analysis (conducted as detailed in section 4.4.6) aimed at determining a possible coupling parameter that could explain the changes in shear strength behaviour observed after the circulation of the alkaline fluid.
The sensitivity analysis was carried out considering four parameters (dry density, macropore void ratio, micropore void ratio and specific surface). It can be seen that the dry density did not permit to explain differences in maximum shear strength that have been observed in the experimental study (Figure 4.60). Even though there is a tendency for the maximum shear strength to increase with an increase in dry density, the calculated variation is much more limited (165-190kPa) compared to what has been observed experimentally for the tested mixtures (from hundred kPa up to several thousands of kPa). The same conclusion can be drawn from the sensitivity analysis for the macropore void ratio (eM).
However, the results of the sensitivity analysis showed that the variation of the maximum deviatoric stress for all the tested samples can be explained mainly by the value of the specific surface of the samples, especially when its value is below 100 $m^2.g^{-1}$ and to a lesser extent by the micropore void ratio. From a physical point of view, specific surface can be used as an indicator of the nature of the material as it reflects its clay content and therefore its mechanical behaviour before circulation. The addition of MX-80 bentonite to the Manois argillite results in a high value of the specific surface, which results in lowering of the mechanical characteristics compared to the initial material (Table 4.16). The addition of lime leads to the flocculation and aggregation of the clay particles that is responsible for a decrease in the specific surface of the Manois argillite, and increase of the micropore void ratio. This was associated with a strong effect on the shear strength behaviour because addition of lime led to the formation of cementitious compounds responsible for the increase in shear strength (Table 4.16) as evidenced by several authors (Little, 1995). The effect of the alkaline water circulation may also alter the specific surface of the tested material. Indeed, the main effect of the alkaline fluid circulation was to induce the dissolution of clay particles (Huertas et al., 2000), that could result in a decrease in the specific surface of the soil. The dissolved compounds may react with the calcium to form cementitious compounds responsible for the increase in shear strength. The formation of new cementitious compounds can lead to a closure of the smallest pores of the soil as evidenced by some researchers who studied lime-treated soils at microstructural level ((Choquette, Berube and Locat, 1987); (Bin et al., 2007)).
Combination of the two parameters, specific surface and micropore void ratio, allowed the explanation of the behaviour of the mixture of Manois argillite and of MX-80 bentonite. This sensitivity analysis shows that the model has also been able to capture and represent the behaviour of the individual mixture. In fact, in case of this mixture, the circulation led to a strong increase of specific surface (-25 $m^2.g^{-1}$) and an increase of the macropore void ratio without significant modification of the micropore void ratio.

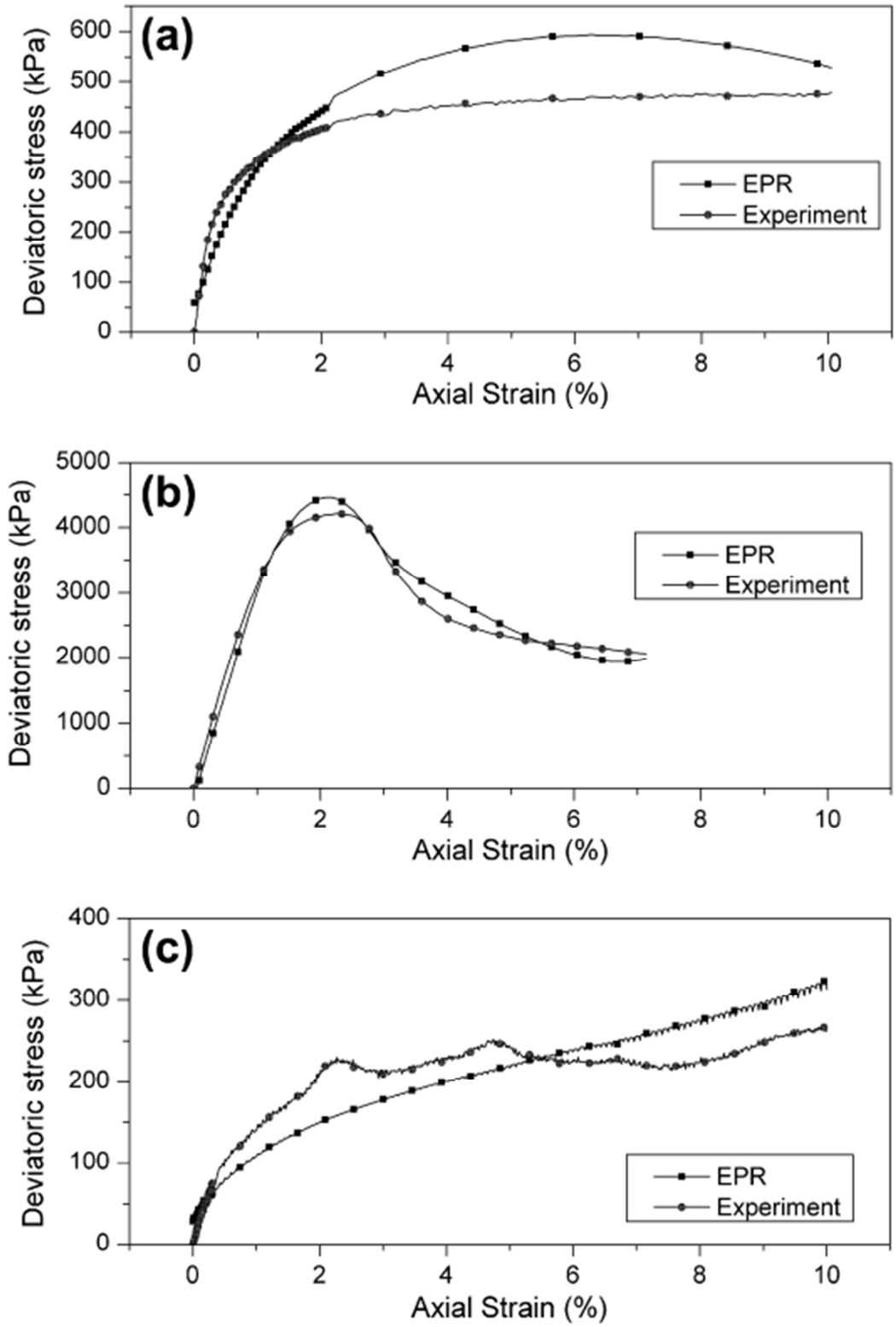

Figure 4.58: Typical training results of the EPR model: (a) Sand-argillite, σ_3'=569kPa, (b) Lime-argillite σ_3'=587, (c) MX-80-argillite, σ_3'=557kPa, after 12 months circulation.

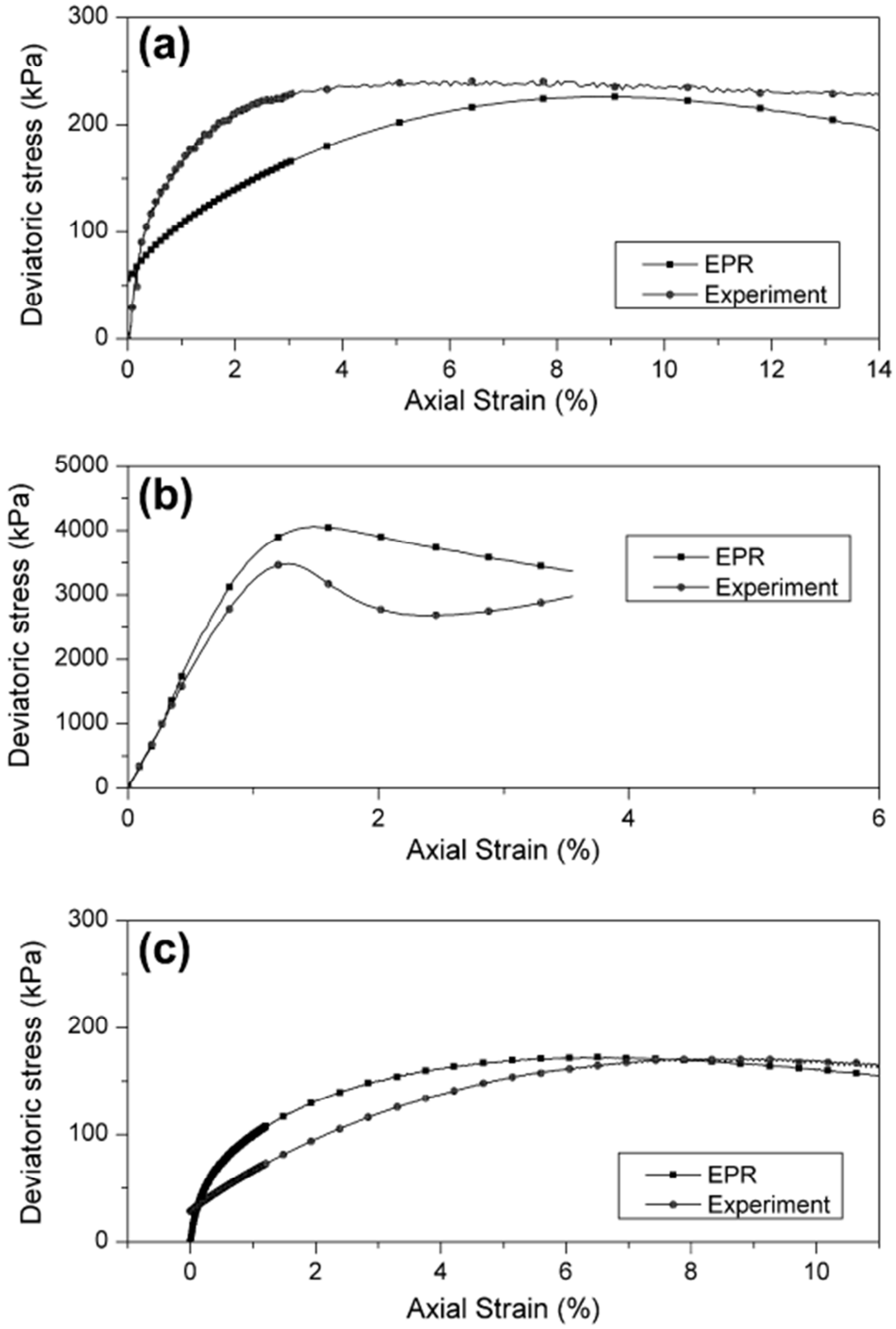

Figure 4.59: Typical testing results of the EPR model: (a) Pure argillite, σ_3'=295kPa, No circulation; (b) Lime-argillite σ_3'=274, 6 month circulation; (c) MX-80-argillite, σ_3'=270kPa, 12 months circulation.

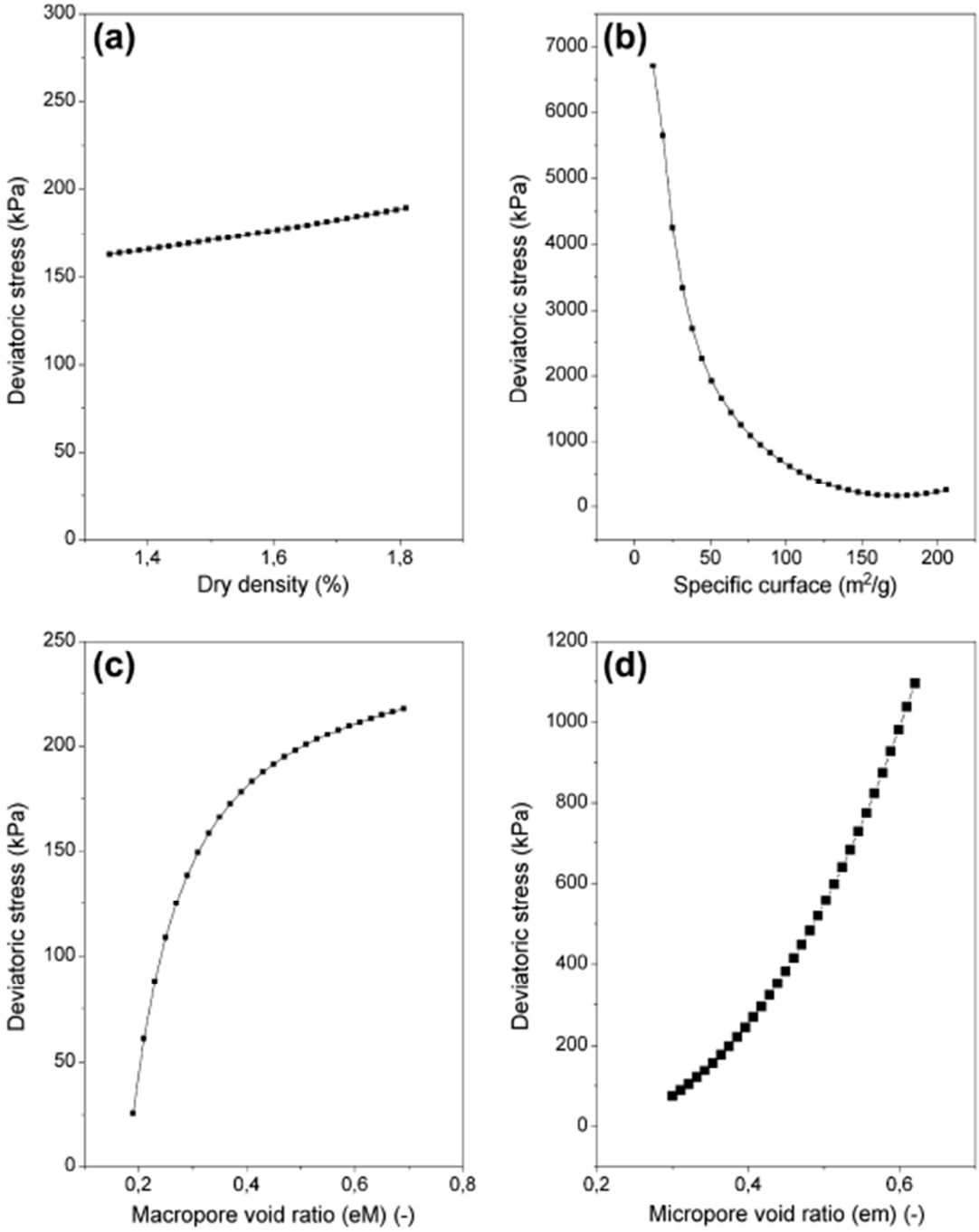

Figure 4.60: Sensitivity analysis considering effect of (a) dry density, (b) specific surface, (c) macroporosity and (d) microporosity

Table 4.16: Properties of the tested materials

Mixture	Circulation period (months)	Water content (%)	Dry weight ($Mg . m^{-3}$)	Specific surface (m^2g^{-1})	Effective friction angle (°)	Effective cohesion (kPa)
Pure argillite	0	23	1.61	156.6	18.6	25.6
	12	27.5	1.54	142	22.2	9.5
50% Argillite + 50% sand	0	15.5	1.83	67.5	28.9	0
	3	17.1	1.86	71.7		
	6	14.9	1.85	67.5	26.8*	0*
	12	16.2	1.88	74.6		
80% Argillite + 20% MX-80	0	25.5	1.54	205.6	18.1	0
	12	34.5	1.34	182.6	13.5	30
96% Argillite + 4% lime	0	25.5	1.55	51.4	39.5	50.3
	3	29	1.49	24.5		
	6	29.9	1.47	19.6	53.7*	282.5*
	12	29.7	1.48	12.2		

[a] No significant influence of circulation duration on shear strength parameter

4.6.5 Discussion and conclusions

Results from a comprehensive study on the impact of the alkaline fluid circulation on mechanical behaviour of several mixtures, made by mixing Manois Argillite and different additives was used to model the complex hydro-mechanical behaviour of the soil during alkaline fluid circulation using the evolutionary polynomial regression (EPR).

Overall, the results showed that the EPR model, trained from pure experimental data, was able to capture and correctly represent many physical characteristics of the behaviour of the different mixtures considered in the study and the effect of the alkaline fluid circulation, with a high accuracy for both training and unseen testing sets of data.

This model was then used to perform a sensitivity analysis in order to identify the best possible coupling parameters between chemical's effect and the shear strength behaviour. It appeared that the most appropriate parameter is the specific surface of the mixture. In the model, the specific surface permit to take into account differences at the initial state (before circulation), reflecting the composition of the mixture, i.e. the nature of the additive, and the differences in their shear strength behaviour. Moreover, specific surface is sensitive to the alkaline fluid circulation duration, and its impact on the shear strength behaviour of each individual mixture. To a lesser extent, the micropore void ratio appeared to be a coupling parameter, even though the shear strength behaviour of the different mixtures is less sensitive to it.

4.7 Conclusions

In this chapter the application of EPR in modelling the stress-strain and volume change behaviour of saturated and unsaturated soils was presented. The temperature effects on

the mechanical behaviour, and also the soil-water characteristic curve in unsaturated soils were modelled. The entire stress paths for stress-strain and volumetric strain-axial strain behaviours were successfully reproduced using the developed models for relevant cases. EPR modelling was also successfully used to find coupling parameters between shear strength behaviour and chemical's effects in compacted soils. Detailed explanations of the modelling procedures and the sensitivity analyses of the developed models were presented.

The results showed that the developed models were capable of predicting complex behaviour of saturated and unsaturated soils accurately.

In the next chapter, further applications of the EPR methodology to other geotechnical and civil engineering problems will be presented.

Chapter 5

OTHER GEOTECHNICAL AND CIVIL ENGINEERING APPLICATIONS OF EPR

5.1 Introduction

This chapter presents the application of EPR to develop models for predicting compaction characteristics and permeability of soils, stability status of soil and rock slopes and the mechanical behaviour of rubber concrete.

Permeability (K), maximum dry density (MDD) and optimum moisture content (OMC) are modelled as functions of some physical properties of soil. EPR models are developed based on results from a series of classification, compaction and permeability tests from literature. The tests included standard Proctor tests, constant head permeability tests and falling head permeability tests conducted on soils made of four components, bentonite, limestone dust, sand, and gravel, mixed in different proportions.

EPR methodology is also introduced as an efficient tool for stability analysis of soil and rock slopes. The main parameters contributing to the behaviour of slopes, namely, unit weight, apparent cohesion, friction angle, slope angle, and pore water pressure are used in the development of the EPR models. The developed models are used to predict the factor of safety of slopes against failure for conditions not used in the model building process.

Evolutionary polynomial regression is also used to predict the mechanical behaviour of rubber concrete. A model is developed relating the compressive strength of rubber concrete to a number of physical parameters that are known to contribute to the mechanical behaviour of rubber concrete.

Data sources and data preparation processes are represented and discussed. Validity and efficiency of the produced models are shown by comparing the proposed model predictions with field measurement, experimental data and conventional models where applicable.

5.2 Modelling of permeability and compaction characteristics of soils

5.2.1 Introduction

In construction of many civil engineering structures such as road embankments, loose soil must be compacted to a desired density and water content. In other projects such as earth dams and compacted soil liners for containing contaminated solid and liquid wastes, the soil should be compacted for the density as well as the permeability requirements. The permeability of compacted soils very much depends on the compaction condition. The required compaction is usually expressed in terms of degree of compaction (dry density) and water content of the soil. To achieve the required degree of compaction, the water content must be near its optimum value. Thus, both the maximum dry density and optimum water content are essential parameters for design of compacted earthwork. Furthermore, for soil lining construction, the permeability of compacted soil liner must be very low. Since permeability, maximum dry density and optimum water content are normally determined from time-consuming laboratory tests, it is desirable to have prediction models capable of predicting compacted soil characteristics based on some easily measurable physical properties of soils.

Many research works have been conducted to relate permeability and compaction characteristics of soils to their physical properties. The physical properties used generally include plasticity characteristics (liquid limit, plastic limit, shrinkage limit, and plasticity index), specific gravity, and grain size distribution that are easily attainable from relatively straightforward laboratory tests. However, the specific index properties used in various correlation equations differ considerably. Rowan and Graham (1948) used gradation, specific gravity and shrinkage limit in their correlation equations. Davidson and Gardiner (1949) eliminated the specific gravity from the equations of Rowan and Graham (1948), but included plasticity index. Turnbull (1948) related the optimum moisture content with gradation, while Jumikis (1946) correlated the optimum moisture content with liquid limit and plasticity index.

Ring et al (1962) developed two sets of correlation equations, one for optimum moisture content and the other for maximum dry density. The physical properties used were liquid limit, plastic limit, plasticity index, D_{50}, content of particles finer than 0.001 mm, and fineness average (FA). The fineness average was determined as one-sixth of the summation of the percentages of soil mass finer than No.10, No.40 and No.200 sieves. Liquid limit alone was correlated with both maximum dry density and optimum moisture content by Ramiah et al. (1970) and Blotz et al. (1998). Linveh and Ishai (1978) also developed some relationships using specific gravity and liquid limit as input. Gupta and Larson (1979) presented a model for predicting packing density of soils from grain size distribution.

The permeability of a soil varies with many factors, such as soil density, water content, degree of saturation, void ratio and soil structure. Available correlations between these factors and permeability include those of Carman (1937), Burmister (1954), Lambe (1951), Michaels and Lin (1954), Olson (1963), Mitchell et al. (1965), and Garcia-Bengochea et al. (1979). Various relationships between permeability and grain size distribution of soils have been reported. Hazen (1911) suggested that, for filter sands having relatively uniform particles, the permeability is directly proportional to the square of the effective grain size, D_{10}. Zunker (1930) developed a theoretical linear relationship, in full logarithmic scales, between the grain size and permeability for

spherical particles of uniform size. Taylor (1948) formulated a theoretical equation, based on the capillary tube model, for flow through porous media, relating the permeability with a representative grain size. Considering of the effect of grain size on permeability, Burmister (1954) recommended that the type of grading (namely, the shape of gradation curve), range of grain size, and the effective grain size (namely, D_{10}) must be taken into account. For a given type of gradation and grain size range, he found that the permeability can be better related with D_{50} than with D_{10}. Horn (1971) related the permeability with the mean grain size on the basis of Zunker's work in 1930. Chen et al. (1977) found that the permeability is strongly related with D_{50}, and Hauser (1978) related the permeability with the aggregate size. Based on the previous research works it can be concluded that the permeability is strongly dependent on grain size distribution. However, a general correlation equation between permeability and gradation applicable to a wide range of soils is not yet available. To develop such a relationship, the entire spectrum of grain size distribution must be considered. More importantly, the density or void ratio of the soil mass should also be considered.

Taking into account a much broader range of influencing factors, Wang and Huang (1984) developed regression equations for predicting maximum dry density, optimum water content, and permeability for two levels of compaction degree (90 and 95%). Najjar et al (1996) used neural networks to determine the optimum moisture content and maximum dry density of soils. Sinha and Wang (2008) proposed models based on artificial neural networks (ANNs) to predict the permeability, maximum dry density, and the optimum moisture content.

EPR models are proposed in this section as alternatives to ANN models suggested by Sinha and Wang in 2008. EPR models were developed to relate permeability (K), maximum dry density (MDD) and optimum moisture content (OMC) to physical properties of soils. The results of EPR model predictions were compared with those of a neural network model, a correlation equation from literature and the experimental data. A parametric study was also conducted to assess the level of contribution of each parameter to the developed models.

5.2.2 Database

Some experimental data from literature (Sinha and Wang, 2008) were used to develop the EPR models. Table 5.1 includes the gradation properties of soils, Table 5.2 contains the compaction test data as well as some physical properties, and Table 5.3 summarizes the permeability test data. The data are from a soil made of four different major components (gravel, sand, limestone dust and bentonite) with different proportions. The bentonite contained Na-Montmorillonite as the primary clay mineral. The limestone dust was a by-product of limestone quarry, which had a grain size ranging from 0.002 mm to 0.047 mm.

The sand component was a well-graded fine aggregate used for making Portland cement concrete. Its grain size ranged from 0.074 mm to 4.76 mm. The gravel component was a coarse aggregate having a particle size range of 4.76–10.05 mm. All the tests were conducted following the standard testing procedures stipulated in the ASTM Standard, e.g., ASTM D-422 for mechanical analysis, ASTM D-423 for liquid limit, and ASTM D-424 for plastic limit tests. The laboratory compaction tests were conducted by using the standard Proctor compaction effort in accordance with the standard test procedures of ASTM D-558. The details of testing procedure and results of analysis have been presented by Sinha and Wang in their 2008 paper.

Table 5.1: Graduation and physical properties of the test soils (Sinha and Wang, 2008)

Soil No.	Nominal gradation (%)				Actual gradation (%)				Specific gravity	Atterberg limits		Grain Size		
	Clay	Silt	Sand	Gravel	Clay	Silt	Sand	Gravel		LL(%)	PL(%)	<No. 4	<No. 40	<No. 200
(1)	(2)	(3)	(4)	(5)	(6)	(7)	(8)	(9)	(10)	(11)	(12)	(13)	(14)	(15)
1	100	0	0	0	84	16	0	0	2.76	495	46	100	100	100
2	80	20	0	0	71	28	1	0	2.76	444	36	100	100	99
3	60	40	0	0	57	41	2	0	2.76	351	36	100	100	98
4	40	60	0	0	44	53	3	0	2.75	203	38	100	99	97
5	20	80	0	0	30	70	0	0	2.87	84	31	100	100	98
6	0	100	0	0	17	83	0	0	2.75	24	22	100	100	97
7	0	60	20	0	13	63	24	0	2.73	0	0	100	88	76
8	0	60	40	0	10	47	43	0	2.72	0	0	100	77	57
9	0	40	60	0	6	31	63	0	2.7	0	0	100	66	37
10	0	20	80	0	3	16	81	0	2.68	0	0	100	55	19
11	0	0	100	0	0	0	100	0	2.67	0	0	100	44	0
12	20	0	80	0	16	3	81	0	2.69	136	25	100	55	19
13	20	20	60	0	20	18	62	0	2.7	132	23	100	66	38
14	20	40	40	0	24	34	42	0	2.73	94	26	100	70	58
15	20	60	20	0	28	50	22	0	2.74	81	27	100	88	78
16	40	40	20	0	40	38	22	0	2.74	222	38	100	88	78
17	40	20	40	0	37	22	41	0	2.72	240	35	100	78	59
18	40	0	60	0	33	6	61	0	2.71	277	29	100	66	39
19	60	0	40	0	50	10	40	0	2.73	389	32	100	78	60
20	60	20	20	0	54	25	21	0	2.74	362	42	100	89	79
21	80	0	20	0	67	18	20	0	2.76	467	39	100	89	80
22	0	0	90	10	0	0	90	10	2.67	0	0	90	40	0
23	0	20	70	10	3	16	71	10	2.72	0	0	90	51	10
24	0	40	50	10	7	32	51	10	2.76	0	0	90	62	39
25	0	60	30	10	10	48	32	10	2.81	0	0	90	74	58
26	0	80	10	10	14	64	12	10	2.86	0	0	90	85	78
27	0	90	0	10	16	72	2	10	2.88	0	0	90	90	88
28	10	10	70	10	10	9	71	10	2.69	75	15	90	51	19
29	10	30	50	10	23	26	41	10	2.75	60	10	90	72	49
30	10	50	30	10	17	42	31	10	2.72	50	10	90	74	59
31	10	70	10	10	21	57	12	10	2.84	45	20	90	85	78
32	10	80	0	10	22	62	2	10	2.86	50	25	90	90	88
33	30	10	50	10	27	12	51	10	2.71	210	30	90	62	39
34	30	30	30	10	30	28	32	10	2.73	175	35	90	73	59
35	30	50	10	10	34	44	12	10	2.74	165	40	90	84	78
36	30	60	0	10	35.6	53	1.8	9.6	2.84	162	47	90	90	89
37	50	10	30	10	44	16	30	10	2.74	342	32	90	74	60
38	50	30	10	10	47	32	11	10	2.74	330	40	90	85	79
39	50	40	0	10	49.2	40	1.2	9.6	2.75	322	37	90	90	89
40	70	10	10	10	61	19	10	10	2.74	445	40	90	85	80

Table 5.1: Continued

Soil No.	Nominal gradation (%)				Actual gradation (%)				Specific gravity	Atterberg limits		Grain Size		
	Clay	Silt	Sand	Gravel	Clay	Silt	Sand	Gravel		LL (%)	PL (%)	<No. 4	<No. 40	<No. 200
(1)	(2)	(3)	(4)	(5)	(6)	(7)	(8)	(9)	(10)	(11)	(12)	(13)	(14)	(15)
41	70	20	0	10	63	26	1	10	2.75	435	40	90	90	89
42	90	0	0	10	76	14	0	10	2.75	495	46	81	90	90
43	0	0	80	20	0	0	81	19	2.67	0	0	81	36	0
44	0	20	60	20	4	15	62	19	2.69	0	0	81	47	19
45	0	40	40	20	7.2	31.2	42.4	19	2.71	0	0	81	58	38
46	0	60	20	20	11	47	23	19	2.72	0	0	81	69	58
47	0	80	0	20	14	64	2	20	2.86	24	22	81	81	78
48	20	0	60	20	17	3	61	19	2.7	170	30	81	47	20
49	20	20	40	20	21	19	41	19	2.71	140	25	81	58	39
50	20	40	20	20	24	34	22	19	2.73	110	25	81	69	58
51	20	60	0	20	28	50	3	19	2.74	110	40	81	80	78
52	40	0	40	20	36	6	39	19	2.72	340	32	81	60	42
53	40	20	20	20	38	22	21	19	2.72	300	40	81	69	60
54	40	40	0	20	41	38	2	19	2.75	285	40	81	80	79
55	60	0	20	20	51	10	20	19	2.74	455	40	81	70	61
56	60	20	0	20	55	25	1	19	2.75	425	40	81	81	80
57	80	0	0	20	68	13	0	19	2.75	495	46	81	81	81

Table 5.2: Compaction test data and gradations of test soils (Sinha and Wang, 2008)

Soil No.	W opt (%)	$\gamma_{d\max}\ (kg/m^3)$	D_{50} (10^{-4} mm)	D_{10} (10^{-5} mm)	Fineness Modulus(F_m)	Uniformity Coefficient (U)	$F_{0.001}$ (%)
(1)	(2)	(3)	(4)	(5)	(6)	(7)	(8)
1	28	1297	3.5	5.6	0.37	10.36	71
2	31	1289	6	5	0.621	22	58
3	29	1362	14	10	0.472	25	45
4	28	1450	29	13	1.123	37.69	33
5	28	1458	42	40	1.282	14	19
6	26	1490	54	140	1.52	4.79	5
7	21	1602	100	300	2.024	0.47	6
8	16	1714	1500	200	2.48	80	4
9	11	1762	3500	160	2.857	225	2
10	10.5	1898	3600	630	3.276	71.43	0
11	14	1826	4500	19000	3.68	2.95	0
12	13	1874	3700	46	3.043	1043.48	13
13	10	1666	2300	40	2.861	850	15
14	20	1618	140	30	2.175	416.67	17
15	24	1546	70	25	1.741	44	19
16	28	1474	42	15	1.527	53.33	31
17	17	1602	85	12	1.924	708.33	31
18	13	1794	2200	11	2.37	290.91	28
19	15	1554	20	5.6	1.865	1517.86	42
20	27	1450	16	7	1.286	54.29	44
21	30	1386	7	5	1.035	24	57
22	13	1890	5500	18000	3.949	4.17	0
23	12.5	2058	4100	600	3.521	96.67	0
24	12	1922	2300	270	3.097	140.74	2
25	16	1788	120	190	2.667	63.16	3
26	22	1706	70	160	2.218	5.94	4
27	24	1618	60	150	1.996	5.13	5
28	10	1914	4200	220	3.417	263.64	8
29	13.5	1962	2500	140	2.972	150	18
30	17.5	1794	120	100	2.538	128	10
31	23.5	1629	65	70	2.114	12.68	11
32	27.5	1578	57	60	1.887	12	12
33	16	1770	2300	18	2.745	2000	22
34	20	1722	120	23	2.323	565.22	24
35	25	1602	60	26	1.916	38.46	25
36	29	1525	41	30	1.666	20	25
37	20	1594	50	6	2.083	1666.67	36
38	28	1498	25	8	1.661	75	38
39	32.5	1450	21	11	1.44	38.18	39
40	27	1474	9.5	5.5	1.406	36.36	50

Table 5.2: Continued

Soil No.	W opt (%)	$\gamma_{d\max}\ (kg/m^3)$	D_{50} (10^{-4} mm)	D_{10} (10^{-5} mm)	Fineness Modulus(F_m)	Uniformity Coefficient (U)	$F_{0.001}$ (%)
(1)	(2)	(3)	(4)	(5)	(6)	(7)	(8)
41	30	1426	9	5	1.2	34	52
42	24	1394	4.4	3.8	0.955	21.05	64
43	8.5	2026	6200	18500	4.218	5.14	0
44	9.5	2122	4600	700	3.796	102.86	2
45	12	2018	3000	280	3.374	160.71	3
46	15	1794	190	190	2.952	78.95	5
47	22.5	1682	70	150	2.482	6.33	6
48	8	1922	4800	40	3.551	1825	14
49	12	1970	2800	35	3.129	1760	16
50	19.5	1738	140	44	2.707	295.45	18
51	26	1618	70	60	2.243	1.83	24
52	11.5	1802	2500	6.8	2.816	6176.47	31
53	20	1714	90	11	2.462	1181.82	31
54	24	1570	40	16	2.03	50	32
55	18	1618	20	6.5	2.212	523.08	43
56	18	1538	15	7.5	1.79	45.33	45
57	30	1474	6	4.4	1.556	28.41	57

Table 0.1: Permeability test data (Sinha and Wang, 2008)

Soil No.	Permeability (10^{-7} cm/s)[k_{90}]	Permeability (10^{-7} cm/s)[k_{95}]	Void Ratio (e_{90})	Void Ratio (e_{95})
(1)	(2)	(3)	(4)	(5)
1	0.00052	0.00036	1.362	1.238
2	0.0005	0.00025	1.377	1.252
3	0.017	0.014	1.225	1.133
4	0.258	0.75	1.107	0.996
5	1	0.64	1.095	1.072
6	90	45	1.174	0.942
7	11	1.15	0.983	0.793
8	270	44	0.762	0.654
9	120	27	0.717	0.627
10	5000	8400	0.568	0.497
11	5211	48	0.653	0.566
12	0.013	0.003	0.594	0.512
13	0.35	0.18	0.817	0.722
14	1.7	1.3	0.912	0.811
15	0.51	0.5	0.969	0.065
16	0.041	0.029	1.064	13.956
17	0.0031	0.00215	0.904	0.804
18	0.001	0.00081	0.678	0.589
19	0.0038	0.0004	0.951	0.849
20	0.0014	0.00091	1.099	0.989
21	0.0007	0.0006	1.204	1.088
22	15000	3200	0.49	0.412
23	800	100	0.468	0.39
24	200	60	0.594	0.511
25	75	20	0.747	0.655
26	350	42	0.862	0.764
27	24	7.5	0.977	0.873
28	10	2.5	0.561	0.479
29	550	25	0.566	0.575
30	40	9	0.733	0.595
31	50	36	0.936	0.834
32	19	12	1.013	0.907
33	0.5	0.04	0.7	0.611
34	0.52	0.42	0.761	0.688
35	5.2	1.2	0.9	0.8
36	6.3	1.7	1.068	0.959
37	0.016	0.0048	0.902	0.802
38	0.043	0.034	1.032	0.925
39	0.19	0.056	1.107	0.966
40	0.0034	0.0028	1.065	0.956

5.2.3 Data preparation

The similar procedure detailed in section4-2-3 was used to choose the most statistically consistent training and testing data sets to be used in training and validation stages in EPR model development process.

5.2.4 EPR model for maximum dry density (MDD)

Five input parameters were used for the EPR model for MDD including dry density of solid phase (γ_s) expressed in (kg/m^3), fineness modulus (Fm), effective grain size (D_{10}) expressed in (mm), plastic limit (PL) expressed in (%), and liquid limit (LL) expressed in percentage (%). The only output was the maximum dry density. The (unit dependent) EPR model developed for maximum dry density is:

$$MDD = -\frac{1.38\times10^{7}(D_{10})}{\gamma_s^2} + 1.92(D_{10}) - 6.61\times10^{-6}(D_{10})\cdot PL^2\cdot LL + 52.35Fm^2 + 1385.07 \qquad 0\text{-}1$$

Figure 5.1 shows a comparison between the results of the EPR model training and testing and the actual experimental data. Table 5.4 presents the values of the coefficient of determination (CoD) for the models. The table shows that the EPR model performs well and represents a very accurate prediction for unseen cases of data.

Table 0.2: Coefficient of determination for predicted MDD values

Model	COD values (%)
Evolutionary Polynomial Regression (EPR)	96 (for unseen testing data)
Artificial Neural Network (ANN)- Sinha and Wang (2008)	98
Wang and Huang (1984)	95

The results of the parametric study are shown in Figure 5.2. The procedure followed is explained in detail in section 4.4.6. It is shown that, according to this model, density of the solid phase, effective grain size, plastic limit and liquid limit have no significant effect on MDD. The main contributing factor appears to be the fineness modulus. To consider this, another model was developed by removing the parameters with negligible effects as:

$$MDD = 214.8\cdot Fm + 1184.39 \qquad 0\text{-}2$$

Figure 5.3 shows a comparison between the results of the EPR model training and testing and the actual experimental data. The values of the coefficient of determination (CoD) for the training and testing stages of the model were 90.78% and 90.29% respectively. Sensitivity analysis results (Figure 5.4) show that increasing fineness modulus (i.e., soil getting coarser) causes the maximum dry density to increase.

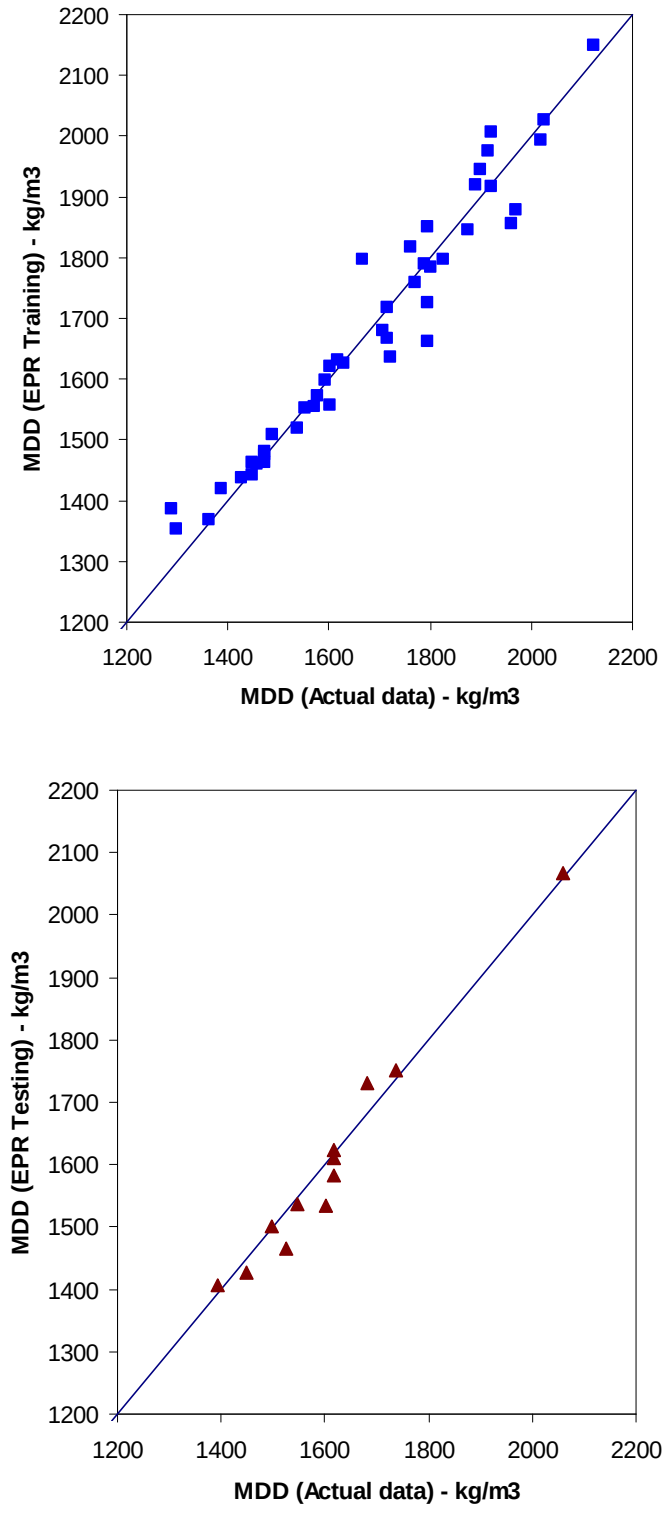

Figure 0.1: Comparison between the predicted maximum dry density and the actual values

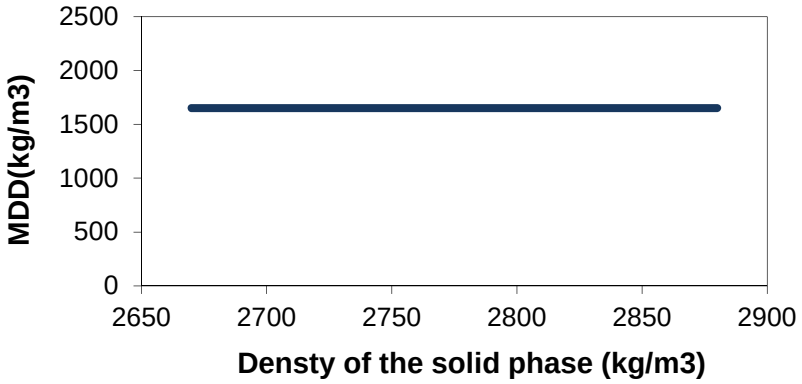

(a)

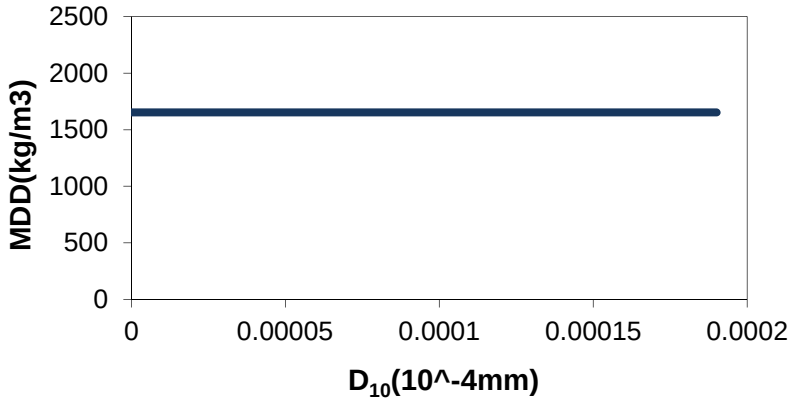

(b)

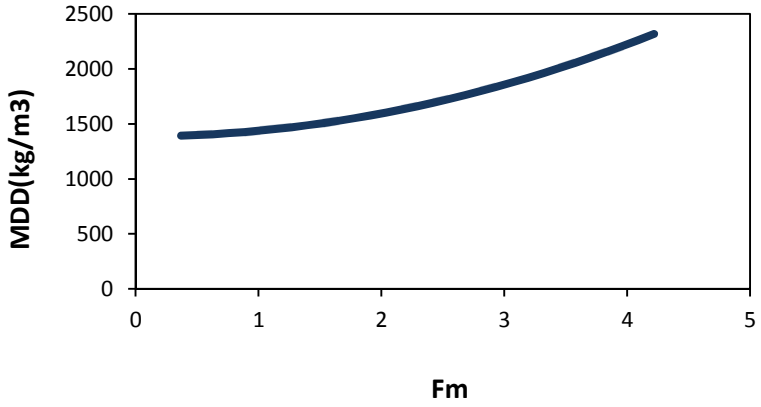

(c)

Figure 0.2: Parametric study results of the maximum dry density against; (a): density of the solid phase of the soil, (b): effective grain size, (c): fineness modulus, (d): plastic limit, (e): liquid limit (to be continued)

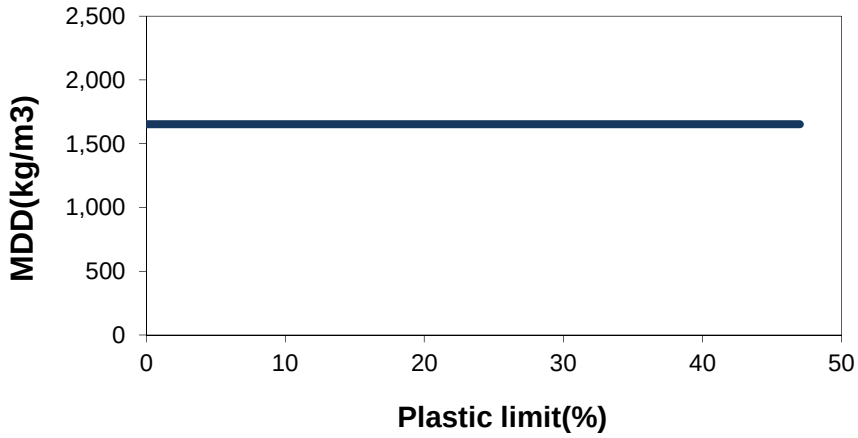

(d)

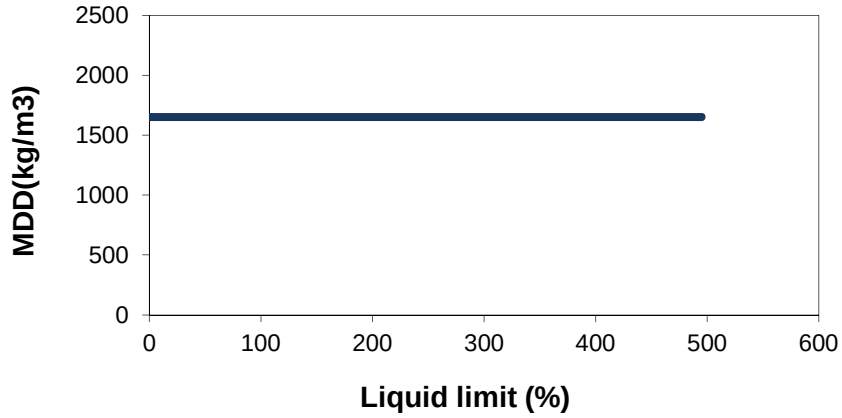

(e)

Figure 5.2; Continued.

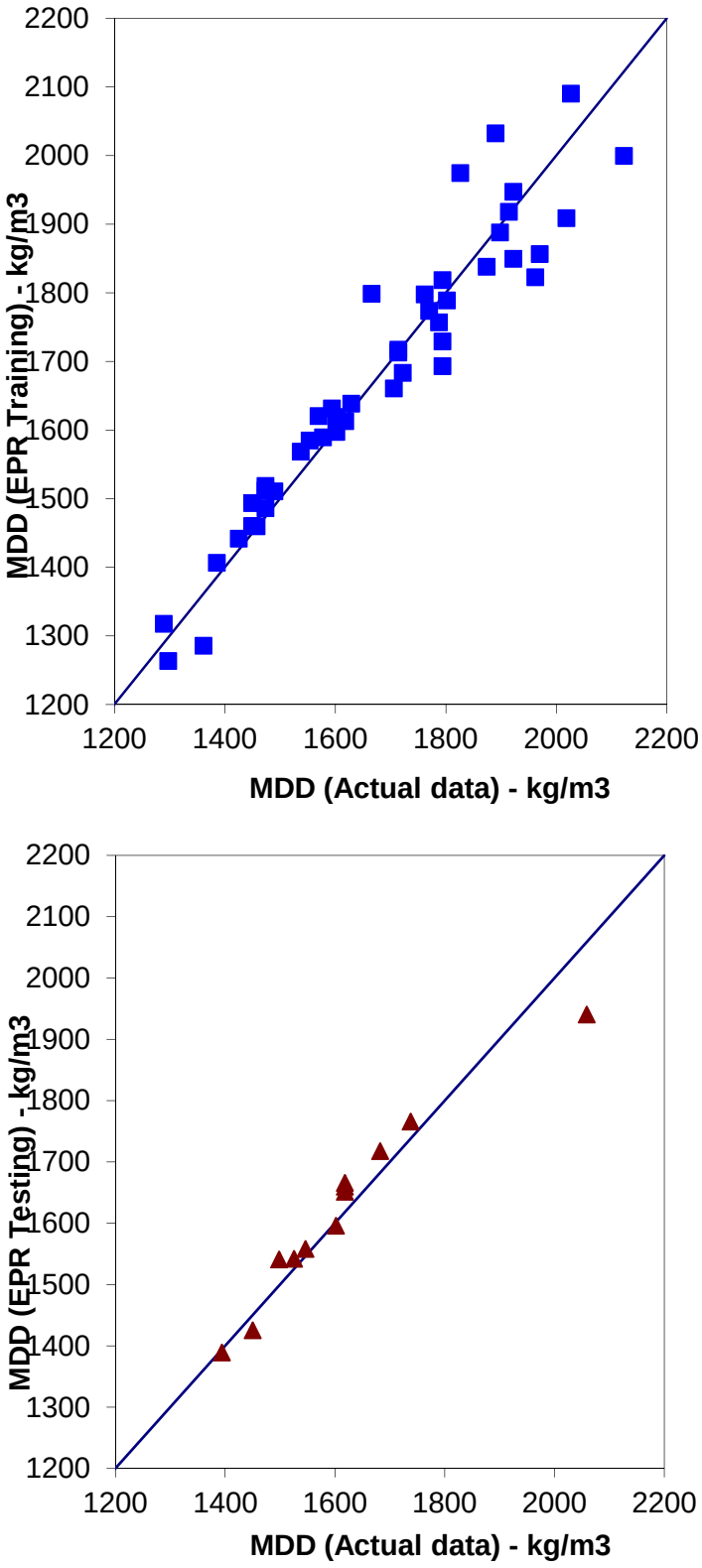

Figure 0.3: Comparison between the predicted maximum dry density and the actual values (Second model-Equation 5-2)

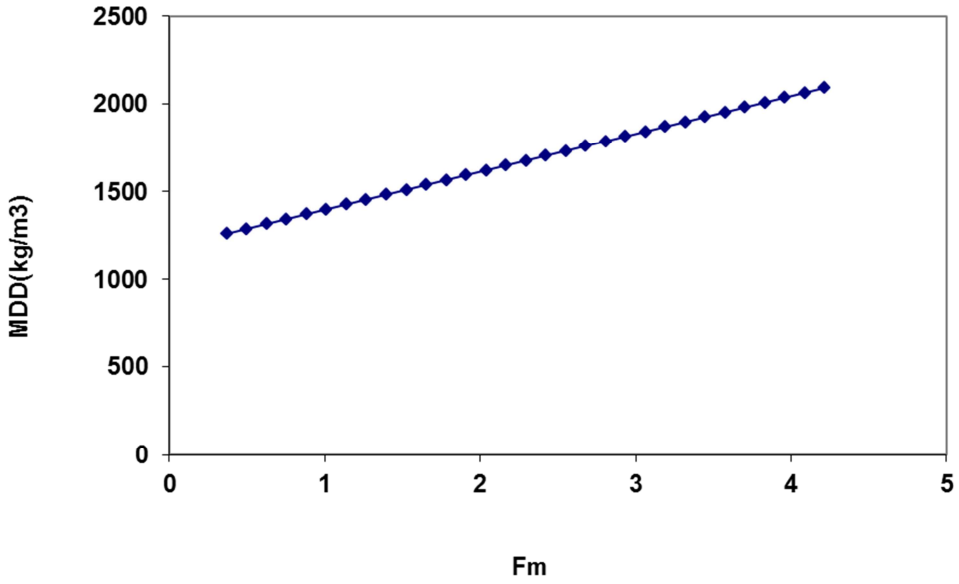

Figure 0.4: Relationship between maximum dry density and fineness modulus (Second model-Equation 5-2)

5.2.5 EPR model for optimum moisture content (OMC)

Three input variables were used to develop the EPR model for OMC including the fineness modulus (Fm), coefficient of uniformity (U), and plastic limit (PL). The EPR model developed to predict the optimum moisture content is:

$$OMC = \frac{9.47}{Fm^3 \cdot U} - \frac{3.57\times10^{-5} PL^3}{Fm^2} - \frac{4.55\times10^{-3} U}{Fm} + 1.72\times10^{-3} PL^2 - 6.36Fm + 34.09 \qquad 0\text{-}3$$

The optimum moisture content of soils predicted using the EPR model was compared with the experimental data (Figure 5.5). The values of coefficient of determination for the models are also shown in Table 5.5. The results indicated excellent performance of the proposed EPR model. Figure 5.6a (sensitivity analysis results - see section 4.4.6) shows that as the fineness modulus increases (the grains get coarser), the optimum moisture content decreases. This is consistent with the expected behaviour (Venkatarama and Gupta, 2008). The effect of coefficient of uniformity on OMC is shown in Figure 5.6b. The higher the coefficient of uniformity, the larger the range of particle sizes in the soil and hence the lower the optimum moisture content (Craig, 1998).

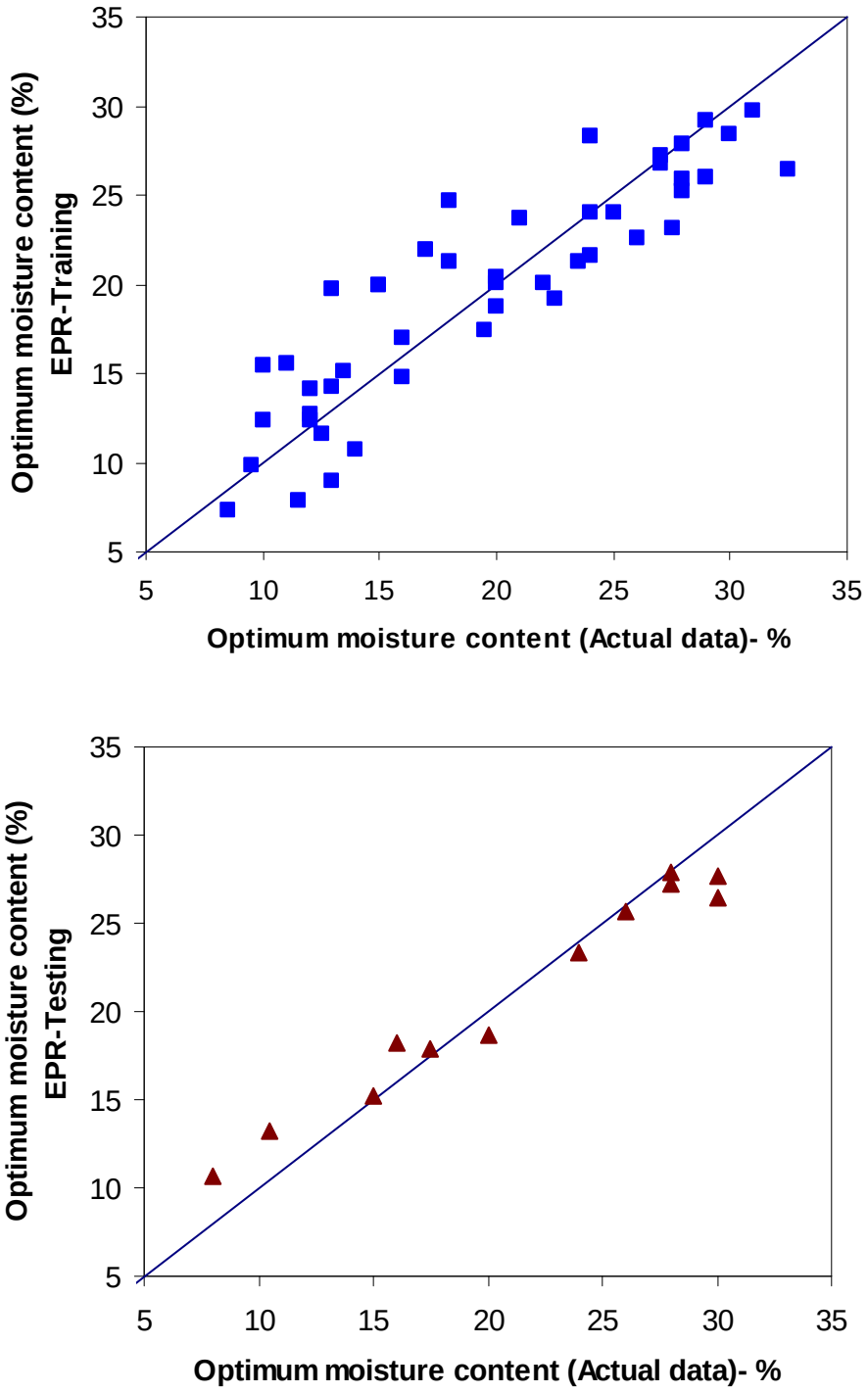

Figure 0.5: Comparison between the predicted and actual optimum moisture content values

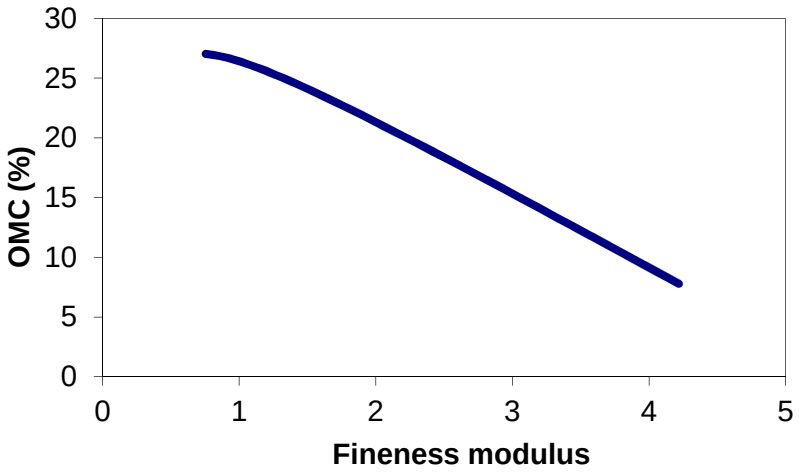

(a)

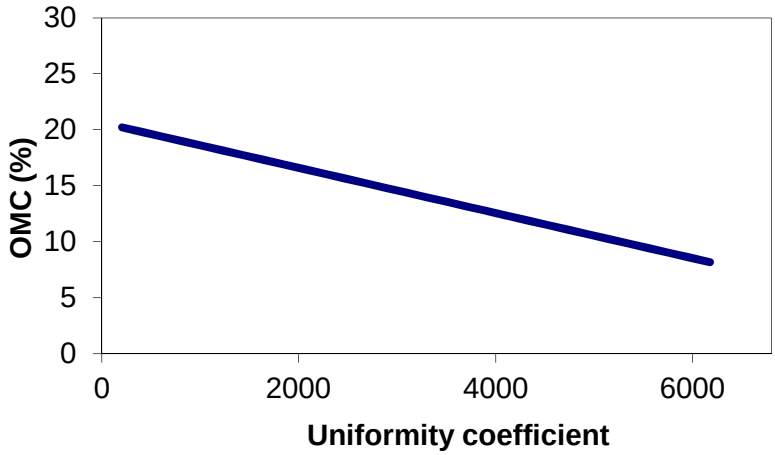

(b)

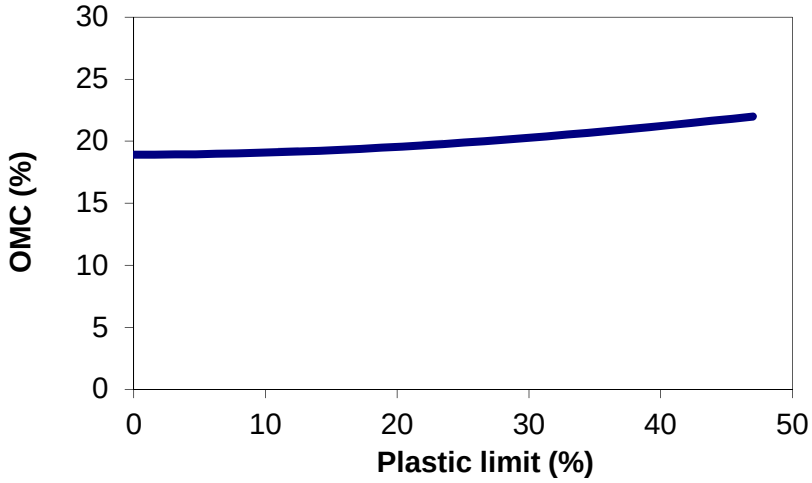

(c)

Figure 0.6: Parametric study results of the optimum moisture content against; (a): fineness modulus of the soil, (b): uniformity coefficient, and (c): plastic limit

Table 0.3: Coefficient of determination for predicted OMC values

Model	COD values (%)
Evolutionary Polynomial Regression (EPR)	94 (for unseen testing data)
Artificial Neural Network (ANN) - (Sinha and Wang, 2008)	92
Wang and Huang (1984)	89

Again, this trend is correctly predicted by the model. Figure 5.6c shows that increasing plastic limit results in the increase in the optimum moisture content due to the increase in the specific surface of the soil grains. A similar trend of variation of optimum moisture content with plastic limit is reported by Sridharan and Nagaraj (2005). The results also show that optimum moisture content is greatly affected by the fineness modulus and the coefficient of uniformity and plastic limit appear to have less effect on the optimum moisture content of soil.

5.2.6 EPR model for coefficient of permeability (K)

Five input parameters were used for the EPR model for the coefficient of permeability including degree of compaction (P) expressed in (%), mean grain size (D_{50}) expressed in (mm), effective grain size (D_{10}) expressed in (mm), plastic limit (PL) expressed in (%), and the liquid limit (LL) expressed in (%). The (unit dependent) EPR model developed to predict the permeability coefficient is:

$$Log_{10}(K) = -\frac{600.25}{P}\left(1+\frac{0.46(D_{50})}{P^2}\right)+\frac{121.96}{(D_{50})^2}-\frac{0.02PL^2}{(D_{50})}+\frac{3.42LL-1983.12}{(D_{10})^3}+$$
$$\frac{1.53\times10^{-9}(D_{50})^3+47.2}{(D_{10})}+5.09\times10^{-4}PL^2\left(1+7.74\times10^{-5}LL(D_{50})-2.66\times10^{-6}LL\cdot PL(D_{50})\right)+13.8 \quad \text{0-4}$$

The results of the developed EPR model are compared with the actual experimental data (Figure 5.7) as well as two other prediction models (Table 5.6). The EPR model gives excellent prediction of the coefficient of permeability of soils. Figure 5.8 shows the results of the parametric study for the EPR permeability model (see section 4.4.6). It is shown that increasing the degree of compaction decreases the volume of voids and hence decreases the permeability of the soil. As the soil becomes coarser (increasing D_{10}) the permeability coefficient increases up to a point after which it increases at a very slow rate. Increasing the plasticity index is an indicator of the greater fines content in the soil and hence results in decrease in permeability (Blotz, Benson and Boutwell, 1998). The results show that the plasticity index has the greatest effect on the permeability while the effects of degree of compaction and effective grain size are relatively moderate.

Table 0.4: Coefficient of determination for predicted K values

Model	COD values (%)
Evolutionary Polynomial Regression (EPR)	92 (for unseen testing data)
Artificial Neural Network (ANN)	90
Wang and Huang (1984)	89

5.2.7 Discussion and conclusion

The process of compaction is extensively employed in the construction of embankments and strengthening sub-grades of roads and runways. In recent years the use of pattern recognition methods such as artificial neural network has been introduced as an alternative method for predicting compaction characteristics and permeability of soils. These methods have the advantages that they do not require any simplifying assumptions in developing the model. However, neural network based models also have some shortcomings as highlighted in chapter 2. In this research a new approach was presented to describe the relationships between permeability and compaction characteristics, and some physical properties of soils.

Three separate EPR models were developed and validated using a database of experiments involving test data on compaction and permeability characteristics of a number of soils. The results of the model predictions were compared with the experimental data as well as results from other perdition models including a neural network. A parametric study was conducted to evaluate the effects of different parameters on permeability and compaction characteristics of soils. Comparison of the results shows that the developed EPR models provide very accurate predictions. They can capture and represent various aspects of compaction and permeability behaviour of soils directly from experimental data.

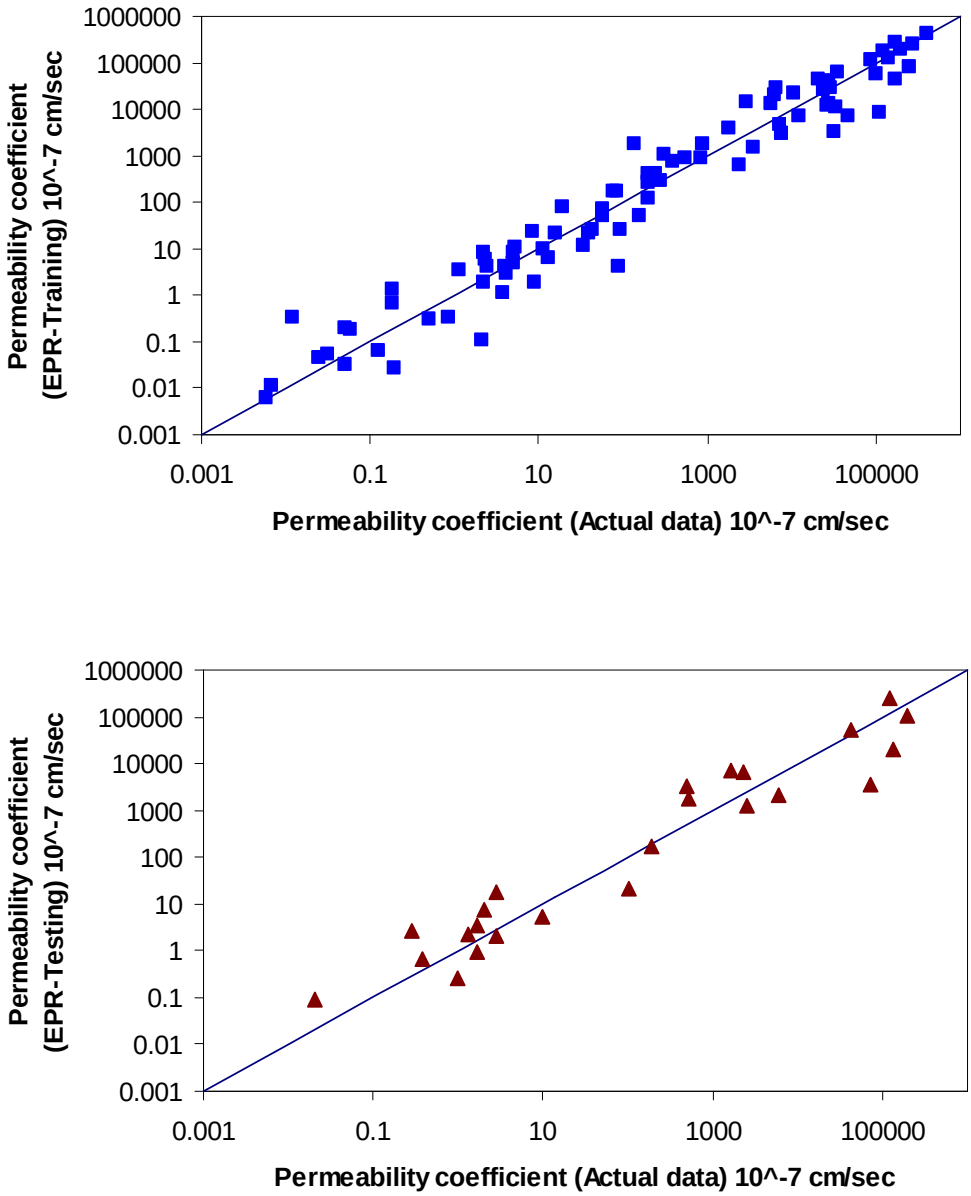

Figure 0.7: Comparison between the predicted permeability coefficient and the actual values

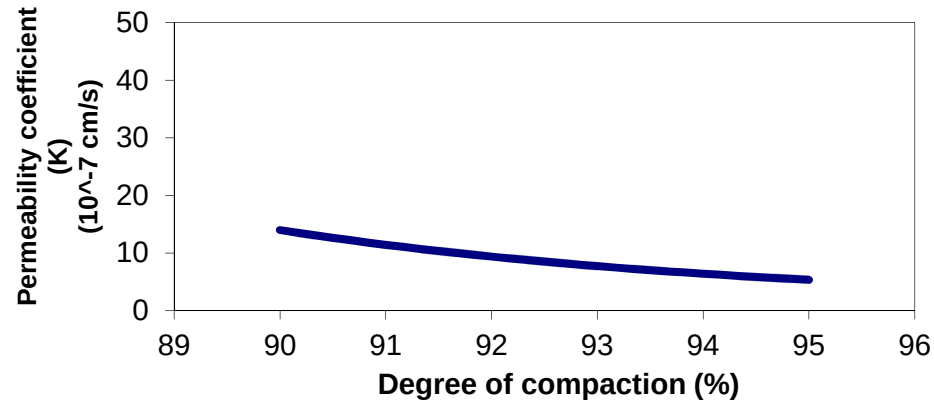

(a)

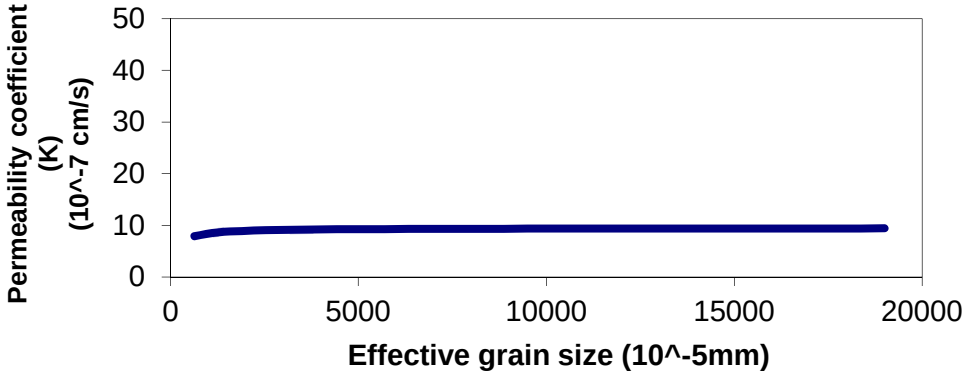

(b)

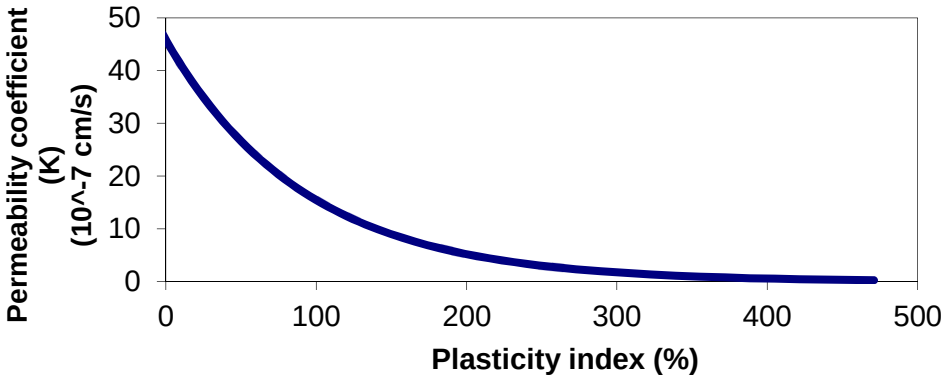

(c)

Figure 0.8: Parametric study results of the permeability coefficient model against; (a): soil compaction, (b): effective grain size, and (c): plasticity index

5.3 A new approach for prediction of the stability of soil and rock slopes

5.3.1 Introduction

Estimation of the stability of a rock or soil slope is a complex problem due to the heterogeneous nature of soil and rock masses, the large number of parameters involved, and the difficulty in determining the geotechnical parameters. In practice, only an approximate general description of the physical and geometric characteristics of the slope can usually be obtained. Therefore, it is difficult to determine the values of the essential input parameters accurately.

Traditional limit equilibrium techniques are the most commonly used methods for analysis of stability of slopes. In this approach, the shape and location of the critical failure surface are assumed rather than determined. It is also assumed that the soil (or rock) moves as a rigid block with movements only occurring on the failure surface. The factor of safety (FS) is defined as the ratio of reaction over action, expressed in terms of moments or forces, depending on the mode of failure and the geometry of the slip surface considered. In rotational mechanisms of failure for example, factor of safety is defined, in terms of moments about the centre of the failure arc, as the ratio of the moment of the resisting shear forces along the failure surface over the moment of weight of the failure mass. These computational methods vary in terms of degrees of accuracy, depending on the degree of appropriateness of the simplifying assumptions for the situation under investigation.

In rock masses, the potential mechanism of failure can be wedge or planar, depending on the orientation of joint sets. In highly fractured rocks this mechanism can be rotational. In evaluating the stability of slope using limit equilibrium methods, it is necessary to determine the shape and location of the critical slip surface and the minimum value of factor of safety corresponding to that surface. This usually involves analyzing a large number of possible trial slip surfaces.

In the methods introduced by Taylor (1937) and Bishop (1961) the slip surface is approximated with an arc of a circle. Other methods e.g. Janbu (1954), Spencer (1967), Sarma (1975), and Hoek and Bray (1981) assume different shapes for the slip surface. The accuracy of these methods depends on the assumptions made in developing the method and the accuracy with which shear strength parameters can be determined. In all cases, it is assumed that the soils are isotropic and homogeneous. These assumptions often lead to reasonable predictions when applied sensibly.

Stability analysis using charts is another method that is less complicated and provides a rapid and potentially useful means of preliminary slope stability estimation (Duncan, 1996).

Although the conventional methods of stability analysis have been widely used for analysis of stability of soil and rock slopes, these methods have a number of shortcomings. For example, the existing methods of stability analysis for slopes on cohesive soils are based on (a) assuming a slip surface and a centre about which it rotates, (b) studying the equilibrium of the forces acting on this surface, and (c) repeating the analysis on several different trial failure surfaces from different centres, until the most critical slip surface is found. The most critical slip surface is the one that yields the lowest factor of safety. In these methods, a number of assumptions and simplifications have been made in order to reduce the computational time and cost and the complexity of the analysis. For example, the failure slip surface is assumed to be of

a specific predetermined shape, and the inter-slice forces may be ignored, etc. However, repeating the procedure for a large number of surfaces can still be computationally intensive and costly.

In recent years, the use of artificial neural networks has been introduced as an alternative approach for analysis of stability of slopes. Sakellariou and Ferentinou (2005) used neural networks to acquire the relationship between the parameters involved in analysis of stability of slopes. They used the models introduced by Hoek and Bray (1981) in order to produce test data to validate the quality of training of their proposed artificial neural network model.

In this research, new models are presented using evolutionary polynomial regression (EPR) for stability analysis of soil and rock slopes. The proposed technique is capable of capturing the behaviour of slopes from the actual (field or experimental) data and making accurate predictions for other unseen cases. EPR models are developed and validated using results from sets of field data. The results show that the proposed approach is very effective and robust in modelling the behaviour of slopes and provides a unified approach to analysis of slope stability problems. Results from a sensitivity analysis show that the models can predict various aspects of behaviour of slopes correctly.

5.3.2 Database

The input data consists of six input parameters in the case of circular failure mechanism for cohesive soils and eight input parameters in the case of wedge failure mechanism for rocks. The output of the EPR models presents a factor of safety that demonstrates the status of stability of the slope.

Two data sets, overall consisting of 67 case studies of slopes with circular critical failure mechanism were used in this study (Sakellariou and Ferentinou, 2005). Of these, 25 cases involve dry soil conditions (13 failed, 12 stable) and 42 cases involve wet conditions (20 failed, 22 stable). The third data set consists of 22 case studies of rock slopes analyzed for wedge failure mechanism. All cases involve dry soil conditions; with 10 cases of failed slope and 12 cases of stable slopes (Sah, Sheorey and Upadhyama, 1994). These data cover a wide range of parameter values.

The main parameters contributing to the stability of a slope can, in general, be categorised in two classes of geotechnical properties and geometrical characteristics of the slope. More specifically, the parameters used for circular failure mechanism in soils (Figure 5.9a) are unit weight (γ), apparent cohesion (c), angle of internal friction (ϕ), slope angle (β), height (H), and pore water pressure parameter (r_u).

The data was divided into two sets (based on the similar statistical procedure introduced in previous sections); one set was used for development of the EPR model and the other one was used for validation and evaluation of the generalization capabilities of the developed EPR model.

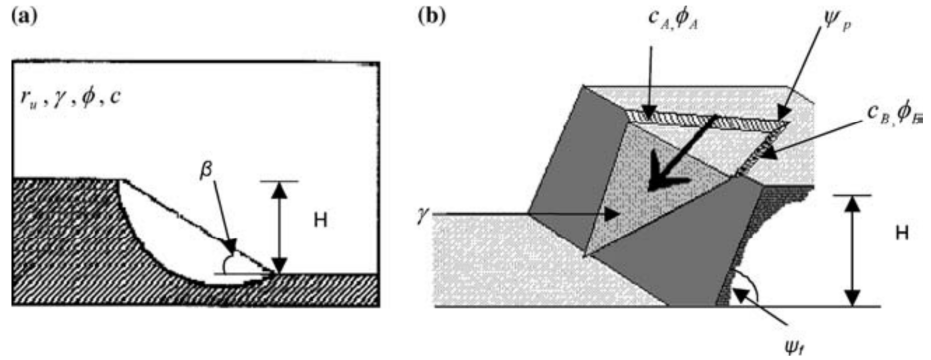

Figure 0.9: (a) Circular failure mechanism; (b) Wedge failure mechanism (Sakellariou and Ferentinou, 2005)

5.3.3 EPR model for circular failure mechanism

From the total of 67 cases in the database, 57 cases were used to develop the EPR model and the remaining 10 cases were used as unseen cases to validate the developed EPR model. Among the resultant equations developed by EPR process the one with the highest value of coefficient of determination (CoD) was selected (Equation 5-5).

$$F_s = -\frac{1.49H}{\gamma^2} - 1.8 \cdot r_u^2 + \tan(\varphi)[2.59 - 2.18\tan(\beta)] + 0.014 \cdot c - 5.19 \times 10^{-5} c^2 + 0.817 \qquad 0\text{-}5$$

Figure 5.10 shows the comparison of the results in terms of factors of safety predicted by the EPR model together with the ones from ANN analysis (Sakellariou and Ferentinou, 2005) and the field data for the training cases. The results of the EPR model predictions were in close agreement with the field data and with values predicted by the ANN model.

Once training was completed, the performance of the trained EPR model was validated using the testing data that were not used during the model development process. The purpose of validation was to examine the capabilities of the trained model to generalize the training to conditions that had not been seen during the training phase. Equation 5-5 was used to predict the factor of safety for the unseen data cases and the results are shown in Figure 5.11. A very good agreement can be seen between the model results and the field data demonstrating the excellent capability of the EPR-based model in generalizing the relationship to unseen cases. The CoD values for the developed EPR models as well as the ANN are shown in Table 5.7.

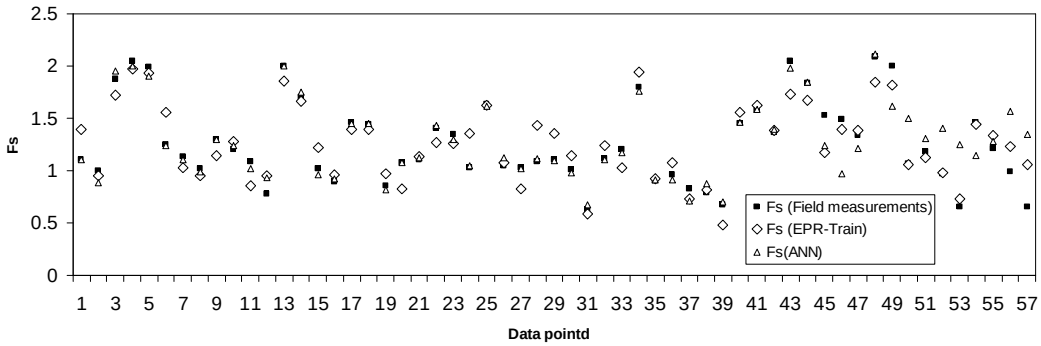

Figure 0.10: Comparison of EPR training results with those from ANN and field measurements for circular failure mechanism.

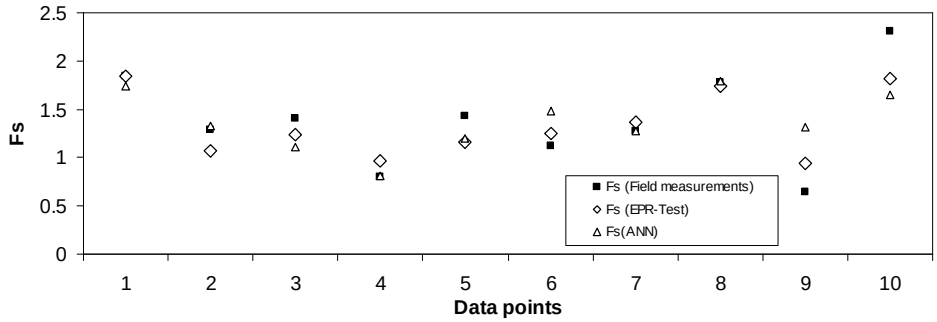

Figure 0.11: Comparison of EPR testing results with ones from ANN and field measurements for circular failure mechanism.

Table 0.5: COD values for ANN and EPR models for soil slopes

Model	COD values for training (%)	COD values for testing (%)
Artificial Neural Network (ANN) Sakellariou and Ferentinou (2005)	97.6	93.7
Evolutionary Polynomial Regression (EPR)	98.3	97.1

It was shown that the EPR model outperforms the ANN model both in terms of the CoD values for the training and testing and also providing a transparent and easy-to-use expression (as opposed to the black box model of ANN).

A parametric study was also carried out following the procedure described in section 4.4.6. The results (shown in Figure 5.12) indicate that:

(i) The factor of safety increases with increasing unit weight, apparent cohesion and angle of friction of the soil and decreases with increasing angle of the slope, height of the slope and pore water pressure in the slope. The trends of variations of all these parameters are consistent with the expected behaviour of slopes.

(ii) The parameters: internal friction angle, apparent cohesion, slope angle and height are the most effective parameters on stability of slopes.

(iii) The effect of unit weight on stability appears to be less than the other contributing parameters, for the cases used in development of this model.

The results of the parametric study show that the developed EPR model has been able to capture, with a very good accuracy, the important physical characteristics of behaviour of slopes and the relationship between the slope stability and its contributing factors.

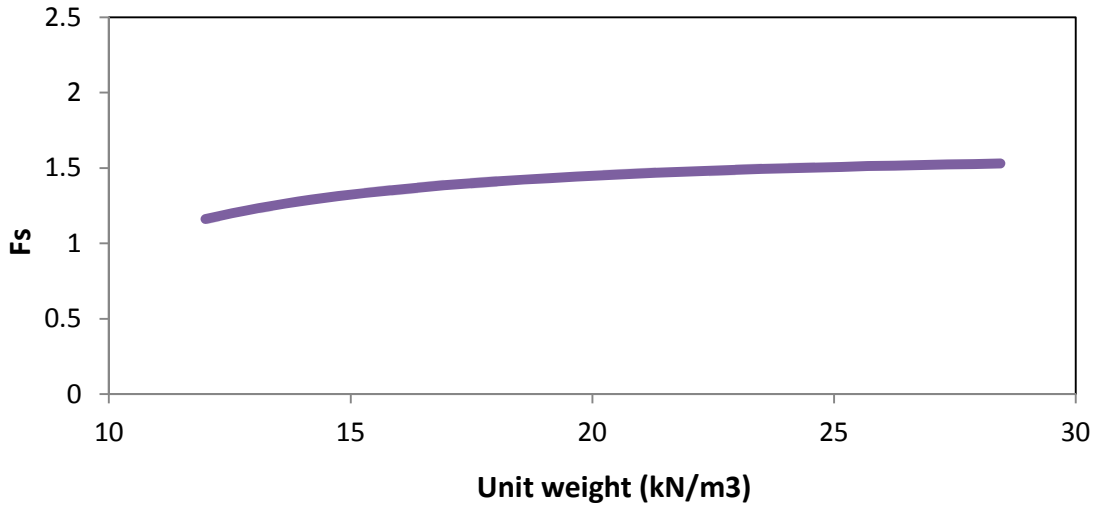

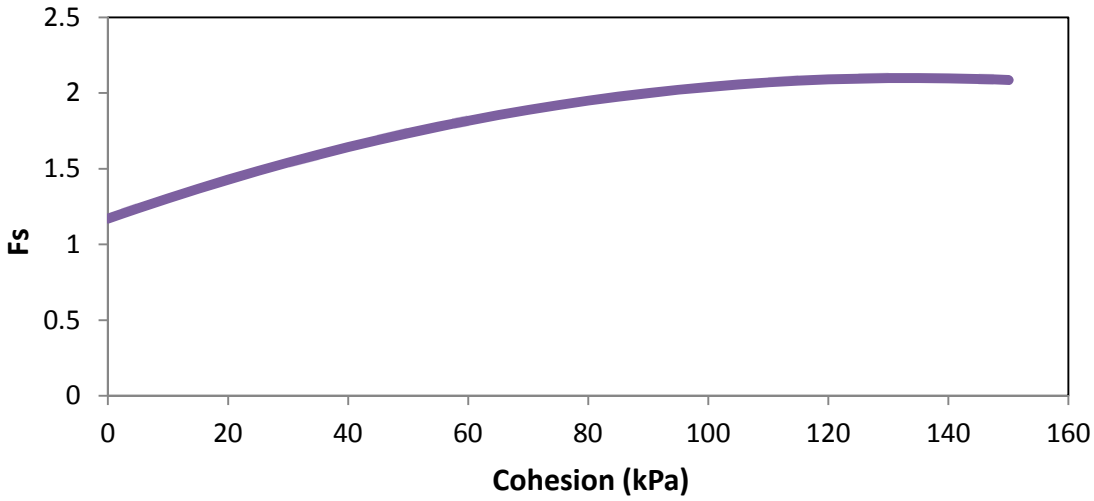

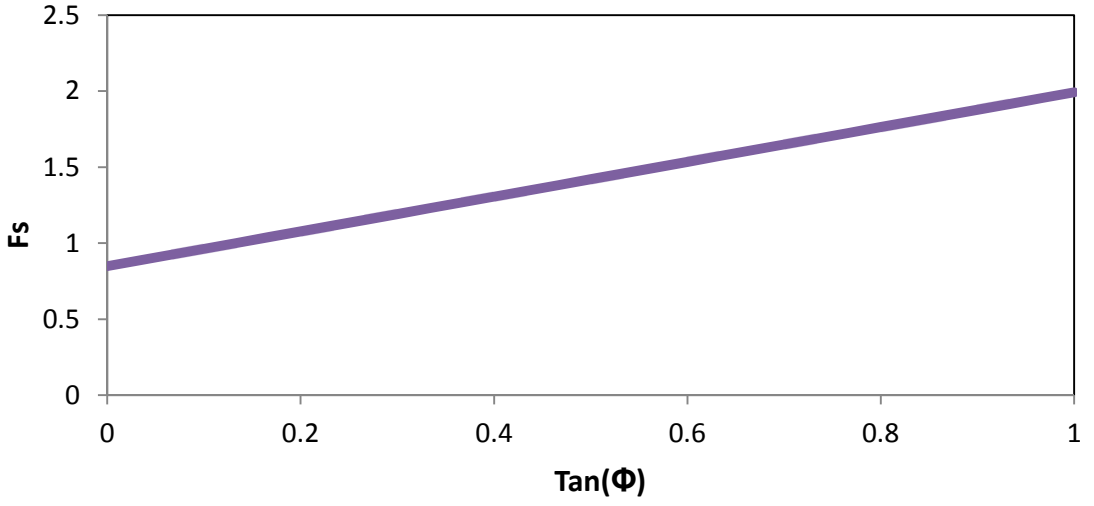

Figure 0.12: Sensitivity analysis results for EPR model developed for circular failure mechanism (to be continued)

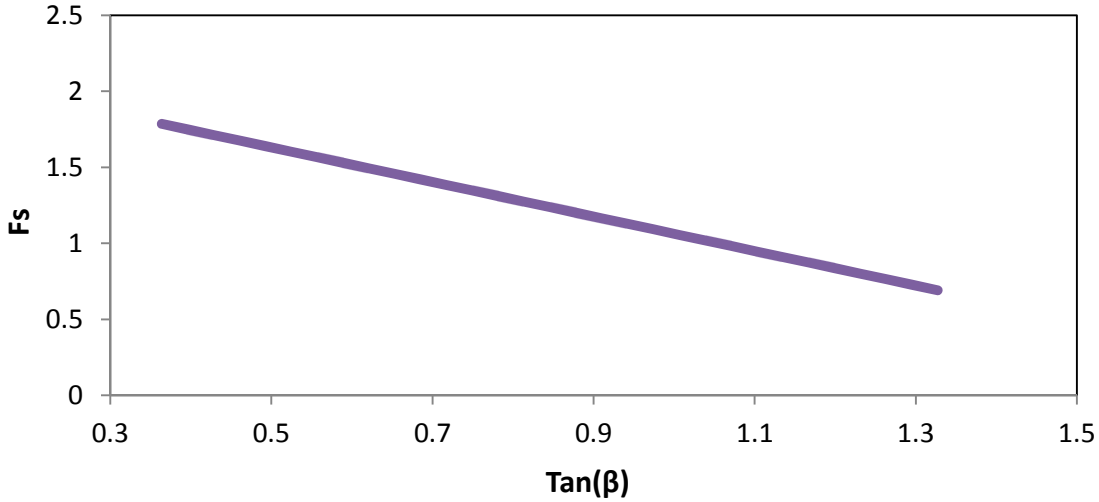

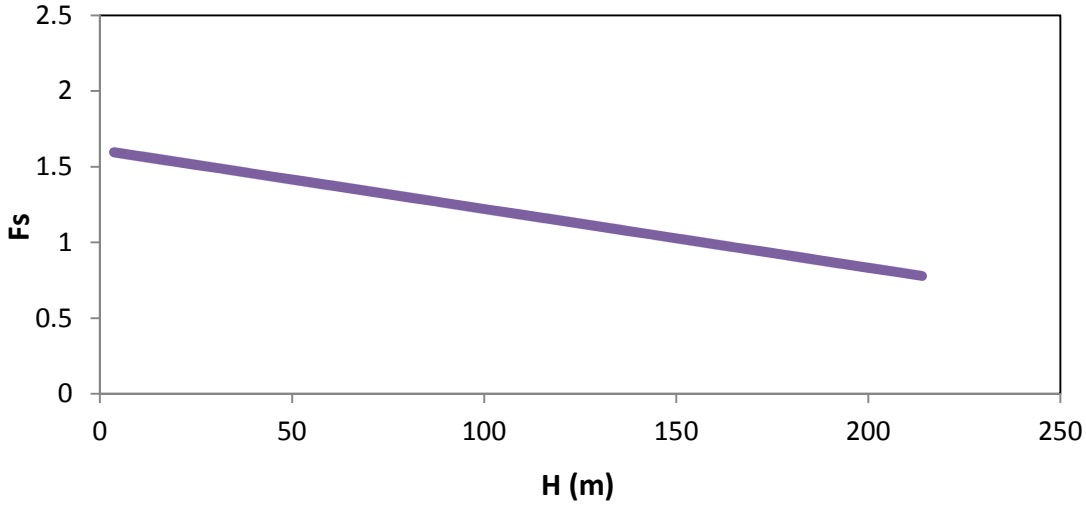

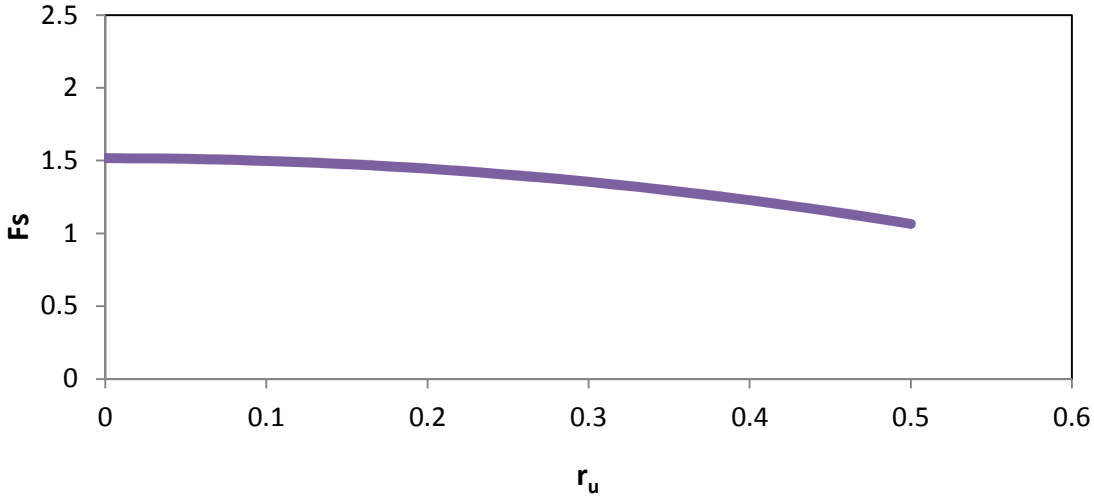

Figure 5.12: Sensitivity analysis results for EPR model developed for circular failure mechanism (continued)

5.3.4 EPR model for wedge failure mechanism

The data set used for development of EPR model for analysis of wedge failure mechanism in rocks consists of 22 case studies. All these cases involve dry soil conditions; with 10 cases of failed slope and 12 cases of stable slopes (Sah, Sheorey and Upadhyama, 1994). The main parameters contributing to the stability of a rock slope are unit weight (γ), apparent cohesions (c_A) and (c_B), angles of internal friction (ϕ_A) and (ϕ_B), angle of the line of intersection of the two joint sets (ψ_p), slope angle (ψ_f) and height (H), where A and B refer to the two joint sets (see figure 5.9b).
20 cases of data were used to develop the EPR model and the remaining 2 cases were used as unseen cases to validate the developed EPR model. From the models developed by the EPR process the one with the highest value of coefficient of determination was selected.

$$F_s = -\frac{0.0028}{(\tan\varphi_B)^3} - \frac{2091}{(H+10)^2} - 0.11(\tan\psi_f)^3 + \frac{229\tan\varphi_A \cdot \tan\varphi_B}{H+10} + 0.015 \cdot c_B + 5\times10^{-4} c_A^2 \cdot \tan\psi_p (\tan\psi_f)^2 + 1.2\times10^{-4}\gamma^3 - 0.88 \quad \text{0-6}$$

Figure 5.13 shows the comparison of the results in terms of factors of safety predicted by the EPR model with the ones from ANN analysis (Sakellariou and Ferentinou, 2005) and field measurements for the training cases. The results of the EPR model are in very close agreement with the field measurements and also with the values predicted by the ANN model.
After training, the performance of the trained EPR model was validated using the testing data that were not used during the model development process. Equation 5-6 was used to predict the factor of safety for the unseen data cases and the results are presented in Figure 5.14. A close agreement can also be seen between the model results and the field data demonstrating the excellent capabilities of the EPR-based model in generalizing the relationship to unseen cases. The CoD values for the developed EPR model and the ANN model are shown in Table 5.8.

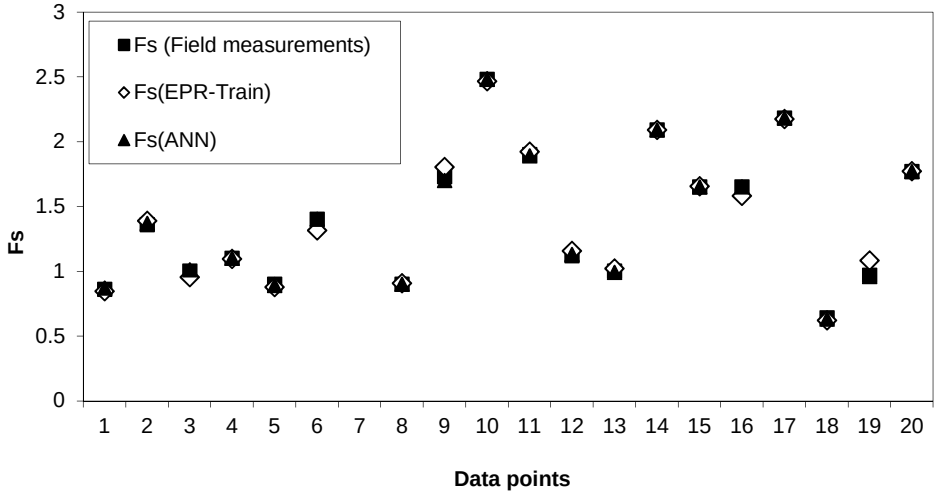

Figure 0.13: Comparison of EPR training results with those from ANN and field data for wedge failure mechanism.

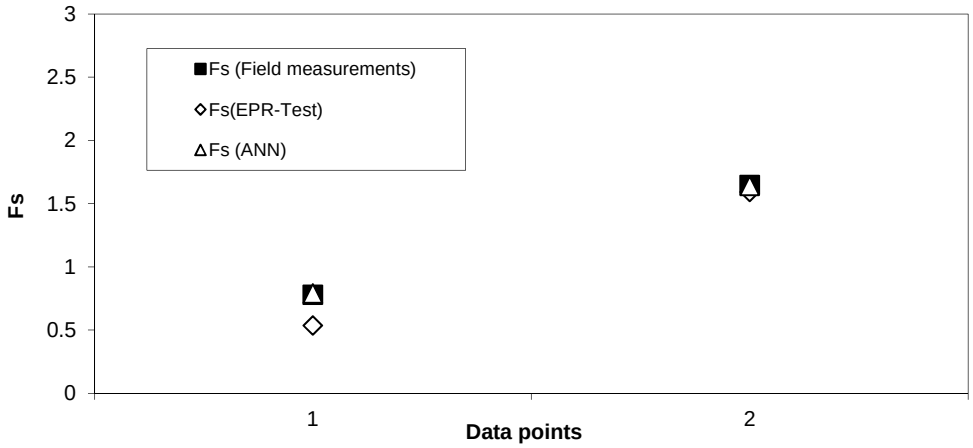

Figure 0.14: Comparison of EPR testing results with those from ANN and field data for wedge failure mechanism

Table 0.6: CoD values for ANN and EPR models for rock slopes

Model	COD values for training (%)	COD values for testing (%)
Artificial Neural Network (ANN) - Sakellariou and Ferentinou (2005)	99.9	-
Evolutionary Polynomial Regression (EPR)	99.7	96.2

It is shown that the results of the EPR model closely match those of the ANN model in terms of the CoD value for the training. It is worth noting that Sakellariou and Ferentinou (2005) did not report the CoD value for the testing data.

Also, the results of the parametric study (see section 4.4.6) indicate that (Figure 5.15):

(i) The factor of safety increases with increasing unit weight, apparent cohesion and internal friction angle on both failure planes and decreases with increasing angle of the slope. The trends of variations of these parameters are consistent with the expected behaviour of slopes.

(ii) The parameters; internal friction angle, apparent cohesion, slope angle and unit weight are the most effective parameters on stability of rock slopes.

(iii) The effect of the joint sets' intersection angle and the slope height on the stability factor of safety appears to be negligible.

5.3.5 Discussion and conclusion

Analysis of stability of soil and rock slopes is a complex geotechnical engineering problem due to the heterogeneous nature of soils and rocks and the participation of a large number of factors involved. Traditional methods are based on simplifying assumptions and usually require trial and error procedures that are time demanding and computationally expensive. In recent years the use of pattern recognition methods such as artificial neural network has been introduced as an alternative method for analysis of stability of slopes based on field data. These methods have the advantage that they do not require any simplifying assumptions in developing the model. However, the neural

network based models also suffer from a number of shortcomings that are highlighted in previous sections.

A new EPR approach was presented in this work for the analysis of stability of soil and rock slopes. Two separate EPR models were developed and validated using a database of case histories involving field data on characteristics of soil and rock and the stability status of slopes. The results of model predictions were compared with field data as well as results from a neural network model. Parametric studies were also conducted to evaluate the effects of different parameters on stability of slopes, and the extent to which the developed models can represent the physical relationships between contributing parameters.

Comparison of the results showed that the developed EPR models provide very accurate predictions for stability of slopes. The developed models present structured and transparent representation of the systems, allowing a physical interpretation of the problem that gives the user an insight into the relationship between the stability status of a slope and various contributing parameters. From practical point of view, the EPR models are easy to use and provide results that are more accurate than the existing methods.

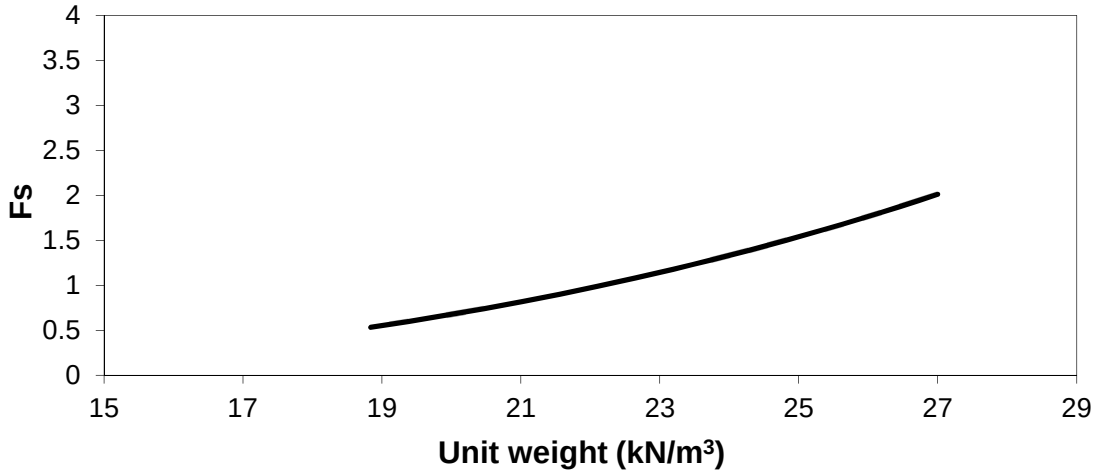

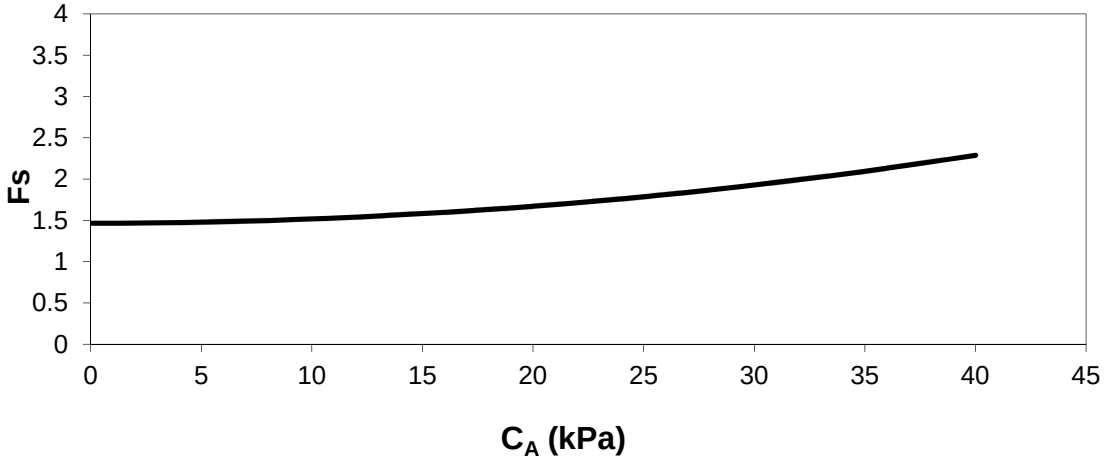

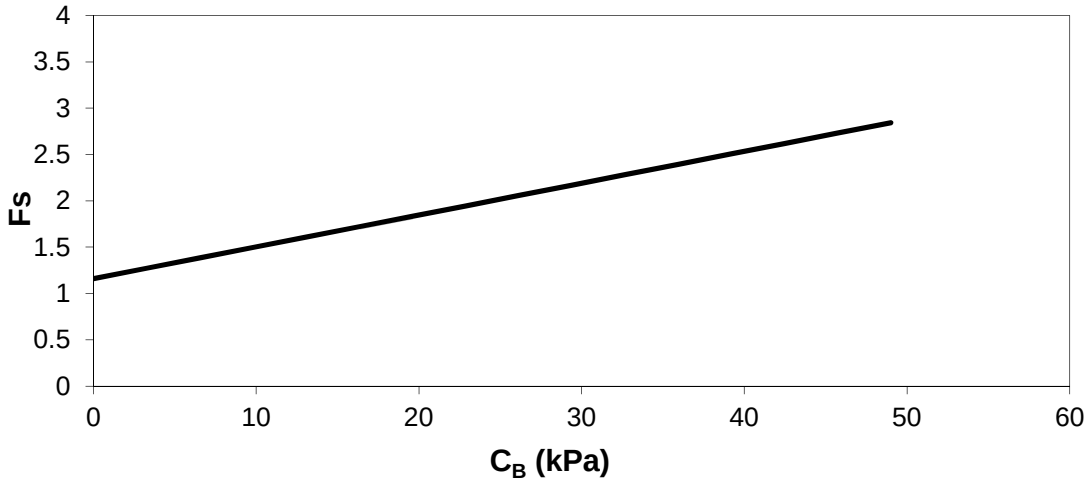

Figure 0.15: Sensitivity analysis results for EPR model developed for factor of safety for wedge failure mechanism (to be continued).

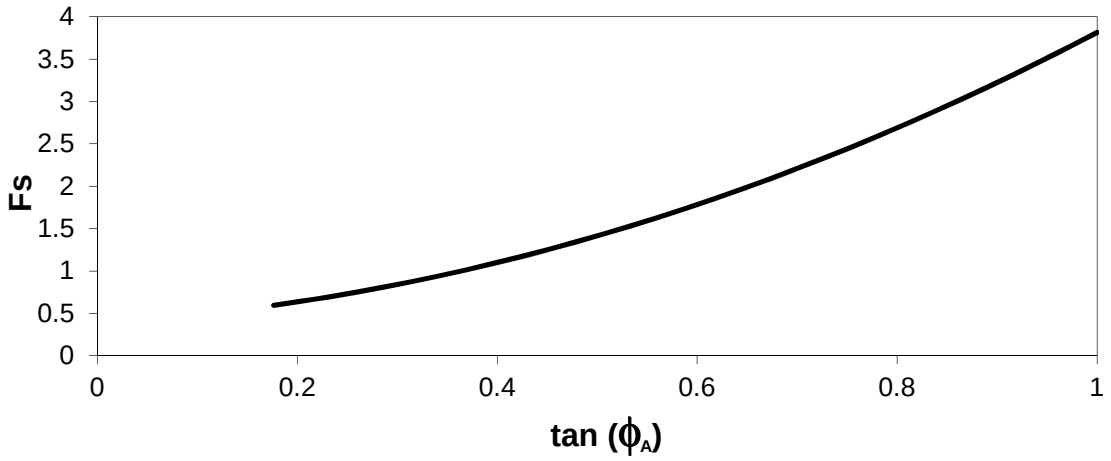

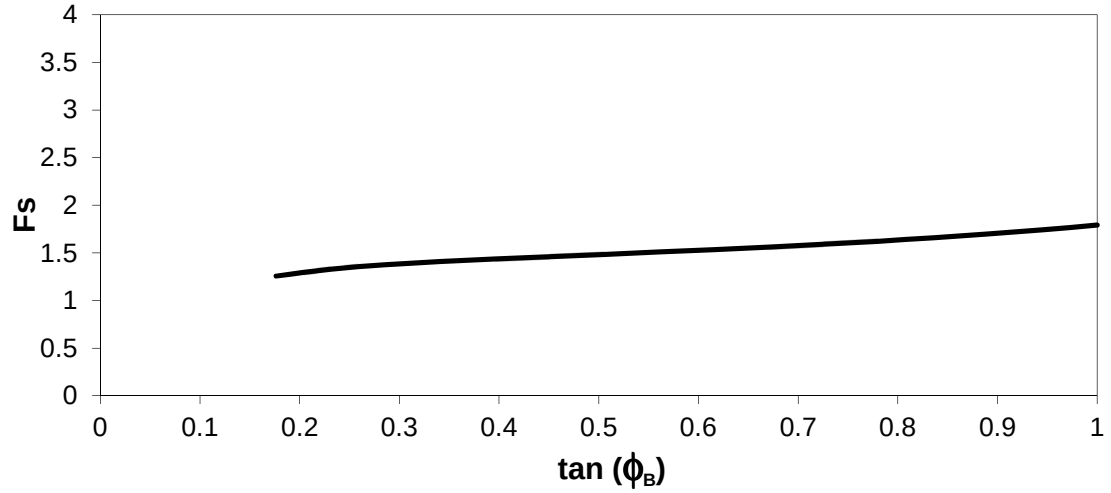

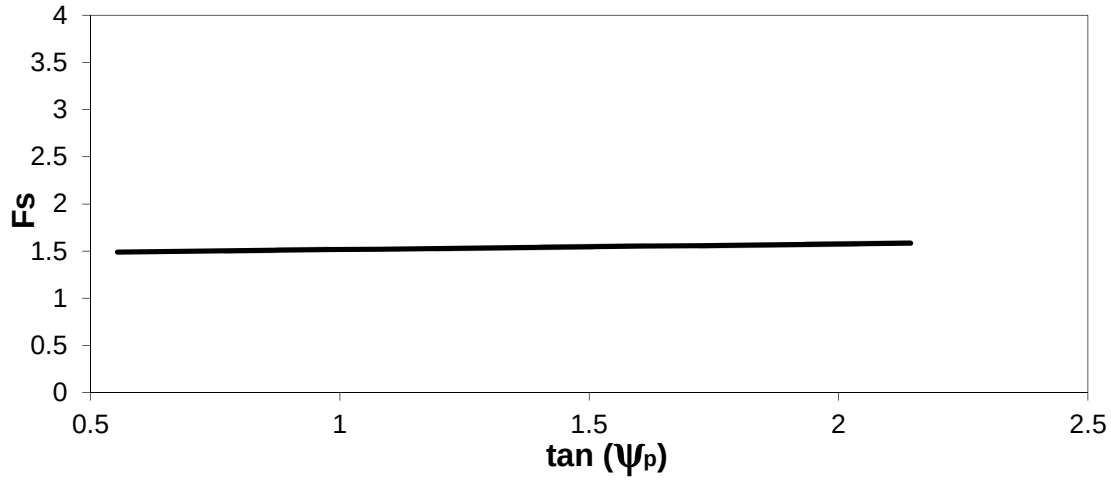

Figure 5.15: Sensitivity analysis results for EPR model developed for factor of safety for wedge failure mechanism (continued).

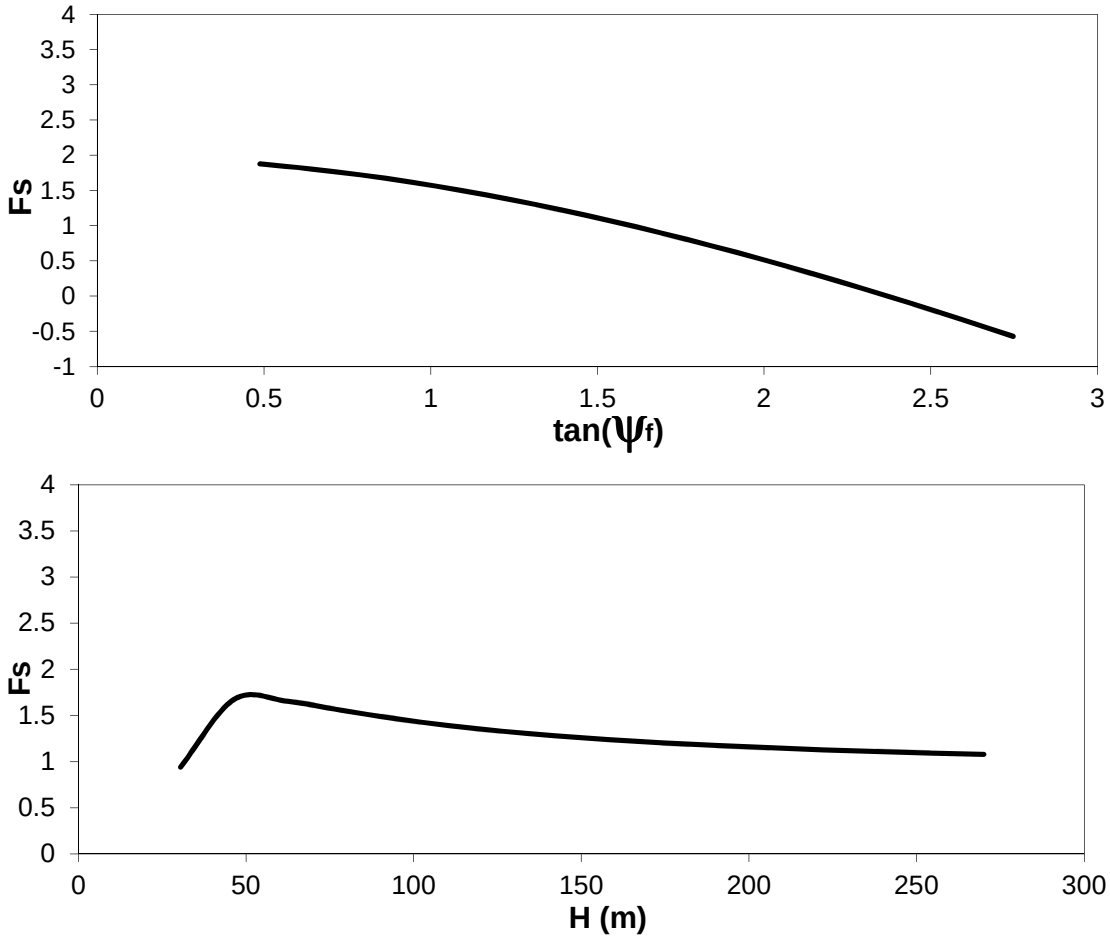

Figure 5.15: Sensitivity analysis results for EPR model developed for factor of safety for wedge failure mechanism (continued).

5.4 Modelling mechanical behaviour of rubber concrete using evolutionary polynomial regression

5.4.1 Introduction

Disposal of waste tyres is one of the most crucial environmental problems all around the world. The conventional solution has been to store them on empty land, which indirectly creates other problems because they become fire hazard or insect and animal habitation ((Siddique and Naik, 2004); (Sukontasukkul and Chaikaew, 2006)). Accumulation of discarded waste tyres has also been a major concern because waste rubber is not easily biodegradable, even after a long period of landfill treatment. A number of innovative solutions have been proposed to meet the challenges of tyre disposal. The use as a fuel or as a component of useful composite materials has been considered as alternative to disposal of the waste rubber ((Williams, Besler and Taylor, 1990), (Eldin and Senouci, 1992) (Eldin and Senouci, 1993), (Sinn, Kaminsky and Janning, 1976), (Farcasiu, 1993), (Atal and Levendis, 1995)). Because of high capital investment involved, using tyres as a fuel for cement kiln is technically feasible but economically may not be very attractive (Siddique and Naik, 2004). Therefore,

recycling of waste tyres in innovative applications seems to be a more effective approach. There has been some interest in using the recycled waste tyre products in a number of applications. In recent years, much research has been carried out to investigate the possibilities for reuse of abandoned tyres by grinding them into small particles (crumb rubber or tyre chips) and using in asphalts, sealants, and rubber sheets. Of particular interest has been the use of waste tyres as aggregate in Portland cement concrete (Sukontasukkul and Chaikaew, 2006). Various researchers have investigated the use of tyre rubber in the production of concrete. Eldin and Senouci (1993) studied the strength and toughness properties of the concretes containing two types of tyre rubber. Khatip and Bayomy (1999) used recycled tyre rubber as aggregate in the concrete mixtures with different rubber contents. Topcu (1995) studied the physical and mechanical properties of the rubber concrete. Benazzouk et al (2003) examined the physico-mechanical properties of cement-rubber composites with two types of rubber aggregates with the aim of developing a highly deformable material. All of these studies have revealed that the addition of rubber aggregates leads to reduction in the basic engineering properties of concrete. The reduction in the strength appears to be more remarkable with increasing the rubber content in the composite. Guneyisi et al (2004) incorporated silica fume into rubber concrete to diminish the strength loss caused by the use of rubber aggregates. The experimental study involved using of both crumb rubber and tyre chips at 2.5%, 5%, 10%, 15%, 25% and 50% by total aggregate volume and a silica fume content of 0%, 5%, 10%, 15%, and 20% by weight of cement. They reported that compressive strength of the produced concretes decreased with the increase in the rubber content. However, the silica fume had a positive effect on increasing the mechanical properties of the rubber concrete. There is ample evidence that the strength of the concrete decreases with the use of tyre rubber in concrete. However, there exists no explicit formulation in literature to predict this strength loss. An appropriate model is required to describe the behaviour of rubber concrete in engineering applications. In this research work EPR is proposed to model the mechanical behaviour of rubber concrete.

5.4.2 Database

Data from an experimental study (Guneyisi et al, 2004) was used to develop an EPR model to describe the compressive strength of rubber concrete. Guneyisi et al (2004) carried out a program of experiments to study the compressive strength of the rubber concrete with and without silica fume. Two types of tyre rubber (crumb rubber and tyre chips) were used as fine and coarse aggregates in the production of rubber concrete mixtures. Six different rubber contents varying from 2.5% to 50% by total volume of aggregate were used. The samples of concrete with silica fume were produced by partial replacement of cement with silica fume at varying amounts of 5–20%. In total, 70 concrete mixtures were tested. Out of the 70 concrete mixtures, 56 cases were used to train the model while the remaining data were used in testing the developed model. The same training and testing datasets as those used by Guneyisi et al (2004) for developing ANN and GP models were used in this study to allow direct comparison between the results of the EPR model with those of ANN and GP models. The training and testing data are shown in Tables 5.9 and 5.10 respectively.

Table 0.7: EPR Training data (Guneyisi, Gesoglu and Ozturan, 2004)

Data No.	C (kg/m3)	SF (kg/m3)	W (kg/m3)	SP (kg/m3)	CA (kg/m3)	FA (kg/m3)	CR (kg/m3)	TC (kg/m3)	Fc (Mpa)
1	450	0.00001	180	13.5	1062.2	687.82	0.00001	0.00001	75.8
2	427.5	22.5	180	13.5	1057.96	685.06	0.00001	0.00001	81
3	405	45	180	13.5	1053.68	682.29	0.00001	0.00001	82.7
4	382.5	67.5	180	13.5	1049.4	679.52	0.00001	0.00001	84
5	350	0.00001	210	5.25	1076.4	697	0.00001	0.00001	53.8
6	332.5	17.5	210	5.25	1073.1	694.8	0.00001	0.00001	56.8
7	315	35	210	5.25	1069.7	692.7	0.00001	0.00001	57.7
8	297.5	52.5	210	5.25	1066.4	690.5	0.00001	0.00001	60.3
9	450	0.00001	180	13.5	1035.7	670.6	5.4	10.1	70.4
10	427.5	22.5	180	13.5	1031.5	667.9	5.4	10	72.5
11	405	45	180	13.5	1027.3	665.2	5.4	10	75.4
12	382.5	67.5	180	13.5	1023.2	662.5	5.4	9.9	78.3
13	350	0.00001	210	5.25	1049.5	679.6	5.5	10.2	47
14	332.5	17.5	210	5.25	1046.2	677.5	5.5	10.1	50.2
15	315	35	210	5.25	1043	675.4	5.5	10.1	52.5
16	297.5	52.5	210	5.25	1039.8	673.3	5.5	10.1	55.4
17	450	0.00001	180	13.5	1009.1	653.4	10.9	20.1	62.8
18	427.5	22.5	180	13.5	1005.1	650.8	10.9	20	67.8
19	405	45	180	13.5	1001	648.2	10.8	19.9	68.2
20	382.5	67.5	180	13.5	996.9	645.5	10.8	19.9	68
21	350	0.00001	210	5.25	1022.6	662.1	11	20.4	51.5
22	332.5	17.5	210	5.25	1019.4	660.1	11	20.3	43.1
23	315	35	210	5.25	1016.3	658.1	11	20.2	46.1
24	297.5	52.5	210	5.25	1013.1	656	10.9	20.2	49.3
25	450	0.00001	180	13.5	956	619	21.8	40.2	50.7
26	427.5	22.5	180	13.5	952.2	616.6	21.7	40	55.3
27	405	45	180	13.5	948.3	614.1	21.6	39.9	56.3
28	382.5	67.5	180	13.5	944.5	611.6	21.5	39.7	55.6
29	350	0.00001	210	5.25	968.8	627.3	22.1	40.7	31.8
30	332.5	17.5	210	5.25	965.8	625.4	22	40.6	35.8
31	315	35	210	5.25	962.8	623.4	21.9	40.5	37.6
32	297.5	52.5	210	5.25	959.8	621.5	21.9	40.4	41.3
33	450	0.00001	180	13.5	902.9	584.7	32.7	60.3	40.3
34	427.5	22.5	180	13.5	899.3	582.3	32.6	60.1	44.5
35	405	45	180	13.5	895.6	579.9	32.4	59.8	45.1
36	382.5	67.5	180	13.5	892	577.6	32.3	59.6	46.4
37	350	0.00001	210	5.25	914.9	592.4	33.1	61.1	24.3
38	332.5	17.5	210	5.25	912.1	590.6	33	60.9	28.8
39	315	35	210	5.25	909.3	588.8	32.9	60.7	31.4
40	297.5	52.5	210	5.25	906.5	587	32.8	60.5	32.8
41	450	0.00001	180	13.5	796.7	515.9	54.5	100.5	26.4
42	427.5	22.5	180	13.5	793.5	513.8	54.3	100.1	29.6
43	405	45	180	13.5	790.3	511.7	54.1	99.7	30.5
44	382.5	67.5	180	13.5	787.1	509.6	53.8	99.3	31.8
45	350	0.00001	210	5.25	807.3	522.7	55.2	101.9	16.2
46	332.5	17.5	210	5.25	804.8	521.1	55	101.5	18.2
47	315	35	210	5.25	802.3	519.5	54.9	101.2	20.1
48	297.5	52.5	210	5.25	799.8	517.9	54.7	100.9	21.2
49	450	0.00001	180	13.5	531.1	343.9	109	201	10.5
50	427.5	22.5	180	13.5	529	342.5	108.5	200.2	11.2
51	405	45	180	13.5	526.8	341.1	108.1	199.4	11.6
52	382.5	67.5	180	13.5	524.7	339.8	107.7	198.6	11.7
53	350	0.00001	210	5.25	538.2	348.5	110.4	203.7	7.1
54	332.5	17.5	210	5.25	536.5	347.4	110.1	203.1	7.2
55	315	35	210	5.25	534.9	346.3	109.7	202.5	8.1
56	297.5	52.5	210	5.25	533.2	345.3	109.4	201.8	8.4

Table 0.8: EPR testing data (Guneyisi, Gesoglu and Ozturan, 2004)

Data No.	C (kg/m3)	SF (kg/m3)	W (kg/m3)	SP (kg/m3)	CA (kg/m3)	FA (kg/m3)	CR (kg/m3)	TC (kg/m3)	Fc (Mpa)
1	360	90	180	13.5	1045.13	676.75	0.00001	0.00001	85.77
2	280	70	210	5.2	1063.1	688.4	0.00001	0.00001	59.7
3	360	90	180	13.5	1019	659.8	5.4	9.9	79.1
4	280	70	210	5.2	1036.5	671.2	5.5	10.1	56.4
5	360	90	180	13.5	992.9	642.9	10.7	19.8	69.4
6	280	70	210	5.2	1009.9	654	10.9	20.1	51.3
7	360	90	180	13.5	940.6	609.1	21.4	39.6	61.7
8	280	70	210	5.2	956.8	619.5	21.8	40.2	41.2
9	360	90	180	13.5	888.4	575.2	32.2	59.3	47
10	280	70	210	5.2	903.6	585.1	32.7	60.4	34.2
11	360	90	180	13.5	783.8	507.6	53.6	98.9	31.8
12	280	70	210	5.2	797.3	516.3	54.5	100.6	23.1
13	360	90	180	13.5	522.6	338.4	107.2	197.8	11.7
14	280	70	210	5.2	531.5	344.2	109.1	201.2	8.6

Table 0.9: COD values (%) for LR, GP, ANN and, EPR models based on testing data

Model	COD values (f_c)
Linear Regression	86.89
Genetic Programming	98.18
Artificial Neural Network (ANN)	99.94
Evolutionary Polynomial Regression (EPR)	99.5

5.4.3 EPR models

From the total of 70 cases in the database, 56 cases were used to develop the EPR model and the remaining cases were used as unseen cases to validate the developed model. Among the resultant equations developed using EPR, the one with the highest value of coefficient of determination (CoD) was selected for the compressive strength parameter (f_c):

$$f_c = -\frac{986.15FA^3}{SP^2 \cdot CA^3 \cdot (W/C)^3} + 6.59\times10^{-3}\left(SP \cdot CR\left(\frac{W}{C}\right)\right)^{0.5} \cdot \left(\frac{CA}{FA}\right)^3 TC - \frac{379.13FA^3}{CA^3 \cdot SP^2}\left(\frac{W}{C}\right)^2 \cdot \left(\frac{SF \cdot CR}{TC}\right)^{0.5} \quad 0\text{-}7$$
$$-1.45\left(SP\left(\frac{W}{C}\right)\right)^{0.5} \cdot \left(\frac{FA}{CA}\right)^3 TC + 100.21$$

where C, SF, W, SP, CA, FA, CR, and TC are cement, silica fume, water, superplasticizer, coarse aggregate, fine aggregate, crumb rubber, and tyre chips contents respectively. The proposed model is also unit dependent. Figures 5.16 and 5.17 show the comparisons between the EPR model predictions with the experimental data for the training and unseen testing cases respectively.

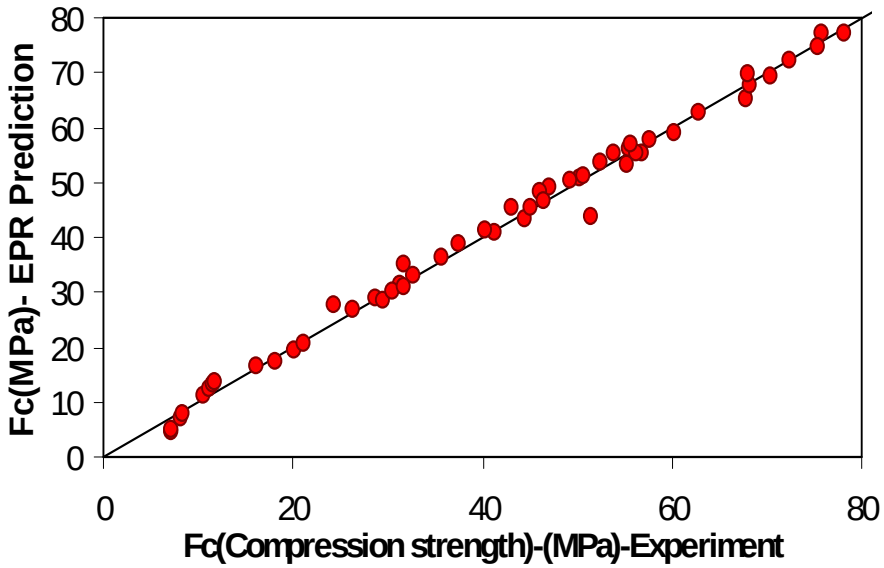

Figure 0.16: Performance of the EPR model on training cases

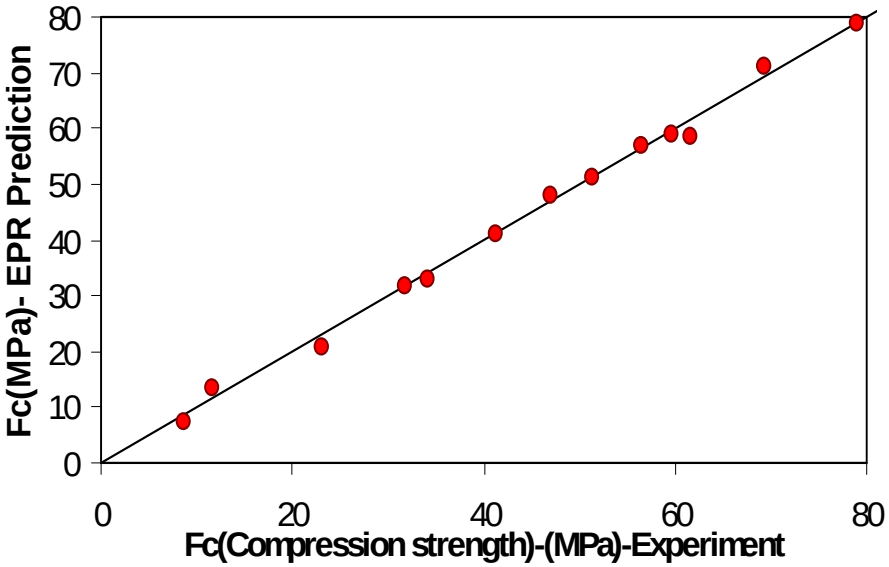

Figure 0.17: Performance of the EPR model on testing cases

A very close agreement between the EPR model predictions and the experimental data can be seen in the graphs. The coefficient of determination value for the EPR model is also compared to the ones for linear regression, artificial neural network and genetic programming techniques. The results are shown in Table 5.11 and indicate that EPR has been able to capture and reproduce the compressive strength behaviour of the rubber concrete with a high accuracy. It is shown that the EPR model outperforms the Linear Regression model and provides results comparable to those of the neural networks and GP models.

The results of the parametric study (see section 4.4.6) for the compressive strength model of the rubber concrete are shown in Figure 5.18. The results show that increasing the amount of fine grained aggregate and tyre chips decreases the compressive strength of the mixture, but any increase in the coarse grained aggregate content improves the compressive strength of the rubber concrete. This is consistent with the expected behaviour of rubber concrete. It is shown that the EPR model developed directly from

experimental data has been able to capture the compressive strength behaviour of rubber concrete correctly.

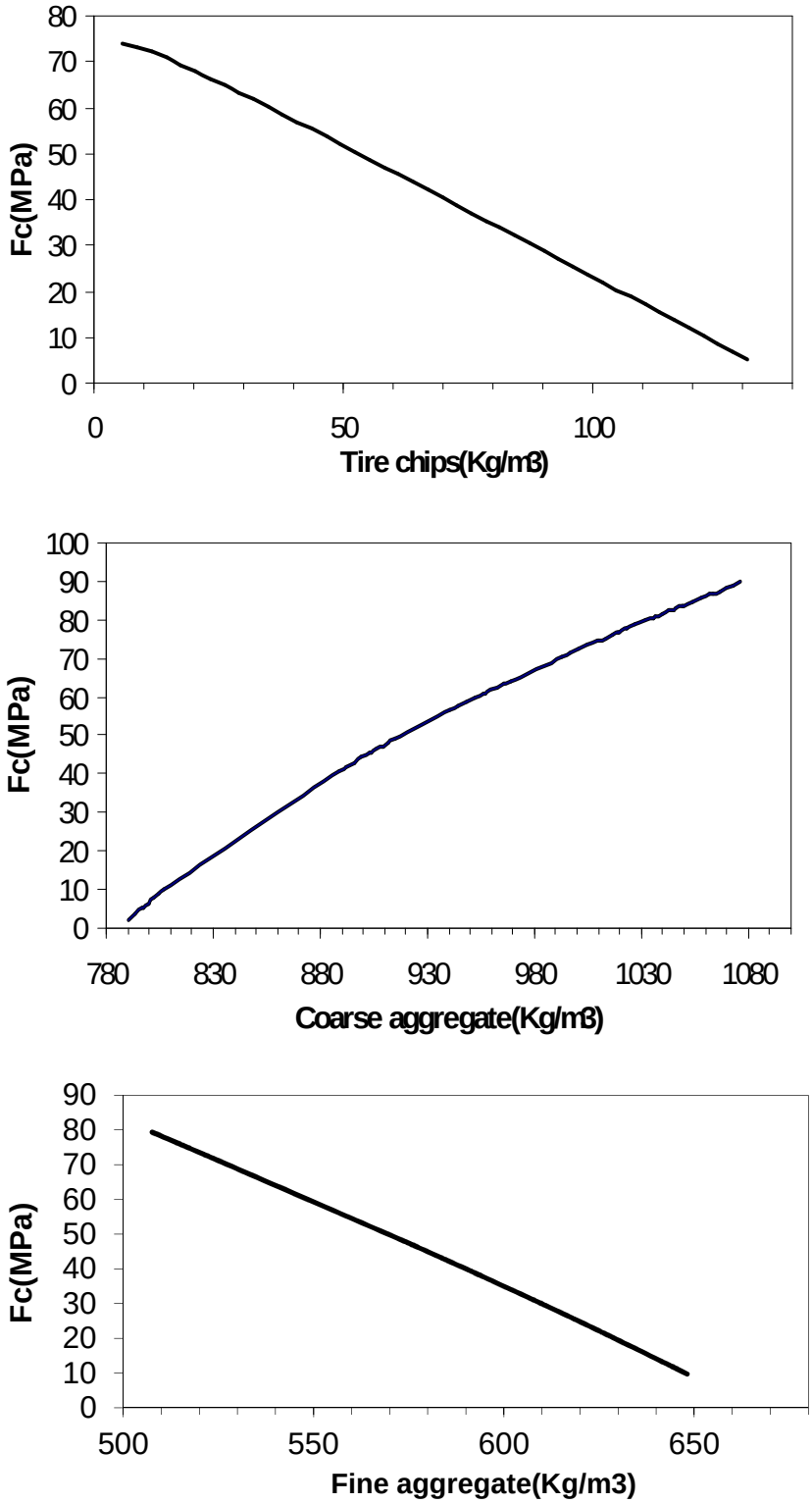

Figure 0.18: Results of the parametric study conducted on the EPR compressive strength model for rubber concrete

5.4.4 Outline and conclusions

Considerable increase in the amount of waste tyres leads to serious environmental problems in many parts of the world. Stockpiling of scrap tyres is undesirable due to the potential fire hazard resulting in environmental damages. These problems produce an urgent need to find new methods of reusing and recycling of waste tyres. As waste tyres do not easily decompose, engineers have been trying to find different ways of reusing them in building industry. The use of waste tyres as aggregate in concrete has been introduced as an effective way of reducing the problems associated with the disposal of this waste material. In order to use rubber concrete as a structural material, an appropriate model is required to describe the behaviour of this composite material.
In this research work, EPR approach was proposed for modelling the compressive strength of the rubber concrete. An EPR model was developed and validated using a database of case histories involving test data on characteristics of rubber concrete. The results of the model predictions were compared with the experimental data and results from linear regression, genetic programming and neural network models. A parametric study was conducted to evaluate the effects of different parameters on compressive strength of the rubber concrete and the extent to which the developed model can represent the physical relationships between the contributing parameters. Comparison of the results showed that the developed EPR model provides accurate predictions for compressive strength of the rubber concrete.

5.5 Conclusions

In this chapter EPR models were developed to represent compaction characteristics (including maximum dry density and optimum moisture content) and permeability of soils. Stability status of rock and soil slopes and also compressive strength of rubber concrete were modelled using the EPR methodology. In all cases parametric studies were conducted and the roles of different contributing parameter in the developed models were analysed in detail. Sensitivity analysis outcomes and also comparing EPR predictions with the results from previously developed models reported in the literature revealed robustness and accuracy of the developed models in predicting the complex behaviour of soil systems and engineering materials.

Chapter 6

SUMMARY, CONCLUSIONS AND RECOMMENDATIONS FOR FUTURE WORK

6.1 Summary of the present work

EPR-based modelling methodology was presented for modelling of behaviour of geomaterials and civil engineering systems. EPR can be described as a hybrid data mining technique that searches for symbolic structures using a genetic algorithm and estimates the constant values of such structures by the least squares method. This is a generic methodology and can be extended to be used for other types of materials and systems. By implementing this methodology the behaviour of the material (e.g. stress-strain behaviour) is captured and represented within evolutionary-based structured polynomial expressions. Models are developed based on training of EPR with raw data directly extracted from laboratory experiments or field measurements without any type of pre-processing. The effectiveness of the proposed approach was validated through application to modelling of various aspects of behaviour of saturated and unsaturated soils and rubber concrete. The developed models showed that using EPR for modelling the behaviour of materials is very promising. No prior assumptions of the material behaviour are made and nothing else but data is used to develop the models.

Where relevant, the EPR models were used to predict the material behaviour over the entire stress paths that had not been seen by EPR at the training stage of the model. The developed models were compared to the existing conventional material models, regression models and artificial neural network models (where available) and their advantages were highlighted. These results showed that EPR can be successfully employed to analyse different geotechnical and other civil engineering problems. Applying the proposed methodology to predict the complex and nonlinear behaviour of geotechnical problems with high levels of success was a firm evidence of excellent capabilities of the EPR methodology.

The following are the achievements of this research in modelling the behaviour of geotechnical and civil engineering materials using the proposed EPR framework:

- Constitutive modelling of unsaturated Soils
- Modelling of soil-water characteristic curve (SWCC) in unsaturated Soils
- Modelling of thermo-mechanical behaviour of unsaturated soils
- Developing models to describe the stress-strain and volume change behaviour of granular soils
- Identification of coupling parameters between shear strength behaviour and chemical effects in compacted soils

A number of other applications are also presented including:

- Modelling of permeability and compaction characteristics of soils
- Prediction of the stability of soil and rock slopes
- Modelling of mechanical behaviour of rubber concrete

Sensitivity analysis (parametric study) was conducted in all modelling cases, taking the advantage of the clear mathematical structure of EPR models, to investigate the effect of different contributing parameters on the developed models and to find out the most and least effective parameters in the behaviour of the desired engineering material / system.

6.2 Limitations of the proposed EPR methodology

EPR models perform very well at interpolation; however, they are not as good at extrapolation and in order to be able to use the developed models for practical purposes, the available training data for developing EPR models must cover the ranges of stresses and strains that will possibly be applied or generated in the real world cases. So, caution should be taken in using EPR model predictions in practical cases if the models are not trained to cover the input data ranges.

Also, similar to other data mining techniques, sufficient data is required for EPR to be able to develop appropriate models and too small databases may not lead to creation of suitable models.

6.3 Conclusions

The evolutionary polynomial regression technique works in a similar way as artificial neural networks and has all the advantages of ANN. But it provides the user with the additional advantage of developing a structured and transparent mathematical representation of the model in the form of a polynomial expression. Different types of functions can be introduced to the EPR by the user based the physical understanding of the problem to help accelerate finding the best possible and the most fit and robust model. EPR provides a unified framework for constitutive modelling of all materials particularly the ones with complicated behaviour and those for which constitutive models are not well developed. All parameters that are known to affect the system can be introduced to be included in the EPR model. More importantly, there is no need for any arbitrary choice of the constitutive (mathematical) models, no material parameters are to be identified and the model is trained directly based on the experimental data and/or field measurements. So, EPR-based material models can be considered as the shortest route from experimental research (data) to material modelling. Additionally, if more experimental data or field measurements become available to the user, the quality

of the EPR prediction can be improved by learning from the additional data through retraining the EPR, and as a result the EPR model becomes more effective, comprehensive and robust.

In spite of some limitations with the proposed methodology (discussed above), the developed models in this thesis showed the robustness and great capabilities of EPR in modelling different aspects of the very complicated constitutive behaviour of saturated and unsaturated soils and other civil engineering problems including stability analysis of slopes and also the compressive strength behaviour of rubber concrete.

6.4 Recommendations for future research work

- The presented methodology was applied to model the complicated shear and volume change behaviour of unsaturated soils considered under anisotropic loading (application of deviatoric stresses). Further investigations can be made to model the behaviour of this type of soils under isotropic loading, different unloading reloading conditions and various stress paths.

- Implementing the developed EPR constitutive models for unsaturated soils into the finite element models is very challenging due to the multi-phase nature of these soils but developing a numerical representation would be very useful in understanding the behaviours of unsaturated soils in more complicated cases.

- Other areas in geotechnical engineering like soil reinforcement, swelling behaviour of fine grained soils and also the behaviour of saturated and unsaturated soils under earthquake loading can also be considered for future applications of the proposed EPR modelling technique to understand the complicated behaviour of the soils and the soil-reinforcement interaction.

- Huge structures like high-rise buildings or different types of dams cause huge stresses in foundations. Because of existence of considerable number of monitoring devices measuring settlements and any other changes in the structures and foundations, the recorded data can be used to develop EPR models for further investigation of the real foundation-structure interactions to provide a better understanding of the problem and reduce the potential risk of damages to these structures that can be very costly in serious cases.

References

ABAQUS. (2007). *User Subroutine Reference Manual* (version 6.8-3 ed.). Dassault Systems.

Abramson, D., & Abela, J. (1992). A Parallel Genetic Algorithm for Solving the School Timetabling Problem. *15 Australian Computer Science Conference*, (pp. 1-11).

Ahangar-Asr, A., Faramarzi, A., & Javadi, A. (2010). A New Approach for Prediction of the Stability of Soil and Rock Slopes. *Engineering Computations*, *27*(7), 878-893.

Ahangar-Asr, A., Faramarzi, A., Javadi, A., & Giustolisi, O. (2011). Modelling Mechanical Behaviour of Rubber Concrete Using Evolutionary Polynomial Regression. *Engineering Computations*, *28*(4), 492-507.

Ahangar-Asr, A., Faramarzi, A., Mottaghifard, N., & Javadi, A. A. (2011, November). Modeling of permeability and compaction characteristics of soils using evolutionary polynomial regression. *Computers & Geosciences*, *37*(11), 1860-1869.

Ahangar-Asr, A., Johari, A., & Javadi, A. A. (2012, June). An evolutionary approach to modelling the soil–water characteristic curve in unsaturated soils. *Computers & Geosciences*, *43*, 25-33.

Alonso, E. E., Gens, A., & Josa, A. A. (1990). Constitutive Model for Partially Saturated Soils. *Geotechnique, 40*(3), 405–430.

Anderson, K., Allard, B., Bengtsson, M., & Magnusson, B. (1989). Chemical composition of cement pore waters. *Cement and Concrete Research, 19*, 327-332.

Aquino, W., & Brigham, J. (2006). Self-learning finite elements for inverse estimation of thermal constitutive models. *International Journal of Heat and Mass Transfer, 49*(15-16), 2466–2478.

Atal, A., & Levendis, Y. A. (1995). Comparison of the combustion behavior of pulverized waste tyres and coal. *Fuel, 74*(11), 1570-1581.

Aubertin, M., Ricard, J. F., & Chapuis, R. P. (1998). A predictive model for the water retention curve: Application to tailings from hardrock mines. *Can. Geotech. J., 35*(1), 55–69.

Baldi, G., Hueckel, T., & Pellegrini, R. (1988). Thermal Volume Changes of Mineral-Water System in Low-Porosity clay Soil. *Canadian Geotechnical Journal, 25*, 807-825.

Bauer, A., & Berger, G. (1998). Kaolinite and smectite dissolution rate in high molar KOH solutions at 35 ºC and 80 ºC. *Applied Geochemistry, 33*, 905-916.

Bauer, A., & Velde, B. (1999). Smectite transformation in high molar KOH solutions. *Clay Minerals, 34*, 259- 273.

Bell, F. G. (1996). Lime stabilization of clay minerals and soils. *Engineering Geology, 42*, 223-237.

Benazzouk, A., Douzane, O., & Queneudec, M. (2003). Effect of rubber aggregates on physico-mechanical behaviour of cement-rubber composites-influence of the alveolar texture of rubber aggregates. *Cem Concr Compos, 25*, 711-720.

Berardi, L., & Kapelan, Z. (2007). Multi-Case EPR Strategy for the Development of Sewer Failure Performance Indicators. *Proceedings of the World Environmental and Water Resources Congress.* Tampa, Florida, USA.

Bertrand, F., & Lyesse, L. (2008). ACMEG-TS: A constitutive model for unsaturated soils under non-isothermal conditions. *Int. J. Numer. Anal. Meth. Geomech., 32*, 1955–1988.

Bin, S., Zhibin, L., Yi, C., & Xiaoping, Z. (2007). Micropore structure of aggregates in treated. *Journal of Materials in Civil Engineering, 19*, 99-105.

Bishop, A. W., & Donald, I. B. (1961). The Experimental Study of Partly Saturated Soil in Triaxial Apparatus. *5th International Conference on Soil Mechanic and Foundation Engineering*, (p. 1321). Paris.

Blotz, L. R., Benson, C. H., & Boutwell, G. P. (1998). Estimating Optimum Water Content and Maximum Dry Unit Weight for Compacted Clays. *Journal of Geotechnical and Geo-Environmental Engineering, ASCE, 124*(9), 907–912.

Boardman, D. I., Glendinning, S., & Rogers, C. D. (2001). Development of stabilisation and solidification in lime-clay mixes. *Géotechnique, 51*, 533-543.

Bolzon, G., Schrefler, B. A., & Zienkiewicz, O. C. (1996). Elastoplastic soil constitutive laws generalized to partially saturated states. *Geotechnique, 46*(2), 279–289.

Booker, J. P., & Smith, D. W. (1989). Behaviour of Heat Source in a Fully Coupled Saturated Thermoelastic Soil. *Proceedings of the 3rd International Symposium on Numerical Models in Geomechanics*, (pp. 399-406). Niagara Falls.

Borja, R. I. (2004). Cam-Clay plasticity. Part V: A mathematical framework for three-phase deformation and strain localization analyses of partially saturated porous media. *Comput. Methods Appl. Mech. Engrg., 193*, 5301–5338.

Boudali, M., Leroueil, S., & Murthy, B. R. (1994). Viscous Behavior of Natural Soft Clays. *13th International Conference on Soil Mechanics and Foundation Engineering.*

Brandl, H. (1981). Alteration of soil parameters by stabilization with lime. *10th Int. Conf. on Soil Mechanics and Foundation Engineering*, *3*, pp. 587-594. Stockholm.

Britto, A. M., Savvidou, C., Maddocks, D. V., Gunn, M. J., & Booker, J. P. (1989). Numerical and Centrifuge Modelling of Coupled Heat Flow and Consolidation around Hot Cylinders Buried in Clay. *Geotechnique, 39*, 13-25.

Brooks, R. H., & Corey, A. T. (1964). *Hydraulic Properties of porous media.* Colorado State University, Fort Collins CO.., Hydrology Paper, No. 3.

Burmister, D. M. (1954). Principles of Permeability Testing of Soils. *Symposium on permeability of soils, ASTM Special Technical Publication, 163*, 3-26.

Burmister, D. M. (1964). Environmental Factors in Soil Compaction. *ASTM Special Publication No. 337.*

Calado, L., De Matteis, G., & Landolfo, R. (2000). Experimental response of top and seat angle semi-rigid steel frame connections. *Materials and Structures, 33*(8), 499–510.

Campanella, R. G., & Mitchell, J. K. (1968). Influence of Temperature Variations on Soil Behavior. *Journal of the Soil Mechanics and Foundations Division, ASCE, 94*(SM.3), 9-22.

Carman, P. C. (1937). Fluid Flows Through Granular Beds. *Trans Inst Chemistry Engineers, 15*, 150-166.

Cekerevac, C., & Laloui, L. (2004). Experimental study of thermal effects on the mechanical behaviour of a clay. *International Journal for Numerical and Analytical Methods in Geomechanics, 28*(3), 209-228.

Chen, C. Y., Bullen, A. G., & Elnaggar, H. A. (1977). Permeability and Related Principles of Coal Refuse. *Trans Res Record, 640*, 49-52.

Cheng, C. T., Ou, C. P., & Chau, K. W. (2002). Combining a fuzzy optimal model with a genetic algorithm to solve multiobjective rainfall-runoff model calibration. *J. of Hydro., 268*((1-4)), 72-86.

Chermak, J. A. (1993). Low temperature experimental investigation of the effect of high pH KOH solutions on the Opalinus shale. *Switzerland. Clays and Clay Minerals, 41*, 365-372.

Choquette, M., Berube, M. A., & Locat, J. (1987). Mineralogical and microtextural changes associated with lime stabilization of marine clays from eastern Canada. *Applied Clay Science, 2*, 215-232.

Claret, F., Bauer, A., Schäfer, T., Griffault, L., & Lanson, B. (2002). Experimental investigation of the interaction of clays with high-ph solutions: a case study from the callovo-oxfordian formation, Meuse-Haute Marne underground laboratory (France). *Clays and Clay Minerals, 50*, 633–646.

Craig, R. F. (1998). *Soil Mechanics* (6 ed.). E&FN Spon.

Cresswell, H. P., & Paydar, Z. (1996). Water retention in Australian soil, description and prediction using parametric functions. *Austral. J. Soil Res, 34*(2), 195–212.

Crilly, T. N. (1996). *Unload-Reload Tests on Saturated Illite Specimens at Elevated Temperatures.* M.Sc. Thesis, University of Manitoba, Winninpeg.

Cui, J. U., Sultan, N., & Delage, P. (2000). A Thermomechanical Model for Saturated Clays. *Canadian Geotechnical Journal, 37*, 607-620.

Cuisinier, O., Deneele, D., & Masrouri, F. (2009). Shear strength behaviour of compacted clayey soils submitted to an alkaline plume. *Engineering Geology, 108*, 177-188.

Cuisinier, O., Javadi, A. A., Ahangar-Asr, A., & Masrouri, F. (2013, March). Identification of coupling parameters between shear strength behaviour of compacted soils and chemical's effects with an evolutionary-based data mining technique. *Computers and Geotechnics, 48*, 107-116.

Cuisinier, O., Masrouri, F., Pelletier, M., Villieras, F., & Mosser-Ruck, R. (2008). Microstructure of a compacted soil submitted to an alkaline plume. *Applied Clay Science, 40*, 159-170.

Davidson, D. T., & Gardiner, W. F. (1949). Calculation of Standard Proctor Density and Optimum Moisture Content from Mechanical Analysis, Shrinkage Factors, and Plasticity Index. *Proceedings HRB , 29*, 447–481.

Dayakar, P., & Rongda, Z. (1999). Triaxial compression behavior of sand and gravel using arti®cial neural networks (ANN). *Computers and Geotechnics, 24*, 207-230.

Delage, P., Sultan, N., & Cui, Y. J. (2000). On the Thermal Consolidation of Boom Clay. *Canadian Geotechnical Journal, 37*, 343-354.

Demars, K. P., & Charles, R. D. (1982). Soil Volume Changes Induced By Temperature Cycling. *Canadian Geotechnical Journal, 19*, 188-194.

Deroo, L. (2002). Expertise sur l'utilisation de l'argilite excavée comme remblai de galerie dans un stockage en formation géologique profonde. *Agence nationale pour la gestion des déchets radioactifs*, (pp. DRP0ISL02.002/3, 131 p.). Paris.

deVeries, D. A. (1958). Simultaneous Transfer of Heat and Moisture in Porous Meia. *Transactions, American Geophysical Union, 39*(5), 909-916.

Dixon, D. A., Gray, M. N., & Thomas, A. W. (1985). A study of the compaction properties of potential clay-sand buffer mixtures for use in nuclear waste disposal. *Engineering Geology, 21*, 247-255.

Doglioni, A. (2004). *A Novel Hybrid Evolutionary Technique for Environmental Hydraulic Modelling.* PhD Thesis, Technical University of Bari, Italy.

Doglioni, A., Giustolisi, O., Savic, D., & Webb, B. (2008). An investigation on stream temperature analysis based on evolutionary computing. *HYDROLOGICAL PROCESSES, 22*(3), 315-326.

Drucker, D., & Prager, W. (1952). Soil mechanics and plastic analysis or limit design. *Q. Applied Mathematics, 10*(2), 157-175.

Dumont, M., Taibi, S., Fleureau, J., Abou Bekr, N., & Saouab, A. (2010). Modelling the effect of temperature on unsaturated soil behaviour. *Comptes Rendus Geoscience, 342*, 892-900.

Duncan, M. (1996). Landslides Investigation and Mitigation. *Soil slope stability analysis(Washington Press)*, 337-371.

Ehlers, W., Graf, T., & Ammann, M. (2004). Deformation and localization analysis of partially saturated soil. *Comput. Methods Appl. Mech. Engrg., 193*, 2885–2910.

Eldin, N. N., & Senouci, A. B. (1992). Use of scrap tyres in road construction. *Journal of Construction Engineering Management, 118*(3), 561-576.

Eldin, N. N., & Senouci, A. B. (1993). Rubber tyre particles as concrete aggregate. *J Mater Civ Eng ASCE, 5*(4), 478-496.

Ellis, G., Yao, C., & Zhao, R. (1992). Neural network modelling of mechanical behaviour of sand. *Proceeding of the 9th ASCE Conference on Engineering Mechanics*, (pp. 421-424). Texas.

Eriksson, L. G. (1989). Temperature Effects on Consolidation Properties of Sulfide Clays. *12th International Conference on Soil Mechanics and Foundation Engineering.*

Erzin, Y. (2004). Strength of Different Anatolian Sands in Wedge Shear,Triaxial Shear, and Shear Box Tests. *The Middle East Technical University, PhD thesis*.

Ewen, J., & Thomas, H. R. (1989). Heating Unsaturated Medium Sand. *Geotechnique, 39*(3), 455-470.

Faramarzi, A. (2011). *Intelligent computational solutions for constitutive modelling of materials in finite element analysis.* PhD thesis: University of Exeter.

Faramarzi, A., Javadi, A. A., & Ahangar-Asr, A. (2013). Numerical implementation of EPR-based material models in finite element analysis. *Computers and Structures*, 118, 100-108

Faramarzi, A., Mehravar, M., Veladi, H., Javadi, A., Ahangar-Asr, A., & Mehravar, M. (2011). A Hysteretic Model for Steel Plate Shear Walls. *Proceedings of the 19th ACME Conference, 5-6 April*, (pp. 69-72). Edinburgh, Heriot-Watt University.

Farcasiu, M. (1993). Another use for old tyres. *Chemtech, 23*(1), 22-24.

Feng, X., & Yang, C. (2004). Coupling recognition of the structure and parameters of non-linear constitutive material models using hybrid evolutionary algorithms. *International Journal for Numerical Methods in Engineering, 59*(9), 1227–1250.

Fossberg, P. E. (1965). Some fundamentals engineering properties of a lime-stabilized clay. *6th Int. Conf. on Soil Mechanics and Foundation Engineering, 1*, pp. 221-225. Montréal.

Fox, P. L., & Edil, T. B. (1996). Effects of Stress and Temperature on Secondary Compression of Peat. *Canadian Geotechnical Journal, 33*, 405-415.

Fredlund, D. G., & Morgenstern, N. R. (1977). Stress State Variables for Unsaturated Soils. *Journal of Geotechnical Engineering Division, ASCE, 103*(GT5), 447-467.

Fredlund, D. G., & Pham, H. Q. (2006). . A volume–mass constitutive model for unsaturated soils in terms of two independent stress state variables. *4th Int. Conf. on Unsaturated Soils, ASCE, 1*, (pp. 105-134). Carefree, Arizona.

Fredlund, D. G., Xing, A., Fredlund, M. D., & Barbour, S. L. (1995). The relationship of the unsaturated soil shear strength to the soil-water characteristic curve. *Canadian Geotechnical Journal, 32*, 440-448.

Fredlund, M. D., Fredlund, D. G., & Wilson, G. W. (1997). Prediction of the soil-water characteristic curve from grain size distribution and volume-mass properties. *Proc. 3rd Brazilian Symp. on Unsaturated Soils*, (pp. 13-23). Rio de Janeiro, Brazil.

Fredlund, M. D., Wilson, G. W., & Fredlund, D. G. (2002). Use of grain-size distribution for estimation of the soil water characteristic curve. *Can. Geotech. J., 39*(5), 1103-1117.

Fu, Q., Hashash, Y., Jung, S., & Ghaboussi, J. (2007). Integration of laboratory testing and constitutive modeling of soils. *Computers and Geotechnics, 34*(5), 330–345.

Furukawa, T., & Hoffman, M. (2004). Accurate cyclic plastic analysis using a neural network material model. *Engineering Analysis with Boundary Elements, 28*(3), 195–204.

Gallipoli, D., Gens, A., Sharma, R., & Vaunat, J. (2003). An elasto-plastic model for unsaturated soil incorporating the effects of suction and degree of saturation on mechanical behaviour. *Geotechnique, 53*(1), 123-135.

Garcia-Bengochea, I., Lovell, C. W., & Altschaeffl, A. G. (1979). Pore Distribution and Permeability of Silty clays. *Journal of Geotechnical Engineering Division, ASCE, 105*(GT7), 839–855.

Gaucher, E. C., Blanc, P., Matray, J. M., & Michau, N. (2004). Modeling diffusion of an alkaline plume in a clay barrier. *Applied Geochemistry, 19*, 1505-1515.

Gawin, D., Baggio, P., & Schrefler, B. A. (1995). Coupled Heat, Water and Gas Flow in Deformable Porous Media. *International Journal for Numerical Methods in Fluids, 20,* 969-987.

Gens, A., & Potts, D. (1988). Critical state models in computational geomechanics. *Engineering Computations, 5*(3), 178 - 197.

Geraminegad, M., & Saxena, S. K. (1986). A Couple Thermoelastic Model for Saturated-Unsaturated Porous Media. *Geotechnique, 36*(4), 539-550.

Ghaboussi, J., & Sidarta, D. (1998). New nested adaptive neural networks (NANN) for constitutive modelling. *Computers and Geotechnics, 22*(1), 29-52.

Ghaboussi, J., Garret, J., & Wu, X. (1991). Knowledge-based modelling of material behaviour with neural networks. *Journal of Engineering Mechanics Division, 117*(1), 153-164.

Ghaboussi, J., Kim, J., & Elnashai, A. (2010). Hybrid modelling framework by using mathematics-based and information-based methods. *IOP Conference Series: Materials Science and Engineering, 10,* pp. 1-9.

Ghaboussi, J., Pecknold, D., Zhang, M., & Haj-Ali, R. (1998). Autoprogressive training of neural network constitutive models. *International Journal for Numerical Methods in engineering, 42*(1), 105-126.

Ghaboussi, J., Sidarta, D., & Lade, P. (1994). Neural network based modelling in geomechanics. *Proceeding of the 8th International Conference on Computer Methods and Advances in Geomechanics*, (pp. 153-164). Morgantown.

Giustolisi, O., & Laucelli, D. (2005). Increasing generalisation of input-output artificial neural networks in rainfall-runoff modelling. *Hydrological Sciences Journal, 50*(3), 439-457.

Giustolisi, O., & Savic, D. (2006). A symbolic data-driven technique based on evolutionary polynomial regression. *Journal of Hydroinformatics, 8*(3), 207-222.

Giustolisi, O., & Savic, D. A. (2009). Advances in data-driven analyses and modelling using EPR-MOGA. *Journal of Hydroinformatics, 11*(3-4), 225-236.

Goldberg, D. (1989). *Genetic Algorithms in Search, Optimization, and Machine Learning.* ADDISON-WESLEY.

Golub, G. H., & Van Loan, C. F. (1993). *Matrix Computations.* London: The John Hopkins University Press.

Graham, J., Tanaka, N., Crilly, T., & Alfaro, M. (2001). Modified Cam-Clay Modelling of Temperature Effects in Clays. *Canadian Geotechnical Journal, 38,* 608-621.

Guneyisi, E., Gesoglu, M., & Ozturan, T. (2004). Properties of rubberized concretes containing Silica fume. *Cem Concr Res, 34*(12), 2309-2317.

Gupta, S. C., & Larson, W. ,. (1979). A Model for Predicting Packing Density of Soils Using Particles-size of Distribution. *Soil Science Society of America Journal, 43*(4), 758–764.

Habibagahi, G., & Bamdad, A. A. (2003). Neural Network framework for mechanical behaviour of unsaturated soils. *Canadian Geotechnical Journal, 40,* 684–693.

Habibagahi, K. (1973). Temperature Effect on Consolidation Behavior of Overconsolidated Soils. *8th International Conference on Soil Mechanics and Foundation Engineering.*

Haj-Ali, R., & Kim, H. (2007). Nonlinear constitutive models for FRP composites using artificial neural networks. *Mechanics of Materials, 39*(12), 1035–1042.

Hardin, B. O. (1985). Crushing of soil particles. *Journal of Geotechnical Engineering, ASCE, 111*(10), 1177-92.

Hashash, Y. M., Song, H., & Osouli, A. (2011). Three-dimensional inverse analyses of a deep excavation in Chicago clays. *International Journal for Numercial and Analytical Methods in Geomechanics, 35*(9), 1059-1075.

Hashash, Y., & Song, H. (2008). The Integration of Numerical Modeling and Physical Measurements through Inverse Analysis in Geotechnical Engineering. *KSCE Journal of Civil Engineering, 12*(3), 165-176.

Hashash, Y., Fu, Q., & Butkovich, J. (2004b). Generalized strain probing of constitutive models. *International Journal for Numerical and Analytical Methods in Geomechanics, 28*(15), 1503–1519.

Hashash, Y., Fu, Q., Ghaboussi, J., Lade, P., & Saucier, C. (2009). Inverse analysis–based interpretation of sand behavior from triaxial compression tests subjected to full end restraint. *Canadian Geotechnical Journal, 46*(7), 768–791.

Hashash, Y., Ghaboussi, J., & Jung, S. (2006b). Characterizing Granular Material Constitutive Behavior Using SelfSim with Boundary Load-Displacement Measurements. *Proceedings of the Tenth Biennial ASCE Aerospace Division International Conference on Engineering, Construction, and Operations in Challenging Environments,* (pp. 1-8). Houston, USA.

Hashash, Y., Ghaboussi, J., Fu, Q., & Marulanda, C. (2006c). Constitutive Soil Behavior Representation via Artificial Neural Networks: A Shift from Soil

Models to Soil Behavior Data. *Proceedings of GeoCongress 2006: Geotechnical Engineering in the Information Technology Age*, (pp. 1-6). Atlanta.

Hashash, Y., Jung, S., & Ghaboussi, J. (2004). Numerical implementation of a neural network based material model in finite element analysis. *International Journal for Numerical Methods in Engineering, 59*(7), 989–1005.

Hashash, Y., Jung, S., & Ghaboussi, J. (2004a). Numerical implementation of a neural network based material model in finite element analysis. *International Journal for Numerical Methods in Engineering, 59*(7), 989–1005.

Hashash, Y., Levasseur, S., Osouli, A., Finno, R., & Malecot, Y. (2010). Comparison of two inverse analysis techniques for learning deep excavation response. *Computers and Geotechnics, 37*(3), 323–333.

Hashash, Y., Marulanda, C., Ghaboussi, J., & Jung, S. (2003). Systematic update of a deep excavation model using field performance data. *Computers and Geotechnics, 30*(6), 477–488.

Hashash, Y., Marulanda, C., Ghaboussi, J., & Jung, S. (2006). Novel Approach to Integration of Numerical Modeling and Field Observations for Deep Excavations. *ASCE Journal of Geotechnical and Geoenvironmental Engineering, 132*(8), 1019-1031.

Hashash, Y., Marulanda, C., Ghaboussi, J., & Jung, S. (2006a). Novel Approach to Integration of Numerical Modeling and Field Observations for Deep Excavations. *ASCE Journal of Geotechnical and Geoenvironmental Engineering, 132*(8), 1019-1031.

Hauser, V. L. (1978). Seepage Control by Particle Size Selection. *Transactions of the ASAE , 21*(4), 691–695.

Hazen, A. (1911). Discussion of Dams on Sand Foundations. *Trans ASCE, 73*, 199–203.

Hoek, E., & Bray, J. W. (1981). *Rock Slope Engineering.* London: Institution of Mining and Metallurgy.

Hogentogler, C. A. (1936). Essentials of Soil Compaction. *HRB.*

Hooke, R. (1675). *A description of helicopes, and some other instruments.* London.

Horn, M. E. (1971). Estimating Soil Permeability Rates. *Journal of the Irrigation and Drainage Division, ASCE, 97*(IR2), 263–274.

Houston, S. L., Houston, W. N., & Williams, N. D. (1985). Thermo-Mechanical Behavior of Seafloor Sediments. *Journal of Geotechnical Engineering, 111*(11), 249-1263.

Hueckel, T., & Baldi, G. (1990). Thermoplasticity of Saturated Clays: Experimental Constitutive Study. *Journal of Geotechnical Engineering, ASCE, 116*(12), 1778-1796.

Hueckel, T., & Pellegrini, R. (1992). Effective Stress and Water Pressure in Saturated Clays during Heating-Cooling Cycles. *Canadian Geotechnical Journal, 29*, 1095-1102.

Huertas, F., Farias, J., Griffault, L., Leguey, S., Cuevas, J., Ramírez, S., . . . Vieillard, P. (2000). Effects of cement on clay barrier performance. *Ecoclay project- Final Report*, 141p.

Hutson, J. L., & Cass, A. (1987). A retentivity function for use in soil water simulation models. *Soil Sci., 38*(1), 105–113.

Janbu, N. (1954). Application of composite slip circles for stability analysis. *Fourth European Conference on stability of earth slopes*, (pp. 43-49).

Javadi, A. A., & Rezania, M. (2008). A New Approach to Constitutive Modelling of Soils in Finite Element Analysis using Evolutionary Computation. *Intelligent Computing in Engineering - ICE08*, (pp. 147-156).

Javadi, A. A., Ahangar-Asr, A., Johari A, A., Faramarzi, A., & Toll, D. G. (2012, August). Modelling stress-strain and volume change behaviour of unsaturated soils using an evolutionary based data mining technique, an incremental approach. *Engineering Applications of Artificial Intelligence, 5*(25), 926-933.

Javadi, A. A., Tan T. P. & Zhang, M. (2003). Neural network for constitutive modelling in finite element analysis. *Computer Assisted Mechanics and Engineering Sciences*, *10*(4), 375-381.

Javadi, A. A., Tan T. P. & Zhang, M. (2004b). Intelligent finite element method: Development of the algorithm. *Proceeding of the 6th World Congress on Computational Mechanics-WCCM VI.* Beijing, China.

Javadi, A. A., & Rezania, M. (2009a). Applications of artificial intelligence and data mining techniques in soil modelling. *Geomechanics and Engineering, An International Journal, 1*(1), 53–74.

Javadi, A. A., Faramarzi, A., & Farmani, R. (2011). Design and Optimization of Microstructure of Auxetic Materials. *Engineering Computations, In press*.

Javadi, A. A., Farmani, R., & Tan T. P. (2005b). A Hybrid Intelligent Genetic Algorithm. *Advanced Engineering Informatics,19*, 255-262.

Javadi, A. A., Johari, A., Ahangar-Asr, A., Faramarzi, A., & Toll, D. G. (2010). Prediction of the behaviour of unsaturated soils using evolutionary polynomial regression: An incremental approach. *5th International Conference on Unsaturated Soils, 6-8 September*, (pp. 837-842). Barcelona, Spain.

Javadi, A. A., Tan, T., & Elkassas, A. (2005). Intelligent finite element method. *Proceeding of the 3rd MIT Conference on Computational Fluid and Solid Mechanics.* Cambridge, Massachusetts, USA.

Javadi, A. A., Tan, T., & Elkassas, A. (2009). Intelligent Finite Element Method and Application to Simulation of Behavior of Soils under Cyclic Loading. In A. Abraham., & a. et (Eds.), *FOUNDATIONS OF COMPUTATIONAL INTELLIGENCE* (Vol. 5, pp. 317-338). Springer-Verlag.

Javadi, A. A., Tan, T., & Elkassas, A. S. (2004a). An intelligent finite element method. *Proceeding of the 11th International EG-ICE Workshop*, (pp. 16-25). Weimar, Germany.

Javadi, A. A., Zhang, M., & Tan, T. (2002). Neural network for constitutive modelling of material in finite element analysis. *Proceedings of the 3rd International Workshop/Euroconference on Trefftz Method*, (pp. 61-62). Exeter, UK.

Johari, A., & Javadi, A. A. (2010). Prediction of a soil-water characteristic curve using neural network. *5th Int. Conf. on unsaturated soils, 1*, (pp. 461-466.). Barrcelona, Spain.

Johari, A., Habibagahi, G., & Ghahramani, A. (2006a). Prediction of soil–water characteristic curve using genetic programming. *Journal of Geotechnical and Geoenvironmental Engineering (ASCE), 5*, 661-665.

Johari, A., Habibagahi, G., & Ghahramani, A. (2006b). Prediction of soil-water characteristic curve using a genetic based neural network. *Scientia Iranica, 13*(3), 284-294.

Jumikis, A. R. (1946). Geology and Soils of the Newark (N.J.) Metropolitan Area. *Journal of the Soil Mechanics and Foundations Division, ASCE , 93*(SM2), 71–95.

Jung, S., & Ghaboussi, J. (2006a). Neural network constitutive model for rate-dependent materials. *Computers and Structures, 84*(15-16), 955–963.

Jung, S., & Ghaboussi, J. (2006b). Characterizing rate-dependent material behaviors in self-learning simulation. *Computer Methods in Applied Mechanics and Engineering, 196*(1-3), 608-619.

Jung, S., & Ghaboussi, J. (2010). Inverse identification of creep of concrete from in situ load-displacement monitoring. *Engineering Structures, 32*(2), 1437-1445.

Jung, S., Ghaboussi, J., & Marulanda, C. (2007). Field calibration of time-dependent behavior in segmental bridges using self-learning simulation. *Engineering Structures, 29*(10), 2692–2700.

Karnland, O. (2005). Laboratory experiments concerning compacted bentonite contacted to high pH solutions. *ECOCLAY II – effects of cement on clay barrier performance – final report. European Commission*, 143-162.

Kessler, B., El-Gizawy, A., & Smith, D. (2007). Incorporating Neural Network Material Models Within Finite Element Analysis for Rheological Behavior Prediction. *Journal of Pressure Vessel Technology, 192*(2), 58-65.

Khalili, N., & Loret, B. (2001). An Elasto-plastic Model for Non-isothermal Analysis of Flow and Deformation in Unsaturated Porous Media: Formulation. *International Journal of Solid and Structures, 38*, 8305-8330.

Khalili, N., Habte, M., & Zargargashi, S. (2008). A fully coupled flow deformation model for cyclic analysis of unsaturated soils including hydraulic and mechanical hystereses. *Computers and Geotechnics, 35*(6), 872-889.

Khatip, Z. K., & Bayomy, F. M. (1999). Rubberized Portland cement concrete. *J Mater Civ Eng ASCE, 11*(3), 206-213.

Kim, J., Ghaboussi, J., & Elnashai, A. (2010). Mechanical and informational modeling of steel beam-to-column connections. *Engineering Structures, 32*(2), 449-458.

Kogho, Y., Nakano, M., & Miyazaki, T. (1993). Theoretical aspects of constitutive modeling for non-saturated soils. *Soils and Foundations, 33*(4), 49-63.

Koza, J. R. (1992). *Genetic Programming: On the Programming of Computers by Natural Selection.* Cambridge, MA.: MIT Press.

Kukreti, A., & Abolmaali, A. (1999). Moment–rotation hysteresis behavior of top and seat angle steel frame connections. *Journal of Structural Engineering , 125*(8), 810–820.

Kuntiwattanakul, P., Towhata, I., Ohishi, K., & Seko, I. (1995). Temperature Effects on Undrained Shear Characteristics on Clay. *Soils and Foundations, 35*(1), 427-441.

Lade, P. (1977). Elasto-plastic stress-strain theory for cohesionless soil with curved yield surfaces. *International Journal of Solids and Structures, 13*(11), 1019-1035.

Lade, P., & Jakobsen, K. (2002). Incrementalization of a single hardening constitutive model for frictional materials. *International Journal for Numerical and Analytical Methods in Geomechanics, 26*, 647-659.

Lagurous, J. G. (1969). Effects of Temperature on Some Engineering Properties of Clay Soils. *an International Conference on Effects of Temperature and Heat on Engineering Behavior of Soils.*

Lambe, T. W. (1951). *Soil Testing for Engineers.* NY: John Wiley and Sons Inc.

Laucelli, D., & Giustolisi, O. (2011). Scour depth modelling by a multi-objective evolutionary paradigm. *Environmental Modelling & Software, 26*(4), 498-509.

Le Runigo, B., Cuisinier, O., Cui, Y. J., Deneele, D., & Ferber, V. (2009). Impact of the initial state on fabric and permeability of a lime treated silt under long term leaching. *Canadian Geotechnical Journal, 46*, 1243-1257.

Lee, K. L., Seed, H. B., & Dunlop, P. (1967). Effect of moisture on the strength of a clean sand. *J. Soil Mech. and Found. Div., ASCE , 93*(6), 17-40.

Leslie, D. D. (1975). Shear strength of rock fill. *Physical Properties Engrg. Study No. 526, U.S. Army Corps of Engrs., Sausalito, CA.*

Lingnau, B. E. (1993). *Consolidated Undrained-Triaxial Behavior of a Sand-Bentonite Mixture at Elevated Temperature.* Manitoba: PhD Thesis, The University of Manitoba.

Lingnau, B. E., Graham, J., & Tanaka, N. (1995). Isothermal Modeling of Sand-Bentonite Mixtures at Elevated Temperatures. *Canadian Geotechnical Journal, 32*, 78-88.

Linveh, M., & Ishai, I. (1978). Using Indicative Properties to Predict the Density-moisture Relationship of Soil. *Trans Res Record , 60p*, 22–28.

Little, D. N. (1995). Stabilization of pavement subgrades and base courses with lime. *National lime association, Arlington*, 219 p.

Lo, K. Y., & Roy, M. (1973). Response of particulate materials at high-pressures. *Soils and Foundations,JSSMFE, 13*(1), 61-76.

Loret, B., & Khalili, N. (2000). A Three Phase Model for Unsaturated Soils. *International Journal for Numerical and Analytical Methods in Geomechanics, 24*, 893-927.

Lu, M., AbouRizk, S., & Hermann, U. (2001). Sensitivity analysis of neural networks in spool fabrication productivity studies. *ASCE Journal of Computing in Civil Engineering, 15*(4), 299-308.

Marachi, N. D., Chan, C. K., Seed, H. B., & Duncan, J. M. (1969). Strength and deformation characteristics of rockfill materials. *Report No. TE-69-5, Dept. of Civil Engrg., Univ. Of California, Berkeley, CA.*

Marcial, D., Delage, P., & Cui, Y. J. (2002). On the high stress compression of bentonites. *Canadian Geotechnical Journal, 39*, 812-820.

Maruyama, S. (1969). Effect of Temperature in Elastic of Clays. *an International Conference on Effects of Temperature and Heat on Engineering Behavior of Soils.*

Matyas, E. L., & Radhakrishna, H. S. (1968). Volume Change Characteristics of Partially Saturated Soils. *Geotechnique, 18*, 432-448.

Michaels, A. S., & Lin, C. S. (1954). The Permeability of Kaolinite. *Industrial & Engineering Chemistry Research (ACS Publications), 46*, 1239–1246.

Milly, P. C. (1982). Moisture and Heat Transport in Hysteretic, Inhomogeneous Porous Media: A Matric Heat-Based Formulation and a Numerical Model. *Water Resources Research, 18*, 489-1098.

Mita, K., Dasari, G., & Lo, K. (2004). Performance of a Three-Dimensional Hvorslev–Modified Cam Clay Model for Overconsolidated Clay. *ASCE International Journal of Geomechanics, 4*(4), 296-310.

Mitchell, J. K., Hopper, D. R., & Campanella, R. C. (1965). Permeability of Compacted. *Journal of the Soil Mechanics and Foundations Division, ASCE, 91*(SM4), 41-65.

Miura, N., & O-Hara, S. (1979). Particle crushing of a decomposed granite soil under shear. *Soils and Foundations, JSSMFE, 19*(3), 1-14.

Miura, N., & Yamanouchi, T. (1975). Effect of water on the behavior of quartz-rich sand under high stresses. *Soils and Foundations, JSSMFE, 15*(4), 23-34.

Mollins, L. H., Stewart, D. I., & Cousens, T. W. (1999). Drained strength of bentonite-enhanced sand. *Géotechnique, 49*, 523-528.

Muir Wood, D. (1990). *Soil Behaviour and Critical State Soil Mechanics.* Cambridge University Press.

Muttil, N., & Chau, K. (2006). Neural network and Genetic Programming for Modelling Coastal Algal Blooms. *International Journal of Environment and Pollution, 28*((3-4)), 223-238.

Najjar, Y. M., Basheer, I. A., & Naouss, W. A. (1996). On the identification of compaction characteristics by neuronets. *Computers and Geotechnichs, 18*(3), 167-187.

Najjar, Y., & Huang, C. (2007). Simulating the stress–strain behavior of Georgia kaolin via recurrent neuronet approach. *Computers and Geotechnics, 34*(5), 346–361.

Neaman, A., Pelletier, M., & Villieras, F. (2003). The effects of exchanged cation, compression, heating and hydration on textural properties of bulk bentonite and its corresponding purified montmorillonite. *Applied Clay Science, 22*, 153-168.

Nezami, E., Hashash, Y., & Ghaboussi, J. (2006). A Model for Large Scale Near-Real Time Simulation of Granular Material Flow. *Proceedings of the Tenth Biennial ASCE Aerospace Division International Conference on Engineering, Construction, and Operations in Challenging Environments*, (pp. 1-8). Houston, USA.

Olson, R. E. (1963). Effective Stress Theory of Soil Compaction. *Journal of the Soil Mechanics and Foundations Division, ASCE, 89*(SM2), 27-45.

Osouli, A., Hashash, Y., & Song, H. (2010). Interplay between Field Measurements and Soil Behavior for Capturing Supported Excavation Response. *ASCE Journal of Geotechnical and Geoenvironmental Engineering, 36*(1), 69-84.

Owen, D., & Hinton, E. (1980). *Finite Element in Plasticity: Theory and Practice.* Swansea: Pineridge Press Limited.

Paaswell, R. E. (1967). Temperature Effects on Clay Soil Consolidation. *Journal of The Soil Mechanics and Foundations Division, ASCE, 93*(SM3), 9-22.

Pastor, M., Zienkiewicz, O. C., & Chan, A. (1990). Generalized plasticity and the modelling of soil behaviour. *Intl. J. Num. Ana. Meth. in Geomechanics, 14*, 151-190.

Pedroso, D. M., & Williams, D. J. (2010). A novel approach for modelling soil water characteristic curves with hysteresis. *Computers and Geotechniques, 37*(3), 374-380.

Penumadu, D., & Zhao, R. (1999). Triaxial compression behaviour of sand and gravel using artificial neural networks (ANN). *Computers and Geotechnics, 24*(3), 207-230.

Pereira, J. H., & Fredlund, D. G. (2000). Volume change behavior of collapsible compacted gneiss soil. *J. of Geotech. and Geoenviron. Eng., 126*, 907–916.

Philip, J. R., & deVeries, D. A. (1957). Moisture Movement in Porous Materials. *Transactions, American Geophysical Union, 39*(2), 222-231.

Plum, R. L., & Esrig, M. I. (1969). Effects of Temperature on Some Engineering Properties of Clay Soils. *an International Conference on Effects of Temperature and Heat on Engineering Behavior of Soils.*

Ponce, V. M., & Bell, J. M. (1971). Shear strength of sand at extremely low pressures. *J. Soil Mech. and Found.Div., ASCE, 97*(4), 625-639.

Pusch, R., Zwahr, H., Gerber, R., & Schomburg, J. (2003). Interaction of cement and smectitic clay – theory and practice. *Appl Clay Sci, 23,* 203–210.

Ramamurthy, T., Kanitar, V. K., & Prakash, K. (1974). Behavior of coarse-grained soils under high stresses. *Indian Geotech. J., 4*(1), 39-63.

Ramiah, B. K., Viswanath, V., & Krishnamurthy, H. V. (1970). Interrelationship of Compaction and Index Properties. *Second Southeast Asian Conference on Soil Engineering*, (pp. 577–587). Singapore.

Ramírez, S., Cuevas, J., Vigil, R., & Leguey, S. (2002). Hydrothermal alteration of «La Serrata » bentonite (Almería, Spain) by alkaline solutions. *Applied Clay Science, 21,* 257- 269.

Raymond, G. P., & Davies, J. R. (1978). Triaxial tests on dolomite railroad ballast. *J. Geotech. Engrg., ASCE, 104*(6), 737-751.

Raymond, G. P., & Diyaljee, V. A. (1979). Railroad ballast load ranking classification. *J. Geotech. Engrg., ASCE, 105*(10), 1133-1153.

Rezania, M., Faramarzi, A., & Javadi, A. (2011). An evolutionary based approach for assessment of earthquake-induced soil liquefaction and lateral displacement. *Engineering Applications of Artificial Intelligence, 24*(1), 142-153.

Rezania, M., Javadi, A. A., & Giustolisi, O. (2008). An Evolutionary-Based Data Mining Technique for Assessment of Civil Engineering Systems. *Journal of Engineering Computations, 25*(6), 500-517.

Ring, G. W., Sallgerb, J. R., & Collins, W. H. (1962). Correlation of Compaction and Classification Test Data. *HRB Bulletin, 325*, 55–75.

Robinet, J. C. (2005). Effects of an alkaline plume on the hydraulic and hydromechanical properties of the bentonite MX-80. *ECOCLAY II– effects of cement on clay barrier performance – final report. European Commission*, 88-104.

Rodwell, W., Baker, A., Schwyn, B., Meyer, T., Michau, N., Snellman, M., & Cuñado, M. (2005). Work package 6: summary and performance assessment. In

ECOCLAY II - Effects of cement on clay barrier performance - Final Report. *European Commission*, 300-313.

Roscoe, K., & Burland, J. (1968). On the Generalized Stress-Strain Behavior of Wet Clays. In J. H. Leckie (Ed.), *Engineering Plasticity* (pp. 535–609). Cambridge: Cambridge University Press.

Rowan, H. W., & Graham, W. W. (1948). Proper Compaction Eliminates Curing Period in Construction Fills. *Civil Engineering , 18*, 450–451.

Rowe, C. W., & Barden, L. (1964). Importance of free ends in triaxial testing. *Journal of the Soil Mechanics and Foundations Division, ASCE, 90*(1), 1-28.

Sah, N. K., Sheorey, P. R., & Upadhyama, L. W. (1994). Maximum likelihood estimation of slope stability. *Int. J. Rock Mech. Min. Sci. Geomech. Abstr., 31*, 47-53.

Sakellariou, M. G., & Ferentinou, M. D. (2005). A study of slope stability prediction using neural networks. *Geotechnical and Geological Engineering, 23*, 419-445.

Sarma, S. K. (1975). Seismic stability of earth dams and embankments. *Geotechnique, 25*(4), 743-761.

Savage, D., Noy, D., & Mihara, M. (2002). Modelling the interaction of bentonite with hyperalkaline fluids. *Applied Geochemistry, 17*, 207-223.

Schofield, D., & Worth, C. (1968). *Critical state soil mechanics.* London: McGraw-Hill.

Sherif, M. A., & Burrous, C. M. (1969). Temperature Effects on The Confined Shear Strength of Saturated, Cohesive Soil. *an International Conference on Effects of Temperature and Heat on Engineering Behavior of Soils.*

Shin, H. (2001). *Neural network based constituive models for finite element analysis.* PhD dissertation University of Wales Swansea, UK.

Shin, H., & Pande, G. (2000). On self-learning finite element code based on monitored response of structures. *Computers and Geotechnics, 27*, 161-178.

Shin, H., & Pande, G. (2001). Intelligent finite elements. *Proceeding of Asian-Pacific Conference for Computational Mechanics-APCOM 01*, (pp. 1301-1310). Sydney, Australia.

Shin, H., & Pande, G. (2002). Enhancement of data for training neural network based constitutive models for geomaterials. *Proceeding of The 8th International Symposium on Numerical Models in Geomechanics-NUMOG VIII*, (pp. 141-146). Rome, Italy.

Shin, H., & Pande, G. (2003). Identification of elastic constants for orthotropic materials from a structural test. *Computers and Geotechnics, 30*(7), 571–577.

Sidarta, D., & Ghaboussi, J. (1998). Constitutive modelling of geomaterials from non-uniform material tests. *Computers and Geotechnics, 22*(1), 53-71.

Siddique, R., & Naik, T. R. (2004). Properties of concrete containing scrap-tyre rubber-an overview. *Waste Management, 24*, 563-569.

Sinha, S. K., & Wang, M. C. (2008). Artificial Neural Network Prediction Models for Soil Compaction and Permeability. *Geotechnical and Geological Engineering, 26*, 47-64.

Sinn, H., Kaminsky, W., & Janning, J. (1976). Processing of plastic waste and scrap tyres into chemical raw materials, especially pyrolysis. *Angew Chem International Edition, 15*(11), 660-672.

Sophocleous, M. A. (1978). *Analysis of Heat and Water Transport in Unsaturated-Saturated Porous Media.* Edmonton: University of Alberta.

Spencer, E. (1967). A method of analysis of the stability of embankments assuming parallel inter-slice forces. *Geotechnique, 17*, 11-26.

Sridharan, A., & Nagaraj, H. B. (2005). Plastic limit and compaction characteristics of fine grained soils. *Ground Improvement, 9*(1), 17–22.

Stasa, F. L. (1986). *Applied Finite Element Analysis for Engineers.* CBS College Publishing.

Sukontasukkul, P., & Chaikaew, C. (2006). Properties of concrete pedestrian block mixed with crumb rubber. *Const Build Mater, 20*, 450-457.

Tanaka, N. (1995). *Thermal Elastic Plastic Behavior and Modeling of Saturated Clays.* PhD Thesis, The University of Manitoba, Manitoba, Canada.

Tanaka, N., Graham, J., & Crilly, T. (1997). Stress-Strain Behaviour of Reconstituted Illitic Clay at Different Temperature. *Engineering Geology, 47*, 339-350.

Taylor, D. W. (1937). Stability of earth slopes. *J. Boston Soc. Civil Eng., 24*, 197.

Taylor, D. W. (1948). *Fundamentals of Soil Mechanics.* NY: John Wiley and Sons Inc.

Thomas, H. R., & He, Y. (1997). A Coupled Heat-Moisture Transfer Theory for Deformable Unsaturated Soil and Its Algorithmic Implementation. *Journal for Numerical and Analytical Methods in Engineering, 40*(18), 3421-3441.

Thomas, H. R., & King, S. D. (1991). Coupled Temperature/ Capillary Potential Variation in Unsaturated Soils. *Journal of Engineering Mechanics, ASCE, 117*(11), 2475-2491.

Thomas, H. R., & Li, C. L. (1997). An Assessment of a Model of Heat and Moisture Transfer in Unsaturated Soil. *Geotechnique, 47*(1), 113-131.

Thomas, H. R., & Sansom, M. R. (1995). Fully Coupled Analysis of Heat, Moisture, and Air Transfer in Unsaturated Soil. *Journal of Engineering Mechanics, ASCE, 121*(3), 392-898.

Timoshenko, S. P., & Goodier, J. N. (1970). *Theory of Elasticity.* McGraw-Hill.

Toll, D. G. (1988). *The behaviour of unsaturated compacted naturally occurring gravel.* (P. Thesis, Ed.) University of London.

Toll, D. G. (1990). A Framework for Unsaturated Soil Behaviour. *Geotechnique, 40*(1), 31–44.

Tomasella, J., & Hodnett, M. G. (1998). Estimating soil water retention characteristics from limited data in Brazilian Amazonia. *Soil Sci., 163*(3), 190–202.

Topcu, I. B. (1995). The properties of rubberized concretes. *Cem Concr Res, 25*(2), 304-310.

Towhata, I., & Kuntiwattanakul, P. (1994). Behavior of Clays undergoing Elevated Temperature. *13th International Conference on Soil Mechanics and Foundation Engineering.*

Towhata, I., Kunttiwattanakul, P., Seko, I., & Ohishi, K. (1993). Volume Change of Clays induced by Heating as Observed in Consolidation Tests. *Soils and Foundations, 33*(4), 170-183.

Tsai, C., & Hashash, Y. (2008). A novel framework integrating downhole array data and site response analysis to extract dynamic soil behavior. *Soil Dynamics and Earthquake Engineering, 28*(3), 181–197.

Turnbull, J. M. (1948). Computation of The Optimum Moisture Content in the Moisture-Density Relationship of Soils. *Second International Conference on Soil Mechanics and Foundation Engineering, IV*, pp. 256–262. Rotterdam.

Uchaipichat, A. (2005). *Experimental Investigation and Constitutive Modelling of Thermo-hydro-mechanical Coupling in Unsaturated Soils.* (P. thesis, Ed.) Sydney, New South Wales, Australia: The University of New South Wales.

Uchaipichat, A., & Khalili, N. (2009). Experimental investigation of thermo-hydro-mechanical beehaviour of an unsaturated silt. *Geotechnique, 59*(4), 339-353.

Van Genuchten, M. T. (1980). A closed-form equation for predicting the hydraulic conductivity of unsaturated soils. *Soil Sci. Soc. of Am. J., 44*, 892-898.

Vanapalli, S. K., Fredlund, D. G., Pufahl, D. E., & Clifton, A. W. (1996). Model for the prediction of shear strength with respect to soil suction. *Canadian Geotechnical Journal, 33*, 379–392.

Venkatarama, B. V., & Gupta, A. (2008). Influence of sand grading on the characteristics of mortars and soil–cement block masonry. *Construction and Building Materials, 22*, 1614-1623.

Wang, M. C., & Huang, C. C. (1984). Soil Compaction and Permeability Prediction Models. *Journal of Environmental Engineering, ASCE, 110*(6), 1063–1083.

Wang, M. C., Benway, J. M., & Arayssi, A. M. (1990). The Effect of Heating on Engineering Properties of Clays. In *Physico-Chemical Aspects of Soil and Related Materials* (pp. 139-158). ASTM.

Wenhua, W., Xikui, L., Charlier, R., & Collin, F. (2004). A thermo-hydro-mechanical constitutive model and its numerical modelling for unsaturated soils. *Computers and Geotechnics, 31*, 155–167.

Wheeler, S. J., & Sivakumar, V. (1995). An elasto-plastic critical state framework for unsaturated soil. *Geotechnique, 45*(1), 35-53.

Wheeler, S. J., Näätänen, A., Karstunen, M., & Lojander, M. (2003). An anisotropic elastoplastic model for soft clays. *Can. Geotech. J., 40*, 403–418.

Williams, P. T., Besler, S., & Taylor, D. T. (1990). The pyrolysis of scrap automotive tyres. *Fuel, 69*(12), 1474-1482.

Wu, T. H. (1957). Relative density and shear strength of sands. *J. Soil Mech. and Found. Div., ASCE, 83*(1), 1161:1-23.

Xie, J. X., Cheng, C. T., Chau, K. W., & Pei, Y. Z. (2006). A hybrid adaptive time-delay neural network model for multi-step-ahead prediction of sunspot activity. *Int. J. of Environ. and Pollution, 28*((3-4)), 364-381.

Youssef, M. S., Sabry, A., & Raml, A. H. (1961). Temperature Changes and Their Effects on Some Physical Properties of Soils. *5th International Conference on Soil Mechanics and Foundations.*

YU, H. S. (1998). CASM: A UNIFIED STATE PARAMETER MODEL. *INTERNATIONAL JOURNAL FOR NUMERICAL AND ANALYTICAL METHODS IN GEOMECHANICS, 22*(8), 621-623.

Yun, G., Ghaboussi, J., & Elnashai, A. (2006a). Neural network-based constitutive model for cyclic behaviour of materials. *Proceeding of the 1st European*

Conference on Earthquake Engineering and Seismology, (pp. 1-9). Geneva, Switzerland.

Yun, G., Ghaboussi, J., & Elnashai, A. (2006b). SELF-LEARNING SIMULATION FOR MODELING OF BEAM-COLUMN CONNECTIONS IN STEEL FRAMES. *Proceeding of the 4th International Conference on Earthquake Engineering.* Taipei, Taiwan.

Yun, G., Ghaboussi, J., & Elnashai, A. (2008a). A new neural network-based model for hysteretic behavior of material. *International Journal for Numerical Methods in Engineering, 73*(4), 447–469.

Yun, G., Ghaboussi, J., & Elnashai, A. (2008b). A design-variable-based inelastic hysteretic model for beam–column connections. *Earthquake Engineering and Structural Dynamics, 37*(4), 535–555.

Yun, G., Ghaboussi, J., & Elnashai, A. (2008c). Self-learning simulation method for inverse nonlinear modeling of cyclic behavior of connections. *Computer Methods in Applied Mechanics and Engineering, 197*(33-40), 2836–2857.

Zapata, C. E., Houston, W. N., & Walsh, K. D. (2003). Soil-water characteristic curve variability. *Advances in Unsaturated Geotechnics, Geotech. Special Pub., 99*, 84–124.

Zhou, Y., Rajapakse, R. K., & Graham, J. (1998). Coupled Heat-Moisture-Air Transfer in Deformable Unsaturated Media. *Journal of Engineering Mechanics, ASCE, 124*(10), 1090-1099.

Zunker, F. (1930). Das Verhalten des Bodens Zum Wasser. *Handbuch der Bodenlehre, 6*, 66-220.